

„Transcriptional regulation of defence gene expression by a VQ-motif containing protein“

Dissertation

Zur Erlangung des Doktorgrades der Naturwissenschaften (Dr. rer. nat.)

der

Naturwissenschaftlichen Fakultät I

– Biowissenschaften –

der Martin-Luther-Universität

vorgelegt

von Herrn Martin Weyhe

geb. am 14.03.1987 in Merseburg

Gutachter:

Prof. Dr. Dierk Scheel | Leibniz Institut für Pflanzenbiochemie, Halle

Prof. Dr. Ulla Bonas | Martin-Luther-Universität Halle-Wittenberg

Prof. Dr. Thorsten Nürnberger | Zentrum für Molekularbiologie der Pflanzen, Tübingen

Verteidigung: 03.07.2019

Index

List of abbreviations.....	VI
1. Introduction	1
1.1. Plant immunity	1
1.1.1 Pattern recognition.....	1
1.1.2. Early MTI responses.....	3
1.1.3. Late MTI responses.....	4
1.1.4 Pathogen effectors and effector-triggered immunity (ETI).....	5
1.2. MAPK cascades	6
1.2.1. MAMP-induced MAPKs	7
1.2.2. MAPK targets involved in immunity	8
1.3. WRKY transcription factors	10
1.3.1 The WRKY domain	10
1.3.2 WRKY function and regulation	10
1.4. VQ-motif containing proteins.....	12
1.4.1. VQs are transcriptional co-regulators	12
1.4.2. MPK3/6-targeted VQs (MVQs)	14
1.5. Aim of the present work.....	16
2. Materials and methods.....	17
2.1. Materials.....	17
2.1.1. Chemicals.....	17
2.1.2. Media.....	17
2.1.3. Bacteria.....	17
2.1.4. Plant material and growth conditions	18
2.2. Methods	18
2.2.1 Molecular cloning	18
2.2.2 Transformation of bacteria.....	19
2.2.3 Generation of MVQ phospho-site mutants.....	19
2.2.4 Genotyping T-DNA insertion lines	19
2.2.5 Generation of CRISPR-Cas9 constructs.....	20
2.2.6 <i>Agrobacterium</i> -mediated plant transformation	20
2.2.7 Quantitative Real-time PCR.....	20
2.2.8 Isolation of genomic DNA.....	20

2.2.9	Southern Blot.....	21
2.2.10	Preparation and transfection of <i>A. thaliana</i> mesophyll protoplasts.....	21
2.2.11	Microscopy	21
2.2.12	Promoter activation assay	22
2.2.13	Microarray analysis.....	22
2.2.15	Expression of recombinant proteins in <i>Escherichia coli</i>	23
2.2.16	Protein purification.....	24
2.2.17	SDS-PAGE and immunoblot analysis	24
2.2.18	Electrophoretic mobility shift assay (EMSA).....	25
2.2.19	DNA-protein interaction assay (DPI-ELISA).....	25
2.2.20	Chromatin Immunoprecipitation followed by sequencing (ChIP-seq)	26
2.2.21	Infection of <i>Arabidopsis thaliana</i> with <i>Botrytis cinerea</i>	26
3.	Results	28
3.1	Subcellular localisation of MVQs	28
3.1.1	MVQs display two distinct subcellular localisation patterns.....	28
3.1.2	Mutation of phosphorylation sites affects localisation of some MVQs	31
3.2	Effects of MVQ1 and other MVQs on defence gene promoter activity	33
3.2.1	MVQ1 dampens MAMP-induced activation of <i>pNHL10</i> via its VQ-motif.....	33
3.2.2	MVQs differentially modulate MAMP-induced activation of <i>pNHL10</i>	35
3.2.3	MVQ1 suppresses MAMP-induced activation of additional defence-related genes ..	38
3.2.4	MVQ1 antagonises WRKY-mediated activation of <i>pNHL10</i>	39
3.3	Confirmation of MVQ1 interactions with WRKY transcription factors	41
3.4	Transcriptome analysis of MVQ1 misexpression lines	44
3.4.1	Characterisation of MVQ1 misexpressing plant lines for transcriptome analysis.....	44
3.4.2	Microarray analysis reveals differentially expressed genes in MVQ1 misexpression lines.....	45
3.4.3.	Effect of altered MVQ1 levels on the transcriptome in control conditions	46
3.4.4.	Impact of MVQ1 on the transcriptome after MAMP-treatment.....	49
3.4.5.	Validation of potential MVQ1-suppressed defence genes by qRT-PCR	53
3.5	Influence of MVQ1 on DNA-binding of WRKYs	55
3.5.1.	EMSAs reveal interactions of MVQ1 with DNA-bound WRKY33.....	55
3.5.2.	MVQ1 stimulates binding of some WRKY-domains to DNA.....	57
3.5.3.	MVQ2-6 can also stimulate binding of WRKY33 cDBD to DNA	59
3.6	Potential MVQ1 targets identified by Chromatin Immunoprecipitation (ChIP).....	61

3.7	The role of MVQ1 in resistance against <i>Botrytis cinerea</i>	65
4.	Discussion	67
4.1	MVQs are potential transcriptional co-regulators of defence genes.....	67
4.2	MVQ1 is a negative regulator of defence gene expression	68
4.3	The molecular mode of action for MVQ1.....	70
4.3.1	Does MVQ1 affect DNA-binding or transcriptional activity of WRKYs?	70
4.3.2	MVQ1 is associated with target gene promoters via WRKYs.....	73
4.3.3	Regulation of MVQ1 activity by MAPKs	74
4.3.4	Integration of MVQ1 into the WRKY network.....	75
5.	Summary	79
6.	Zusammenfassung	80
7.	References	81
8.	Appendix	93
8.1	List of Figures.....	93
8.2	List of Tables	94
8.3	List of Supplementary Figures	94
8.4	List of Supplementary Tables	94
8.5	List of Supplementary Data Files (see compact disc)	95
8.5	Supplementary figures	96
8.6	Supplementary tables.....	103
	Danksagung	121
	Curriculum vitae	122
	Eidesstattliche Erklärung	123

List of abbreviations

ABA	abscisic acid	CERK1	CHITIN ELICITOR RECEPTOR KINASE
ABI5	ABSCISIC ACID-INSENSITIVE 5	ChIP	chromatin immunoprecipitation
ACC	1-amino-cyclopropane-1-carboxylate	CIPK	CBL-INTERACTING PROTEIN KINASES
ACS	ACC-SYNTHASE	CFP	CYAN FLUORESCENT PROTEIN
Amp	ampicillin	cGMP	cyclic guanosine monophosphate
ASR3	ARABIDOPSIS SH4-RELATED 3	CNGC	CYCLIC NUCLEOTIDE-GATED ION CHANNEL
At	<i>Arabidopsis thaliana</i>	CRCK3	CaM-BINDING RLCK 3
ATP	adenosine triphosphate	CTD	carboxy-terminal domain
BAK1	BRI1-ASSOCIATED KINASE 1	d	diameter
Bc	<i>Botrytis cinerea</i>	DAMP	damage-associated molecular pattern
BiFC	bimolecular fluorescence complementation	DBD	DNA-binding domain
BIK1	BOTRYTIS-INDUCED KINASE 1	DEG	differentially expressed genes
BIR2	BAK1-INTERACTING RLK 2	dpi	days post infection
bHLH	basic helix-loop-helix	eATP	extracellular ATP
BR	brassinosteroid	EDS1	ENHANCED DISEASE SUSCEPTIBILITY 1
BRI1	BR-INSENSITIVE 1	EDTA	ethylenediaminetetraacetic acid
bZIP	basic leucine zipper	EFR	EF-Tu RECEPTOR
Cam	chloramphenicol	EF-Tu	ELONGATION FACTOR THERMO UNSTABLE
CaM	CALMODULIN	EGF	EPIDERMAL GROWTH FACTOR
CAMTA	CaM-BINDING TRANSCRIPTION ACTIVATOR	elf18	bacterial elongation factor EF-Tu-derived 18 amino acid peptide
CC	coiled-coiled	EMSA	electrophoretic mobility shift assay
CBL	CALCINEURIN B-LIKE PROTEIN	ERF	ETHYLENE RESPONSIVE ELEMENT BINDING FACTOR
CBP60g	CaM-BINDING PROTEIN 60g		
CDKC	CYCLIN-DEPENDENT KINASE C		
CDPK	CALCIUM-DEPENDENT PROTEIN KINASE		

ET	ethylene	MAPK	MITOGEN-ACTIVATED PROTEIN KINASE
EV	empty vector		
FDR	false discovery rate	MAPKK	MAPK KINASE
FLS2	FLAGELLIN SENSING 2	MAPKKK	MAPKK KINASE
flg22	bacterial flagellin-derived 22 amino acid peptide	MKP1	MAPK PHOSPHATASE 1
FRK1	FLG22-INDUCED RECEPTOR-LIKE KINASE 1	MKS1	MAPK SUBSTRATE 1
GFP	GREEN FLUORESCENT PROTEIN	MTI	MAMP-triggered immunity
GO	gene ontology	MVQ	MPK3/6-TARGETED VQ-PROTEIN
GST1	GLUTATHIONE-S-TRANSFERASE 1	NADPH	nicotinamide adenine dinucleotide phosphate
GUS	β -GLUCURONIDASE	Nb	<i>Nicotiana benthamiana</i>
HA	human influenza hemagglutinin	NBS	nucleotide binding site
HIN1	HARPIN INDUCED 1	NDR1	NON-RACE SPECIFIC DISEASE RESISTANCE 1
IGS	indole glucosinolates	NHL10	NDR1/HIN1-LIKE 10
IPTG	isopropyl- β -D-thiogalactopyranosid	NLP	NECROSIS AND ETHYLENE-INDUCING PEPTIDE 1-LIKE PROTEIN
JA	jasmonate	NLR	NBS-LRR-R-PROTEIN
JAV1	JASMONATE-ASSOCIATED VQ MOTIF 1	NPR1	NONEXPRESSOR OF PR-GENES 1
JAZ	JASMONATE-ZIM-DOMAIN PROTEIN	Nt	<i>Nicotiana tabacum</i>
Kan	kanamycin	OE	overexpression
LPS	lipopolysaccharides	OG	oligogalacturonides
LRR	leucine-rich repeat	PAD3/4	PHYTOALEXIN-DEFICIENT 3/4
LUC	LUCIFERASE	PAGE	polyacrylamide gel electrophoresis
LYK	LysM-CONTAINING RLK	PAMP	pathogen-associated molecular pattern
LysM	lysine motif	PAT1	ARABIDOPSIS HOMOLOG OF YEAST PAT1
Ma	<i>Musa acuminata</i>	PBL	PBS1-LIKE KINASE
MAMP	microbe-associated molecular pattern	PBS1	AVRPPHB SUSCEPTIBLE 1
		Pc	<i>Petroselinum crispum</i>

Abbreviations

PCR	polymerase chain reaction	RPS2	RESISTANT TO <i>Pseudomonas syringae</i> 2
PEP	PLANT ELICITOR PEPTIDE		
PEPR	PEP RECEPTOR	RRS1	RESISTANCE TO <i>Ralstonia solanacearum</i> 1
PIP	PAMP-INDUCED PEPTIDE	RT	room temperature
PIF1	PHYTOCHROME-INTERACTING FACTOR 1	SA	salicylic acid
PGN	peptidoglycan	SAR	systemic acquired resistance
Pmut	phosphosite-mutant	SDS	sodium dodecyl sulfate
Poly-dIdC	poly-deoxy-inosinic-deoxy-cytidylic acid	SEM	standard error of the mean
PR	PATHOGENESIS-RELATED GENE	SIPK	SA-INDUCED PROTEIN KINASE
PRR	pattern recognition receptor	SOBIR	SUPPRESSOR OF BIR1
PROPEP	PLANT ELICITOR PEPTIDE PRECURSOR	Spec	spectinomycin
PTI	PAMP-triggered immunity	SUMM2	SUPPRESSOR OF <i>mkk1 mkk2</i>
PUB	PLANT U-BOX PROTEIN	TF	transcription factor
pv.	pathovar	TIR	TOLL-INTERLEUKIN RECEPTOR
qRT-PCR	quantitative real-time PCR	TSS	transcription start site
R	resistance	TZF9	TANDEM ZINC FINGER PROTEIN 9
RALF	RAPID ALKALINISATION FACTOR	UTR	untranslated region
RBOHB/D/E/F	RESPIRATORY BURST OXIDASE HOMOLOG B/D/E/F	WIPK	WOUND-INDUCED PROTEIN KINASE
RIN4	RPM-INTERACTING PROTEIN 4	WT	wild type
RLCK	RECEPTOR-LIKE CYTOPLASMATIC KINASE	Y2H	yeast two-hybrid
RLK	RECEPTOR-LIKE KINASE	YFP	YELLOW FLUORESCENT PROTEIN
RLP	RECEPTOR-LIKE PROTEIN	ZAT10	ZINC FINGER PROTEIN ZAT10
RNAPII	RNA POLYMERASE II		
ROS	reactive oxygen species		
RPM1	RESISTANCE TO <i>Pseudomonas syringae</i> pv. <i>maculicola</i> 1		

1. Introduction

1.1. Plant immunity

Plants, as photoautotrophic organisms, provide the nutritional basis for animals and most microbes. Microorganisms can interact with plants in mutualistic relationships (e.g. mycorrhiza, rhizobia), which are beneficial for both partners. In contrast, pathogenic microbes colonise plants to extract nutrients, causing disease and reduction in fitness. Pathogens called biotrophs acquire nutrients from living host cells, while necrotrophs kill the host cell and feed off dead or dying tissue. Hemi-biotrophic pathogens initially invade living cells and switch to a necrotrophic life style during later stages of infection.

Plants evolved an immune system to ward off pathogens that in turn acquired mechanisms to evade plant immunity in an ongoing evolutionary arms race (Jones and Dangl 2006). Unlike higher vertebrates, plants lack an adaptive immune system with specialised immune cells and therefore rely on innate immunity (Nurnberger et al. 2004). For optimal plant fitness, growth and defence need to be adaptively balanced according to the current environmental situation. Immune responses are thus tightly regulated by complex signaling networks to avoid for example excessive allocation of limited resources to defence pathways in absence of pathogens.

Plant diseases threaten global food security since they cause an estimated loss of 10 % in food production (Oerke 2006). A detailed understanding of plant immune responses and the underlying signaling networks is important to increase food security and to reduce the use of pesticides i.e. by breeding of resistant plant varieties.

1.1.1 Pattern recognition

Preformed physical barriers, such as cuticular waxes and the cell wall, build the first line of defence against invading pathogens. To detect potential pathogens that breached those preformed barriers, plants employ pattern recognition receptors (PRR), which recognise microbe- or pathogen-associated molecular patterns (MAMPs/PAMPs) and initiate MAMP- or PAMP-triggered immunity (MTI/PTI). MAMPs are characteristic microbial molecules that are usually conserved and critical for pathogen fitness (Macho and Zipfel 2014). Typical examples are chitin oligomers from fungal cell walls, lipopolysaccharides (LPS) from Gram-negative bacteria and peptidoglycans (PGN) from Gram-positive bacteria (Wan et al. 2008; Ranf et al. 2015; Gust et al. 2007). Well characterised proteinaceous MAMPs include peptides derived from bacterial translation elongation factor EF-Tu (Kunze et al. 2004) or from flagellin, which forms the filament of bacterial flagella (Zipfel et al. 2004). Besides MAMPs, which are

non-self molecules, plants are able to detect plant-derived damage-associated molecular patterns (DAMPs) that are released by cell disruption during pathogen or herbivore attack. Examples of DAMPs are extracellular adenosine triphosphate (eATP) (Choi et al. 2014) or cell wall fragments called oligogalacturonides (OGs) (Ferrari et al. 2013).

Presence of pathogens or wounding can additionally trigger production and secretion of small peptides like plant elicitor peptides (PEPs) (Huffaker, Pearce, and Ryan 2006), rapid alkalisation factors (RALFs) (Stegmann et al. 2017) or PAMP-induced peptides (PIPs) (Hou et al. 2014). These peptides modulate immune responses upon perception by PRRs and are referred to as phytocytokines because of similarities to metazoan cytokines (Gust, Pruitt, and Nurnberger 2017).

MAMPs, DAMPs and phytocytokines are perceived by PRRs at the cell surface. PRRs include receptor-like kinases (RLKs) and receptor-like proteins (RLPs). While both RLKs and RLPs are composed of a ligand-binding ectodomain and a transmembrane domain, RLKs additionally possess an intracellular kinase domain, which is lacking in RLPs. Due to lack of a kinase domain, RLPs rely on interaction with the regulatory LRR-RLK SUPPRESSOR OF BIR1-1 (SOBIR1) to form a bimolecular equivalent of a genuine RLK (Liebrand et al. 2013; Couto and Zipfel 2016). PRRs can be grouped according to the identity of their ectodomain. Proteins and peptides are typically bound by ectodomains containing leucine-rich repeats (LRRs) (Chinchilla et al. 2006; Zipfel et al. 2006; Yamaguchi, Pearce, and Ryan 2006), while lysine motifs (LysM) bind carbohydrate-containing ligands like chitin and PGN (Miya et al. 2007; Willmann et al. 2011). Epidermal growth factor (EGF)-like ectodomains bind OGs (Brutus et al. 2010) and lectin-type PRRs detect eATP and LPS (Choi et al. 2014; Ranf et al. 2015).

One of the best-studied plant PRRs is the flagellin receptor FLAGELLIN SENSING 2 (FLS2), an LRR-RLK from *Arabidopsis thaliana*. It recognises a conserved 22 amino acid epitope of flagellin (flg22) with its LRR ectodomain (Zipfel et al. 2004). Upon ligand binding, FLS2 heterodimerises with another RLK BRI1-ASSOCIATED KINASE 1 (BAK1) that serves as a co-receptor for flg22 (Sun et al. 2013). In the absence of flg22, both FLS2 and BAK1 are associated with the receptor-like cytoplasmatic kinase (RLCK) BOTRYTIS-INDUCED KINASE 1 (BIK1). After flg22-perception, BIK1 is phosphorylated by BAK1 and in turn phosphorylates FLS2 and BAK1 before it dissociates from the PRR-complex and triggers downstream responses (Lu et al. 2010; Zhang et al. 2010).

Interestingly, the regulatory kinase BAK1 also associates with the brassinosteroid (BR) receptor BR-INSENSITIVE 1 (BRI1) and thus provides a link to regulation of plant growth (Li et al. 2002). BAK1 interacts with additional PRRs, such as the EF-Tu receptor (EFR) recognising EF-Tu-derived peptides elf18 and elf26, the PEP receptors (PEPRs) PEPR1 and PEPR2 (Tang et al. 2015), and several LRR-RLP-SOBIR1 complexes e.g. RLP23-SOBIR1, which recognises the nlp20 fragment of microbial NECROSIS AND ETHYLENE-INDUCING PEPTIDE 1-LIKE PROTEINS (NLPs) (Albert et al. 2015). BAK1 is required for all these signalling pathways and its importance was further illustrated in a study investigating LRR-

RLK interaction networks, where it was found to be the most interconnected LRR-RLK (Smakowska-Luzan et al. 2018).

CHITIN ELICITOR RECEPTOR KINASE 1 (CERK1) seems to act as a regulatory RLK analogous to BAK1 in case of LysM-domain PRRs. It forms a complex with the chitin receptor LysM-CONTAINING RLK 5 (LYK5) and its homolog LYK4 during chitin perception in *A. thaliana* (Cao et al. 2014). Additionally, CERK1 is recruited by two RLPs LysM-DOMAIN PROTEIN 1 (LYM1) and LYM3 that recognise PGN (Willmann et al. 2011). Although chitin perception is independent of BAK1, BIK1 is activated, which thus constitutes a converging point for different MAMP or phytoytokine signals including chitin, elf18, Pep1 and flg22. On the other hand, the RLCK PBS1-LIKE KINASE 27 (PBL27) is specifically activated after chitin perception (Shinya et al. 2014).

1.1.2. Early MTI responses

The most rapid responses that occur within minutes after MAMP-treatment are changes in ion flux at the plasma membrane, an increase in intracellular Ca^{2+} concentration, production of reactive oxygen species (ROS) and activation of MITOGEN-ACTIVATED PROTEIN KINASES (MAPKs) and CALCIUM-DEPENDENT PROTEIN KINASES (CDPKs or CPKs) (Fig. 1).

How activated PRRs trigger increase of intracellular Ca^{2+} is not well understood and the identity of main calcium channels involved remains elusive (Yuan et al. 2017). In case of PEPR1, Qi et al. (2010) suggest that upon perception of PEPs, a guanylyl cyclase domain of PEPR1 produces cGMP, which activates a cyclic nucleotide-gated ion channel (CNGC) triggering PEP-induced Ca^{2+} rise. Furthermore, the RLCKs BIK1 and PBL1 are important for MAMP-induced Ca^{2+} signalling (Ranf et al. 2014) indicating a role as (possibly indirect) link between PRRs and Ca^{2+} -channels.

Increased intracellular Ca^{2+} -levels are sensed by Ca^{2+} -binding proteins like calmodulins (CaMs), CALCINEURIN B-LIKE PROTEINS (CBLs) and CPKs (Seybold et al. 2014). Binding of Ca^{2+} by CaMs triggers conformational changes that affect downstream responses. Some CaMs interact with transcription factors (TFs) to regulate gene expression. CaM-BINDING PROTEIN 60g (CBP60g) and CaM-BINDING TRANSCRIPTION ACTIVATOR 3 (CAMTA3) are examples of CaM-interacting TFs that are involved in immunity (Wang et al. 2009; Zhang et al. 2014). CBLs interact with CBL-INTERACTING PROTEIN KINASES (CIPKs) to build a bimolecular sensor/kinase pair. Binding of Ca^{2+} by CBLs leads to activation of interacting CIPKs. In contrast to CBL/CIPKs, CPKs combine Ca^{2+} -sensing and kinase activity in one protein. CPK4, CPK5, CPK6 and CPK11 are positive regulators of flg22 signalling (Boudsocq et al. 2010), important for defence gene activation and phosphorylate WRKY TFs (Gao et al. 2013).

CPKs and CBL/CIPKs connect Ca^{2+} -signalling with ROS production by targeting the two NADPH oxidases RESPIRATORY BURST OXIDASE HOMOLOG D & F (RBOHD, RBOHF), which are responsible for ROS

generation during MTI. While a module of CBL1, CBL9 and CIPK26 enhances activity of RBOHF (Drerup et al. 2013), RBOHD is positively regulated by CPK5 (Dubiella et al. 2013). RBOHD is furthermore phosphorylated by BIK1 and PBL1, which is crucial for full MAMP-induced ROS production (Li, Li, et al. 2014; Kadota et al. 2014). Thus, RLCKs provide a direct link between PRR activation and ROS generation. ROS serve as antimicrobial agents and signalling molecules that are involved in cell-to-cell signal propagation and stomatal closure (Qi et al. 2017).

MAPKs are typically activated in a hierarchical manner with a MAPK kinase kinase (MAPKKK) activating MAPK kinase (MAPKK), which in turn activates MAPKs. MAPKs phosphorylate target proteins thus modulating properties like enzymatic activity, stability, localisation or interaction with other molecules. MAPK cascades and their function in immunity are described in detail in chapter 1.2.

1.1.3. Late MTI responses

Following the described early MTI signalling events, activated MAPKs, CPKs, CIPKs and CaMs relay signals from the plasma membrane to the cytoplasm and nucleus thereby triggering transcriptional changes and the production of other signalling molecules e.g. hormones. Ethylene (ET), salicylic acid (SA) and jasmonates (JA) are the major phytohormones regulating plant immunity and their biosynthesis is induced by MAMPs within hours (Yu et al. 2017). In general, ET and JA play an important role in defence responses against necrotrophs, while SA is involved in defence against biotrophs and hemi-biotrophs by promoting cell death (Glazebrook 2005). SA is furthermore essential in establishing systemic acquired resistance (SAR) to subsequent infections. However, the signalling networks of the three hormones are strongly interconnected and collectively contribute to MTI (Hillmer et al. 2017). MAMP treatment leads to massive transcriptional reprogramming (Denoux et al. 2008). While expression of defence-related genes is induced, photosynthesis-related genes are suppressed probably to favour defence over growth (Lewis et al. 2015). More details on transcriptional regulation of immunity are given in chapters 1.2 and 1.3.

Transcriptional changes during MTI ultimately translate into physiological responses, which prevent pathogen entry or growth. Examples are the closure of stomata, deposition of callose as well as production and secretion of antimicrobial compounds. Of note, transcripts of many components of MTI-signalling like *FLS2*, *EFR*, *BIK1*, *RBOHD*, *MAPKs* and *PROPEPs* (precursors of PEPs) are induced upon MAMP-treatment, hence providing positive transcriptional feedback that ensures sustained immune responses (Li et al. 2016).

1.1.4 Pathogen effectors and effector-triggered immunity (ETI)

During co-evolution with plants, adapted plant pathogens evolved effectors (either small molecules or proteins) to interfere with MTI or host metabolism and successfully establish host infection (Bozkurt et al. 2012). Bacteria secrete effectors into the host cell via a type-III secretion system. How effectors of filamentous pathogens like fungi and oomycetes are translocated into host cells is not well understood but seems to require vesicular transport (Lo Presti and Kahmann 2017). Virtually all key components of MTI are targeted by effectors. For example, the *Pseudomonas syringae* effector AvrPto is a kinase inhibitor that targets kinase domains of FLS2, BAK1, EFR and CERK1 to prevent MAMP-signalling (Xiang et al. 2008). Further downstream, the RLCK BIK1 is a target of *P. syringae* AvrPphB and the *Xanthomonas campestris* effector AvrAC, which interfere with BIK1 function by cleavage (AvrPphB) or uridylation (AvrAC) (Su, Spears, et al. 2018). MAPK cascades are additional important targets of several effectors. PexRD2, an effector from the oomycete *Phytophthora infestans*, interacts with MAPKKKε from *Nicotiana benthamiana* to prevent activation of downstream MAPKs and cell death response (King et al. 2014), while *P. syringae* HopAI1, a phosphothreonine lyase, inactivates MPK3, MPK4 and MPK6 in *A. thaliana* (Zhang et al. 2007). AvrRpt2, a cysteine protease from *P. syringae*, specifically suppresses activation of MPK4 and MPK11 (Eschen-Lippold et al. 2016). Some effectors interfere with MTI on multiple levels like HopF2 from *P. syringae*, which targets BAK1, BIK1, MKK5 and RPM-INTERACTING PROTEIN 4 (RIN4) (Zhou et al. 2014). RIN4 is involved in the regulation of proton pumps and stomatal opening (Lee et al. 2015). Its importance as a key component of plant immunity is illustrated by the fact that RIN4 is targeted by several *P. syringae* effectors, including AvrB, AvrRpm1, AvrRpt2, HopF2, AvrPto, and AvrPtoB (Deslandes and Rivas 2012).

To counter effector-triggered susceptibility plants deploy intracellular receptors to detect the activity of pathogen effectors. These receptors are nucleotide binding site (NBS)-LRR containing proteins (NLRs), which, once activated, induce effector-triggered immunity (ETI). The prominent effector target RIN4 for example is guarded by RESISTANCE TO *Pseudomonas syringae* pv. *maculicola* 1 (RPM1), which detects phosphorylation of RIN4 caused by AvrRpm1 or AvrB (Liu et al. 2011). RESISTANT TO *P. syringae* 2 (RPS2) is another NLR activated by AvrRpt2-mediated cleavage of RIN4 (Day et al. 2005). RPS5 recognises activity of AvrPphB by guarding AVRPPHB SUSCEPTIBLE 1 (PBS1), a close homolog of BIK1. Interestingly, PBS1 has no detectable function in MTI, but rather represents a decoy to detect AvrPphB activity (Qi et al. 2014). Recently, it became evident that a number of NLRs contain integrated domains (NLR-IDs), which resemble effector targets. These domains serve as “integrated decoys” and enable the NLR to directly detect effector activities. Of note, NLRs with an integrated RIN4-domain are present in barley, rice and apple (Sarris et al. 2016). Analysis of NLR-IDs will probably facilitate the discovery of previously unknown effector targets in the future.

MTI and ETI share signalling components including Ca^{2+} , ROS and MAPKs and distinction between MTI and ETI can be nebulous (Thomma, Nurnberger, and Joosten 2011). However, during ETI, MAPK activation is typically prolonged compared to MTI and ROS burst originates mainly from the chloroplast (Su, Yang, et al. 2018). ENHANCED DISEASE RESISTANCE 1 (EDS1) and PHYTOALEXIN-DEFICIENT 4 (PAD4) constitute a signalling hub, which activates SA-signalling and cell death and is employed by a subclass of NLRs containing a TIR-domain.

1.2. MAPK cascades

MAPK cascades are conserved eukaryotic signalling modules that translate external stimuli into intracellular responses. Typically sequential phosphorylation events involving MAPKKKs and MAPKK lead to the activation of MAPKs by phosphorylation of their T(E/D)Y activation motifs. Activated MAPKs phosphorylate serine-proline (SP) or threonine-proline (TP) phosphorylation sites in target proteins. The *A. thaliana* genome encodes 12 MEKK-type MAPKKKs, 10 MAPKKs and 20 MAPKs that are engaged in different MAPKKK/MAPKK modules depending on the signalling context. In addition to the MEKK-type MAPKKKs, 48 RAF-related kinases exist in *A. thaliana*, but so far evidence is lacking for these kinases to be *bona fide* MAPKKKs (Group 2002).

MAPK cascades are involved in regulation of plant immunity, development (Xu and Zhang 2015) and responses to abiotic stress. The latter is showcased by the identification of a cascade comprised of MAPKKK17/18, MKK3 and MPK1/2/7/14, which regulates stress signalling in response to abscisic acid (ABA) (Danquah et al. 2015). Notably, completely different stimuli can result in activation of the same MAPKs. For instance, a module comprised of the MAPKKK YODA, MKK4/5 and MPK3/6 regulates different developmental aspects like inflorescence architecture, embryonic cell differentiation and patterning of stomata as well as immune responses (Bergmann, Lukowitz, and Somerville 2004; Sopena-Torres et al. 2018). The same MKK4/5-MPK3/6 module under control of different MAPKKKs (MAPKKK3/5) is critical in plant immunity as well (Sun et al. 2018). In the context of cold stress, the MKK4/5-MPK3/6 module is involved in phosphorylation of the transcriptional regulator ICE1 to mediate its degradation and attenuate expression of cold-responsive genes (Li et al. 2017). Specificity of MAPK signalling is ensured by spatiotemporal expression of up-stream signalling components (e.g. RLKs) and MAPK-targets (Xu and Zhang 2015). Activated MAPK can be inactivated by phosphatases to regulate magnitude and duration of MAPK signalling (Anderson et al. 2011).

1.2.1. MAMP-induced MAPKs

MAMP perception activates two distinct MAPK kinase cascades comprising MEKK1, MKK1/2, MPK4 and MKK4/5, MPK3/6 respectively as summarised in Fig. 1 (Asai et al. 2002; Qiu, Zhou, et al. 2008). Additionally, the MPK4 homolog MPK11 was found to be activated by flg22 treatment (Bethke et al. 2012).

Just recently, MAPKKK3/5 were identified to be the upstream MAPKKKs of MPK3/6 in response to multiple MAMP stimuli including flg22, elf18 and chitin as well as the phytocytokine Pep2 (Bi et al. 2018). In the same study the authors reported MAPKKK5 to be phosphorylated by MPK6 in order to increase MPK3/6 activation in a positive feedback loop. In an analogous manner MPK4 phosphorylates MEKK1 to increase its own activation (Bi et al. 2018).

RLCKs from subfamily VII were suspected to be the missing link between PRRs and MAPKKK activation, since effectors that target these components prevent MAPK activation (Feng et al. 2012). But probably due to redundant functions of the 46 members, mutant analyses mostly failed to pinpoint specific RLCKs required for MAMP-mediated MAPK activation. However, BIK1 and PBL1 are important for Pep-induced MAPK activation (Yamada, Yamashita-Yamada, et al. 2016). PBL27 was shown to specifically connect the chitin receptors with MAPKKK5 (Yamada, Yamaguchi, et al. 2016), while opposed to these findings Rao et al. (2018) found that chitin-mediated MAPK activation was not altered in the *pbl27* mutant or mutants of related RLCKs but rather abolished by deletion of six members of RLCK VII subgroup 4.

While MPK3/6 are regulating immunity in a mainly positive manner, MPK4 was historically described as a negative regulator of immunity because of constitutive immune responses in the *mekk1*, *mkk1/2* and *mpk4* mutants that result in a dwarfed phenotype. This view was challenged by the discovery of SUMM2, an NLR that guards the MPK4 cascade. SUMM2 associates with two MPK4 substrates: the RLCK CRCK3 and PAT1, a component of the RNA decapping machinery. Phosphorylation of these substrates by MPK4 inactivates SUMM2. If PAT1 or CRCK3 are not phosphorylated due to mutations or effector activity, an ETI response is induced (Roux et al. 2015; Zhang et al. 2017). Surveillance of the MPK4 cascade by an NLR strongly suggests that MPK4 activity is important for immune responses.

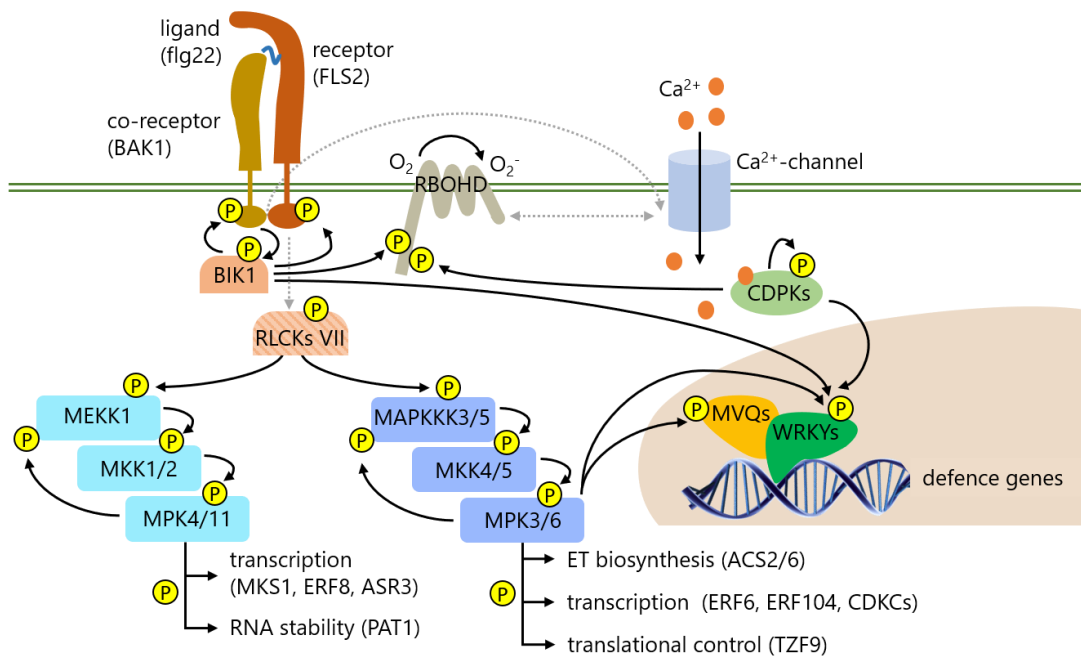


Fig. 1 Scheme of flg22-triggered responses: The bacterial MAMP flg22 is recognised by FLAGELLIN SENSING 2 (FLS2), which recruits the co-receptor BRI1-ASSOCIATED KINASE 1 (BAK1). The RECEPTOR-LIKE CYTOPLASMIC KINASE (RLCK) BOTRYTIS-INDUCED KINASE 1 (BIK1) is phosphorylated by BAK1 leading to several transphosphorylation events at the receptor complex. MAMP elicitation triggers influx of Ca²⁺ and reactive oxygen species (ROS) production by RESPIRATORY BURST OXIDASE HOMOLOG D (RBOHD). Calcium signals are decoded by Ca²⁺-sensors such as CALCIUM-DEPENDENT PROTEIN KINASES (CDPKs/CPKs). CPK5 phosphorylates RBOHD to promote ROS-production and WRKY transcription factors to modulate transcription. RBOHD activity is additionally regulated by BIK1 phosphorylation. A nuclear fraction of BIK1 is able to phosphorylate WRKYs. Other RLCKs from group VII are activated by the receptor complex to trigger activation of two MITOGEN-ACTIVATED PROTEIN KINASE (MAPK) cascades resulting in the activation of MPK4, MPK11 on the one hand and MPK3, MPK6 on the other hand. MAPKs increase activity of their upstream MAPKKK by phosphorylation in a positive feedback loop. Active MAPKs modulate transcription of defence genes by phosphorylation of transcription factors as emphasised here in case of MPK3/6 and WRKYs. Furthermore, they seem to be involved in regulation of RNA stability and translation. MPK3/6 promote ethylene (ET) biosynthesis and phosphorylate a subgroup of proteins containing a VQ-motif termed MPK3/6-TARGETED VQ-PROTEINS (MVQs) (see 1.4.2). P indicates phosphorylation events. Dashed lines indicate functional interactions that might be indirect. MKS1 - MAPK SUBSTRATE 1; ERF - ETHYLENE RESPONSIVE ELEMENT BINDING FACTOR; ASR3 - ARABIDOPSIS SHA4-RELATED 3; ACS2/6 - ACC-SYNTHASE; CDKC - CYCLIN-DEPENDENT KINASE C; TZF9 - TANDEM ZINC FINGER PROTEIN 9

1.2.2. MAPK targets involved in immunity

The output of MAPK signalling is defined by the MAPK target proteins and how phosphorylation affects their properties. MPK4 and MPK11 phosphorylate ETHYLENE RESPONSIVE ELEMENT BINDING FACTOR 8 (ERF8), to reduce ERF8 turnover and positively regulate immunity, since higher ERF8 levels lead to enhanced resistance against bacteria (Cao et al. 2018). At the same time MPK4 also negatively regulates immunity by targeting the trihelix TF ARABIDOPSIS SH4-RELATED 3 (ASR3). ASR3 suppresses most flg22-induced genes and phosphorylation by MPK4 enhances its DNA-binding affinity (Li et al. 2015). The aforementioned MPK4 substrate PAT1 is involved in mRNA decay, but how phosphorylation

by MPK4 affects its function is not clear (Roux et al. 2015). Another target of MPK4 is MAPK SUBSTRATE 1 (MKS1), which harbours a VQ-motif and interacts with WRKY33 (Andreasson et al. 2005). Upon phosphorylation of MKS1, the WRKY33-MKS1 module is released from a ternary complex with MPK4 and subsequently activates the *PAD3* promoter to induce biosynthesis of camalexin, which is the main phytoalexin of *A. thaliana* (Qiu, Fiil, et al. 2008). Resistance to *P. syringae* and *Hyaloperonospora arabidopsidis* is reduced in *mks1* mutants, while MKS1 overexpression lines are more susceptible to the necrotrophic fungus *Botrytis cinerea* (Petersen et al. 2010). This suggests opposing roles of MKS1 as a positive regulator of defence against biotrophs and a negative regulator of resistance to necrotrophic pathogens.

Interestingly, WRKY33, a key transcriptional regulator of camalexin biosynthesis, is a substrate of MPK3/6. Its phosphorylation by MPK3/6 is required for induction of camalexin biosynthesis in response to *B. cinerea* (Mao et al. 2011). The induction of biosynthesis of antimicrobial compounds seems to be an important function of MPK3/6 since camalexin, indole glucosinolates (IGS) and agmatine accumulate in plants displaying sustained MPK3/6 activation caused by expression of a constitutively active MKK5 variant (Lassowskat et al. 2014). In this context Xu et al. (2016) demonstrated that the MPK3/6 target ERF6 is involved in reprogramming of IGS biosynthesis. Another ERF (ERF104) interacts specifically with MPK6 and is released upon flg22 treatment to promote expression of defensins (Bethke et al. 2009). MPK3/6 also activate defence gene expression by phosphorylating cyclin-dependent kinase C (CDKCs) (Li, Cheng, et al. 2014). Activated CDKCs in turn phosphorylate the C-terminal domain (CTD) of an RNA polymerase II (RNAPII) subunit. The phosphorylation pattern at the CTD of RNAPII regulates recruitment of gene-specific TFs and thereby orchestrates defence gene transcription (Li, Cheng, et al. 2014). MPK3 regulates chromatin remodelling in response to flg22 by targeting the histone deacetylase HD2B, which is important for immunity (Latrasse et al. 2017).

Besides their role in transcriptional reprogramming, MPK3/6 directly control ET biosynthesis by phosphorylating two isoforms of ACC-synthase (ACS), the rate-limiting enzyme in ET biosynthesis. Phosphorylation increases stability of ACS2 and ACS6 leading to enhanced ET production that promotes expression of ET-responsive defence genes (Han et al. 2010).

Identification of TANDEM ZINC FINGER 9 (TZF9) as substrate of MPK3/6 suggests, that MPKs might also be involved in post-transcriptional regulation. TZF9 binds RNA and is located in processing-bodies which are cytoplasmic protein complexes responsible for mRNA decay or translational arrest (Maldonado-Bonilla et al. 2014). Phosphorylation reduces TZF9 stability, but its role in post-transcriptional control needs to be further investigated.

1.3. WRKY transcription factors

WRKY transcription factors constitute one of the largest families of transcriptional regulators in plants (Rushton et al. 2010) with 74 members in *A. thaliana*.

1.3.1 The WRKY domain

Determining feature of all WRKYs is the WRKY domain - a conserved DNA-binding domain consisting of about 60 amino acids harbouring a WRKYGQK heptapeptide in the N-Terminus and a C-terminal zinc-finger structure (Eulgem et al. 2000).

Crystal structure analysis revealed that the WRKY domain forms a five stranded anti-parallel β -sheet, which partially enters into the major groove of target DNA (Yamasaki et al. 2012; Duan et al. 2007). While the WRKYGQK heptapeptide is directly involved in sequence-specific binding of the W-box (TTGACC/T) in promoters of target genes, the zinc-finger stabilises the tertiary structure crucial for DNA-binding activity (Maeo et al. 2001).

WRKYs are divided into three major groups according to the number of WRKY-domains and the type of zinc finger motif (Eulgem et al. 2000). Group I comprises members with two WRKY domains of a C₂H₂-type zinc finger, group II WRKYs possess a single WRKY domain with a C₂H₂-motif, whereas group III contains proteins with a single C₂HC-type WRKY domain. Group II can be further divided into five subgroups IIa-e. Recent phylogenetic analyses proposed regrouping of WRKYs into four WRKY lineages: groups I + IIc, groups IIa + IIb, groups IId + IIe and group III (Rinerson et al. 2015).

Although WRKYs underwent a lineage-specific expansion in green plants, members can also be found in diplomonads, amoebae and ancient fungi. Several lines of evidence suggest that these non-plant WRKYs were acquired through lateral gene transfer (Rinerson et al. 2015).

1.3.2 WRKY function and regulation

When bound to their target sequence, WRKYs can activate or repress transcription. Some WRKYs display both functions depending on the promoter context (Miao et al. 2004). They control a broad range of processes including responses to abiotic stress (Wang et al. 2014) as well as development of seeds (Wang et al. 2010), pollen (Guan et al. 2014) and trichomes (Pesch et al. 2014), senescence (Chen et al. 2017) and the biosynthesis of secondary metabolites (Schlottenhofer and Yuan 2015).

Importantly, some WRKYs play a major role in plant immune responses (Pandey and Somssich 2009; Asai et al. 2002) and expression of 49 out of 72 tested members was responsive to SA-treatment or *P.*

syringae infection (Dong, Chen, and Chen 2003). The relevance of WRKYs in plant immunity is further illustrated by the fact that they are targeted by the bacterial effector PopP2, which interferes with DNA-binding by acetylation of the WRKY domain (Le Roux et al. 2015). RESISTANCE TO RALSTONIA SOLANACEARUM 1 (RRS1), an NLR with an integrated decoy WRKY domain, detects PopP2 activity and triggers ETI (Sarris et al. 2015).

The enormous functional diversity of WRKYs, although most WRKYs are binding to the W-box, raises the question of how specificity of WRKYs towards their target promoters is achieved. To some extent the nucleotides adjacent to the core TTGACC/T influence the DNA-binding affinity as demonstrated by Ciolkowski et al. (2008). In addition, variants of the canonical WRKYGQK sequence e.g. WRKYGKK in AtWRKY50 display altered DNA-binding specificities (Brand et al. 2013; Hussain et al. 2018).

Interestingly, W-boxes are statistically enriched in WRKY promoters and binding of WRKYs to their own promoter or those of other family members has been reported (Hsu et al. 2013; Birkenbihl, Kracher, and Somssich 2017). This suggests that WRKYs act within a complex network of auto- and cross-regulation.

A study on parsley (*Petroselinum crispum*) PcWRKY1, the orthologue of AtWRKY33, indicates that W-boxes in promoters of PcWRKY1 and PcPATHOGENESIS-RELATED GENE 1 (PR1) are constitutively occupied by WRKY repressors (Turck, Zhou, and Somssich 2004). In response to MAMP treatment PcWRKY1 transiently binds to its own and the PR1 promoter thus probably replacing pre-bound WRKYs. This mechanism was further corroborated by chromatin immunoprecipitation followed by DNA sequencing (ChIP-seq) in *A. thaliana* (Birkenbihl et al. 2018). Flg22-inducible WRKY18, WRKY33 and WRKY40 bind to their own promoters and those of other flg22-inducible WRKYs specifically after flg22 treatment, while in absence of a stimulus these promoters are occupied by other constitutively expressed WRKYs.

The transcriptional activity of WRKYs is regulated by protein-protein interactions. WRKY-WRKY-interactions, which seem to be restricted to group IIa, IIb, IIc and group III WRKYs (Chi et al. 2013), were shown to have antagonistic or cooperative effects on DNA binding. For example, AtWRKY60 enhances binding of AtWRKY18 to a DNA probe, while it reduces the DNA-binding activity of WRKY40 (Xu et al. 2006).

Besides homo- and heterodimerisation, WRKYs also interact with other proteins. In a screen for MAPK-targets, Popescu et al. (2009) identified a number of WRKYs to be phosphorylated by different MAPKK/MAPK modules. The role of the MAPK substrate WRKY33 in plant immunity was already mentioned in 1.2.2. The homolog of WRKY33 in *N. benthamiana* is NbWRKY8, which is together with closely related WRKYs activated by the MAPK3/6 homologs SA-INDUCED PROTEIN KINASE (SIPK) and WOUND-INDUCED PROTEIN KINASE (WIPK) (Adachi et al. 2015). Phosphorylation of these WRKYs

stimulates expression of the RBOHD ortholog *NtRBOHB* and is required for ROS-burst during ETI triggered by the *P. infestans* effector Avr3a and elicitor INF1-mediated MTI.

A new signalling route in which WRKY33, WRKY50 and WRKY57 are phosphorylated by a nuclear fraction of BIK1 to repress JA and SA production was recently uncovered (Lal et al. 2018). Upon elf18-perception BIK1 is phosphorylated, which in turn inhibits its phosphorylation activity towards the WRKYs and triggers JA and SA signalling. Furthermore, proteins containing a VQ-motif (VQs) emerge as interactors of WRKYs from group I and IIc (Cheng et al. 2012; Pecher et al. 2014). A detailed account on these proteins and their functions will be given in the following chapter.

1.4. VQ-motif containing proteins

A short VQ-motif is the hallmark of VQ proteins and its core sequence FhxxVQxhTG, where x represents any residue and h represents hydrophobic residues, is conserved in *A. thaliana* (Fig. 2) and other plant species (Pecher et al. 2014; Dong et al. 2018). VQs are found in all land plants including mosses and liverworts and the *A. thaliana* genome encodes 34 members. VQs were thought to be plant-specific until a recent study reported putative VQs in nematodes, fungi and bacteria (Jiang, Sevugan, and Ramachandran 2018). However, most of these non-plant VQs contained only partial VQ-motifs and their function in these organisms remains elusive.



Fig. 2 Consensus VQ-motif: The 18 amino acid VQ-motif of all 34 VQs from *Arabidopsis thaliana* as graphical representation (<http://weblogo.berkeley.edu>) (Crooks et al. 2004). Overall stack height indicates sequence conservation at a given position and height of symbols indicates relative frequency of amino acids.

1.4.1. VQs are transcriptional co-regulators

Over the last decade, VQs have been reported to regulate plant growth and development (Lei et al. 2017; Li, Jing, et al. 2014), responses to abiotic stress (Ye et al. 2016) and defence responses against pathogens (Lai et al. 2011) and herbivores (Hu, Zhou, et al. 2013). VQs are transcriptional co-regulators since all VQs, which were analysed in detail so far, interact with TFs to modulate downstream responses. Direct binding of DNA by VQs has not been reported yet. The most prevalent VQ interaction partners are WRKYs with at least 20 of the 34 *A. thaliana* VQs being experimentally proven WRKY

interactors. All WRKYs for which interaction with VQs was demonstrated belong to the phylogenetically closely related groups I and IIc.

VQs can act as co-repressors like VQ20, which together with its WRKY partners WRKY2 and WRKY34 represses expression of three MYB TFs to control pollen development (Lei et al. 2017; Lei, Ma, and Yu 2018). Similarly, JASMONATE-ASSOCIATED VQ MOTIF 1 (JAV1) also named VQ22 is part of a repressor complex including JASMONATE-ZIM-DOMAIN PROTEIN 8 (JAZ8) and WRKY51 that negatively regulates biosynthesis of JA (Yan et al. 2018). Upon herbivore attack, Ca²⁺ activates CaM-dependent phosphorylation of JAV1 leading to disintegration of the repressor complex and activation of JA biosynthesis.

In contrast, SIB1 (VQ23) and SIB2 (VQ16) interact with WRKY33 and stimulate its DNA-binding activity (Lai et al. 2011). *sib1* and *sib2* mutants are more susceptible to *B. cinerea* infection, while SIB1 overexpression plants are more resistant in a WRKY33-dependent manner. In other cases, VQs antagonise the activity of their interacting WRKY. For example, banana (*Musa acuminata*) MaWRKY26 activates JA biosynthesis genes to mediate cold stress tolerance in banana fruits and interaction with MaVQ5 interferes with this activity (Ye et al. 2016).

Interaction between VQs and WRKYs requires the VQ-motif. Deletion of the whole motif or replacement of valine and glutamine with aspartate and leucine (VQ to DL) abolishes VQ-WRKY interactions (Pecher et al. 2014; Cheng et al. 2012). Group IIc WRKYs and the C-terminal WRKY domain of group I WRKYs contain conserved aspartate residues in close proximity to the WRKYGQK heptapeptide, which are probably required for interaction with VQs (Cheng et al. 2012).

Apart from WRKYs, some VQs were reported to interact with other TFs. VQ29 is an interactor and co-activator of PHYTOCHROME-INTERACTING FACTOR 1 (PIF1), a member of the BASIC HELIX-LOOP-HELIX (bHLH) family (Li, Jing, et al. 2014). Both VQ29 and PIF1 positively regulate cell elongation in order to repress seedling de-etiolation. VQ29-PIF1 interaction is not affected by mutation of the VQ-motif, suggesting existence of a different interaction domain. Another example is the BASIC LEUCINE ZIPPER (bZIP) ABA-INSENSITIVE 5 (ABI5), which is a central TF mediating ABA signalling. During seed germination, VQ18 and VQ26 interact with ABI5 to interfere with its transcriptional activity and render germinating seedlings less responsive to ABA (Pan et al. 2018).

Furthermore, VQ12 and VQ29, which are negative regulators of resistance against *B. cinerea*, were demonstrated to form homo- and heterodimers (Wang, Hu, et al. 2015). The C-terminus but not the VQ-motif is required for these interactions, but the molecular mechanism of VQ12/29 function and the relevance of dimerisation remains to be determined.

1.4.2. MPK3/6-targeted VQs (MVQs)

The first evidence of a link between VQs and MAPK signalling was established by (Andreasson et al. 2005) who identified MKS1 (VQ21) as a substrate of MPK4 (see 1.2.2).

A yeast two-hybrid (Y2H) screen with MPK3 or MPK6 as bait identified VQ4, VQ32 and VQ33 as potential interactors that were subsequently confirmed by bimolecular fluorescence complementation in protoplasts (Pecher et al. 2014). These results prompted Pecher et al. (2014) to systematically screen 32 of the 34 *A. thaliana* VQs in an *in vitro* kinase assay for phosphorylation by activated MPK3 and MPK6. Ten VQs were found to be phosphorylated by both kinases and renamed MPK3/6-TARGETED VQ PROTEINS (MVQs). Two independent phosphoproteomic studies used transgenic plants with constitutively active *PcMKK5^{DD}* (or *NtMEK2^{DD}* respectively) under control of an inducible promoter to activate MPK3/6 and identify potential targets (Hoehenwarter et al. 2013; Lassowskat et al. 2014). MVQ1 (VQ) was isolated in both screens, which further underpins its role as a MPK3/6 target.

An extensive Y2H-screen of all MVQs against 59 WRKYs revealed interactions of almost all MVQs with group I and IIc WRKYs (Pecher et al. 2014). MVQ-WRKY interactions depend on an intact VQ-motif, since DL mutants are not able to interact (Fig. 3). MVQ8 did not interact with any tested WRKY and MVQ9 could not be interpreted due to auto-activation in the Y2H. A previous study however reported that MVQ9 (IKU1) interacts with WRKY10 (MINI3) to positively regulate endosperm growth and seed size (Wang et al. 2010). Another MVQ whose function has been studied is MVQ10 (VQ9). MVQ10 antagonises the positive role of WRKY8 during salt stress responses through interaction with WRKY8 and interference with its DNA-binding activity (Hu, Chen, et al. 2013).

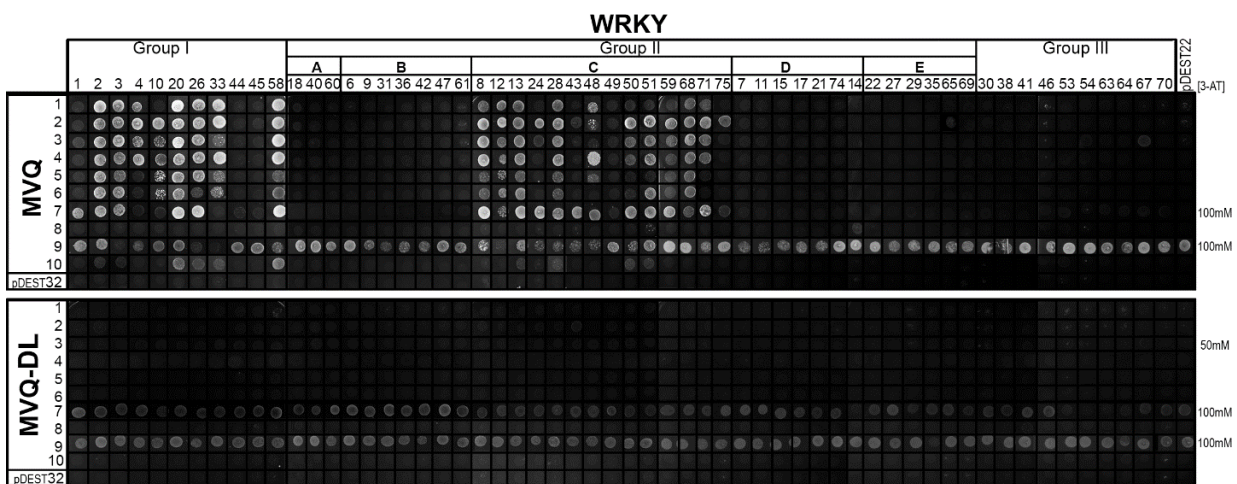


Fig. 3 Yeast two-hybrid (Y2H) analysis of MVQ-WRKY interactions: Data and image taken from Pecher et al. (2014). MVQs (upper table) or variants with a VQ to DL mutation in the VQ-motif (lower table) were screened for interaction with WRKYs in a Y2H analysis. MVQs (except MVQ8) specifically interact with WRKYs from group I and IIc as indicated by growth of yeast cells in selection medium (-His/-Ade). Last lanes represent empty vector controls pDest22/32 respectively. MVQ9, MVQ7^{DL} and MVQ9^{DL} displayed considerable auto-activation, hindering assessment of interaction with WRKYs in these cases.

Evidence for *in vivo* phosphorylation of MVQs after MAMP-treatment was provided by transient expression experiments in protoplast (Pecher et al. 2014). Upon flg22 treatment of protoplasts expressing MVQs, gel mobility shifts were observed for MVQ1-6 and MVQ10 in immunoblot analysis. Inhibition of the mobility shifts by phosphatase treatment demonstrates *in vivo* phosphorylation of these proteins. Furthermore, protein abundance of some MVQs is decreased in flg22-treated protoplast. In case of MVQ1, blocking of *de novo* protein synthesis with cycloheximide unravelled degradation upon MAMP-treatment, which is abolished by mutation of all MVQ1 phosphorylation sites. Promoter activity assays employing the promoter of the defence marker gene *NDR1/HIN1-LIKE 10 (NHL10)* fused to a luciferase reporter gene suggest, that MVQ1 is able to suppress MAMP-induced *pNHL10* activity. A role of MVQ1 in negative regulation of plant immunity is further supported by MVQ1 overexpression (OE) lines displaying impaired MAMP-induced resistance against *P. syringae* (Pecher et al. 2014).

1.5. Aim of the present work

Plant VQs are transcriptional co-regulators that interact with TFs to modulate gene expression. A group of VQs termed MVQs are targeted by MAMP-activated MAPKs MPK3/6, possibly to regulate MVQ protein abundance. Most MVQs interact with WRKY TFs in a VQ-motif-dependent manner and first lines of evidence implicate MVQ1 in transcriptional regulation of MTI responses.

The mode of action, however, is poorly understood and MVQ1 target genes are not identified yet.

This work aims to provide insights into the role of MVQs in transcriptional reprogramming upon MAMP perception. The objective is to investigate all ten MVQs with respect to subcellular localisation and the ability to modulate gene expression driven by defence gene promoters, which is followed by a detailed analysis of MVQ1.

A major challenge in understanding MVQ1 function is the identification of genes and pathways that are controlled by MVQ1, which is addressed using a transcriptomics approach in the present work. Furthermore, this work intends to shed light on the molecular mechanisms underlying transcriptional co-regulation by analysing the potential influence of MVQ1 on WRKY-DNA interactions.

In doing so, we ultimately aim to obtain insights into the importance of MVQ1 in plant immunity and potentially pave the road for plant breeders to use this knowledge to create plants with elevated stress resistance.

2. Materials and methods

2.1. Materials

2.1.1. Chemicals

Chemicals were acquired from Carl Roth, SIGMA Aldrich, Merck, or Applichem GmbH if not specified otherwise. Primers were obtained from Eurofins Genomics. The enzymes cellulase R10 and macerozyme R10 were acquired from Yakult Pharmaceuticals.

Flg22 and elf18 were synthesized in house by Petra Majovsky using an EPS221 peptide synthesiser (Abimed).

2.1.2. Media

Lysogeny broth (LB) medium (Luria/Miller):

10 g/l tryptone; 5 g/l yeast extract; 5 g/l NaCl. 15 g/l agar-agar were added for solid LB medium

1x Murashige and Skoog (MS) medium:

4,4 g/l MS salts including vitamins (Duchefa); 5 g/l sucrose; 0,5 g/l MES; pH adjusted to 5,6 with KOH.

2.1.3. Bacteria

The *Escherichia coli* strain DH5 α (Thermo) was used for molecular cloning. For expression of proteins the *E. coli* strains BL21 (DE3) RIL (Agilent) or KRX (Promega) were used except for full-length WRKY33 which was expressed in BL21 DE3 magic (kindly provided by Dr. Michal Sikorski, Institute of Bioorganic Chemistry, Poznan, Poland). All strains were grown in LB-medium at 37°C if not indicated otherwise.

Agrobacterium tumefaciens strain GV3101 was used for *Agrobacterium*-mediated transformation of *A. thaliana* and grown in LB-medium at 28°C.

Antibiotics were used in the following concentrations: Ampicillin (100 μ g/ml), Chloramphenicol (25 μ g/ml), Gentamycin (10 μ g/ml), Kanamycin (50 μ g/ml), Rifampicin (80 μ g/ml), Spectinomycin (50 μ g/ml), Tetracycline (10 μ g/ml)

2.1.4. Plant material and growth conditions

For all experiments *Arabidopsis thaliana* ecotype Columbia-0 (Col-0) or mutants in Col-0 background were used. Seeds of the *mvq1* mutant (SALK _107266) were obtained from NASC. MVQ1 overexpression lines were generated by *Agrobacterium*-mediated transformation (as described in 2.2.6). Plants were grown on soil in phytochambers and phytocabinets under short day conditions (8 h light/16 h dark) at 22°C. For chromatin immunoprecipitation (ChIP) experiments seedlings were grown in sterile conditions. Seeds were surface sterilized with ethanol and subsequently grown in 1x MS medium supplemented with 0.5% sucrose and 0.1% claforan.

2.2. Methods

2.2.1 Molecular cloning

The Gateway system (Invitrogen) was employed for all cloning procedures. pENTR/D-TOPO and pDonr221 entry clones of MVQ1-10, MVQ1-10^{DL} and MVQ1^{Pmut} (generated by Dr. Pascal Pecher, Lee lab, IPB Halle), WRKYs (provided by Prof. Imre Somssich, MPIZ, Cologne) and different WRKY DBDs (provided by Dr. Luise Brand, ZMBP Tübingen (Brand et al. 2013)) were cloned into respective destination vectors (Tab. 1) using LR-clonase (Invitrogen) according to manufacturer's instructions.

Tab. 1 Gateway compatible destination vectors used in this study

Name	Selection markers	Structure	Source
pUBC-GFP	SpecR, BarR	pUBQ10- GW -GFP-T35	Grefen et al. (2010)
pUBN-GFP	SpecR, BarR	pUBQ10-GFP- GW -T35	Grefen et al. (2010)
pENSG-CFP	AmpR, BarR	p35S-CFP- GW	Feys et al. (2005)
pUGW15	AmpR	p35S-N-3xHA- GW	Nakagawa et al. (2007)
pUGW18	AmpR	p35S-N-4xc-Myc- GW	Nakagawa et al. (2007)
pE-SPYCE	AmpR	p35S-HA-cYFP- GW	Walter et al. (2004)
pE-SPYNE	AmpR	p35S-c-Myc-nYFP- GW	Walter et al. (2004)
pEarleyGate203	KanR, BarR	35S-c-Myc- GW -OCS	Earley et al. (2006)
pDestN110	AmpR	pT7-lacO-SD-10xHis- GW	Dyson et al. (2004)
pET-Dest42	AmpR, CamR	pT7-lacO- GW -V5-6xHis	Invitrogen
pET-Dest42m2	AmpR, CamR	pT7-lacO-SD-GFP- GW -V5	Dr. Luise Brand, ZMBP Tübingen, Germany
pMCSG84	AmpR	pT7-lacO-SD-8xHis-NusA-TEVsite- MCS -6xHis	Michal Sikorski, Institute of Bioorganic Chemistry, Poznan, Poland

MVQs without stop codon for C-terminal fusions were cloned with the pENTR/SD/D-TOPO cloning kit (Invitrogen) following manufacturer's instructions using primers listed in Tab. S1. Mutation of the VQ-residues to DL for generation of MVQ3^{DL} entry clones was achieved by site-directed mutagenesis as described by Palm-Forster, Eschen-Lippold, and Lee (2012) using pENTR/SD/D-TOPO MVQ3 as template with primers in Tab. S2.

2.2.2 Transformation of bacteria

E. coli strains were transformed by heat shock transformation. Competent cells (50 µl) were thawed on ice and the plasmid (50 ng) was added. Cells were incubated with plasmids on ice for 20 min before applying a heat shock (42°C, 45 s). Subsequently 200 µl of LB Medium were added and the bacteria were grown for 1 h at 37°C, 120 rpm before they were plated out on LB Media supplemented with respective antibiotics.

Agrobacterium strain GV3101 was transformed by cold-shock transformation. Competent cells (200µl) were thawed on ice and plasmid DNA (1 µg) was added followed by incubation on ice for 20 min. Cells were shock-frozen in liquid nitrogen for 1 min and subsequently thawed at 37°C for 5 min. After adding 1 ml LB medium bacteria were incubated at 37°C, 120 rpm for 2-3 h before being plated on LB medium supplemented with antibiotics.

2.2.3 Generation of MVQ phospho-site mutants

Mutant versions of MVQ2-6 in which all potential SP and TP phosphorylation sites (Fig. S2) are mutated to AP and with *attB*-sites added to N- and C-terminus, were generated by gene synthesis (GeneArt, Thermo Fisher Scientific) as part of Florian Rist's master thesis. The construct was cloned into entry vectors using BP-clonase (Invitrogen) according to manufacturer's instructions.

2.2.4 Genotyping T-DNA insertion lines

Seeds of T-DNA insertion lines for MVQ1-10 (see Fig. S11) were ordered from NASC. For DNA isolation and PCR, the REExtract-N-Amp tissue PCR Kit (Sigma-Aldrich) was used according to manufacturer's protocol. Primers used for genotyping were designed as suggested by the SALK T-DNA primer design software (Alonso et al. 2003) and are listed in Tab. S3.

2.2.5 Generation of CRISPR-Cas9 constructs

In order to generate transgenic plant lines with deletions in *MVQ* genes, target sites for CRISPR-Cas9 editing (Belhaj et al. 2015) were identified with the CHOPCHOP tool (<http://chopchop.cbu.uib.no/>) for each gene. For cloning of constructs, the molecular toolkit described by Ordon et al. (2017) was employed. More specifically two targets per *MVQ* were chosen and guide sequences loaded in pDGE5 and pDGE8 shuttle vectors using oligonucleotides listed in Tab. S7. Shuttle vectors were cloned in the multiplex genome editing vector pDGE4 encoding Cas9 under control of a parsley ubiquitin promoter.

2.2.6 *Agrobacterium*-mediated plant transformation

Transgenic *A. thaliana* lines were generated by *Agrobacterium*-mediated transformation with the floral dip method described in (Logemann et al. 2006). Lines expressing c-Myc-tagged *MVQ1* under control of the 35S promoter were generated using the pEarleyGate203 vector (Earley et al. 2006).

2.2.7 Quantitative Real-time PCR

RNA was isolated from plant tissue using the TRIzol (Thermo) reagent according to manufacturer's instructions. For synthesis of cDNA the RevertAid (Thermo) cDNA synthesis kit was used using the supplier's protocol. Diluted cDNA (1:10) was added to EvaGreen qPCR Mix (Bio & Sell) following manufacturer's instructions. Primers used for qRT-PCR are listed in Tab. S4. The PCR-program was performed in MX3005P cyclers (Agilent) and consisted of an initial activation step (15 min at 95°C), followed by 40 cycles of 15 s 95°C and 40 s 60°C. After additional 2 min at 95°C a melting curve was recorded (30 s 55°C, 30 s 95°C).

2.2.8 Isolation of genomic DNA

For isolation of genomic DNA 400 µl extraction buffer (200 mM Tris-HCl, pH 7.5; 250 mM NaCl; 25 mM EDTA; 0.5 % SDS) were added to ground plant material (1 adult leaf) and vortexed vigorously. After centrifugation (5 min, 10 000 rpm) 300 µl of the supernatant were mixed with the same amount of isopropanol. DNA was pelleted by centrifugation (5 min, 10 000 rpm), washed with EtOH (70 %) and the dry pellet dissolved in water.

2.2.9 Southern Blot

Genomic DNA was digested with EcoRI (Thermo) and separated on an agarose gel. Southern blotting was performed as described by Southern (2006). The probe was generated by amplification of a fragment in the Basta resistance gene using primers listed in Tab. S5 and the pEarleyGate203 vector as template. Phusion high fidelity polymerase (Thermo) was used for PCR according to manufacturer's protocol. After separation of PCR products on an agarose gel the desired fragment (405 bp) was cut out and isolated with the Fragment CleanUp kit (Invisorb). The DNA (25 ng) was labelled with ^{32}P - α -ATP using the Megaprime DNA labelling kit (GE Healthcare) following the supplier's instructions.

2.2.10 Preparation and transfection of *A. thaliana* mesophyll protoplasts

Fully expanded leaves from 4-week old plants were harvested and used for protoplast isolation as described by Yoo, Cho, and Sheen (2007) with the following changes: After infiltration of leaf strips with enzyme mix, digestion was carried out in the dark for 3 h at 18°C and the protoplast solution was kept on ice for subsequent washing steps. Plasmid DNA for transfection of protoplast was prepared with a Plasmid Maxi Kit (Qiagen) and transfection of protoplast was performed with 10 μg DNA per 100 μl protoplasts according to (Yoo, Cho, and Sheen 2007). After transfection protoplasts were aliquoted and incubated in the dark at 18°C for 14-16 h before use in different assays. For protein expression analysis protoplasts (300 μl) were pelleted and frozen in liquid nitrogen after removal of supernatant. 12 μl of 4x loading buffer were added to the pellet and incubated at 95°C for 3 min.

2.2.11 Microscopy

Protoplasts were analysed by confocal laser scanning microscopy with an LSM710 (Zeiss) 14-16 h after transfection. For localisation studies protoplasts were transfected with pUBN/C plasmids (Grefen et al. 2010) coding for GFP-MVQ fusion proteins. GFP was excited with a 488 nm argon laser and emission recorded from 500-550 nm. CFP-ERF104 served as a nuclear marker in protoplasts transfected with pENSG-ERF104 (provided by Dr. Gerit Bethke, Lee lab, IPB Halle). CFP fluorescence between 480 and 520 nm was recorded in a second track after excitation with a 458 nm laser pulse.

For bimolecular fluorescence complementation (BiFC) protoplasts were co-transfected with pE-SPYNE and pE-SPYCE constructs (Walter et al. 2004) coding for nYFP-WRKYs or cYFP-MVQ1/MVQ1^{DL} respectively. Reconstituted YFP was excited with a 514 nm laser and emissions detected between 500 and 570 nm.

2.2.12 Promoter activation assay

Promoter activation assays were conducted as described in (He et al. 2006) but Luciferase expression was driven by promoters of *NHL10*, *GST1* (constructs provided by Dr. Lennart Eschen-Lippold, Lee lab, IPB Halle), *ZAT10* and *WRKY33* (constructs provided by Xiyuan Jiang, Lee lab, IPB Halle) instead of *FRK1*. A *pUBQ10-GUS* construct was co-transfected for normalisation (Sun and Callis 1997). Protoplast were additionally transfected with *pUGW15* vectors encoding proteins of interest (Nakagawa et al. 2007). 200 μ M luciferin (Invitrogen) was added to protoplast suspension 14-16 h after transfection and aliquots (90 μ l) of 3 biological replicates were transferred to microtiter plates (Greiner). After 20 min the protoplasts were elicited with 100 nM flg22, elf18 or water as a control and luciferase activity recorded with a Luminoscan Ascent plate reader (Thermo).

To measure GUS-activity protoplast extracts were prepared by adding extraction buffer (50 mM NaPO₄ pH 7.0; 1mM EDTA; 0.1 % TritonX; 10 mM mercaptoethanol) to the protoplast suspension followed by vortexing of the sealed plate. 50 μ l of protoplast extract were mixed at 4°C with 10 mM 4-Methylumbelliferyl- β -D-glucuronide dissolved in extraction buffer. 20 μ l of this mix was transferred to 200 μ l stop buffer (0.2 M Na₂CO₃) (t_0), while the rest of the mix was incubated at 37°C for 20 min. Subsequently 20 μ l were transferred to stop buffer (t_{20}) and both time points were measured with a Twinkle LB790 plate reader (Berthold) (excitation filter 355 nm; emission filter 466 nm). Previously recorded luminescence was divided by the difference of GUS activity (t_{20} - t_0) for normalisation.

2.2.13 Microarray analysis

Leaves of six week old plants (Col-0, *mvq1*, MVQ1 OE line K11) were infiltrated with 1 μ M flg22 or water as a control in three biological replicates and harvested 1 h later. RNA was extracted with the RNeasy kit (Qiagen) and treated with DNaseI (Qiagen) following manufacturer's protocol. Quality of RNA was assessed with the Qiaxcel capillary electrophoresis system (Qiagen). RNA (100 ng) with estimated RNA integrity number (RIN) \geq 8 (Schroeder et al. 2006) was used for synthesis of labelled cDNA and hybridisation to Affymetrix 1.1 ST exon arrays employing the GeneChip WT PLUS reagent kit (Affymetrix) following manufacturer's instructions. Hybridised array strips were imaged with the GeneAtlas system (Affymetrix) and preprocessed by Affymetrix Power Tools (v. 1.15.1).

Processing and statistical analysis of raw data was performed by Dr. Benedikt Athmer (Tissier lab, IPB Halle) using R package xps and adapting analysis pipeline from (Balcke et al. 2017). Raw data sets were normalized by robust multiarray averaging including quantile normalisation. Data were filtered for undetected probe sets to remove background noise as described by (Lockstone 2011), using detection above background tests at the exon-level. Undetected probe sets were excluded prior to differential

gene expression analysis. Hybridisation signal above background was detected for 14,461 genes on the chips. Linear models were fitted with Bioconductor's limma package (Ritchie et al. 2015) and adjustment of p values was performed using Benjamini and Hochberg false discovery rate (FDR) (<0.05) procedure (Benjamini and Hochberg 1995). Differentially expressed genes were identified by a significance threshold of 0.05 and a minimal log₂-fold change of ± 1 . Differentially expressed genes were scaled by calculating z-scores. Scaled data was analysed and hierarchically clustered with the TIGR-MEV tool version 4.9 (<http://mev.tm4.org>) using Pearson correlation and average linkage clustering or Hopach clustering (see file 1 and file 2 of supplemental data on CD) respectively.

2.2.14 *In silico* data analysis

Sets of differentially regulated genes were analysed for interaction networks in the STRING database (Szklarczyk et al. 2017) with the STRING tool version 10.5 (<https://string-db.org/>). All networks were created with high confidence interaction score of 0.9 except the network of downregulated genes in *mvq1* vs. WT (H₂O) for which the score was 0.7 due to relatively low number of genes in the list (21).

Gene ontology (GO) analysis was performed with the online tool provided by the GO consortium (<http://www.geneontology.org/>) that uses the PANTHER database (Mi et al. 2017) version 13.1. Enrichment of GO terms was tested by Fisher's exact test using Bonferroni correction for multiple testing.

Analysis and visualisation of overlaps in gene lists was conducted using Venny version 2.1 (<http://bioinfogp.cnb.csic.es/tools/venny/>) by Juan Carlos Olivero (Spanish National Center for Biotechnology, Madrid)

Pscan (Zambelli, Pesole, and Pavesi 2009) version 1.5 (<http://159.149.160.88/pscan/>) was employed as a tool for identification of enriched transcription factor (TF) binding sites from the JASPAR 2018_NR database (Khan et al. 2018) analysing the -500 bp region of genes in a given list.

2.2.15 Expression of recombinant proteins in *Escherichia coli*

For subsequent protein purification MVQ1 and MVQ1^{DL} were expressed via pDestN110 in KRX cells according to Promega guidelines. After induction with 0.1 % rhamnose bacterial cultures were grown for 20 h at 18°C, 120 rpm. WRKY33 was expressed as a His-tagged NusA-fusion with the pMCSG48 vector in BL21 DE3 magic cells (construct and cells provided by Michal Sikorski, Institute of Bioorganic Chemistry, Poznan, Poland). Bacteria were grown in selective LB at 37°C, 120 rpm until an OD₆₀₀

between 0.4 and 0.6 was reached. After induction with 0.5 mM IPTG cells were grown at 18°C, 120 rpm for 20 h. For preparation of crude protein extracts used in DPI-ELISA, MVQ1-6, MVQ8 and respective MVQ^{DL} mutants were expressed via pET-Dest42 in BL21 DE RIL cells according to the protocol by (Brand et al. 2010). Bacteria were lysed on ice using a SONOPULS homogenizer (Bandelin) with a VS70T or MS73 probe sonicating for six cycles consisting of 15 s pulse and 15 s pause each at 60 % output. The lysed cells were spun down at 2200 g for 20 min at 4°C and the crude protein extract (supernatant) was measured in a Bradford assay (BioRad). Subsequently 0.2 % biotin free BSA and 1mM DTT was added before aliquots were stored at -20°C. Due to precipitation protein extracts had to be used within three days for downstream applications. DNA-binding domains (DBDs) of WRKY11, WRKY33 (N- and C-terminal) and WRKY50 were expressed via pET-Dest42m2 in the same way.

2.2.16 Protein purification

Bacteria were spun down at 5000 g, 4°C for 20 min and the pellet was dissolved in lysis buffer (0.1 M Na₂HPO₄/NH₂PO₄ buffer system, pH 8.0; 0.3 M NaCl; 10 mM imidazole). Protease inhibitor HP-mix (Serva) was added in 1:100 dilution. Cells were lysed with Lysozyme (Applichem) in 1 mg/ml concentration for 30 min on ice and subsequently treated with sonication (as described for crude protein extracts in 2.2.13). TritonX (1 %) was added to the lysate but DNase treatment was omitted due to presence of DNA probes in downstream applications. After centrifugation at 20 000 g, 4°C for 40 min. The supernatant was mixed with nickel affinity agarose beads Ni-NTA (Qiagen) according to manufacturer's instructions and rotated at 4°C for 1 h. Beads were spun down at 1000 g, 4°C for 1 min and washed with wash buffer I (= lysis buffer with 40 mM imidazole), followed by washing with wash buffer II (= wash buffer I with 0.5 M NaCl) and another washing step with wash buffer I. Proteins were eluted with elution buffer (= lysis buffer with 0.5 M imidazole). Purified proteins were dialysed at 4°C over night using SnakeSkin dialysis tubes (Thermo) in 20 mM Tris/HCl, pH 7.5 buffer.

2.2.17 SDS-PAGE and immunoblot analysis

Protein samples were mixed with 4x loading buffer (125 mM Tris/HCl pH 6.8; 4 % SDS; 20 % glycerol; 5 % mercaptoethanol; 0.01 % bromophenol blue), incubated for 5 min at 95°C and separated via SDS-PAGE using discontinuous gel-electrophoresis with 10-12 % separation gels (10 % Acrylamide-bis; 0.375 M Tris/HCl pH 8,8; 0,1 % SDS; 0,2 % TEMED; 0,04 % APS), 5% stacking gels (5 % Acrylamide-bis; 0.125 M Tris/HCl pH 6,8; 0,1 % SDS; 0,2 % TEMED; 0,04 % APS) and 1x running buffer (25 mM Tris; 192 mM glycine; 0,1% SDS). Subsequently, the proteins were transferred semi-dry onto nitrocellulose membranes (Parablot NCL, Macherey-Nagel) in transfer buffer (20 % MeOH; 25 mM Tris; 15 mM

glycine; 1 % SDS) for 60 min with 0.8 mA per cm² of membrane. Membranes were then blocked in 5 % blocking solution (5 % milk powder in TBS-T (50 mM Tris/HCl pH 7.6; 150 mM NaCl; 0.1 % tween 20)) for 1 h at RT. Membranes were incubated with the antibodies (Tab. 2) in 3 % blocking solution either over night at 4°C or for 1h at room temperature (RT). For detection of signals the ECL Prime Kit (Amersham) was used according to manufacturer's instructions.

Tab. 2 List of antibodies used in this work

Antibody	anti-HA	anti-c-Myc	anti-His	anti-GFP	anti-V5	anti-mouse-HRP
Concentration	1:1000	1:1000	1:3000	1:5000	1:7500	1:10 000
Supplier	Eurogentec	Sigma-Aldrich	Sigma-Aldrich	Takara Clontech	Thermo	Sigma-Aldrich
Organism	mouse	mouse	mouse	mouse	mouse	rabbit

2.2.18 Electrophoretic mobility shift assay (EMSA)

DNA probes were generated by mixing of complementary oligonucleotide pairs listed in Tab. S6 in annealing buffer (10 mM Tris, pH 7.5; 50 mM NaCl, 1 mM EDTA). After incubation at 95°C for 5 min the oligonucleotides were annealed by cooling down at RT for 1 h. 0.5 pmol of the Cy5-labelled probe were mixed with Ficoll (4 % final conc.) and incubated with purified protein in 0.25 mM NaCl for 15 min at RT. To reduce unspecific interactions 0.2 µg of poly-deoxy-inosinic-deoxy-cytidylic acid (poly-dIdC) (Sigma-Aldrich) were added. For competition unlabelled probe was pre-incubated for 10 min with the protein before incubation with labelled probe.

Acrylamide gels (8 %) in TAE buffer (40 mM Tris; 20 mM acetic acid; 1 mM EDTA) were pre-run at 150 V for 30 min at 4°C. After loading of samples, gels were run at 100 V, 4°C until bromophenol blue that had been pre-run for 5 min reached the end of the gel. Cy5 signals were imaged with a Typhoon FLA9500 (GE Healthcare) using a laser of 635 nm wavelength and quantified with ImageQuant software (GE Healthcare)

2.2.19 DNA-protein interaction assay (DPI-ELISA)

The DPI-ELISA was performed following the protocol from Brand et al. (2010), but DNA-bound proteins were detected via GFP fluorescence instead of enzyme-linked antibodies. Biotin-labelled DNA-probes were generated with the oligonucleotides listed in Tab. S7 and immobilised to streptavidin-coated 384 well plates (Greiner). Dilutions (1:10) of protein extracts containing GFP-tagged WRKY DBDs or GFP expressed from cells carrying the empty vector were pre-incubated with undiluted crude extracts containing His-tagged MVQs or empty vector control in a 1:1 fashion for 20 min at RT. Subsequently the mixture was incubated with the probes on the plate for 1 h at RT. After washing with TBS (50 mM

Tris/HCl pH 7.6; 150 mM NaCl) the GFP signal was read out with a Varioscan Flash (Thermo) using excitation wavelength of 485 nm and emission of 510 nm. When crude protein extracts containing different WRKY-DBD-GFP fusions were compared, GFP fluorescence of the extracts was utilised as a proxy for “protein concentration”. Concentrations of extracts were adjusted according to fluorescence of the extract with the weakest signal by dilution.

2.2.20 Chromatin Immunoprecipitation followed by sequencing (ChIP-seq)

ChIP-seq experiments were conducted by Dr. Rainer Birkenbihl (Somssich lab, MPIZ Cologne). Seedlings of WT (Col-0) and MVQ1 OE (K11) were grown in sterile conditions (see 2.1.4) in a light chamber at 22°C under long-day conditions (16 h light/8 h dark) for 12 days. Subsequently seedlings were treated with flg22 by replacing the growth medium with medium containing 1 mM flg22 or medium without flg22 as a control. ChIP was performed with anti c-Myc antibody M4439 (Sigma Aldrich) applying a protocol by (Gendrel et al. 2005) with modifications as described in (Birkenbihl, Diezel, and Somssich 2012). To prepare the ChIP-seq libraries the DNA was first amplified by two rounds of linear DNA amplification (Shankaranarayanan et al. 2011). Libraries were constructed with the DNA Smart ChIP-seq kit (Clontech Laboratories) and sequenced at the Max Planck Genome Centre in Cologne with a HiSeq2500 system (Illumina).

ChIP-seq data was processed and analysed by Dr. Barbara Kracher (MPIZ Cologne) as described in (Liu et al. 2015). For identification of genomic DNA regions enriched in sequencing reads in the ChIP sample compared to input control as well as in inoculated compared to mock treated samples, the peak calling algorithm of the QuEST program version 2.4 (Valouev et al. 2008) was used. To search for conserved binding motifs in the MVQ1 binding regions, for each peak the 500-bp sequence surrounding the peak maximum was extracted and submitted to the online version of MEME-ChIP for CentriMo search (Bailey and Machanick 2012). Number and percentage of peak regions containing a certain motif were extracted with the online version of FIMO (Grant, Bailey, and Noble 2011) with a p value threshold of 0.001. ChIP-seq data were visualised with the Integrative genomic viewer (IGV) browser (Thorvaldsdottir, Robinson, and Mesirov 2013).

To identify all locations of the W-box motif (TTGACT/C) in the complete Arabidopsis genome, the R function “matchPattern” was used (Pagès, 2016; <https://bioconductor.org/packages/release/bioc/>).

2.2.21 Infection of *Arabidopsis thaliana* with *Botrytis cinerea*

Permanent cultures of the *B. cinerea* strain B05.10 were provided by Dr. Lennart Eschen-Lippold (Lee lab, IPB Halle) and transferred to a sterile pot containing half a peach (canned peaches from PENNY

supermarket). The fungus was grown for 5 days at 22°C under UV-light to trigger sporulation. The sporulating mycelium was removed from the peach with a forceps, transferred into 20 ml B5-Glcmedium (3.16 g/l solid Gamborg B5 medium with vitamins (Duchefa), 2 % glucose) and mixed by vortexing.

After filtering of the spore solution through a 20 µm nylon net (Merck Millipor) spores were counted and adjusted to 2×10^5 spores/ml. Germination of spores was initiated by adding 1 M potassium phosphate buffer, pH 6.4 to a final concentration of 10 mM and spores were kept for 1 h at RT for germination. Fully expanded leaves of six week old *A. thaliana* plants were inoculated with 10 µl droplets of the spore solution and plant trays were sealed with parafilm to ensure high humidity. The infected leaves were harvested 3- and 4-days post infection (dpi) to document symptoms. For determination of fungal biomass leaves were harvested 2 and 3 dpi and leaf discs (d = 8 mm) were punched out at the inoculation sites. Four leaf discs from the same plant were pooled in one sample and DNA was extracted with a genomic DNA isolation kit (Sigma-Aldrich) according to supplier's protocol. During extraction, plant DNA was spiked with plasmid DNA (pCR2.1 containing the potato *StNOX* gene) as reference. The extracted DNA was diluted (1:10) and subjected to qRT-PCR analysis (see 2.2.7) using primers listed in Tab. S4. Amount of fungal *BcCutA* was referenced to the amount of plasmid DNA (*StNOX*) via a standard curve of diluted pCR2.1-*StNOX*.

3. Results

3.1 Subcellular localisation of MVQs

Almost all MVQs interact with WRKY transcription factors in a Y2H screen (Pecher et al. 2014). Occurrence of MVQ-WRKY interactions *in planta* would require at least partially overlapping localisation patterns between MVQs and nuclear WRKYs. Indeed MVQ9 (IKU1) and MVQ10 (VQ9), the only MVQs analysed with respect to their localisation so far, are nuclear proteins (Wang et al. 2010; Hu, Chen, et al. 2013). For all other MVQs there is only predicted localisation data from the Subcellular Proteomic Database (<http://suba.plantenergy.uwa.edu.au>) available, as listed in (Cheng et al. 2012). According to these predictions MVQ1-2 are targeted to mitochondria and the nucleus, while MVQ3-6 localise to plastids and the nucleus and MVQ7-10 are exclusively located in the nucleus. One aim of this work was to analyse subcellular localisation patterns of all MVQs and to validate these *in silico* predictions experimentally.

3.1.1 MVQs display two distinct subcellular localisation patterns

To investigate subcellular localisation of MVQs, genes of all ten members were cloned to express GFP-MVQ fusion proteins under the control of the moderate *UBIQUITIN10* promoter using the pUBN-GFP vector (Grefen et al. 2010). In case of MVQ3, for which cleavage of N-terminal tags was previously shown (Pecher, unpublished data), a C-terminal GFP-fusion was used (pUBC-GFP). *A. thaliana* mesophyll protoplasts were transfected with plasmids expressing GFP-tagged MVQ1-10 and analysed 16 hours later by confocal laser scanning microscopy.

The conserved VQ-residues are essential for MVQ-WRKY interactions (Pecher et al. 2014) and might influence the subcellular localisation of MVQs. Therefore MVQ-variants, in which VQ residues have been exchanged for DL, were included in the analysis.

The ten MVQs displayed two distinct subcellular localisation patterns. GFP-tagged MVQ1-6 were located in the cytoplasm and the nucleus (Fig. 4 A-F). Within the nucleus the GFP signal was evenly distributed with lower signals in the nucleolus. In contrast, GFP-fusions of MVQ7-10 localised to the nucleus exclusively (Fig. 4 G-J) and the GFP signal was concentrated in small punctate structures (see enlarged image segments in Fig. S1).

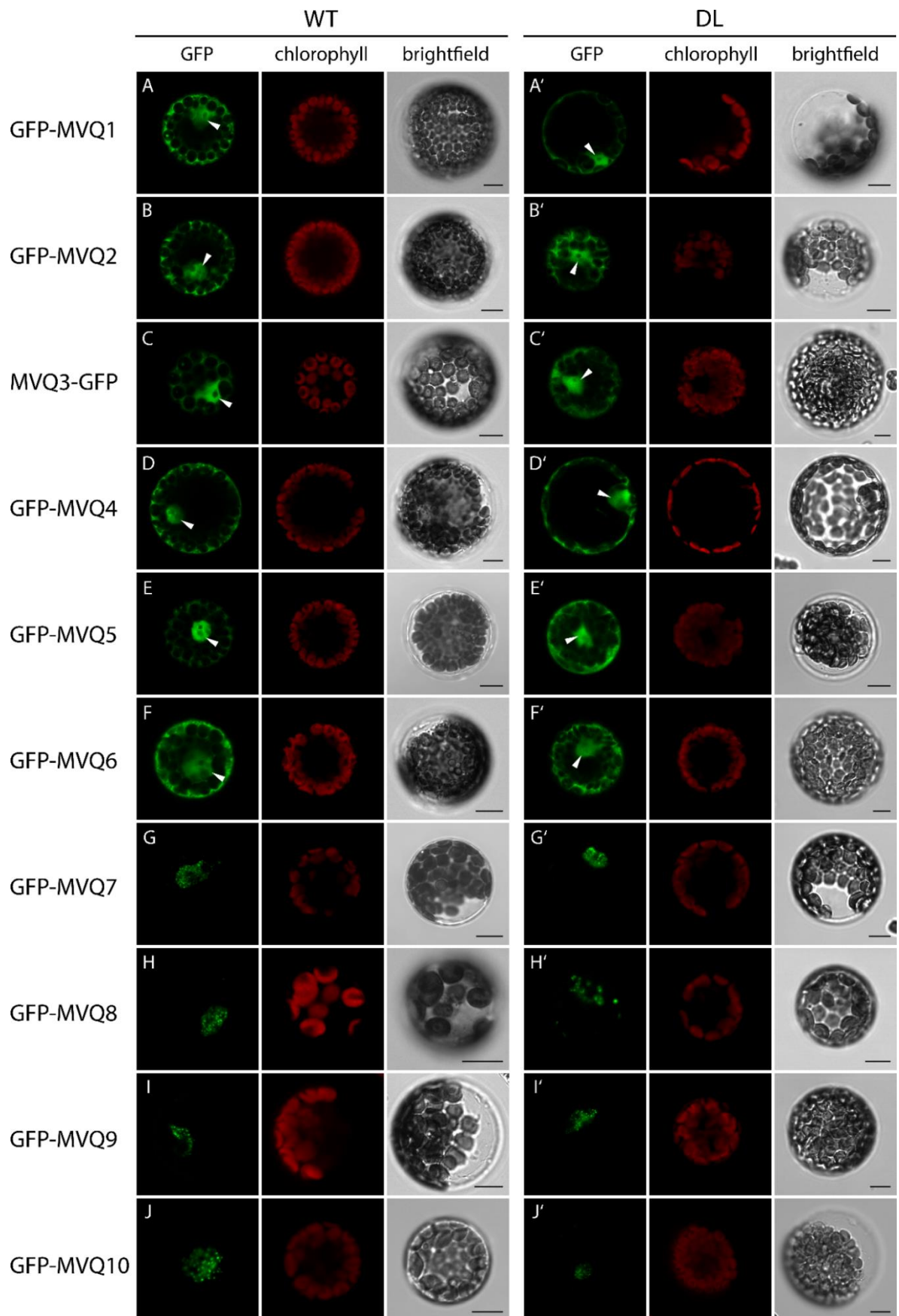


Fig.4 For legend see next page.

Fig. 4 Subcellular localisation of MVQ1-10 and respective VQ-mutants in *A. thaliana* protoplasts: Protoplasts were transfected with plasmids expressing GFP-tagged MVQ1-10 (**A-J**) and respective MVQ^{DL} variants (**A'-J'**) and analysed by confocal laser microscopy 16 h after transfection. GFP-fluorescence (1st panel), chlorophyll fluorescence (2nd panel) and brightfield images (3rd panel) were recorded in different channels. Scale bars represent 10 μ m. White triangles indicate the nuclear proportion of GFP signal in (**A-F**) and (**A'-F'**). Images are representative of three independent experiments with similar results.

The nature of these punctate structures is currently unknown but they resemble the dynamic light-regulated nuclear foci described by Kaiserli et al. (2015), which are speculated to be sites of transcriptional activity. Interestingly, WRKY18 and WRKY40 have been reported to be in similar nuclear bodies (Geilen and Bohmer 2015).

Mutation of the strictly conserved VQ residues to DL did not seem to affect localisation of any GFP-tagged MVQ ((Fig. 4 A'-F'), suggesting that the interaction with WRKYs might not be required for nuclear localisation of MVQs. There was no overlap between chlorophyll fluorescence (as a marker for chloroplasts) and GFP signals of any of the MVQs, thus refuting SUBA-predictions for plastid localisation of MVQ3-6.

Furthermore speckle-like signals throughout the protoplast would be expected in case of mitochondrial localisation for MVQ1 & 2 as predicted by SUBA. Since the GFP-signal was quite evenly distributed in the cytoplasm in both cases, mitochondrial localisation seems rather unlikely. However co-localisation of MVQ1 & 2 with a mitochondria-staining dye (mitotracker) or other markers would be required to exclude this possibility.

Western blot analysis confirmed, that the protoplasts expressed the full-length GFP-MVQ fusions and no free GFP was detected (Fig. 5). MVQ4- and MVQ6-GFP-fusions show additional bands running higher than the expected size (56 kDa instead of 52 kDa and 54 kDa instead of 48 kDa respectively). This might be explained by phosphorylation, which was reported before for these proteins (Pecher et al. 2014).

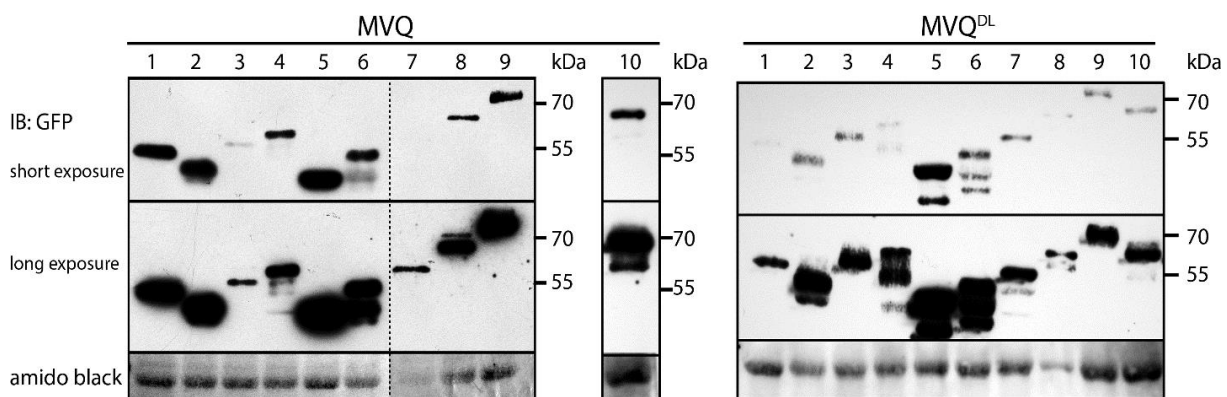


Fig. 5 Expression of GFP-tagged MVQs in *A. thaliana* protoplasts: Protein extracts from protoplasts were subjected to SDS-PAGE and Western blot analysis using anti-GFP antibody. Two different exposure times are shown. Amido black staining of the RuBisCO large subunit served as a measure of loading. The dotted line indicates that the image was spliced from the same blot.

To provide further evidence, that the observed punctate structures in Fig. 4 G-J/G'-J' are located inside the nucleus, protoplasts were co-transfected with plasmids expressing GFP-fusions of MVQ1 and MVQ8-10 and an ERF104-CFP fusion that served as a nuclear marker. MVQ1 and ERF104 showed overlapping localisation in the nucleus with additional GFP-MVQ1 signals in the cytoplasm (Fig. 6 A). Localisation of GFP-tagged MVQ8-10 overlapped with that of ERF104-CFP (Fig. 6 B-D) thus confirming exclusively nuclear localisation of these GFP-MVQ fusions. ERF104-CFP was generally rather uniformly distributed within the nucleus (with only occasional concentrations e.g. Fig. 6 B).

In contrast GFP-fusions of MVQ8-10 displayed the punctate localisation pattern that was already observed in Fig. 4 G-J.

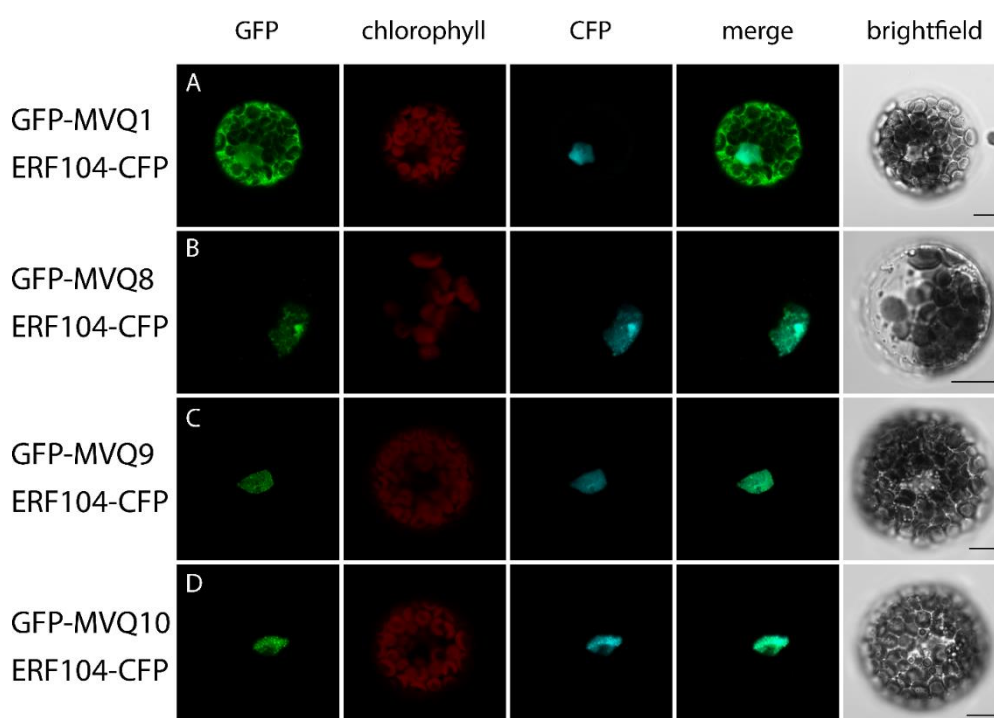


Fig. 6 Co-localisation of MVQs with nuclear marker ERF104: Protoplasts were co-transfected with plasmids expressing ERF104-CFP and GFP-tagged MVQ1 (A), MVQ8 (B), MVQ9 (C) or MVQ10 (D). GFP-fluorescence (1st panel), chlorophyll fluorescence (2nd panel), CFP-fluorescence (3rd panel) and brightfield image (5th panel) were recorded in different channels 16 h after transfection. 4th panel shows overlay of GFP- and CFP fluorescence. Scale bars represent 10 μ m. Images represent three independent experiments with similar results.

3.1.2 Mutation of phosphorylation sites affects localisation of some MVQs

MVQs are phosphorylated by the MAPKs MPK3 and MPK6 and for MVQ1-6 phosphosites have been mapped by mass spectrometry (Pecher et al. 2014). Phosphorylation was reported to negatively affect the stability of some MVQs. To investigate whether phosphorylation might also alter subcellular localisation, GFP-tagged phosphosite-mutants of MVQ1-6 (Pmut) were analysed in transfected protoplasts. In case of MVQ1, it was demonstrated that mutation of those phosphorylation sites, which

had previously been detected by mass spectrometry, is not sufficient to prevent *in vivo* phosphorylation of MVQ1 in response to flg22. Only when all 12 potential SP and TP phosphorylation sites in MVQ1 are mutated to alanine-proline (AP), phosphorylation was abolished (Pecher et al. 2014). Accordingly, all potential SP and TP phosphorylation sites were mutated to AP in MVQ2-6 phosphosite-mutants (see Fig. S2 for overview of potential phosphosites in MVQ1-6).

MVQ1-6 were located in the cytoplasm and nucleus (Fig. 7 A-F). The respective phosphosite-mutants of MVQ1, MVQ2 and MVQ6 showed the same localisation pattern (Fig. 7 A',B',F'), while phosphosite-mutants of MVQ3-5 were exclusively found in the nucleus (Fig. 7 C'-E'). In case of GFP-tagged MVQ5^{Pmut}, GFP signals were concentrated in small nuclear foci resembling those of MVQ7-10.

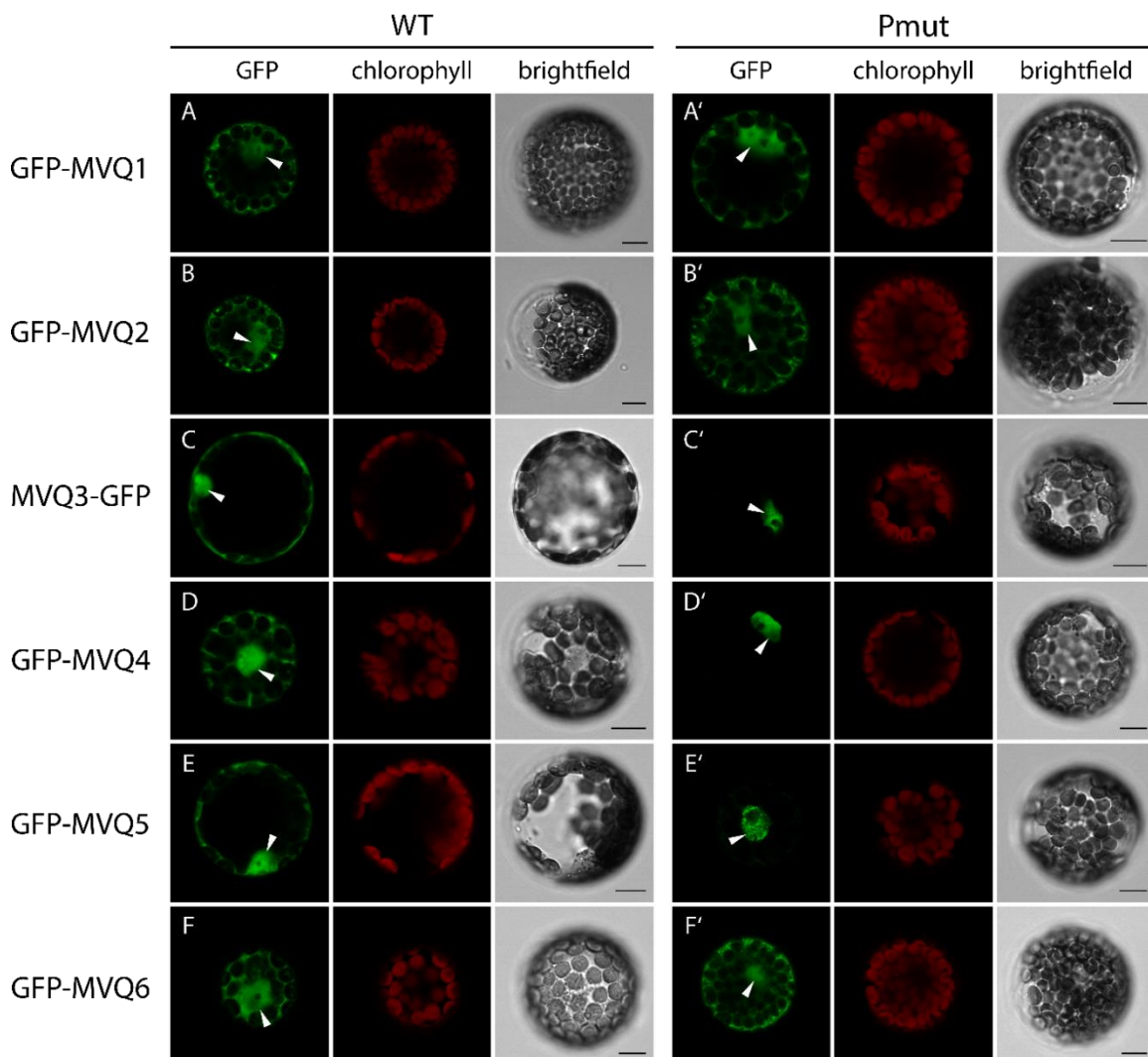


Fig. 7 Subcellular localisation of MVQ1-6 and respective phosphosite-mutants (Pmut) in *A. thaliana* protoplasts: Protoplasts were transfected with plasmids encoding GFP-tagged MVQ1-6 (A-F) and respective Pmut variants (A'-F') and analysed by confocal laser microscopy 16 h later. GFP-fluorescence (1st panel), chlorophyll fluorescence (2nd panel) and brightfield images (3rd panel) were recorded in different channels. Scale bars represent 10 μ m. White triangles indicate the nuclear proportion of GFP signal in (A-F) and (A'-F'). Images are representative of three independent experiments with similar results.

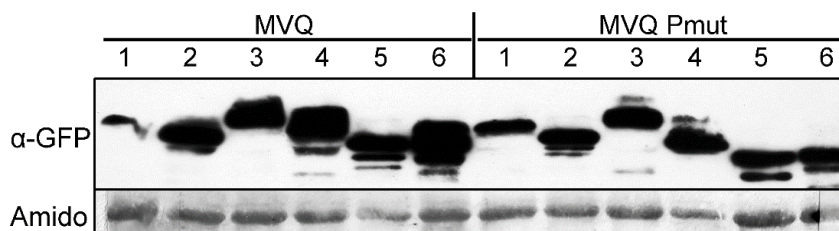


Fig. 8 Expression of GFP-tagged MVQ1-6 and respective phosphosite-mutants (Pmut) in *A. thaliana* protoplasts: Protein extracts from protoplasts expressing GFP-tagged MVQ1-6 or respective MVQ Pmut variants were subjected to SDS-PAGE and Immunoblot analysis using anti-GFP antibody. Amido black staining served as a measure of loading.

These results suggest, that MVQ3-5 might undergo subcellular re-localisation upon phosphorylation from nucleus to cytoplasm, which is inhibited in the phosphosite-mutant. However, it cannot be excluded that mutation of all phosphosites (12 sites in MVQ3, 14 sites in MVQ4 and 5 sites in MVQ5 (Fig. S2)) might impair correct folding of MVQs and result in mislocalisation. Expression analysis confirms, that protoplasts expressed the GFP-tagged MVQs (Fig. 8)

3.2 Effects of MVQ1 and other MVQs on defence gene promoter activity

All MVQs are present in the nucleus (section 3.1), targeted by MAMP-activated MAPKs and most of them interact with WRKY TFs (Pecher et al. 2014). These findings suggest a potential role of MVQs in the regulation of defence gene expression. To investigate this hypothesis, a luciferase-based reporter assay was employed to measure activities of defence gene promoters after MAMP-treatment.

To this end, *A. thaliana* protoplasts were co-transfected with three plasmids: the first plasmid is the reporter construct encoding *Luciferase* driven by promoters of MAMP-responsive genes, while a second “effector” plasmid is constitutively expressing MVQs (or CFP as a control) with an HA-tag. The third plasmid *pUBQ10-β-GLUCURONIDASE (GUS)* served as a transfection normalisation reference.

3.2.1 MVQ1 dampens MAMP-induced activation of *pNHL10* via its VQ-motif

NHL10 is a marker gene for early defence responses and its induction via the MAPK pathway has previously been demonstrated (Boudsocq et al. 2010). When the *pNHL10-LUC* reporter construct was expressed in protoplasts, the activity of the *NHL10* promoter did not change after treatment with water (Fig. 9 A). Furthermore, promoter activity was similar in protoplasts expressing MVQ1 and those expressing CFP as a control. After treatment of protoplasts with flg22 (100 nM) a transient rise in *NHL10* promoter activity was observed with a peak of more than 2-fold induction around 60 min after

treatment (Fig. 9 B). When MVQ1 is overexpressed, *NHL10* promoter activity still flg22-inducible but from 30 min onwards the activity was significantly lower in comparison to the CFP control and the peak of activity at 60 min could not be detected.

Treatment with another bacterial MAMP (100 nM elf18) also resulted in induction of the *NHL10* promoter but the activity was slightly higher (up to 2.7-fold) and reached a plateau instead of a peak when compared with flg22-treatment (Fig. 9 C). In the case of elf18 treatment, MVQ1 expression resulted in significantly lower promoter activity already from 5 min onwards.

Expression of MVQ1 (or CFP) in protoplasts was confirmed by western blot analysis (Fig. 9 D, where the additional bands for MVQ1 might indicate phosphorylation of MVQ1 during handling of the protoplasts).

These results confirmed previous experiments (Pecher et al. 2014), showing that MVQ1 seems to be able to suppress MAMP-induced activation of a defence gene promoter.

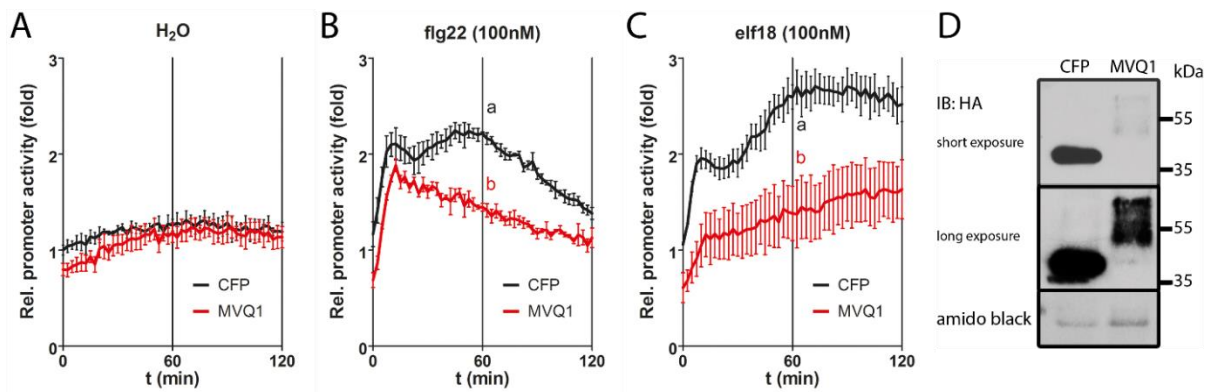


Fig. 9 Effect of MVQ1 on the promoter activity of defence marker gene *NHL10*: *A.* *thaliana* protoplasts were transfected with the *pNHL10-LUC* reporter construct and *p35S-MVQ1* or *p35S-CFP* as control and incubated for 16 h. Luciferase activity was measured after treatment with water (**A**), or the MAMPs flg22 (**B**) and elf18 (**C**), normalised to an expression reference (*pUBQ10-GUS*) and is depicted as mean fold-change ($n=3$) compared to water-treated CFP-transfected control ($t=0$). Error bars indicate standard errors. Statistically different groups at $t=60$ (two-way ANOVA with Bonferroni multiple comparison post-test $p<0.05$) are denoted by letters. (**D**) Protein extracts from protoplasts were subjected to SDS-PAGE and Immunoblot analysis using anti-HA antibody. Amido black staining serves as a measure of loading.

However, while repeating this assay we noticed that the effect of MVQ1 on the induction of *pNHL10-LUC* can be quite variable between experiments (Tab. 3). This variation could be in part due to the differential protoplast handling or the non-sterile conditions used. For an unbiased view, all independent experiments are shown and the average effect plotted as the difference in promoter activity (i.e. mean promoter activity values in the control were subtracted from those in protoplasts overexpressing the tested MVQs). Hence negative values indicate a suppression effect, while positive values show enhancement of promoter activity.

Fig. 10 A summarises 25 independent experiments in which the effect of MVQ1 on activity of *pNHL10* after treatment was determined. Each grey curve represents the difference in *pNHL10* activity after

MVQ1 overexpression in the individual experiments and the average difference is plotted as a coloured curve. MVQ1 displayed, on average, a slight reduction of *pNHL10* activity at the activation peak 60 min after flg22-treatment (Fig. 10 A red curve). In 12 of 25 experiments MVQ1 overexpression led to significantly lower promoter activity at this time point, while in 2 experiments a significant stimulation was observed (Tab. 3). In the remaining 11 experiments, no significant difference to the CFP control was observed. These findings indicated that the suppressive effect of MVQ1 on the flg22-induced activation of *pNHL10* in protoplasts is rather variable.

Besides effects from protoplast handling, variability of the MVQ1 effect might be explained by phosphorylation and subsequent degradation of MVQ1 as demonstrated in (Pecher et al. 2014). Indeed, western blot analysis showed additional bands running higher than the expected size for MVQ1, which are absent in the MVQ1 phosphosite-mutant MVQ1^{Pmut} (Fig. 11) and hence indicative for phosphorylation. We postulate, that MVQ1^{Pmut} might be more stable and thus suppresses *pNHL10* activation more robustly. In fact, the suppression of *pNHL10* activity by MVQ1^{Pmut} is generally more pronounced compared with the native MVQ1. However, overexpression of MVQ1^{Pmut} did not have statically significant effects on *pNHL10* activity in 7 out of 13 experiments (Tab. 3) suggesting that phosphorylation is not the only source of variability.

Induction of *pNHL10* by MAMPs is probably mediated by WRKYs since it depends on the presence of two W-boxes (Pecher et al. 2014). Thus, suppression of *pNHL10* induction by MVQ1 might depend on its ability to interact with WRKYs via the VQ-motif. To test this hypothesis, the DL mutant of MVQ1 was included in the assay. Interestingly MVQ1^{DL} led to substantially enhanced activity of *pNHL10* in 11 out of 18 experiments (Fig. 10 B, Tab. 3) suggesting that MVQ-WRKY-interaction might indeed be necessary for the suppressive effect of MVQ1.

3.2.2 MVQs differentially modulate MAMP-induced activation of *pNHL10*

Potential influence of the other nine MVQs on defence gene expression was investigated by means of the protoplast transient expression assay described above. Most of the MVQs were able to modulate flg22-mediated *pNHL10* induction, (Fig. 10). An exception is MVQ2, which generally did not alter *pNHL10* activity when compared to CFP control (Fig. 10 D). But the results in this case varied substantially between the six independent experiments (Tab. 3), so that interpretation of these results is difficult.

On the whole, MVQ3, 4, 6, 7 slightly suppressed the induction of *pNHL10* to a similar extent as MVQ1 (Fig. 10 E, F, H, I).

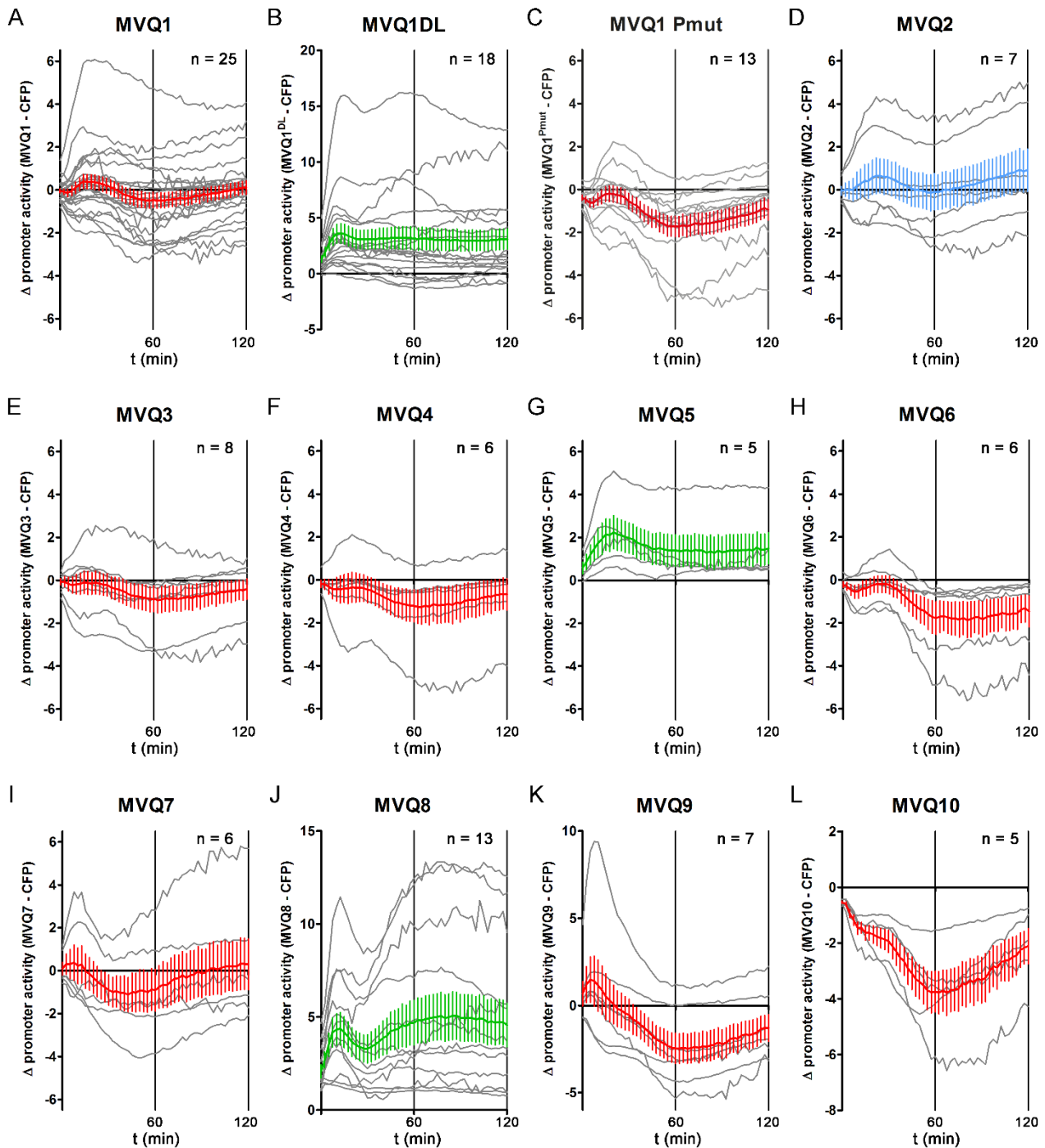


Fig. 10 Effect of MVQs on promoter activity of defence marker gene *NHL10*: *A. thaliana* protoplasts were transfected with the *pNHL10-LUC* reporter and *p35S-MVQs* or *p35S-CFP* as control. 16 h later, Luciferase activity was measured after treatment with 100 nM flg22 and normalised to an expression reference (*pUBQ10-GUS*). Δ promoter activity is the difference of luciferase activity in presence of MVQs subtracted by the luciferase activity in the CFP control. Values from individual experiments are plotted as grey curves. Coloured curves represent mean values of all experiments for each MVQ with error bars indicating standard errors. red = suppression, green = stimulation, blue = no effect. Note differences in scale of y-axis for B, J, K and L.

Suppression in these cases seemed to be more robust in comparison to MVQ1, since statistically significant lower promoter activity at 60 min was observed in the majority of experiments (Tab. 3). By comparison, *pNHL10* induction was strongly and robustly suppressed by overexpression of MVQ9 and MVQ10 (Fig. 10 K, L). In contrast to the other MVQs, overexpression of MVQ5 and MVQ8 stimulated *pNHL10* activity. In both cases, but particularly for MVQ8, this included a boost in the basal *pNHL10* activity prior to MAMP treatment. Apparently, members of the MVQ subfamily are able to negatively or positively modulate promoter activation of the early defence marker gene *NHL10* upon MAMP-treatment with different strength.

Tab. 3 Summary of MVQ effects on flg22-induced promoter activity of *NHL10*: Listed are numbers of experiments with different effects on activity of *pNHL10* 60 min after flg22-treatment. Effects are defined as statistically different in comparison to CFP control at t=60 (two-way ANOVA with Bonferroni multiple comparison post-test $p < 0.05$). Numbers in brackets indicate total number of experiments n.

effect on <i>pNHL10</i>	MVQ1	MVQ1 ^{DL}	MVQ1 ^{Pmut}	MVQ2	MVQ3	MVQ4
stimulation	2 (25)	11 (18)	- (13)	2 (7)	- (8)	- (6)
suppression	12 (25)	1 (18)	6 (13)	3 (7)	5 (8)	5 (6)
no effect	11 (25)	6 (18)	7 (13)	2 (7)	3 (8)	1 (6)

	MVQ5	MVQ6	MVQ7	MVQ8	MVQ9	MVQ10
	3 (5)	- (6)	1 (6)	12 (13)	- (7)	- (5)
	- (5)	5 (6)	3 (6)	- (13)	5 (7)	5 (5)
	2 (5)	1 (6)	2 (6)	1 (13)	2 (7)	- (5)

For all the experiments, MVQ expression was verified by western blot analysis (Fig. 11). For MVQ1-4, additional shifted bands were observed, indicative for phosphorylation of those proteins as described in (Pecher et al. 2014).

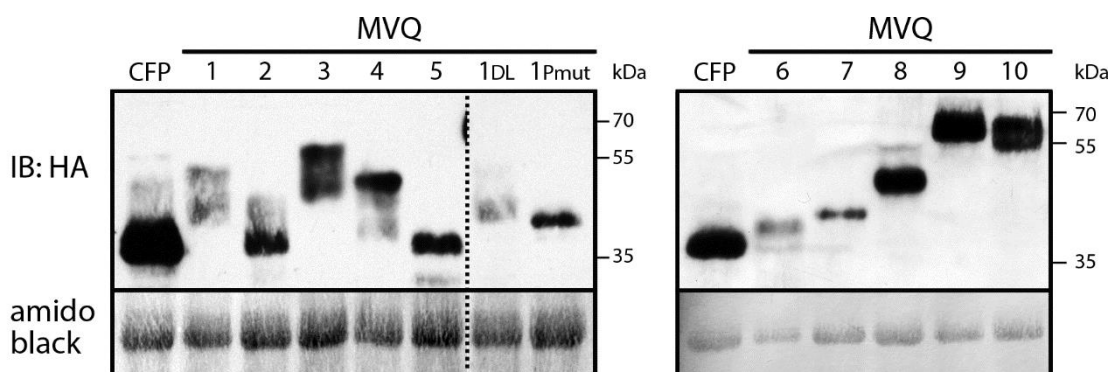


Fig. 11 Expression of HA-tagged MVQs in *A. thaliana* protoplasts: Protein extracts of protoplasts expressing HA-tagged MVQ1-10, MVQ1^{DL}, MVQ1^{Pmut} or CFP were subjected to SDS-PAGE and Immunoblot analysis using anti-HA antibody. Amido black staining of RuBisCO large subunit serves as a measure of loading. The dotted line indicates that the image was spliced from the same blot.

3.2.3 MVQ1 suppresses MAMP-induced activation of additional defence-related genes

In order to investigate, if MVQ1 is able to antagonise MAMP-mediated induction of defence-related genes in general, we extended the analysis to promoters of additional flg22-responsive genes other than *NHL10*.

WRKY33 is up-regulated upon treatment of *A. thaliana* seedlings or cell cultures with flg22 (Navarro et al. 2004) and its promoter contains seven W-boxes, three of which are critical for MAMP-responsiveness (Lippok et al. 2007). Activity of p*WRKY33* was transiently induced by flg22 in the protoplast assay with a peak activity between 50 and 60 min after elicitation (Fig. 12 A). Upon overexpression of MVQ1, the activity of p*WRKY33* was significantly lower compared to CFP control in two out of three experiments, while there was no significant difference in one experiment.

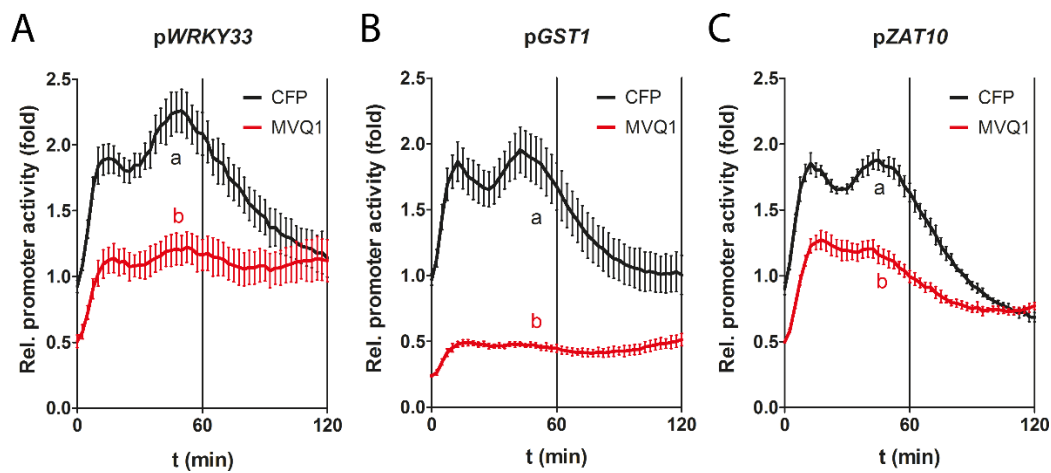


Fig. 12 Effect of MVQ1 on flg22-triggered activation of defence gene promoters: *A. thaliana* protoplasts were transfected with plasmids encoding a luciferase reporter under control of (A) p*WRKY33*, (B) p*GST1* and (C) p*ZAT10* and p*35S-MVQ1* or p*35S-CFP* as control. Luciferase activity was measured after treatment with flg22 (100 nM), normalised to an expression reference (p*UBQ10-GUS*) and is depicted as mean fold-change (n=3) compared to water-treated CFP-transfected control (t=0). Error bars indicate standard errors. Statistically different groups at peak of activity (two-way ANOVA with Bonferroni multiple comparison post-test p<0.05) are denoted by letters. Representative graphs of three independent experiments are shown.

GLUTATHIONE S-TRANSFERASE 1 (*GST1*) is a defence marker gene, for which activation by flg22 in the protoplast system has previously been demonstrated (Asai et al. 2002). Its promoter contains six W-boxes. p*GST1* responded to flg22 treatment similar to p*WRKY33* and p*NHL10*. In all three experiments expression of MVQ1 robustly led to significantly lower activity of p*GST1* in comparison to the control (Fig. 12 B).

SALT TOLERANCE ZINC FINGER (*STZ/ZAT10*) plays a role in responses to oxidative stress as well as salt and drought stress. Navarro et al. (2004) have identified *ZAT10* to be transcriptionally activated upon flg22-treatment. The promoter region of *ZAT10* contains 16 W-boxes and direct regulation by *WRKY43* has been demonstrated (Geilen et al. 2017). Activation of p*ZAT10* after flg22 elicitation was significantly reduced by MVQ1 overexpression (Fig. 12 C) in two out of three experiments, while in one

experiment MVQ1 stimulated activity of *pZAT10* compared to the CFP control. Expression of CFP control and MVQ1 was confirmed by Western Blot (Fig. 13).

The suppressive effect of MVQ1 could be observed in most experiments with all three promoters. Thus, MVQ1 might potentially be able to suppress MAMP-mediated transcriptional activation of a number of defence-related genes.

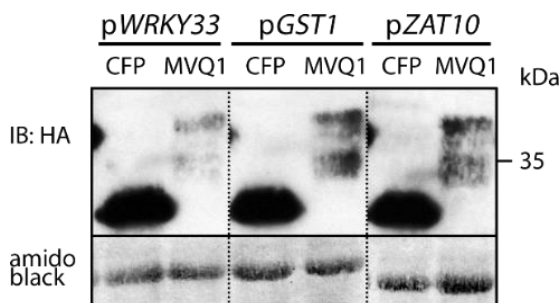


Fig. 13 Expression of MVQ1 and CFP in *A. thaliana* protoplasts: Protein samples from protoplasts expressing the respective promoter-reporter constructs and HA-tagged MVQ1 or CFP were subjected to SDS-PAGE and Immunoblot analysis using anti-HA antibody. Amido black staining of RuBisCO large subunit served as a measure of loading. The dotted line indicates that the image was spliced from the same blot.

3.2.4 MVQ1 antagonises WRKY-mediated activation of *pNHL10*

All four defence gene promoters, which were analysed in the reporter assays, contain several *W*-boxes and thus might be regulated by WRKYs. We hypothesise, that suppression of MAMP-induced activation of these promoters by MVQ1 requires binding of WRKYs because MVQ1^{DL} failed to suppress the *NHL10* promoter activity.

To take a closer look at the possible connection between MVQ1 and WRKY-mediated regulation we took advantage of a *NHL10* promoter fragment containing -198 bp upstream of the putative transcription start site (TSS). This fragment can be activated by MAMP treatment, although the amplitude of activation is lower, compared to the full promoter. Two *W*-boxes present in the fragment are essential for its activation since mutation of these sites renders the fragment unresponsive to MAMPs (Pecher et al. 2014). When transfected together with a CFP control, the *pNHL10*-198-fragment displayed a basal promoter activity, which is lower in protoplast transfected with the *W*-box mutated *pNHL10*-198 (Fig. 14 A, B black curves). Basal activity might be regulated by endogenous WRKYs in the protoplasts, which cannot contribute to promoter activity when the *W*-boxes are mutated. Overexpression of WRKY33 using the pUGW18 vector (Nakagawa et al. 2007) significantly enhanced *pNHL10*-198 activity (Fig. 14 A, green curve), while WRKY33-mediated activation of the promoter fragment was prohibited when a fragment with mutated *W*-boxes was used (Fig. 14 B), illustrating the requirement of these WRKY DNA-binding sites for activation of the promoter by WRKY33.

Expression of the phosphosite-mutant of MVQ1, which was used because it is more stable than the WT-version, did not affect basal *pNHL10-198* activity compared to the CFP control. But when WRKY33 was co-expressed with MVQ1^{Pmut}, the promoter activity of the fragment remained on the basal level suggesting that MVQ1^{Pmut} might be able to inhibit WRKY33-mediated activation of *pNHL10-198*. Since MVQ1 physically interacts with WRKY33 in a yeast two-hybrid screen (Pecher et al. 2014), it is tempting to speculate, that interaction between MVQ1^{Pmut} and WRKY33 might antagonize the ability of WRKY33 to enhance activity of the *pNHL10-198* fragment. WRKY33 protein level was comparable between the protoplasts expressing WRKY33 and CFP and those expressing WRKY33 and MVQ1^{Pmut} (Fig. 14 C) and thus unaffected by MVQ1^{Pmut}.

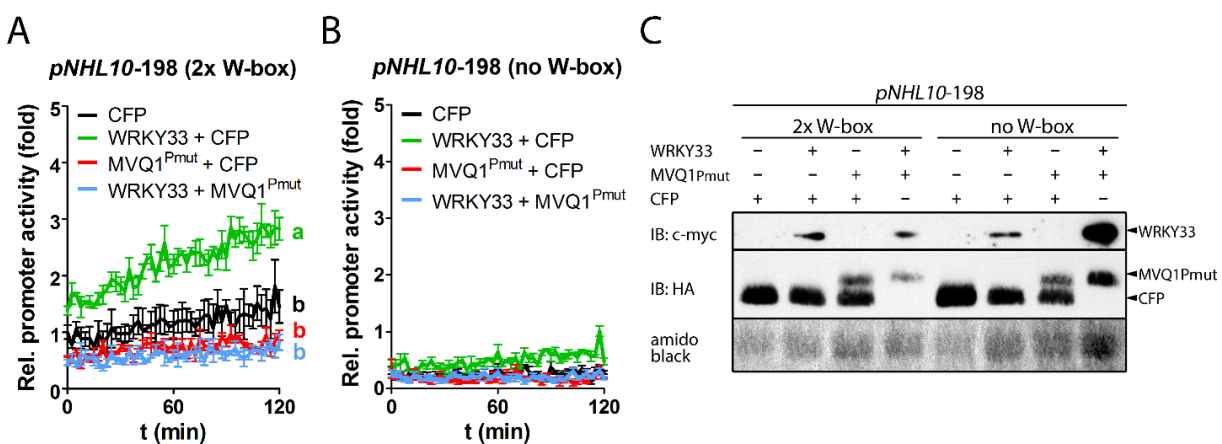


Fig. 14 Effect of WRKY33 and MVQ1^{Pmut} on activity of a -198 bp fragment of *pNHL10*: Protoplast were transfected with plasmids expressing luciferase under control of a -198 bp fragment of the *NHL10* promoter containing two W-boxes (A) or a version of the same *pNHL10* fragment with mutated W-boxes (B). Additionally, *p35S-MVQ1^{Pmut}*, *p35S-WRKY33* and *p35S-CFP* or combinations of those constructs were transfected. 16 h after transfection luciferin was added to the protoplasts and luciferase activity monitored, normalised to expression reference (*pUBQ10-GUS*) and is depicted as mean fold-change (n=3) compared to CFP-transfected control of *pNHL10-198* (t=0). Error bars indicate standard errors. Statistically different groups (two-way ANOVA with Bonferroni multiple comparison post-test p<0.05) are denoted by letters. (C) Protein extracts were subjected to SDS-PAGE and immunoblot analysis using anti-HA and anti-c-Myc antibodies. Amido black staining of RuBisCO served as a measure of loading.

3.3 Confirmation of MVQ1 interactions with WRKY transcription factors

MVQ1 physically interacts with WRKYs specifically from the subgroups I and IIc depending on the VQ-residues (Pecher et al. 2014). Since these data were generated in a yeast two-hybrid screen, MVQ1-WRKY interactions warrant further examination *in planta*. To this end, we employed a bimolecular fluorescence complementation assay (BiFC) in protoplasts. BiFC or Split-YFP exploits the fact that non-fluorescent N-terminal and C-terminal fragments of YFP can reconstitute the fluorophore when brought in close proximity e.g. when fused to proteins that interact with each other.

For the analysis of MVQ1-WRKY interactions MVQ1 or MVQ1^{DL} were fused to the C-terminal half of YFP (cYFP) under control of *p35S* with an additional N-terminal HA-tag in the pESPYCE-vector. Three representative WRKYs from three different groups were expressed as fusion proteins with c-Myc tagged N-terminal half of YFP (nYFP) under the control of *p35S* (in the pESPYNE-vector). Constructs were transiently expressed in *A. thaliana* protoplasts and analysed for YFP reconstitution 16 h later. YFP signals were frequently observed in protoplasts expressing cYFP-MVQ1 and nYFP-WRKYs from the group I (WRKY2, 20, 33) and group IIc (WRKY 28, 68) indicating interactions of these proteins with MVQ1 *in planta*. All YFP signals were located in the nucleus, which was marked by CFP-tagged ERF104 (Fig. 15 A-C, E, F). In contrast no reconstitution of YFP signal was detected after co-expression of cYFP-MVQ1 and nYFP-fused WRKY30, 46 and 64 from group III (Fig. 15 G-I). The group IIc WRKY12 apparently did not interact with MVQ1 in the assay, since no fluorescence was observed after co-expression with the respective YFP-fragment fusions. Co-expression of cYFP-MVQ1^{DL} with any of the nYFP-WRKY constructs did not result in reconstitution of the YFP signal (Fig. 15 A'-I') corroborating the notion that the VQ-residues are essential for MVQ1-WRKY interactions.

Expression of YFP fragment fusions with WRKYs or MVQ1/MVQ1^{DL} was confirmed by immunoblot analysis (Fig. 16 A-C). Protein levels of cYFP-MVQ1 and cYFP-MVQ1^{DL} were quite equal. Expression of respective nYFP-WRKY fusions was comparable between samples co-expressing cYFP-MVQ1 or cYFP-MVQ1^{DL}.

Additional shifted MVQ1 signals, that might indicate phosphorylation, were detected by immunoblot analysis. To address if MVQ1 phosphorylation might be a prerequisite for its interaction with WRKYs, BiFC analysis with non-phosphorylatable MVQ1 was performed. Reconstitution of YFP signals was observed when cYFP-MVQ1^{Pmut} was paired with nYFP-WRKY2, WRKY33 or WRKY68, suggesting that phosphorylation of MVQ1 is not required for interaction with these WRKYs (Fig. S3).

The BiFC results confirm that MVQ1-WRKY interactions detected in a yeast two-hybrid screen by Pecher et al. (2014) also occur in living plant cells. Apart from WRKY12 that did not interact with MVQ1

in BiFC (although it did in yeast), all other tested representatives of group I and IIc WRKYs were able to interact with MVQ1, while members of group III were not.

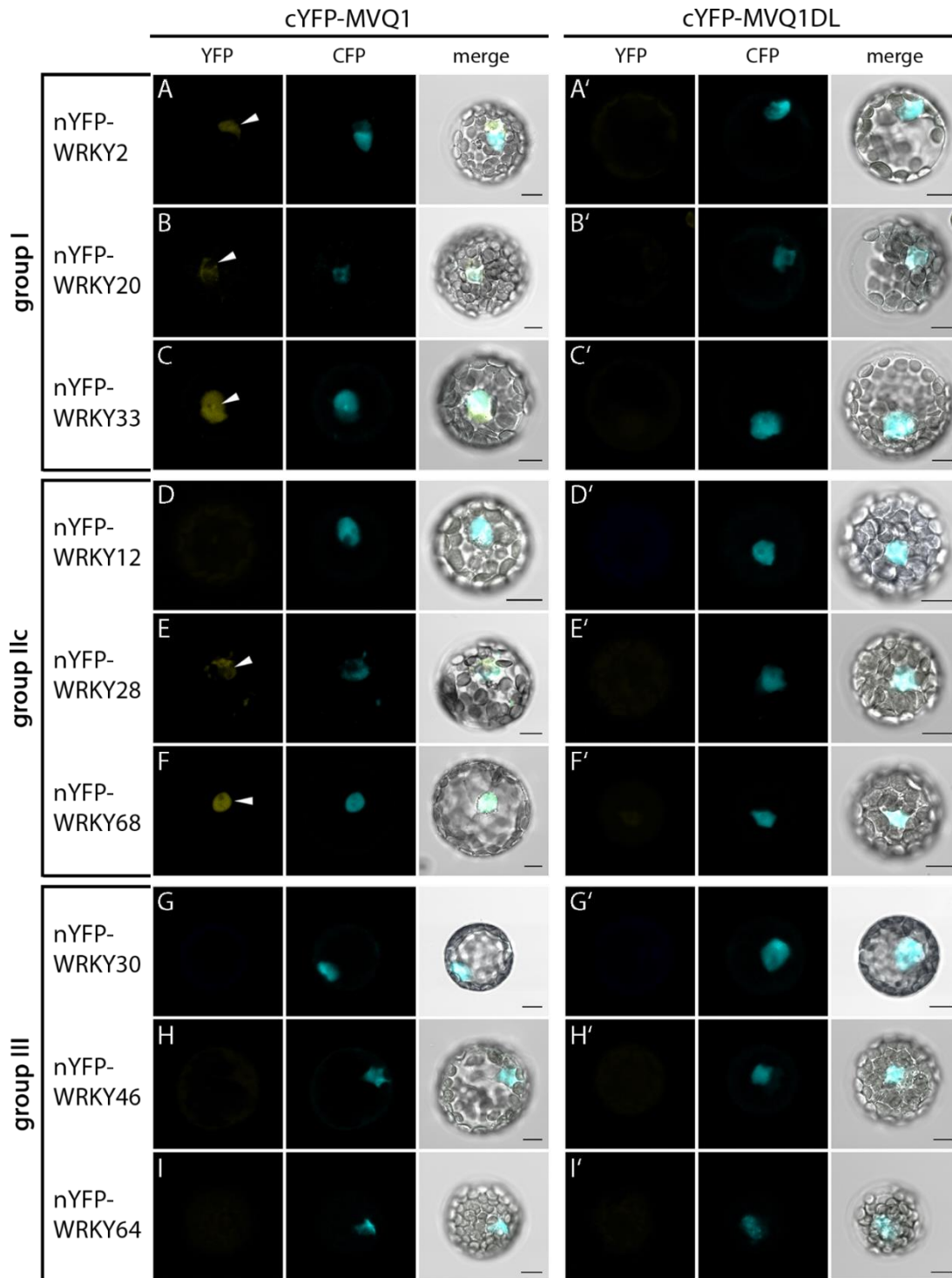


Fig. 15 Bimolecular fluorescence complementation of cYFP-MVQ1 and cYFP-MVQ1^{DL} with nYFP-WRKYs: *A. thaliana* protoplasts were co-transfected with plasmids encoding cYFP-MVQ1 or cYFP-MVQ1^{DL} and n-YFP tagged WRKYs from subgroup I (A-C), subgroup IIc (D-F) and subgroup III (G-I). A plasmid encoding ERF104-CFP was additionally transfected serving as a nuclear marker. YFP reconstitution was analysed 16 h after transfection by confocal laser scanning microscopy. YFP-fluorescence (1st panel), CFP-fluorescence (2nd panel) and brightfield image were recorded in different channels and merged (3rd panel). Scale bars represent 10 μ m. White triangles highlight YFP signals. Images are representative of three independent experiments with similar results.

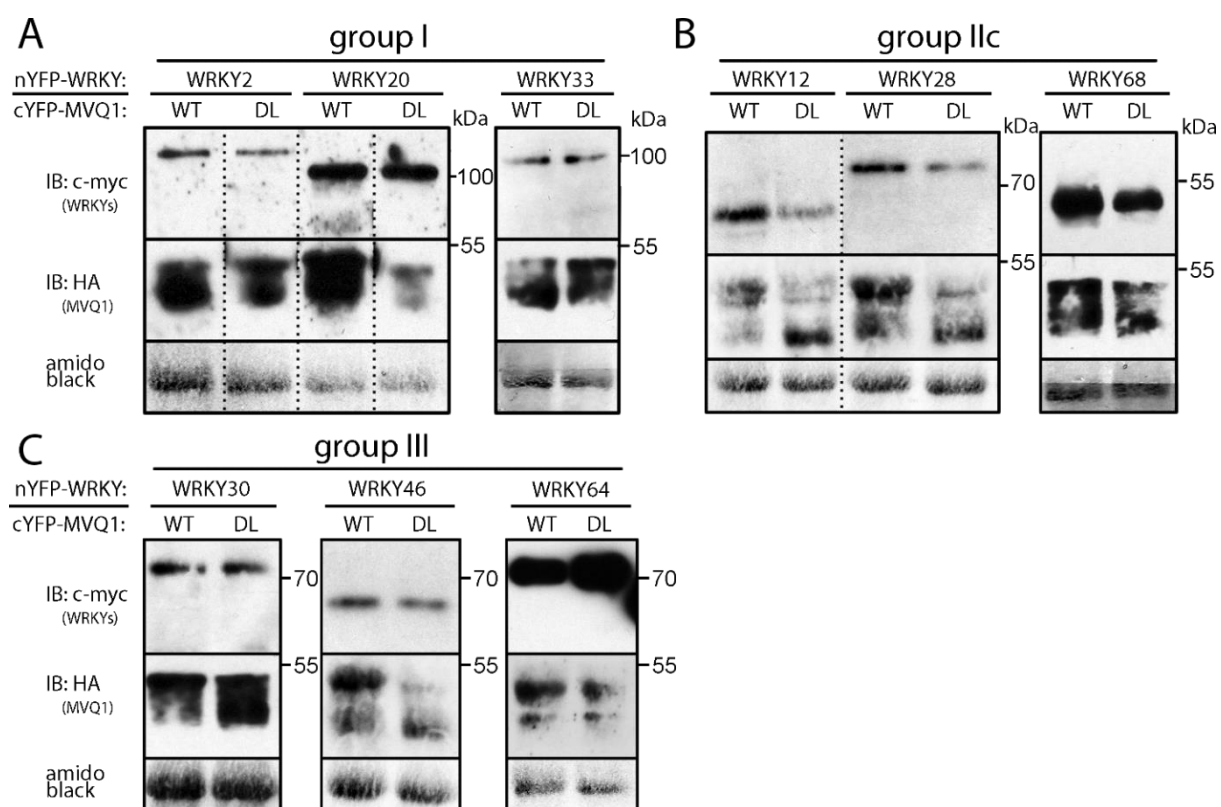


Fig. 16 Expression of nYFP-WRKY and cYFP-MVQ1/MVQ1^{DL} in *A. thaliana* protoplasts: Proteins extracts from protoplasts expressing nYFP-WRKY fusion protein and cYFP-MVQ1 fusions were subjected to SDS-PAGE and Immunoblot analysis using anti-c-Myc to detect nYFP-WRKYs from group I (**A**), group IIc (**B**) and group III (**C**). Blots were subsequently stripped and re-probed with anti-HA antibody to detect cYFP-MVQ1/MVQ1^{DL}. Amido black staining of RuBisCO served as a reference for loading. Dotted lines indicate rearrangement of lanes from the same blot, while unconnected boxed lanes are derived from distinct blots.

3.4 Transcriptome analysis of MVQ1 misexpression lines

MAMP-perception leads to extensive transcriptional reprogramming e.g. induction of defence genes (Navarro et al. 2004). Dampening of MAMP-induced defence gene promoter activation by MVQ1 was demonstrated by example of selected reporter genes in the protoplast system (section 3.2.1 and 3.2.3). If these examples represent a general function of MVQ1 in plants, a considerable influence of MVQ1 on MAMP-induced changes in the transcriptome would be expected.

To address this hypothesis and potentially identify MVQ1-regulated candidate genes, a global transcriptome analysis was performed in order to compare transcriptional responses to flg22-treatment between WT plants, and plant lines with altered MVQ1 expression.

3.4.1 Characterisation of MVQ1 misexpressing plant lines for transcriptome analysis

For transcriptomic analysis, plant lines with altered MVQ1 expression needed to be selected. The *mvq1* mutant (SALK_107266) is a T-DNA insertion line carrying the insertion within the coding region of MVQ1 (Fig. 17 A). The exact position of the T-DNA insertion was determined by sequencing a PCR product containing the T-DNA-plant genomic sequence interface. MVQ1 OE-lines were generated by means of agrobacterium-mediated plant transformation (using the binary vector pEarleyGate203, Earley et al. (2006)). In these lines, expression of c-Myc-tagged MVQ1 is controlled by the strong 35S promoter. Southern blot analysis identified line K11 to likely contain only one copy number of the transgene (Fig. S4). Therefore, K11 was selected for further analysis.

To confirm lack of *MVQ1* transcripts in *mvq1* and overaccumulation in K11 respectively, transcript levels of *MVQ1* were determined by qRT-PCR (Fig. 17 B). The relative transcript level of *MVQ1* ($2^{-\Delta\Delta CT}$ using *PP2A* as a reference gene) reached 51 in MVQ1 OE K11 and was significantly higher (about 30 times) compared to WT (1.7). In *mvq1* significantly lower transcript levels were detectable (0.1), which represent about 6 % of the levels in WT. Both *mvq1* and MVQ1 OE line K11 do not display any obvious phenotypes.

Expression of c-Myc-tagged MVQ1 in K11 was confirmed by immunoblot analysis (Fig. 17 C). An unspecific signal was detected in all samples (upper band), whereas a band of the size expected for MVQ1 was exclusively present in samples from the transgenic line. MVQ1 protein levels could not be assessed in WT and *mvq1* because there is no specific antibody against MVQ1 available.

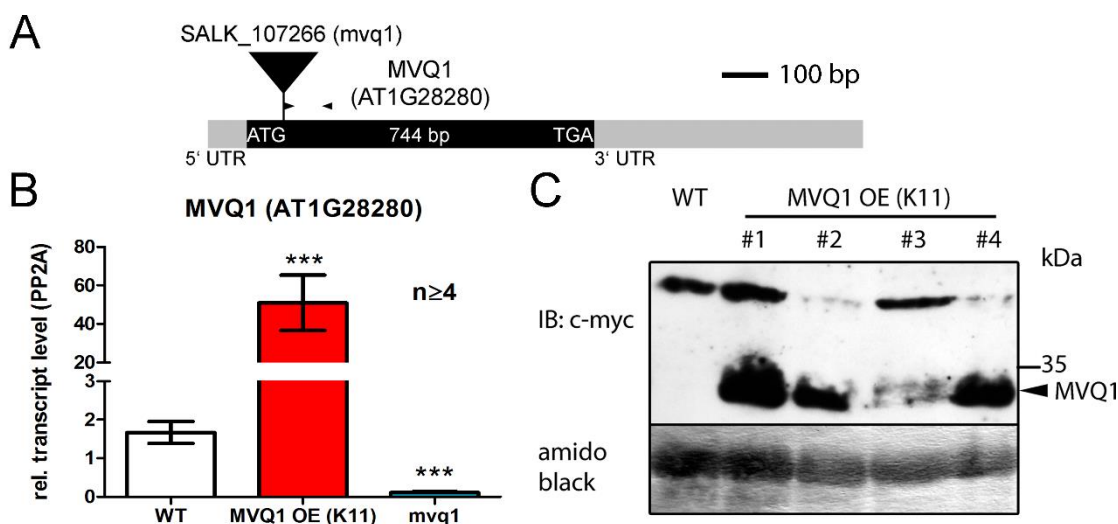


Fig. 17 Characterisation of MVQ1 overexpressing line (MVQ1 OE K11) and T-DNA insertion line *mvq1*: **(A)** Scheme drawn to scale of the MVQ1 (At1g28280) locus with coding region (black box) and UTRs (grey boxes). Location of T-DNA insertion is depicted by black triangle and arrowheads represent primers used for qRT-PCR. **(B)** RNA was extracted from leaves of indicated plant lines and used for cDNA synthesis and subsequent analysis by qRT-PCR. PP2A served as reference gene. Relative transcript levels are represented by $2^{-\Delta ct}$ and error bars indicate SEM. Two-tailed t-test was performed after log₂ transformation; *** $p \leq 0.001$ $n=5$ except MVQ1 OE (K11) $n=4$. Note break in y-axis for better visualisation of columns. **(C)** Protein extracts from leaves of WT and four sibling plants from the MVQ1 K11 OE-line were subjected to SDS-PAGE and immunoblot analysis using anti-c-Myc to detect MVQ1. MVQ1 signals are indicated by a black arrow. Anti-c-Myc detected a second unspecific band in all extracts. Amido black staining of RuBisCO served as loading reference.

3.4.2 Microarray analysis reveals differentially expressed genes in MVQ1 misexpression lines

For comparative transcriptome analysis of WT (Col-0), MVQ1 OE K11 and *mvq1*, leaves were infiltrated with flg22 (1 μ M) or water as a control and harvested one hour later. RNA was extracted for subsequent cDNA synthesis, labelling and hybridisation to microarray chips (Affymetrix® 1.1 ST exon array). Array strips were read out using the GeneAtlas™ system and raw data was statistically analysed and processed by Dr. Benedikt Athmer. Signal above background was detected for 14,461 genes (see file 1 of supplementary data on CD). When comparing the datasets of different genotypes and treatments, genes were defined as differentially regulated with a fold change ≥ 2 (upregulated) or ≤ 0.5 (downregulated) and a false discovery rate (FDR) adjusted p -value < 0.05 .

Comparing the transcriptomes of MVQ1 OE and *mvq1* with WT plants under control conditions revealed that overexpression of MVQ1 resulted in differential expression of 1070 genes (639 up-, 431 down-regulated), whereas only 138 (117 up, 21 down) differentially expressed genes (DEGs) were detected in *mvq1* (Tab. 4). Upon treatment with flg22, the transcriptomes of *mvq1* and WT were quite similar (only 1 upregulated gene). In flg22-treated MVQ1 OE 434 DEGs (199 up, 235 down) were observed.

The comparatively low number of DEGs in the *mvq1* mutant especially in flg22 treated samples might indicate, that loss of MVQ1 does not affect the transcriptome as much as MVQ1 overexpression. This could be explained by potentially redundant functions of closely related MVQs (e.g. MVQ2-4).

Tab. 4 Differentially expressed genes in MVQ1 misexpression lines: Listed are numbers of up- and down-regulated genes in MVQ1 OE (K11) and *mvq1* compared to WT after treatment with water or 1 μ M flg22 respectively.

	water		flg22	
	up	down	up	down
MVQ1 OE vs. WT	639	431	199	235
<i>mvq1</i> vs. WT	117	21	1	0

3.4.3. Effect of altered MVQ1 levels on the transcriptome in control conditions

To get a better understanding which processes might be influenced by altered transcriptomes in *mvq1* and MVQ1 OE in control conditions (absence of flg22), we sought to match DEG identities with data on function of those genes. To this end, gene ontology (GO) enrichment analysis was performed using the PANTHER online tool on the GO consortium website (www.geneontology.org). GO terms for biological function of the respective DEGs were tested for enrichment against the whole *A. thaliana* genome list as background. Additionally, network analysis was performed based on the STRING database (Szklarczyk et al. 2017) to identify interactions of proteins encoded by DEGs.

Results of the STRING network analysis of the up- and downregulated genes in *mvq1* compared to WT are summarised in Fig. 19. Among the 117 upregulated genes, 48 are clustered in a network containing genes involved in the biogenesis of ribosomes. A second network contains genes encoding for chaperones. Accordingly GO terms like “ribosome biogenesis”, “RNA processing”, “nuclear transport” and “translation” and other GO terms related to these processes were enriched (Tab. S8).

Only few genes (21) were downregulated in *mvq1*. Five of those are part of a network containing genes involved in defence response. “Response to hypoxia” and “defence response” were identified as overrepresented GO terms for genes downregulated in *mvq1* (Tab. S9).

More than 600 genes were upregulated in the MVQ1 OE line compared to WT, which clustered in ten distinct networks during STRING analysis (Fig. 18). Genes involved in sulphate and nitrate metabolism were grouped together (blue cluster). Other networks contained genes coding for enzymes involved in the biosynthesis of indoles (purple cluster) fitting to the GO-overrepresentation of “indole-containing compound biosynthetic process”. Genes important for biosynthesis of phenylpropanoids

(black cluster) were connected with ethylene biosynthesis genes (red cluster) and stress-related TFs (brown cluster).

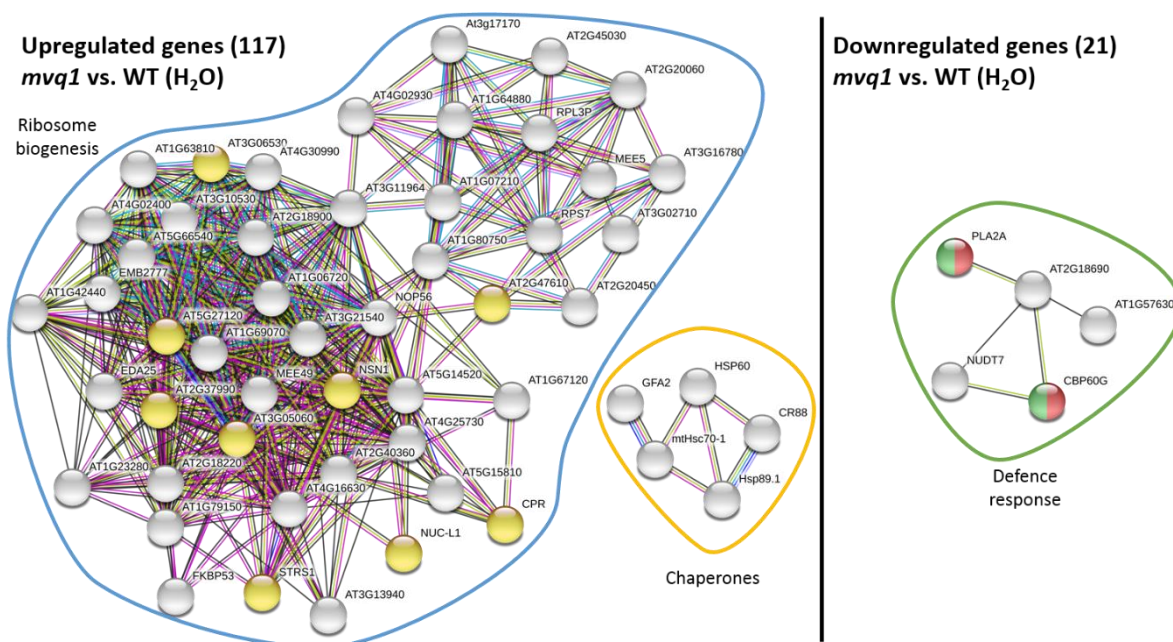


Fig. 19 STRING network analysis of differentially expressed genes in *mvq1* vs. WT under control conditions: Networks containing at least 4 nodes were constructed with a minimal required interaction score of 0.9 for upregulated genes (left) and 0.7 for downregulated genes (right). Interactions between nodes are based on curated databases (blue line), experiments (pink line), co-expression (black line) and textmining (green line). Genes assigned to highly overrepresented GO terms (by STRING) are displayed in yellow (ribosome biogenesis), green (defence response) and red (response to external stimulus) nodes.

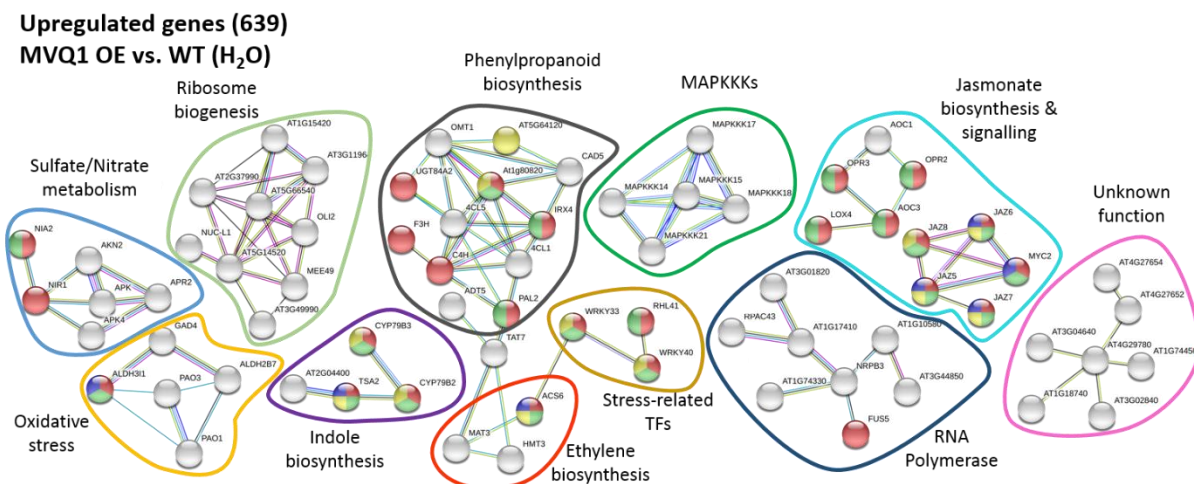


Fig. 18 STRING network analysis of upregulated genes in MVQ1 OE vs. WT under control conditions: Networks of at least 4 nodes were constructed with a minimal required interaction score of 0.9. Interactions between nodes are based on curated databases (blue line), experiments (pink line), co-expression (black line) and textmining (green line). Genes assigned to highly overrepresented GO terms (by STRING) are displayed in yellow (defence response), green (response to stress), blue (response to hormone) and red (response to stimulus) nodes.

Two distinct networks were associated with JA (turquoise circle). One network contained genes responsible for JA biosynthesis, and the other JA signalling components such as JAZ repressors and MYC2. Coinciding with overrepresentation of the GO terms “JA metabolic process” and “response to wounding”. Additional networks contained genes involved in oxidative stress (yellow cluster), ribosomal biogenesis (bright green cluster), a group of genes connected to RNA-Polymerase II (dark blue cluster), five MAPKKs (dark green cluster) and 7 genes with unknown function (pink cluster). 25 groups of GO terms were enriched in MVQ1 OE upregulated genes (Tab. S10). The most highly enriched included specific terms like: “respiratory burst“, “response to chitin“ and “JA metabolic process“. These can be summarised in general GO terms like “defence response“, “response to hormone“ and “response to stress“, which were enriched as well.

Analysis of the genes that are downregulated in MVQ1 OE revealed five networks (Fig. 20). The most extensive network consisted of 41 genes with roles in photosynthesis (green cluster). Furthermore 15 genes, involved in chlorophyll biosynthesis were grouped together (blue cluster). In line with this, GO terms related to “photosynthesis“, “response to light“ and “chlorophyll biosynthesis“ were highly enriched (Tab. S11). Genes associated with oxidative stress, constituted another network (red cluster) coinciding with enrichment of the GO term “oxidation-reduction process“. Four genes connected to cell wall modification were grouped together (black cluster). Similar to the upregulated genes, the downregulated genes contained a network of ribosome biogenesis genes (yellow cluster), although no rRNA- or ribosome-related GO terms were enriched.

Downregulated genes (431) MVQ1 OE vs. WT (H₂O)

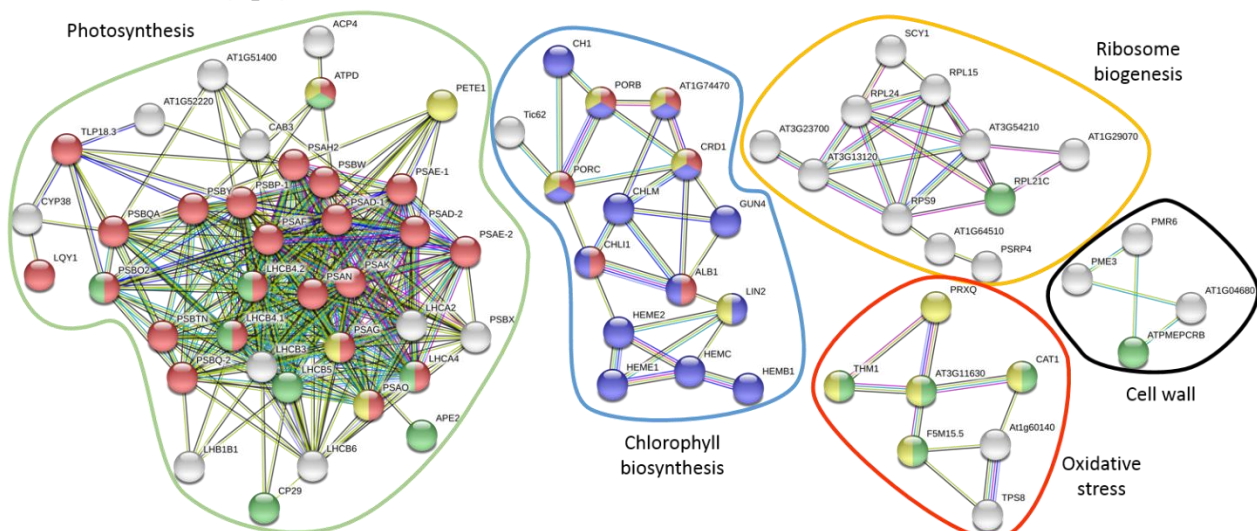


Fig. 20 STRING network analysis of genes downregulated in MVQ1 OE vs. WT under control conditions: Networks of at least 4 nodes were constructed with a minimal required interaction score of 0.9 Interactions between nodes are based on curated databases (blue line), experiments (pink line), co-expression (black line) and textmining (green line). Genes assigned to highly overrepresented GO terms (by STRING) are displayed in red (photosynthesis), yellow (oxidation-reduction), green (abiotic stimulus) and blue (chlorophyll biosynthesis) nodes.

In summary, it can be stated that under control conditions genes involved in ribosome biogenesis (e.g. *RPLs*) and protein folding (chaperones), both important for translation are upregulated in *mvq1* compared to WT, while only few genes involved in defence response (e.g. *PHOSPHOLIPASE A 2A*) are downregulated.

In the MVQ1 OE line mainly genes involved stress response and/or biosynthesis of hormones and metabolites (JA, ET, phenylpropanoids, indoles) are upregulated, while genes involved in photosynthesis and connected processes (chlorophyll biosynthesis, oxidative stress) are downregulated. This could indicate that MVQ1 overexpression potentially induces a stress response while simultaneously limiting photosynthesis. In case of genes associated with ribosome biogenesis some representatives are upregulated while others are downregulated in MVQ1 OE, which possibly indicates a change in ribosome composition.

3.4.4. Impact of MVQ1 on the transcriptome after MAMP-treatment

One major aim of the present work was to investigate the influence of MVQ1 on MAMP-induced changes in the transcriptome. In this context, gene expression profiles of plants that were infiltrated with flg22 (1 μ M) for 1 h were compared to transcriptomes of plants of the same genotype after water infiltration.

In WT plants, flg22 treatment for 1 h led to upregulation of nearly 1000 genes. At the same time 454 genes were downregulated compared to water control (Fig. 21).

The upregulated genes were highly enriched for GO terms typically associated with MTI (e.g. “defence response”, “response to fungus, bacterium, oomycete”, “respiratory burst”, “cell death” etc.), while downregulated genes were enriched for GO terms related to growth and metabolism (Tab. S12). This result resembles transcriptomic responses to flg22 treatment that have been described before (Denoux et al. 2008) thereby confirming that the deployed flg22 was active.

In *mvq1* plants, 80 % of flg22-activated genes in WT were upregulated as well. Additionally, 385 genes with enriched GO terms related to defence response (Tab. S14) were specifically upregulated after flg22 treatment in the *mvq1* background. This underpinned the similarity of responses to flg22 in WT and *mvq1* (see Tab. 4), and suggests that *mvq1* might even be slightly hypersensitive to flg22, since more genes are upregulated upon flg22 treatment compared to WT.

In contrast the MVQ1 OE line did not react strongly to flg22 treatment. Only 23 % (233) of the genes upregulated in WT by flg22 are upregulated in MVQ1 OE as well. There were 160 additional genes upregulated by flg22 in MVQ1 OE, but GO-enrichment analysis revealed, that a large fraction of these genes is encoding proteins involved in photosynthesis and translation (Tab. S15). The majority of these

genes emerged as upregulated in the flg22/water comparison because they were downregulated in MVQ1 OE vs. WT under control conditions and returned to “WT-level” after flg22-treatment.

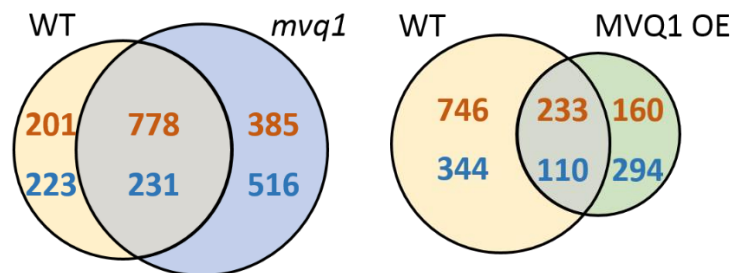


Fig. 21 Comparison of differentially expressed genes in flg22- vs. water treated plants from different genotypes: VENN diagrams show the number of DEGs in flg22-treated samples versus the water control of the same genotypes. WT is compared to *mvq1* (left) and MVQ1 OE (right). Circle sizes are proportional to number of DEGs. Red numbers indicate up-, blue numbers downregulated genes. Overlapping regions contain genes that are differentially regulated in both respective phenotypes.

These results support our hypothesis that MVQ1 might act as a suppressor of MAMP-induced defence genes expression. To investigate potential “targets” of suppression by MVQ1, focus was set on those genes that were upregulated by flg22 in WT, but failed to be induced in MVQ1 OE.

To this end, all differentially regulated genes between the treatments (flg22, water) in a given genotype (WT, MVQ1 OE) or between genotypes under a given treatment (total 2596 genes), were subjected to hierarchical clustering analysis. Z-scores were calculated and the scaled data was hierarchically clustered in the TIGR-MEV software. Relative changes in gene expression between WT and MVQ1 OE after water or flg22 treatment were visualised in a heatmap (Fig. 22). The 2596 genes were grouped into 29 clusters according to similarity in gene expression profiles. Expression of genes of interest should be highly induced after flg22 treatment in WT compared to water treatment, but should not be or only weakly induced by flg22 in the MVQ1 OE line. Four distinct gene clusters met these criteria.

Despite generally similar expression profiles, the four clusters displayed slight differences in expression patterns. For example, the expression of genes from the green cluster in the MVQ1 OE line is hardly affected by flg22 treatment, while expression of genes in the yellow cluster is even lower in MVQ1 OE lines upon flg22 treatment compared to the respective water control (Fig. 22).

Taking all four clusters together, 404 genes could be identified for which flg22-induced activation was suppressed in the MVQ1 OE line (see file 4 of supplementary data on CD). The gene set contains several RLKs (e.g. *FRK1*, *BAK1*, *WAKL2*, 3, 7, seven different *cysteine-rich RLKs* and ten *lectin RLKs*), intracellular receptors (11 TIR-type and 2 CC-type *NLRs*), transcription factors (e.g. *WRKY45*, *WRKY47*, *WRKY53*, *bZIPs*, *bHLHs*, *MYBs*, *ERF14*), elicitor peptide precursors (*PROPEP2*, 3) and important defence signalling components such as *EDS1*, *PAD4* and *NPR1*.

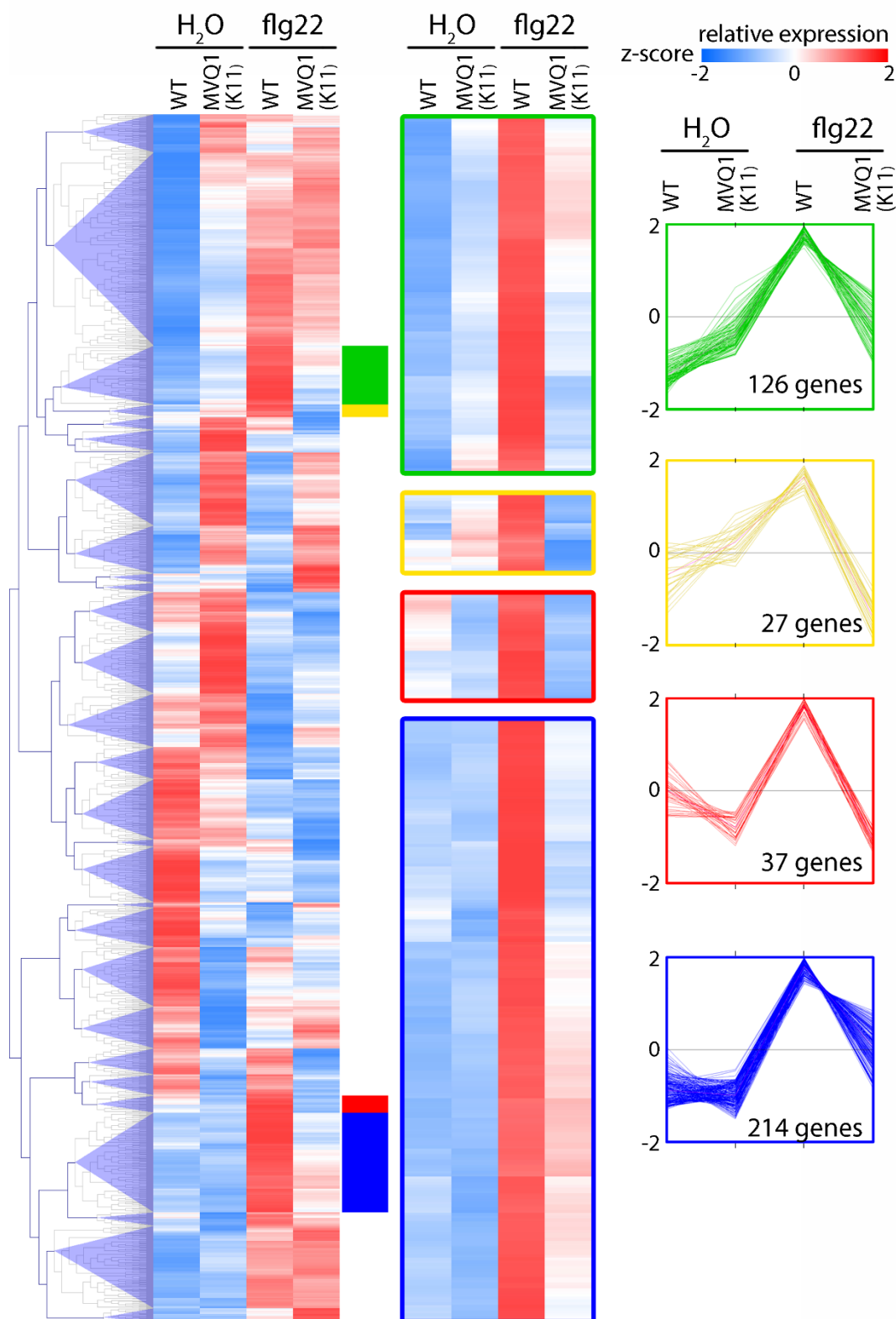


Fig. 22 Hierarchical clustering analysis of genes regulated by MVQ1 and/or flg22: Scaled expression data of 2596 genes, that are differentially regulated in MVQ1OE (K11) vs. WT or flg22 vs. H₂O. Each row represents a gene with z-scores representing relative expression levels on a colour scale, blue = low expression (-2), red = high expression (2). **Left panel:** Hierarchical clustering was performed using Pearson correlation and average linkage clustering in TIGR-MEV. Tree branches leading to distinct clusters are highlighted in purple. Four identified clusters of interest are marked by coloured blocks. **Middle panel:** Gene expression heatmaps of selected clusters (increased magnitude). **Right panel:** Summary of gene expression profiles for selected clusters.

Results

Tab. 5 lists a selection of prominent defence-related genes, which were suppressed in MVQ1 OE. Typical early defence marker genes like *FRK1*, *NHL10* and *GST1* were also present in this list, which is in line with results from promoter activation assays that demonstrated MVQ1-mediated suppression of flg22-induced activation of *pNHL10* and *pGST1* (see 3.2.1, 3.2.3). These results illustrate that MVQ1 overexpression might negatively affect expression of genes involved in defence-related signalling on different levels from receptors to transcription factors.

Tab. 5 Selected flg22-activated genes that are suppressed in MVQ1 OE: Genes highlighted in grey were used for validation by q-PCR. FC = fold change; Cluster = corresponding coloured clusters used in Fig. 22 (b = blue, g = green, r = red)

Gene ID	Gene name	FC 1h flg22		Description	Cluster
		WT	MVQ1 OE		
AT2G19190	<i>FRK1</i>	27.17	2.47	receptor-like kinase; defence signalling	b
AT2G35980	<i>NHL10</i>	7.03	2.72	induced during defence responses and senescence	b
AT4G23810	<i>WRKY53</i>	6.21	1.15	WRKY transcription factor; resistance against bacteria	g
AT2G32680	<i>RLP23</i>	6.19	1.30	receptor-like protein; defence signalling	b
AT5G64905	<i>PROPEP3</i>	5.88	2.31	elicitor peptide 3 precursor	b
AT5G57220	<i>CYP81F2</i>	5.41	2.52	Cytochrome P450; indole glucosinolate biosynthesis	b
AT1G02930	<i>GST1</i>	4.25	1.75	Glutathione-S-transferase 1; defence response	g
AT1G22070	<i>TGA3</i>	4.03	1.97	bZIP transcription factor; NPR1-interactor	b
AT3G48090	<i>EDS1</i>	3.41	2.24	lipase-like gene; defense signal transduction	b
AT4G33430	<i>BAK1</i>	3.25	2.50	receptor-like kinase; defence signalling	b
AT1G64280	<i>NPR1</i>	2.43	1.44	key regulator of SA-mediated systemic acquired resistance	g
AT3G25070	<i>RIN4</i>	2.31	1.41	RPM1 interacting protein 4	g
AT1G18570	<i>MYB51</i>	2.16	0.88	transcriptional regulator of indole glucosinolate biosynthesis	r
AT3G52430	<i>PAD4</i>	2.11	0.96	lipase-like gene; defense signal transduction; EDS1 interactor	r
AT4G16890	<i>SNC1</i>	1.77	1.08	TIR-NB-LRR-type resistance protein	r

Results from the microarray analysis support the notion of MVQ1 as a negative regulator of MTI. Since MVQ1 interacts with WRKYs, dampening of transcriptional response to flg22 by MVQ1 may occur via WRKYs. If that is true, one would expect enrichment of W-boxes in promoters of the 404 identified genes suppressed by MVQ1. The gene list was therefore subjected to Pscan, a tool that scans promoter sequences for overrepresentation of known TF-binding motifs. Binding motifs of 43 different WRKYs, which all contain the core W-box (TTGAC[T/C]) are most over-represented with p-values in the range of 10^{-25} to 10^{-11} . The database used by Pscan contains motif information for single TFs and does not pool members of a family even if the binding motifs are nearly identical. Apart from W-boxes, Pscan identified binding sites for bZIPs, so called G- and C-boxes, ([G/C]ACGT) and binding sites for zinc-finger proteins of the C2H2-type (AAAG). Those are over-represented with p-values between 10^{-5} to $5 \cdot 10^{-4}$. For a detailed list of all identified TF-binding motifs (see Tab. S16).

3.4.5. Validation of potential MVQ1-suppressed defence genes by qRT-PCR

In order to validate MVQ1-suppressed defence-related genes identified by microarray analysis with an additional method, four of those genes were selected (Tab. 5) and analysed by qRT-PCR in a set of independently grown plants. A second independent MVQ1 OE line (K42) was included in the analysis, to exclude that the observed changes in gene expression are caused by position effects of the transgene in MVQ1 OE (K11). Plants were infiltrated with water or flg22 (1 μ M) and samples were taken 1 h and 2 h after treatment. Following isolation of RNA, cDNA was synthesised and subsequently subjected to qRT-PCR. For the analysis of K11 plants samples treated for 1 h or 2 h with flg22 or water were generated in a single experiment. Due to a limited number of K42 plants in the initial experiment, samples were generated in two separate experiments: one in which all plants (Col-0, K42) were harvested 1 h after treatment with flg22 or water and another one, in which samples were taken 2 h after treatment (see individual plots for 1 h and 2 h in this line Fig. 23).

MVQ1 overexpression in samples from both MVQ1 OE lines was examined by qRT-PCR and shown to range from 10- to 20-fold induction of transcripts compared to WT samples (Fig. S5).

The amount of *FRK1* transcript was found to be significantly lower in K11 compared to WT 2 h after flg22 treatment. In the K42 line *FRK1* transcripts accumulated to a lesser extent than in the WT 1 h and 2 h after flg22 treatment as well as 2 h after water treatment. *NHL10* transcript levels were lower in both MVQ1 OE lines (K11, K42) compared to WT 2 h after treatment with flg22. Transcript levels of *RLP23* did not differ significantly between WT- and K11-samples at any time point, while in K42 samples they were significantly lower 2 h after treatment with water and flg22 compared to WT. In K11 plants, induction of *PROPEP3* transcripts was significantly reduced 2 h after flg22 treatment in comparison to WT, while in K42 plants significantly lower *PROPEP3* transcript levels were observed 1 h after flg22 elicitation.

The qRT-PCR results confirmed that flg22-mediated induction of *FRK1*, *NHL10* and *PROPEP3* is suppressed in the MVQ1 OE K11 line. In contrast to the microarray, in which those genes were suppressed already 1 h after treatment with flg22, significant differences to WT samples could only be observed 2 h after flg22 treatment. Suppression of *RLP23* induction on the other hand could not be confirmed by qRT-PCR in the K11 MVQ1 OE line.

Flg22-induced transcriptional activation of all four tested genes was suppressed in a second independent MVQ1 OE line (K42) with significantly lower transcripts of *FRK1*, *NHL10* and *RLP23* at 2 h after flg22 treatment and lower transcripts of *PROPEP3* 1 h after flg22 elicitation. Despite differences in timing of the response, transcript quantification by qRT-PCR largely confirmed the microarray data on suppression of flg22-induced activation of defence-related genes by MVQ1 overexpression in two independent plant lines.

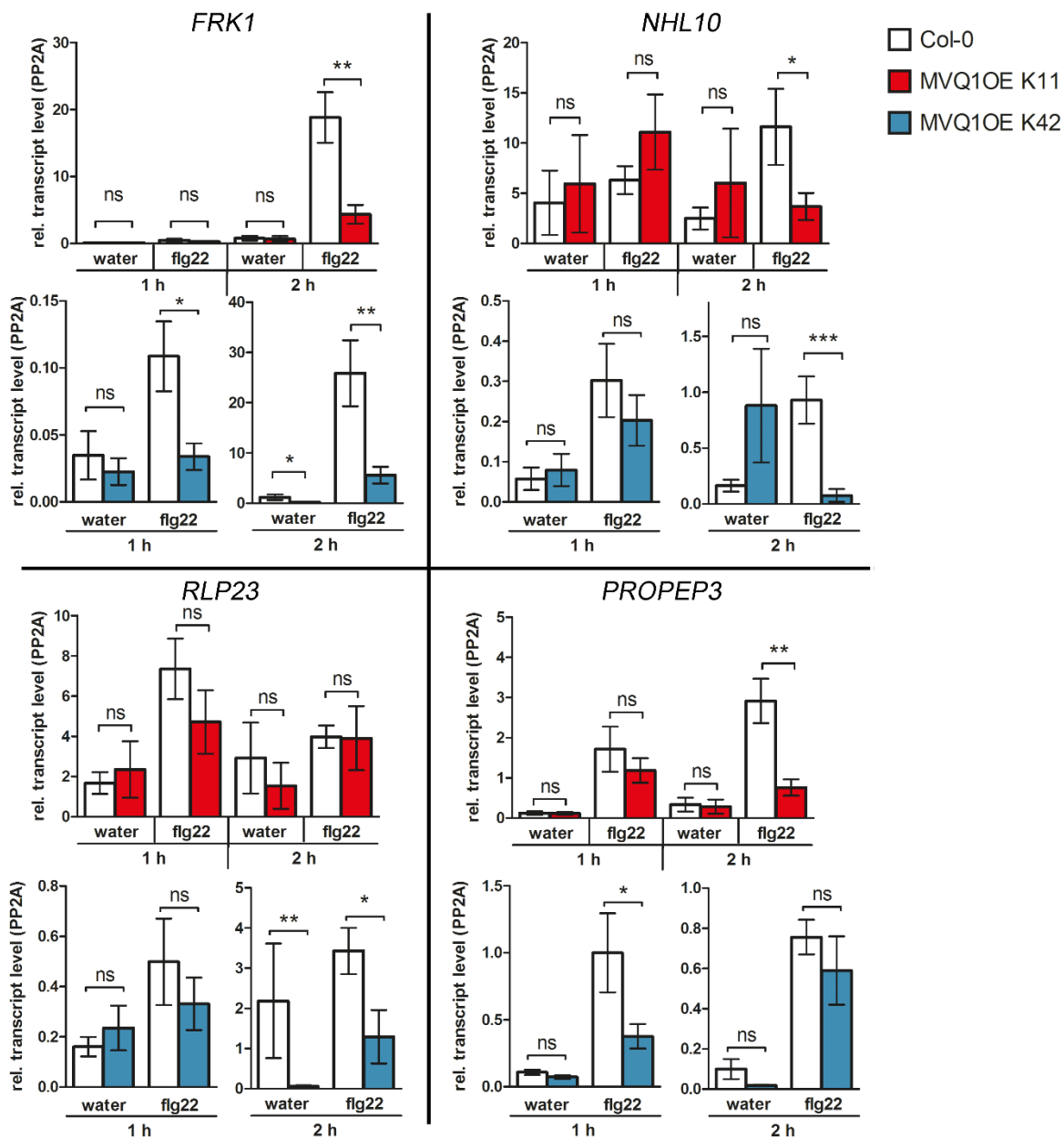


Fig. 23 Expression analysis of selected genes in two MVQ1 OE lines after *fig22* treatment by qRT-PCR: WT (Col-0) and plants from two independent MVQ1 OE lines (K11 and K42) were infiltrated with 1 μ M *fig22* or water as a control and samples were harvested after 1 h and 2 h. RNA was extracted for subsequent cDNA synthesis and analysis by qRT-PCR. *PP2A* served as a reference gene. For Col-0/K11 comparison, samples were derived from one experiment. For Col-0/K42 comparison, samples were derived from two independent experiments (one experiment for each time point) and therefore measured independently (see individual y-axis). Data is shown as mean and SEM, $n \geq 5$. Asterisks indicate statistically significant differences between Col-0 and respective MVQ1 OE plants (unpaired two-tailed t-test after \log_2 transformation, * $p \leq 0.05$, ** $p \leq 0.01$, *** $p \leq 0.001$, ns – not significant).

3.5 Influence of MVQ1 on DNA-binding of WRKYs

The presented transcriptomic data corroborates the hypothesis that MVQ1 might act as a negative regulator of MTI. It raises the subsequent question of how MVQ1 suppresses expression of MAMP-activated genes. Considering that MVQ1 interacts with WRKYs (3.3) and is able to antagonise WRKY-mediated promoter activation (3.2.4) it is tempting to speculate that WRKYs are involved in MVQ1-mediated suppression of gene expression. One possible scenario could be that MVQ1-WRKY interactions might change properties of WRKYs and hence interfere with DNA-binding or transcriptional activity.

3.5.1. EMSAs reveal interactions of MVQ1 with DNA-bound WRKY33

To address the question, whether presence of MVQ1 alters DNA-binding properties of WRKYs, an electrophoretic mobility shift assay (EMSA) was employed. A W-box containing sequence from the parsley PR1-1 promoter called W2 (Rushton 2002) was used as a DNA-probe. His-tagged full-length WRKY33 was expressed in *E. coli* as a NusA-fusion to promote solubility (pMCSG48-vector) and extracted for subsequent purification and dialysis. Purified WRKY33 or His-tagged NusA from the empty vector (EV) control were incubated with Cy5-labelled W2-probe and analysed by EMSA. Immunoblot analysis showed that full length proteins were expressed (Fig. 24 C). In case of EV and WRKY33 additional bands of lower molecular weight were present in the purified extracts. These lower bands might represent degradation products.

When no protein was present, the labelled DNA probe ran through the gel and could be found at the bottom of the gel (free probe). Incubation with WRKY33 (4 µg) resulted in retardation of a proportion of the probe in the gel causing a band shift and suggesting interaction between WRKY33 and the W2-probe (Fig. 24 A). Incubation with the EV control that contained His-tagged NusA did not lead to retardation of the probe demonstrating that WRKY33 and not NusA is binding to the DNA.

Interaction of WRKY33 with the W2-probe is concentration-dependent since higher amounts of WRKY33 resulted in stronger signals of the bound probe (quantification in Fig. 24 D). Pre-incubation of WRKY33 with unlabelled W2-probe in 40-fold excess drastically reduced signal intensity of the shifted band thus showing that WRKY33 binds the unlabelled W2-probe too. Mutation of the W-box in the W2-probe abolished retardation in the gel emphasising its requirement for interaction with WRKY33 (Fig. 24 B).

Pre-incubation of WRKY33 with MVQ1 resulted in a slightly stronger retardation of the probe which was more pronounced when increased concentrations of MVQ1 were used. The observed “supershift”

indicated that the protein bound to the probe was larger than WRKY33 alone and might be explained by formation of a WRKY33-MVQ1-DNA complex. MVQ1^{DL} was not able to induce a supershift demonstrating that MVQ1-WRKY-interaction is required for supershift formation.

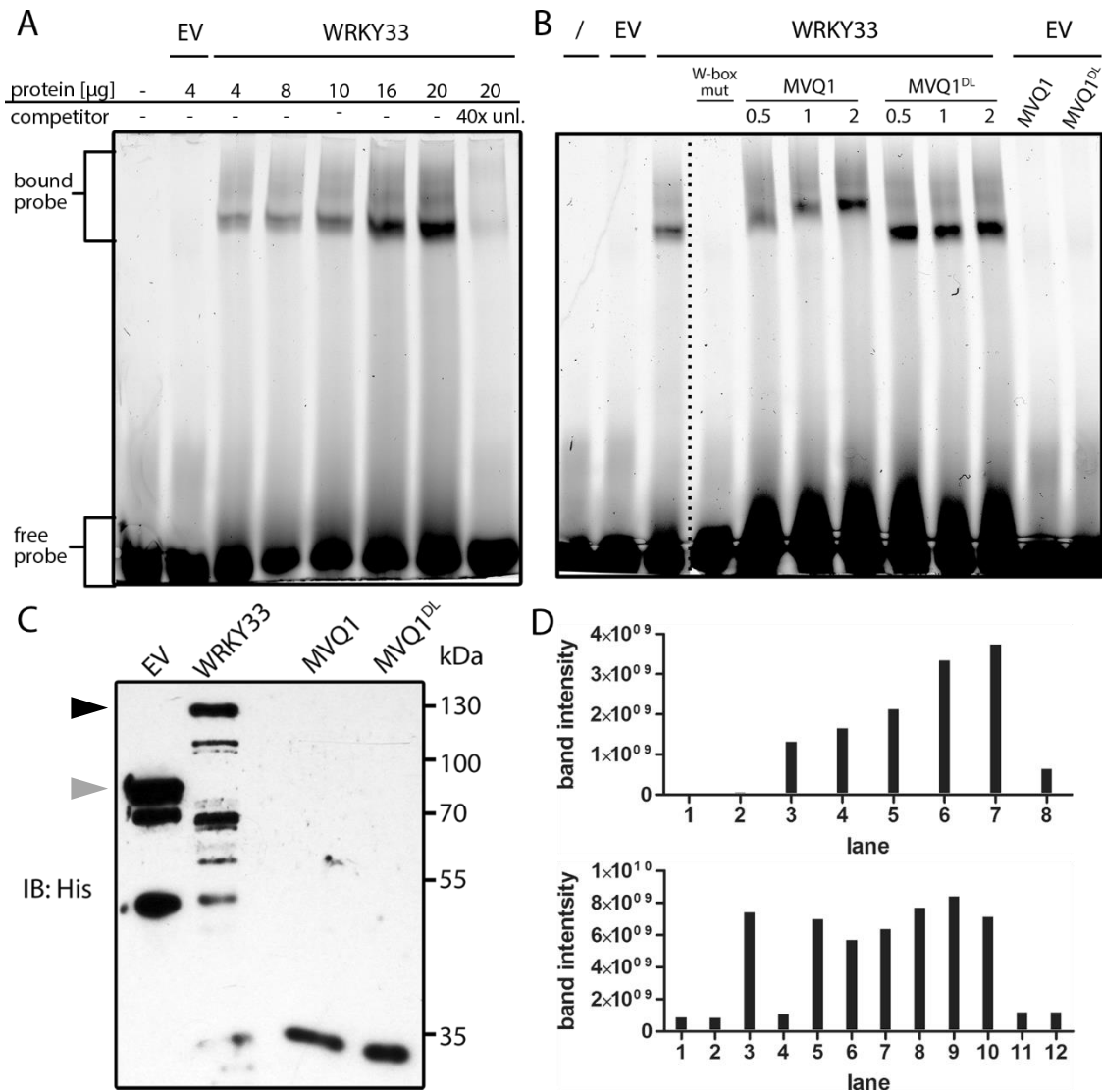


Fig. 24 MVQ1 binds to a WRKY33-DNA complex: (A) EMSA of Cy5-labelled W2-probe incubated with different amounts of WRKY33 and empty vector (EV) as control. Numbers indicate amount of WRKY33 in µg. Last lane shows competition with 40-fold excess of non-labelled W2-probe. (B) EMSA of Cy5-labelled W2-probe incubated with WRKY33 (8 µg) and EV (8 µg) in presence or absence of MVQ1/MVQ1^{DL}. Numbers indicate amount of MVQ1/MVQ1^{DL} in µg. In lane 4 WRKY33 was incubated with Cy5-labelled W2-probe harbouring a mutated W-box (W2-mut). Similar results like (A) and (B) were obtained in three independent experiments. (C) *E. coli* protein extracts were purified using Ni-NTA and subjected to SDS-PAGE followed by immunoblot analysis with anti-His. Black triangle highlights band for full-length NusA-WRKY33 fusion and grey triangle indicates band of His-tagged NusA in the empty vector control. (D) Quantification of EMSA signals was performed using 'ImageQuant'. Areas of same size around the bound probe band were used for signal quantification. Upper diagram displays band intensities for (A) and lower diagram for (B).

When MVQ1 or MVQ1^{DL} were incubated with the EV control and the W2-probe without WRKY33, no retarded band was observed, suggesting that these proteins are not able to bind the W2-probe directly.

Quantification of the signal, for which areas around the defined bands were included, did not reveal strong differences between samples that contained WRKY33 alone, together with MVQ1 or MVQ1^{DL} respectively. Thus, MVQ1 did not seem to interfere with the DNA-binding ability of WRKY33 but rather seemed to interact with WRKY33 at the DNA in a complex.

3.5.2. MVQ1 stimulates binding of some WRKY-domains to DNA

Quantification of EMSA signals did not reveal any reduction of DNA binding of WRKY33 in the presence of MVQ1. To corroborate these results with a quantitative assay, a modified DNA-protein-interaction enzyme-linked immunosorbent assay (DPI-ELISA) as described by Brand et al. (2010) was performed. This assay allows GFP-based detection of binding of proteins of interest to respective DNA probes.

To this end, biotinylated DNA-probes containing an intact W-box (W2) or a mutated version (W2^{mut}) were immobilised on a streptavidin-coated plate.

These plates were incubated with *E. coli* extracts containing recombinant DNA-binding domains (DBD) of WRKYs from three different subgroups: WRKY11 (group IIc), WRKY33 (group I) and WRKY50 (group IIc). WRKY DBDs were expressed with N-terminal GFP- and a C-terminal V5-tag (using the pET-Dest42m2 vector, Brand unpublished). After washing, GFP-fluorescence was measured to quantify the amount of GFP-WRKY DBD fusion protein bound to the DNA probe. Extracts containing WRKY DBDs were pre-incubated with extracts containing MVQ1 or the mutant version MVQ1^{DL} or EV control to assess potential influence of MVQ1 on DNA-binding of WRKY DBDs. MVQ1 and MVQ1^{DL} were expressed with C-terminal His- and V5-tags in *E. coli* (using the pET-Dest42 vector, Brand et al. (2010)). Like all group I WRKYs, WRKY33 has an N-terminal (nDBD) and C-terminal DBD (cDBD). Based on Y2H data from Cheng et al. (2012), who investigated interaction between MVQ1 and WRKY DBDs, we expected MVQ1 to interact with WRKY33 cDBD, but not with WRKY33 nDBD or WRKY11 DBD. BiFC experiments, in which nYFP-WRKY DBD fusions and cYFP-MVQ1 fusions were co-expressed in protoplasts, confirmed that MVQ1 can interact with WRKY33 cDBD, but not with WRKY33 nDBD or WRKY11 DBD (Fig. S7). Interestingly WRKY50 DBD interacted with MVQ1 as well although full-length WRKY50 failed to interact with MVQ1 in a Y2H screen (Pecher et al. 2014) .

Bacterial extracts from strains expressing GFP from the EV control were incubated with both DNA probes to determine background GFP-fluorescence signals in absence of WRKY DBDs (Fig. 25 A). This low-level background fluorescence was independent of the presence of the W-box in the DNA-probe. It was also unaffected by pre-incubation with extracts containing MVQ1 or MVQ1^{DL}. When WRKY11

DBD was incubated with the W2-probe, GFP signals were significantly higher compared to samples incubated with W2-mut, which only reached background levels. Since GFP-fluorescence is a measure for the amount of tagged protein, which is bound to the DNA probe, this result shows that WRKY11 DBD specifically interacts with the W2-probe harbouring an intact W-box. Pre-incubation of WRKY11 DBD with extracts containing MVQ1 or MVQ1^{DL} did not result in altered GFP-fluorescence when compared to the corresponding EV control (Fig. 25 B).

WRKY33 cDBD bound to the W2-probe as indicated by significantly higher GFP-fluorescence compared to the mutant version. Interestingly the GFP-signal in WRKY33 cDBD samples incubated with W2-probe was significantly increased after pre-incubation with MVQ1 extract to more than 3-fold in comparison to MVQ1^{DL} or EV control (MVQ1: 0.836 +/- 0.074 as opposed to EV: 0.240 +/- 0.027 and MVQ1^{DL}: 0.247 +/- 0.043) (Fig. 25 C). When using the W2-mut probe no influence of MVQ1 on GFP-fluorescence was observed. Thus, MVQ1 might promote WRKY33 cDBD binding to the W2-probe.

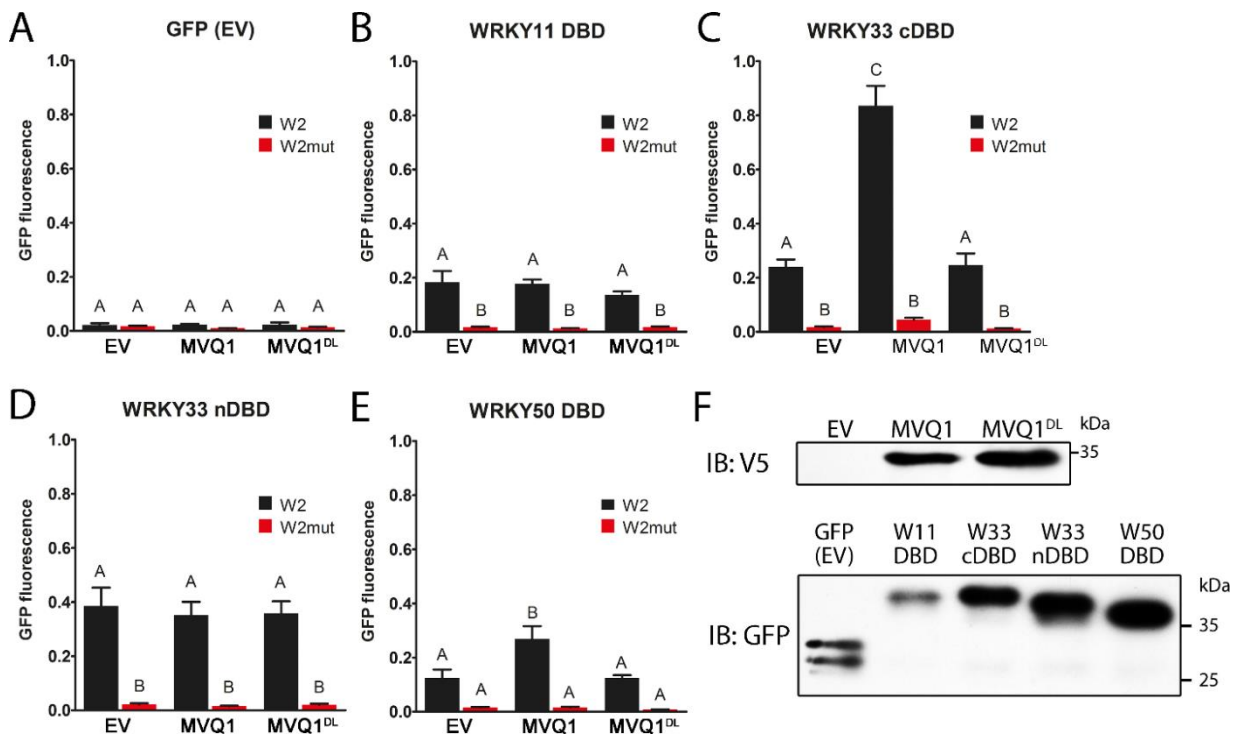


Fig. 25 Effect of MVQ1 on DNA binding of WRKY DBDs: Crude *E. coli* extracts containing (A) GFP (EV control) or GFP-tagged DNA-binding domains (DBD) of (B) WRKY11, (C) WRKY33 cDBD, (D) WRKY33 nDBD or (E) WRKY50 were pre-incubated with bacterial extracts containing MVQ1, MVQ1^{DL} or EV control and incubated with immobilised W2-probe or W2-mut harbouring a mutation in the W-box. After washing, GFP signal was quantified to assess the amount of WRKY DBD bound to the probe. Three independent extracts were used in independent experiments. Bars represent mean values with error bars indicating SEM. Statistically different groups are denoted by letters (One-way ANOVA, Bonferroni multiple comparison post-test $p \leq 0.05$). (F) Bacterial protein extracts were subjected to SDS-PAGE and immunoblot analysis using antibodies against GFP (WRKY DBDs) or the V5 epitope (MVQ1)

Extracts containing WRKY33 nDBD displayed GFP-fluorescence above background level when incubated with the W2-probe, suggesting DNA-protein interaction. Pre-incubation with MVQ1 however, did not have any effect on GFP fluorescence of WRKY33 nDBD in comparison with the controls (Fig. 25 D).

In the case of WRKY50 DBD, GFP fluorescence was not statistically different between samples that were incubated with the W2-probe and those incubated with W2-mut in presence of EV. However, in the presence of MVQ1 extract and the W2-probe, GFP-fluorescence is higher and statistically different suggesting interaction between WRKY50 DBD and the W2-probe. This is not the case with the W2-mut probe or in presence of MVQ1^{DL} extracts.

Thus, it is likely that binding of WRKY50 DBD to the W2-probe is weak (and therefore prone to type II statistical error) and is only detectable, when enhanced by including MVQ1.

Two DNA-probes derived from *AtNHL10* promoter and a third from *AtWRKY33*, which contain one W-box each, were tested in an additional experiment to exclude generation of artefacts by use of the parsley-derived W2-probe. All three probes and the W-box mutant versions were incubated with WRKY33 cDBD extracts after pre-incubation with MVQ1, MVQ1^{DL} or EV extracts respectively. WRKY33 cDBD interacted specifically with a W-box containing probe derived from the *NHL10* promoter (W1) and the interaction was stimulated in presence of MVQ1, while in the case of W2 from *pNHL10* and W2 from *pWRKY33* interaction with WRKY33 cDBD was detected after pre-incubation with MVQ1 exclusively (Fig. S8).

Taken together these results suggest, that presence of MVQ1 might increase binding ability of some WRKY DBDs to their target sequence or in case of WRKY50 DBD enabling them to bind in the first place. Interaction between MVQ1 and WRKY DBDs is apparently necessary for MVQ1-induced increased binding to the target sequence since this effect was only observed for WRKY DBDs, which interact with MVQ1. The importance of MVQ1-WRKY DBD interaction is further supported by the fact that MVQ1^{DL} fails to stimulate DNA binding of WRKY DBDs.

3.5.3. MVQ2-6 can also stimulate binding of WRKY33 cDBD to DNA

The presented results raised the question, whether MVQ1 is the only MVQ, which is able to stimulate binding of WRKY DBDs to DNA. To investigate this, interaction of WRKY33 cDBD with W2 or W2mut probes was analysed after pre-incubation with MVQ2-6 and or respective EV and MVQ^{DL} controls. Additionally MVQ8 was included, since this MVQ (in contrast to MVQ1-6) does not interact with WRKY33 in BiFC assays (Weyhe, unpublished) or Y2H (Pecher et al. 2014).

The low background signals caused by incubation of EV (GFP) crude extract with the probes was comparable to those from previous experiments (Fig. 25 A) and not affected by pre-incubation with

any of the MVQs (Fig. 26 A). All tested MVQs except MVQ8 were stimulating or rather enabling binding of WRKY33 cDBD to the W2-box compared to respective EV or MVQ^{DL} controls (Fig. 26 B). The W2-mut probe was not bound by WRKY33 cDBD even in presence of MVQs. Immunoblot analysis of the bacterial extracts showed that protein amounts of native MVQs and the respective MVQ^{DL}s were usually comparable (Fig. 26 C). In contrast, the amount of different MVQs in the extract differed considerably (e.g. MVQ5 vs. MVQ6) suggesting that direct quantitative comparisons between different MVQs concerning their ability to promote binding of WRKY33 cDBD to the W2-probe are inept. These results illustrate that stimulation of WRKY DBD-DNA-interaction might be a general feature of several MVQs and that ability of MVQs to interact with WRKY is an essential prerequisite.

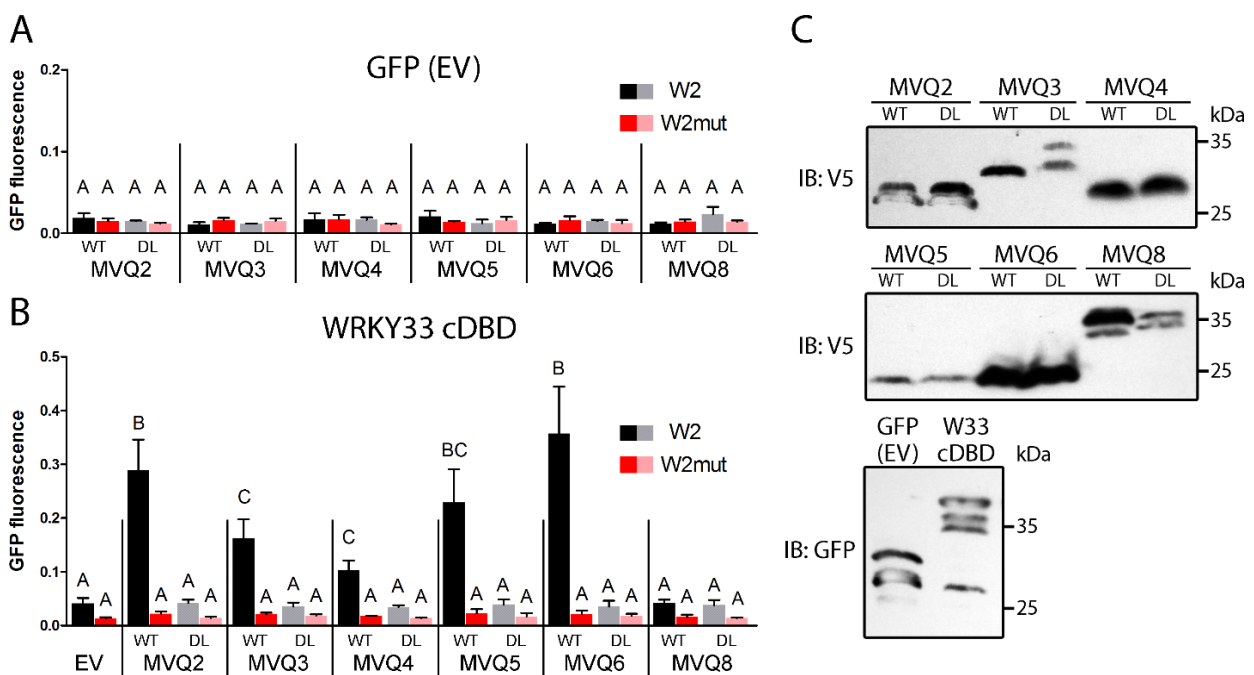


Fig. 26 Effect of different MVQs on DNA binding of WRKY33 cDBD: Crude *E. coli* extracts containing (A) GFP (EV control) or GFP-tagged C-terminal DNA-binding domain (cDBD) of WRKY33 (B) were pre-incubated with bacterial extracts containing MVQ2-6, MVQ8, respective MVQ^{DL}-versions or EV control and incubated with immobilised W2-probe or W2-mut harbouring a mutation in the W-box. After washing, GFP signal was quantified to assess the amount of WRKY DBD bound to the probe. Three independent extracts were used in independent experiments. Bars represent mean values with error bars indicating SEM. Statistically different groups are denoted by letters (One-way ANOVA, Bonferroni multiple comparison post-test $p \leq 0.05$). (C) Bacterial protein extracts were subjected to SDS-PAGE and immunoblot analysis using antibodies against GFP (WRKY33 cDBD) or the V5 epitope (MVQs)

3.6 Potential MVQ1 targets identified by Chromatin Immunoprecipitation (ChIP)

EMSA results showed that MVQ1 can be in a complex with DNA through interaction with WRKY33. Therefore, it seemed feasible to use MVQ1 OE plants for chromatin immunoprecipitation (ChIP) experiments, which allows identification of DNA sequences associated with MVQ1. To see potential changes in DNA-association of MVQ1 after MAMP-treatment samples were treated with 1 μ M flg22 for 1 h or with media as control treatment. First, expression of c-Myc-tagged MVQ1 in seedlings from the MVQ1 OE line K11 was confirmed for the chosen conditions (Fig. 27 A). ChIP-seq analysis was performed by Dr. R. Birkenbihl in the group of Prof. Dr. I. Somssich at the MIPZ in Cologne (2.2.20). Basically, seedlings of WT (Col-0) and MVQ1 OE (K11) were grown in sucrose-supplied MS-medium at long-day conditions and after 12 days treated for 1 h by media exchange with medium containing flg22 (1 μ M) or control medium. For ChIP, samples were subjected to cross-linking followed by chromatin extraction, sonication and immunoprecipitation. The precipitated DNA was purified and processed for library construction and subsequent sequencing. Potential MVQ1-associated regions were identified using the QuEST program searching for DNA-regions enriched in sequencing reads in the MVQ1 OE line compared to WT control.

In the control samples, 220 binding sites could be detected that corresponded to 220 distinct target genes, while in flg22-treated samples 36 binding sites and target genes were detected of which 24 were also identified in control samples (Fig. 27 B, complete list in file 5 of supplementary data on CD). Manual inspection of binding sites in the Integrative Genomic Viewer (IGV) browser (Thorvaldsdottir, Robinson, and Mesirov 2013) revealed that the number of sequence reads at binding sites is reduced in flg22-treated samples compared to the control (see example Fig. 27 C). Upon closer inspection of the 12 binding sites exclusive to the flg22-treated samples in the IGV browser, these sites had comparable or even higher numbers of sequence reads in control samples. Thus, possibly due to stringent peak calling parameters used, these sites may have been missed being classified as MVQ1 targets in the control sample.

These findings indicate that flg22-treatment does not lead to an exchange of MVQ1-targets but in general negatively affects binding of MVQ1 to DNA-targets, most likely through changes in its interaction with WRKY TFs.

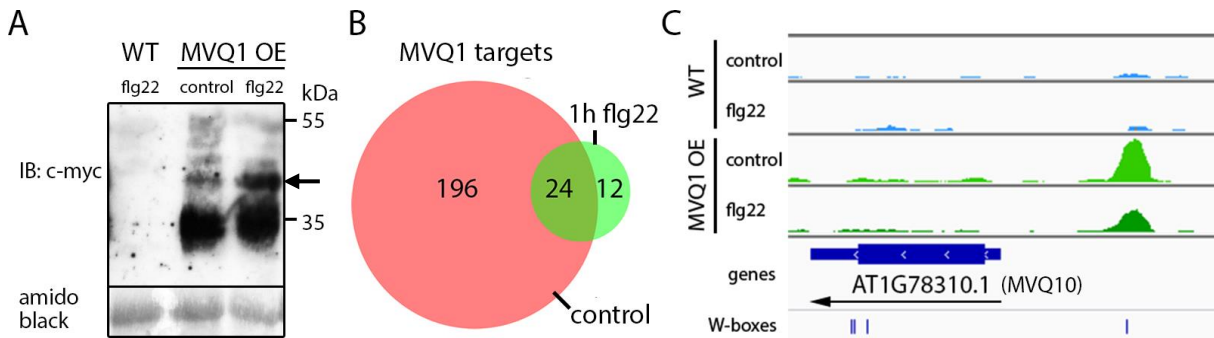


Fig. 27 ChIP-seq reveals target genes bound by MVQ1 in MVQ1 OE line: (A) Seedlings (Col-0; MVQ1 OE K11) were grown in medium (1/2 MS + 0.5 % Sucrose) at long-day conditions. After 12 d seedlings were treated with 1 μ M flg22 or media control for 1 h and subsequently subjected to protein extraction, SDS-PAGE and immunoblot analysis using c-Myc antibody. Arrow indicates bands that could correspond to phosphorylated MVQ1. (B) VENN-diagramm displays target genes identified in control (red) and flg22-treated samples (green) by ChIP-seq analysis. (C) Integrative Genomic Viewer (IGV) image of MVQ10 (AT1G78310) locus with read coverage histograms indicating binding of MVQ1 in WT (blue) and MVQ1 OE samples (green) in control conditions or upon flg22 treatment. 5th row displays gene structures and location of W-boxes is marked by blue lines (last row).

In support of a role of MVQ1 in transcriptional regulation, most of the binding sites were found in promoter regions (57 % in annotated 1000 bp promoters) compared to genomic sequences (27 %). To identify DNA-motifs within the MVQ1 binding region CentriMo motif search was employed by Dr. B. Kracher (MPIPZ, Cologne) searching 500 bp around MVQ1 binding peaks. W-boxes were identified in 87 % of MVQ1 binding sites (Fig. 28 A) and they were highly enriched in close proximity to the binding peak of MVQ1 (central enrichment). Additionally, C-boxes which are binding sites of bHLH and bZIP TFs were identified in 57 % of MVQ1 binding sites but central enrichment was much lower compared to W-boxes (Fig. 28 B). These data indicate that MVQ1 interacts with DNA at W-boxes most probably

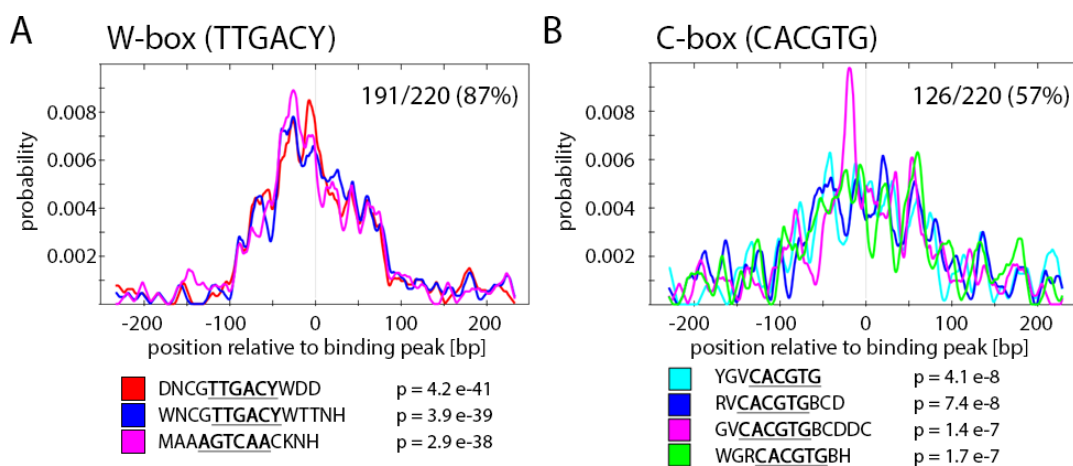


Fig. 28 Motifs present in MVQ1 binding regions: Motif position probability graphs were generated using CentriMo motif search in MVQ1 binding site 500 bp regions. Data was generated by Dr. B. Kracher (MPIPZ, Cologne). Identified motifs belonged to W-box (A) and C-box motifs (B). Graphs display the probability of a specific motif to occur at a certain position. Numbers in the upper right corner indicate total occurrence rate of the respective motif family in all binding site areas. Motif sequences and respective central enrichment p-values are shown beneath the graphs.

indirectly through interaction with WRKY TFs. bHLH or bZIP TFs could also be involved in regulation of some MVQ1 targets since their DNA-binding motif (C-box) was identified as well in MVQ1 binding sites. Analysis of all 232 identified MVQ1 target genes with regard to involvement in biological processes revealed overrepresentation of GO terms related to defence (“response to chitin”), signalling (“response to hormones”, “protein phosphorylation”, “regulation of transcription”) and “response to stress” (Tab. S17).

Tab. 6 lists some selected MVQ1 target genes with known function. A closer look at the target list revealed 37 MVQ1 target genes coding for TFs of which ERFs constitute the biggest group (10) followed by WRKYs (7) and Zinc-finger proteins (5). Interestingly *MVQ10* and *TPL*, both transcriptional co-regulators are also MVQ1 targets. Furthermore, 13 *RLKs* and 2 *RLPs* are among the MVQ1 target genes. These results illustrate that MVQ1 probably binds to genes that are mainly involved in detection of stimuli and in transcriptional regulation.

Tab. 6 Selected target genes of MVQ1: Listed is a selection of genes, which are close to MVQ1 binding peaks in untreated MVQ1 OE line samples. Location of the binding peak and the respective ChIP-score, which is a measure of confidence, are indicated.

AGI number	Gene name	peak location	score ChIP	Description
AT4G18170	<i>WRKY28</i>	intergenic	30.10	WRKY transcription factor 28
AT4G17500	<i>ERF1</i>	intergenic	25.09	Ethylene-responsive binding factor 1
AT1G78310	<i>MVQ10</i>	promoter-TSS	21.89	VQ motif-containing protein
AT4G24240	<i>WRKY7</i>	exon 3	16.88	WRKY transcription factor 7
AT2G23320	<i>WRKY15</i>	intergenic	15.39	WRKY transcription factor 15
AT2G17120	<i>LYM2</i>	promoter-TSS	15.28	LysM domain-containing GPI-anchored protein 2
AT5G49520	<i>WRKY48</i>	intergenic	14.82	WRKY transcription factor 48
AT4G01720	<i>WRKY47</i>	promoter-TSS	14.03	WRKY transcription factor 47
AT1G27730	<i>ZAT10</i>	intergenic	13.68	Zinc finger protein STZ/ZAT10
AT5G46350	<i>WRKY8</i>	promoter-TSS	13.11	WRKY transcription factor 8
AT2G38470	<i>WRKY33</i>	promoter-TSS	12.31	WRKY transcription factor 33
AT5G25910	<i>RLP52</i>	promoter-TSS	12.09	Receptor-like protein 52
AT1G15750	<i>TPL</i>	promoter-TSS	11.86	TOPLESS; transcriptional repressor
AT4G34390	<i>XLG2</i>	promoter-TSS	11.52	extra-large GTP-binding protein 2
AT3G07040	<i>RPM1</i>	promoter-TSS	10.18	Resistance to <i>P.syringae maculicola</i> 1

Among the 232 MVQ1 target genes that were identified by ChIP-seq was *WRKY33*, for which suppression of promoter activity by MVQ1 overexpression was demonstrated in promoter activation assays (see 3.2.3). This suggests, that MVQ1 might suppress flg22-induced activation of the *WRKY33* promoter by binding to it, probably indirectly via WRKYs.

Neither other genes tested in the promoter activation assay, nor genes that were confirmed by qRT-PCR to be suppressed in MVQ1 OE lines after flg22 treatment (see 3.4.5), were identified by the peak calling algorithm as MVQ1 targets. These loci were thus manually inspected in the IGV browser for MVQ1 binding peaks, which were possibly filtered out during peak calling (false negatives).

Inspection of *NHL10*, *GST1* and *ZAT10* revealed MVQ1 binding peaks in the promoter of *GST1* and *ZAT10* that were smaller compared to the peak in the *WRKY33* promoter but especially in flg22-treated samples well above WT-background (Fig. 29, 1st row). Interestingly, *ZAT10* displayed one high additional MVQ1 binding peak in the 3'UTR and another one upstream of the 1000 bp promoter. All binding peaks were in close proximity to W-boxes. In contrast, no binding peak was observed at the *NHL10* locus.

Of those genes, whose suppression of flg22-mediated induction in MVQ1 OE lines was confirmed by qRT-PCR (see 3.4.5), only *PROPEP3* showed an obvious MVQ1 binding peak close to W-boxes in the promoter region (Fig. 29, 2nd row). *FRK1* exhibits a small MVQ1 binding peak in the promoter, which is hardly higher than some background signals in the WT control samples. Based on this data it is difficult to state whether *FRK1* is bound by MVQ1 or not. The *RLP23* locus did not display any MVQ1 binding peaks.

In summary, MVQ1 seems to be associated with promoters of *WRKY33*, *GST1*, *ZAT10* and *PROPEP3*, which results in suppression of MAMP-induced activation of these genes.

Loci like *NHL10* and *RLP23*, which are not bound by MVQ1, might be suppressed in MVQ1 OE lines because MVQ1 binds and suppresses genes encoding components that activate expression of these loci that hence represent indirect targets.

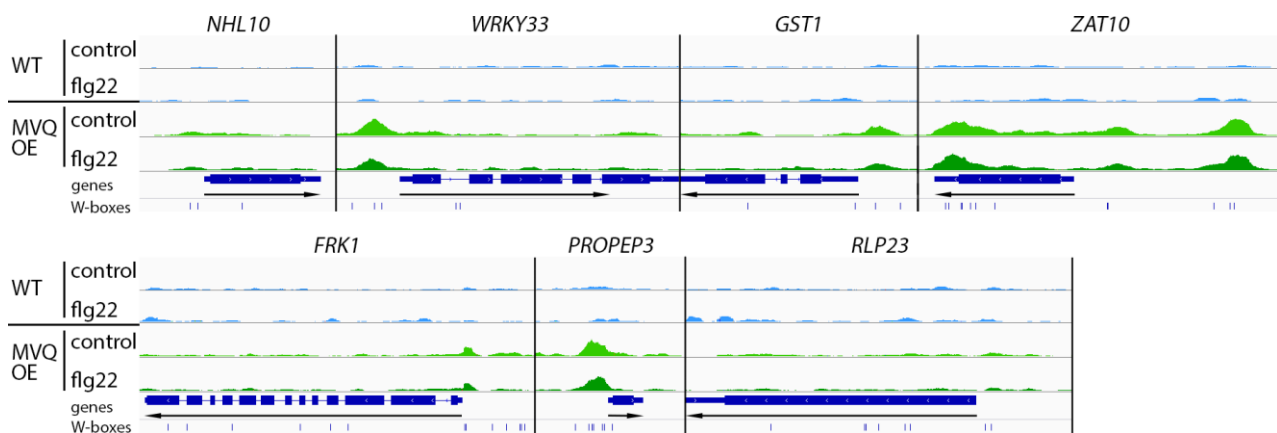


Fig. 29 MVQ1 binding to different loci: Integrative Genomic Viewer (IGV) images of ChIP-seq results for *NHL10* (AT2G35980), *WRKY33* (AT2G38470), *GST1* (AT1G02930), *ZAT10* (AT1G27730), *FRK1* (AT2G19190), *PROPEP3* (AT5G64905) and *RLP23* (AT2G32680) loci. Read coverage histograms indicate binding of MVQ1 in WT (blue) and MVQ1 OE samples (green) in control conditions or upon flg22 treatment. 5th row displays gene structures and location of W-boxes is marked by blue lines (last row).

3.7 The role of MVQ1 in resistance against *Botrytis cinerea*

The data presented in this work indicate that MVQ1 negatively affects MAMP-induced activation of defence-related genes. As a consequence of reduced defence gene expression, defence responses against pathogen attacks might also be influenced by MVQ1. Resistance to the necrotrophic fungus *B. cinerea* has previously been shown to depend on WRKY33 as *wrky33* mutants are more susceptible than WT plants (Zheng et al. 2006; Birkenbihl, Diezel, and Somssich 2012). Since MVQ1 interacts with WRKY33 and might possibly interfere with WRKY-mediated defence gene activation, we were interested whether interaction between *A. thaliana* and *B. cinerea* is influenced by MVQ1 overexpression.

To address this question, leaves of 5-week old WT-plants and plants from two independent MVQ1 OE lines were challenged with *B. cinerea* (strain B05.10) by droplet inoculation with a spore suspension ($10 \mu\text{l } 2 \times 10^5$ spores/ml). Disease symptoms became visible between two and three days post infection (dpi), when necrotic lesions were formed at the inoculation site. The lesions grew further accompanied by wilting and yellowing of the leaves (Fig. 30 A) until the tissue was macerated at 5 dpi.

Quantification of lesion size revealed a certain degree of variability as indicated by scattering of the data points in Fig. 30 B. However, line K11 but not line K42 displayed significantly larger lesion diameters compared to WT already at 3 dpi. At 4 dpi, lesions on leaves of both MVQ1 OE lines were significantly larger than those on WT leaves. The enhanced disease symptoms observed in both MVQ1 OE lines suggest that they might be more susceptible to this *B. cinerea* strain than the WT.

Another way to assess the fungal infection process is quantification of fungal biomass by measuring the amount of genomic fungal DNA at the infection site. To this end, leaf discs ($d = 8$ mm) were harvested at the inoculation site at 2 and 3 dpi. After extraction of DNA, *BcCUTINASE A* (*CutA*) was quantified and referenced to a plasmid control, with which samples had been spiked beforehand.

B. cinerea biomass was analysed in three independent experiments (Fig. 30 C). In all three experiments fungal biomass did not differ between MVQ1 OE lines and WT plants at 2 dpi. Three days after infection in fungal biomass was higher in the K11 line compared to WT only in one out of three experiments, while in the K42 line it was significantly lower in one out of three experiments. Apart from those two cases, no significant differences in fungal biomass compared to WT plants were detected in the MVQ1 OE lines. Overexpression of MVQ1 thus seems to have no effect on *B. cinerea* (B05.10) biomass during the timeframe investigated. Analysis of fungal biomass at later time points e.g. 4 dpi, when lesion sizes significantly differed between WT and MVQ1 OE lines, was hampered by collapse of the harvested tissue and therefore not feasible with the described method.

4. Discussion

4.1 MVQs are potential transcriptional co-regulators of defence genes

Proteins with a conserved VQ-motif (VQs) emerged in the last decade as novel transcriptional co-regulators of plant development and responses to biotic and abiotic stresses (Jing and Lin 2015). Ten MVQs constitute a subgroup of the VQ protein family and are phosphorylated by MAMP-responsive MAPKs MPK3/6. All MVQs (except MVQ8) interact with WRKY TFs from subgroup I and IIc in a Y2H analysis (Pecher et al. 2014).

Hence, MVQs might potentially play a role in transcriptional regulation downstream of MAPKs during MTI. In line with this hypothesis, results of a defence gene promoter activation assay in protoplasts gave a first hint that MVQs might be able to modulate flg22-induced activation of defence gene promoters in a positive (MVQ5 and MVQ8) or negative (MVQ1, 3, 4, 6, 7, 9, 10) manner. The subcellular localisation patterns of MVQs fit to their potential role as transcriptional (Co-) regulators since all of them can be found in the nucleus; in fact, MVQ7-10 are exclusively nuclear-localised.

The protoplast-based promoter activation assay is a rapid and facile screen for testing effects of overexpression (i.e. on defence gene promoter activity). However, it presents some drawbacks that need to be considered and might account in part for variability observed between different experiments. Generation and transformation of protoplasts imposes stress on the cells. The digestion of the plant cell wall by fungal enzymes may release cell wall fragments that potentially serve as DAMPs, which might affect subsequent MAMP response. Furthermore, contamination of protoplasts with microbes cannot be excluded during non-sterile protoplast preparation. Despite these risks, experiments in seedlings and protoplasts yielded comparable results in the context of MAMP-induced Ca^{2+} -influx (Maintz et al. 2014) demonstrating that use of protoplasts in the analysis of MAMP-triggered responses is generally feasible.

The variability in the promoter activation assays might also be explained by phosphorylation of some MVQs during handling of protoplasts. This was indicated in immunoblots that displayed mobility shifts for some MVQs (MVQ1-4). Thus, even in absence of MAMPs a proportion of these MVQs might be phosphorylated. Phosphorylation of MVQs can negatively affect protein stability as demonstrated for MVQ1 (Pecher et al. 2014). Other studies reported regulation of subcellular localisation through phosphorylation of proteins by MAPKs. The heat shock protein HsfA2 is targeted by MPK6, while the TF VIP1 is a substrate of MPK3 and phosphorylation promotes nuclear localisation of both proteins (Djamei et al. 2007; Evrard et al. 2013).

In fact, phosphosite-mutants of MVQ3, MVQ4 and MVQ5 were exclusively located in the nucleus while the native versions localised to the nucleus and cytoplasm indicating that phosphorylation of these proteins might promote cytoplasmic localisation. Phosphorylation by MPK3/6 could provide a mechanism to abolish transcriptional regulation activity of these MVQs by relocalisation out of the nucleus. On the other hand, it cannot be excluded that mutation of all phosphosites in these proteins impairs protein folding and leads to localisation artefacts.

In order to enable further functional characterisation of MVQs in plants, T-DNA insertion lines were analysed to identify plant lines with reduced *MVQ* expression. However, T-DNA insertion lines with reduced *MVQ* expression could only be identified in case of MVQ1, MVQ7 and MVQ8 respectively (Fig. S11). While this work subsequently focused on the characterisation of MVQ1, the CRISPR-Cas9 system was used in parallel to generate *mvq* knock-out mutant lines (selection still in process), which will be a valuable genetic tool to investigate MVQ functions in the future (for list of gRNA targets see Tab. S7).

4.2 MVQ1 is a negative regulator of defence gene expression

In order to effectively use limited resources, plants need to prioritise either growth or defence, depending on external and internal signals (Huot et al. 2014). Negative regulation is therefore important to fine-tune immune responses and avoid excessive activation of defence, which would result in reduced fitness.

Consequently, all aspects of MTI from signal perception and transduction to transcriptional regulation are tightly controlled by negative regulators.

At the level of PRRs the PRR-complex formation prior to ligand binding is inhibited by pseudokinases like BAK1-INTERACTING RLK 2 (BIR2), which interacts with BAK1 to prevent its association with FLS2 in absence of flg22 (Halter et al. 2014). Additionally, PLANT U-BOX PROTEINs (PUB12 and PUB13) directly ubiquitylate FLS2 leading to its degradation and attenuation of flg22-signalling (Lu et al. 2011). Further downstream, protein turnover of the RLCK BIK1 is promoted by CPK28-mediated phosphorylation (Monaghan et al. 2014).

Phosphorylation events at the PRR complex, at the RLCKs and in MAPK cascades are crucial for signal transduction during immune response. Hence, phosphatases that dephosphorylate activating residues in RLKs, RLCKs or MAPKs are important negative regulators of MTI. For example, PROTEIN PHOSPHATASE 2A (PP2A) dephosphorylates BAK1 to dampen immunity (Segonzac et al. 2014), while MAPK PHOSPHATASE 1 (MKP1) negatively regulates MPK6 activity (Anderson et al. 2011).

Negative regulation of immunity at the transcriptional level can be mediated by action of transcriptional repressors or the retardation of transcriptional activators in inhibitory complexes. WRKY33 is kept in such an inhibitory complex together with MPK4 and the VQ protein MKS1 (Qiu, Fiol, et al. 2008). Upon MAMP elicitation, MPK4 is activated and phosphorylates MKS1, which leads to the release of MKS1-WRKY33 and activation of WRKY33-targeted genes.

The trihelix TF ASR3 was characterised as a transcriptional repressor of defence gene expression. Transcriptomic analysis revealed that transcription of most flg22-activated genes is enhanced in *asr3*, while flg22-mediated activation is impaired in an ASR3 OE line (Li et al. 2015). In line with these results the *asr3* mutant exhibits enhanced disease resistance to *P. syringae*. MAMP-triggered phosphorylation of ASR3 by MPK4 results in increased binding to its target genes (i.e. *FRK1*) and therefore is part of a negative feedback loop fine-tuning MTI.

Several lines of evidence provided in the present work support a role of MVQ1 as a negative regulator of defence gene expression. In protoplasts MVQ1 overexpression lead to suppression of flg22-induced activation of promoters from four defence-related genes (*NHL10*, *WRKY33*, *ZAT10* and *GST1*). Furthermore, a genome-wide transcriptomic analysis of the response to flg22 in an MVQ1 OE line and WT plants uncovered 404 genes whose flg22-mediated induction was strongly reduced in the MVQ1 OE line compared to WT 1 h after flg22 treatment. Among those genes were prominent defence marker genes and signalling components like receptor kinases, NLRs and TFs. Thus, MVQ1 seems to be involved in repression of a set of flg22-inducible genes. This is reminiscent of ASR3 but unlike ASR3, MVQ1 does not contain a typical repressor motif and probably acts indirectly via interactions with WRKYs. Similar to the VQ MKS1, MVQ1 might be part of an inhibitory complex (as discussed in 4.3). The repressive effect of MVQ1 on many flg22-activated genes explains the previous observation that flg22-induced resistance against *P. syringae* is impaired in MVQ1 OE lines (Pecher et al. 2014).

Infection assays with the necrotrophic fungus *B. cinerea* hinted at a possible negative role of MVQ1 in resistance of *A. thaliana* to this pathogen. While necrotic lesions were significantly larger in MVQ1 OE lines, no significant changes in *B. cinerea* biomass were detected. However, in two previous experiments under the same conditions *B. cinerea* biomass was significantly increased in the MVQ1 OE line K11 when compared to WT (Fig. S9). Fungal biomass is commonly considered to be a more accurate measure of pathogen infection since development of disease symptoms (i.e. necrotic lesions) depends on the physiological status of the plant, which can potentially be affected by MVQ1 overexpression (pleiotropic effects).

The lack of a clear susceptibility phenotype in MVQ1 OE lines might be due to use of the B05.10 strain in this work. This strain can infect Col-0 plants, which are on the other hand fairly resistant against two other *B. cinerea* strains: BMM1 and 2100 (Liu et al. 2017). Resistance towards BMM1 and 2100 depends on WRKY33, since the *wrky33* mutant is susceptible to these strains. Liu et al. (2017)

demonstrated that B05.10 is able to hamper the accumulation of WRKY33 on protein and transcript level during infection, which affects downstream responses like camalexin production. Therefore, interfering with WRKY33-mediated responses by overexpression of MVQ1 might not strongly affect growth of this strain as it suppresses WRKY33-mediated responses anyway. It will be interesting to assess, whether the WRKY33-dependent resistance towards BMM1 or 2100 is affected in MVQ1 OE lines.

Several VQs (VQ5, VQ12, VQ20, MKS1, JAV1, VQ25 and VQ29) have been reported to negatively regulate resistance against *B. cinerea* (Petersen et al. 2010; Cheng et al. 2012; Hu, Zhou, et al. 2013; Wang, Hu, et al. 2015). The modes of action and involved pathways are barely understood except for JAV1 (VQ22), which is part of a repressor complex that includes JAZ8 and WRKY51 and suppresses JA-mediated defence responses against herbivores and necrotrophs (Yan et al. 2018).

In contrast SIB1 (VQ23) and SIB2 (VQ19) are positive regulators of WRKY33-mediated resistance against *B. cinerea* (Lai et al. 2011). Besides increasing experimental evidence, the significance of VQs in plant immunity is indirectly supported by the recent identification of NLRs with a VQ-motif as “integrated domain or decoy” in rice, wheat, apple and rape (Sarris et al. 2016). Integration of the VQ-motif into NLRs implies that VQs (or a specific VQ) represent virulence target(s) of as yet unknown effectors. Alternatively, the VQ-motif may dock the NLR to specific chromatin regions through its interacting endogenous WRKY transcription factor(s).

4.3 The molecular mode of action for MVQ1

Transcriptomic data generated in the present work supports the notion that MVQ1 is negatively affecting transcriptional reprogramming during MTI. A major aim was to obtain insights into the molecular mechanisms that underlie MVQ1 function as a transcriptional co-regulator.

To this end the effects of MVQ1-WRKY interactions on WRKY-DNA binding were addressed in DNA-protein interaction assays and DNA-targets of MVQ1 were identified by CHIP-seq.

4.3.1 Does MVQ1 affect DNA-binding or transcriptional activity of WRKYs?

MVQ1 interacts with WRKYs from subgroup I and IIc as demonstrated by Y2H-assays (Pecher et al. 2014) and interactions were confirmed *in planta* for selected MVQ1-WRKY pairs using BiFC (see 3.3). MVQ1^{DL}, which is unable to interact with WRKYs, fails to suppress the flg22-induced activation of the *NHL10* promoter and in absence of a MAMP stimulus, MVQ1 was able to antagonise WRKY33-

mediated activation of *NHL10*. Furthermore, W-boxes are enriched in a set of genes, whose flg22-mediated induction is suppressed by MVQ1 (Tab. S16). These findings suggest that MVQ1 affects defence gene expression by targeting WRKY TFs. In order to further corroborate or challenge this hypothesis, it would be intriguing to analyse transcript levels of flg22-inducible genes in MVQ1^{DL} OE lines.

A simple model, in which MVQ1 interacts with WRKYs to prevent their binding to DNA and subsequent activation of transcription, could explain suppression of flg22-induced gene expression in MVQ1 overexpressing protoplasts and plant lines. As VQs interact with WRKYs in close proximity to the WRKY-DBD (Cheng et al. 2012), it is tempting to propose that VQ-WRKY interactions sterically interfere with DNA-binding of WRKYs. Results from Hu, Chen, et al. (2013), who observed decreased DNA-binding of WRKY8 after incubation with MVQ10 (VQ9), support this idea.

In contrast MKS1, SIB1 and SIB2 increase binding of WRKY33 to target DNA, although its transcription-activating activity was unaffected in plants overexpressing SIB1 (Lai et al. 2011). In a more recent study Jiang and Yu (2016) demonstrated that WRKY33 and WRKY57 competitively bind to a W-box in the promoters of *JAZ1* and *JAZ5* to either repress (WRKY33) or activate (WRKY57) gene expression. SIB1 and SIB2 influenced this competition in favour of WRKY33 (Jiang and Yu 2016).

EMSA experiments showed that MVQ1 (but not MVQ1^{DL}) is part of a MVQ1-WRKY33-DNA complex as indicated by the occurrence of a supershift of the W-box containing probe when WRKY33 had been pre-incubated with MVQ1. Pre-incubation with MVQ1 did not seem to drastically affect binding of WRKY33 to the probe. Quantitative data from DNA-protein interaction assays on the other hand suggests that MVQ1 is able to increase DNA-binding of WRKY DBDs significantly. This assay quantified binding of GFP-tagged WRKY DBDs to immobilised DNA-probes by measuring GFP fluorescence. MVQ1 specifically stimulated DNA-binding of interacting WRKY DBDs. These data imply that MVQ1 does not inhibit WRKY DNA-binding by steric interference but possibly rather stimulates WRKY DBD-DNA interactions.

To explain the negative regulation of MTI by MVQ1 in accordance with these results, one could envision two alternative scenarios. In the first scenario (Fig. 31 A) MVQ1 increases the DNA-binding of WRKYs, which act as repressors of MAMP-responsive genes, thus inhibiting the replacement of these WRKY repressors by activators upon a stimulus. This way MVQ1 could influence competition of different WRKYs for W-boxes as it was suggested for SIB1 and WRKY33/57 competition (Jiang and Yu 2016).

The second scenario (Fig. 31 B) assumes that the transcription activation activity of WRKYs is affected by the interaction with MVQ1. Transcription activation requires recruitment of general TFs and RNAPII to the promoter. A multiprotein complex called mediator connects specific TF (i.e. WRKYs) with RNAPII and facilitates preinitiation complex formation (Mathur et al. 2011). The mediator complex in plants

consists of 33 subunits (six of which are plant-specific), which integrate regulatory signals to activate or repress transcription in response to developmental or stress signals (Yang, Li, and Qu 2016). WRKY33 was demonstrated to physically interact with the mediator subunit MED16 for transcriptional activation of two defence genes (*PDF1.2* and *ORA59*) during defence response against *Sclerotinia sclerotiorum* (Wang, Yao, et al. 2015).

In the second scenario binding of MVQ1 to WRKYs could potentially influence or interfere with the interaction between WRKYs and the mediator complex to repress activation of transcription.

Information on the 3-dimensional structure of MVQ1 or other VQs, which is lacking until now, could enable modelling of the structure of VQ-WRKY complexes and would further advance our understanding of the molecular mode of action of VQs like MVQ1. To decide which of the two proposed scenarios is better reflecting the *in vivo* situation, it will be important to determine the identity of MVQ1-interacting WRKYs (see 4.3.4) using e.g. co-immunoprecipitation (Co-IP) followed by mass spectrometry analysis and to identify potential connections to the mediator complex.

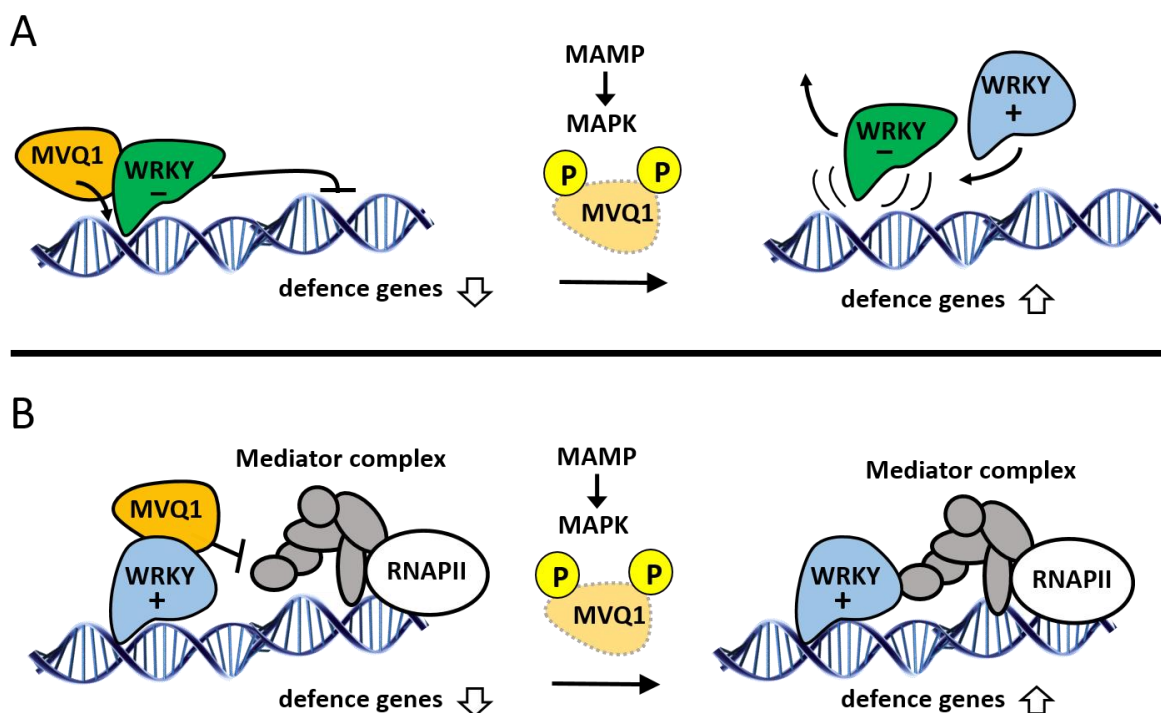


Fig. 31 Two alternative models describing the molecular mode of action of MVQ1: (A) MVQ1 interacts with WRKY repressors to increase their DNA-binding activity resulting in repression of target genes. MAPK-mediated phosphorylation and subsequent degradation of MVQ1 or its dissociation from the complex negatively affects DNA-binding of the WRKY. WRKYs can subsequently be substituted by other WRKYs with different transcriptional activity. **(B)** MVQ1 interacts with WRKYs, which are acting as transcriptional activators, to prevent their interaction with the transcriptional machinery. MAPK-mediated phosphorylation and subsequent degradation of MVQ1 or dissociation from the complex allows the WRKYs to activate transcription by recruiting the transcriptional machinery (Mediator complex and RNA-Polymerase II).

4.3.2 MVQ1 is associated with target gene promoters via WRKYs

Engagement of MVQ1 in a complex with WRKY33 and DNA-probe *in vitro* prompted the investigation of potential DNA targets of MVQ1 by ChIP-seq analysis of MVQ1 OE plants. MVQ1 binding peaks corresponding to 220 genes in untreated samples and 36 genes in flg22-treated samples respectively were identified. This dataset represents the first experimental evidence of association of a VQ with DNA *in planta*.

The search for motifs in the DNA sequences close to MVQ1 binding peaks revealed that W-boxes are present in 87 % of the targets and strongly enriched at the centre of the binding peak, suggesting indirect binding of MVQ1 to DNA mainly via WRKYs. In fact, comparison of the 220 MVQ1 targets with *in vivo* ChIP targets of WRKY18, WRKY33 and WRKY40, which were identified by Birkenbihl, Kracher, and Somssich (2017) showed considerable overlap of 111, 102 and 115 genes respectively. Analysis of the 25 MVQ1 targets with the highest ChIP-score integrating ChIP-seq data for WRKY18, WRKY33 and WRKY40 as well as targets, which were precipitated with an anti-all WRKY antibody that recognises at least 27 different WRKYs (Birkenbihl et al. 2018) showed that all of those MVQ1 binding peaks correlated with WRKY binding peaks at the same position (Fig. S10). In most cases the targets were targeted by all three WRKYs (2 h after flg22 treatment), but there are examples of MVQ1 targets like *MVQ10* that are only bound by WRKY33, whereas others are targeted by WRKY18 and WRKY40 but not WRKY33 (Fig. S10).

C-boxes, which can be bound by bZIP and bHLH TFs, are present in 57 % of MVQ1 binding regions and also enriched at the peak centre but with lower p-values compared to W-boxes. MVQ1 could therefore potentially also be associated with DNA-bound bZIP and bHLH TFs, although evidence for physical interaction between these proteins and MVQ1 is lacking so far. On the other hand VQ29 was reported to interact with the bHLH TFs PIF1 and PIF3 (Li, Jing, et al. 2014) while VQ18 and VQ26 interact with the bZIP ABI5.

Comparison of the identified MVQ1 target genes with RNA-seq data from Birkenbihl, Kracher, and Somssich (2017) that were generated under conditions comparable to the ChIP-seq experiment (as opposed to microarray data in this work) demonstrated that 118 of the 220 genes targeted by MVQ1 are upregulated (≥ 2 fold) 1 h after flg22 treatment in WT plants, while only 5 are downregulated illustrating that MVQ1 mainly targets flg22-inducible genes.

As MVQ1 overexpression negatively affected flg22-mediated induction of 404 genes (see 3.4.4) the question, whether these genes are directly targeted by MVQ1 arises. Comparison of both gene lists uncovered little overlap between the 404 genes and the 220 MVQ1 targets since only 14 genes are targeted by MVQ1 and display reduced flg22-mediated induction in MVQ1 OE plants. This could partly be attributed to differences of the experimental systems (seedlings in liquid culture vs. leaves of adult

soil-grown plants). Apart from that, MVQ1 might target genes coding for signalling components, whose altered transcript levels in turn affect flg22-induced activation of other genes, which would hence be indirect targets of MVQ1.

Furthermore, additional MVQ1 targets might not have been identified by the ChIP algorithm due to stringent peak calling parameters. Manual inspection of genes, whose flg22-induced activation was suppressed by MVQ1 overexpression either in promoter activation assays (3.2.1 & 3.2.3) or in qRT-PCR experiments (3.4.5) revealed additional MVQ1 binding peaks that were missed during automated peak calling (Fig. 29).

PROPEP3 and three of the promoters tested in the activation assays (*pWRKY33*, *pGST1*, *pZAT10*) are direct targets of MVQ1. In contrast *pNHL10* seems not to be a direct MVQ1 target. But since *NHL10* transcripts levels are lower in MVQ1 OE lines after flg22 treatment compared to WT, it might be an indirect target. Requirement of additional regulators for control of *pNHL10* might also explain higher variability of the suppressive effect of MVQ1 on *pNHL10*, when compared to the three promoters, which are directly targeted by MVQ1.

The 232 MVQ1 targets (220 in control samples, 12 additional ones in flg22-treated samples, see file 5 of supplementary data on CD) identified by the algorithm probably represent only the tip of the iceberg since manual data inspection led to the identification of additional binding peaks. The fact that MVQ1 most likely does not interact directly with target DNA aggravates problems in efficient crosslinking and hence makes ChIP-seq a challenging task. The ChIP-seq analysis was performed with two replicates, but in the second replicate ChIP-seq failed, due to insufficient amount and quality of recovered DNA. Thus, all results need to be treated with caution until validation by another ChIP-seq replicate or ChIP-qPCR. Nevertheless, the ChIP-seq data set strongly suggests that MVQ1 is associated with some flg22-inducible genes via WRKY TFs mainly in promoter regions to repress transcriptional activation. Additional indirect target genes might be modulated by MVQ1-targeted regulators.

4.3.3 Regulation of MVQ1 activity by MAPKs

MVQ1 is phosphorylated by the MAMP-responsive MAPKs MPK3 and MPK6 and MVQ1 levels are reduced upon treatment with flg22 (Pecher et al. 2014). Phosphorylation of MVQ1 by the two MAPKs triggers its degradation as indicated by increased stability of an MVQ1 variant, in which all phosphosites were mutated. Degradation of repressors is a common strategy to ensure rapid activation of preformed signalling modules.

There are for instance striking similarities to innate immune responses in mammals that involve the NFκB TFs. In absence of inflammatory signals, INHIBITOR OF NFκB (IκB) interacts with NFκB and masks nuclear localisation signals (NLS), which results in cytoplasmic retention of the TFs (Karin 1999).

Recognition of bacterial LPS or proinflammatory cytokines by receptors triggers activation of the I κ B KINASE (IKK) complex (Hoesel and Schmid 2013). IKK phosphorylates I κ B leading to its ubiquitination and subsequent degradation. NF κ B enters the nucleus and activates expression of genes involved in inflammation.

ChIP-seq of samples from MVQ1 OE plants, which were treated with flg22 for 1 h, identified much lower binding peaks and consequently fewer targets compared to control samples. Interestingly the protein amount of Myc-tagged MVQ1 did not drastically change after flg22 treatment (Fig. 27A) probably due to strong activity of the 35S promoter that controls MVQ1 expression in the MVQ1 OE line. This raises the possibility that association of MVQ1 with DNA is not only controlled by phosphorylation-induced degradation. Phosphorylation of MVQ1 might also affect the MVQ1-WRKY interaction. This hypothesis could be tested by fluorescence lifetime imaging (FLIM) of Förster resonance energy transfer (FRET) between WRKYs and MVQ1, which are labelled with the respective fluorescent proteins. Comparison of the FLIM-FRET between protoplasts transfected with a constitutively active MAPKK (i.e. MKK5^{DD}) and an inactive control would provide valuable insights into the effect of phosphorylation on MVQ1-WRKY interactions. One could also quantify WRKY-interactions of MVQ1 phosphosite mutants and phosphomimic mutants i.e. by means of split-Luciferase assay, bearing in mind that mutation of 12 putative MAPK-phosphorylation sites (Fig. S2) might affect protein folding.

Another intriguing but unsolved question is whether MVQ1 is part of an inhibitory complex that involves interacting WRKYs and possibly MPK3 or MPK6 as it is proposed for MPK4, MKS1 and WRKY33 (Qiu, Fiil, et al. 2008). Co-immunoprecipitation of tagged MVQ1 and subsequent mass spectrometry analysis might be a good way to address this question.

4.3.4 Integration of MVQ1 into the WRKY network

WRKYs are important transcriptional regulators of plant defence responses. The enrichment of W-boxes in promoters of *WRKY* genes suggest extensive auto- and cross-regulation, establishing an intricate network of positive and negative feedback loops that govern the transcriptional response to pathogen attacks (Eulgem and Somssich 2007; Llorca, Potschin, and Zentgraf 2014).

In response to flg22 treatment 27 WRKYs are transcriptionally activated within one hour, which in almost all cases correlates with enhanced protein levels, while transcript and protein levels of 17 other WRKYs are unaffected (Birkenbihl et al. 2018).

A concept proposing that functionally important W-boxes are bound by constitutively expressed WRKYs and that MAMP treatment induces expression of a set of inducible WRKYs, which replace the pre-bound WRKYs to activate transcription was put forward by Turck, Zhou, and Somssich (2004) based

on ChIP results obtained in parsley. This hypothesis was further confirmed in *A. thaliana* by the finding that WRKY40 and WRKY33 bind their target genes in response to flg22 treatment, while no binding occurred in untreated samples (Birkenbihl, Kracher, and Somssich 2017). Among the WRKY33/40 targets are 30 *WRKY* genes (22 inducible, 6 not expressed, 2 constitutive) whose promoters are pre-occupied by other WRKYs, which were precipitated with an anti-all WRKY antibody in absence of flg22 (Birkenbihl et al. 2018). Interestingly, microarray data shows that transcript levels of flg22-inducible, but not those of constitutively expressed, WRKYs are increased upon treatment with the protein synthesis inhibitor cycloheximide (William et al. 2004). This suggests that expression of these inducible *WRKY* genes is negatively regulated by pre-existing proteins, which are most likely constitutively expressed WRKYs.

Our ChIP-seq results identified seven *WRKY* genes (WRKY7, 8, 15, 28, 33, 47, 48), all of which belong to the flg22-inducible group, as direct targets of MVQ1. In case of WRKY33 and WRKY47, suppression of flg22-mediated induction by MVQ1 could also be demonstrated in the present work. This could be a hint that MVQ1 together with constitutively expressed *WRKY*s might be involved in repression of flg22-induced *WRKY*s. This is supported by the fact that *WRKY*s belonging to group I and thus being potential VQ-interactors are clearly overrepresented among constitutively expressed *WRKY*s (Birkenbihl et al. 2018). Repression of defence genes by a WRKY-MVQ1 repressor complex could be a mechanism to prevent untimely defence responses. MAMP treatment results in release of repression through MAPK-mediated phosphorylation of MVQ1 resulting in degradation or dissociation from the WRKY interactor. Since *MVQ1* transcripts are induced in response to flg22-treatment (Fig. S6), MVQ1 might also serve to shut down defence responses after the MAMP stimulus is over.

The WRKY network in MTI is very robust, probably due to functional redundancy, since simultaneous elimination of three highly connected hubs (WRKY18, 33, 40) does not alter seedling responses to flg22 or flg22-induced resistance to bacteria (Birkenbihl et al. 2018). Complexity of the network is increased enormously by WRKY-VQ interactions which may differentially affect WRKY functions as co-activators or co-repressors.

WRKY33 is an example for a TF with dual functions. While in it binds to promoters of genes involved in ET-response or camalexin biosynthesis such as *PAD3* and *CYP71A12* to activate their transcription (Mao et al. 2011; Liu et al. 2015), it represses more than 75 % of its binding targets in response to *B. cinerea* infection (Liu et al. 2015). Among the repressed targets are many SA-related genes associated with cell death. WRKY33 function as either a transcriptional repressor or activator might depend on interactions with VQs such as MVQ1 and MKS1 and its recruitment to distinct protein complexes. The fact that ten MVQs are targeted by MPK3/6 and MKS1 is regulated by MPK4 adds another layer of complexity to the network as phosphorylation might facilitate substitution of WRKY-interacting MVQs with other VQs thereby modulating transcription (Weyhe et al. 2014). Potential functional redundancy of some

VQs (i.e. closely related MVQ1-4) might explain why mutants of these genes don't display obvious phenotypes and thus were not retrieved in mutant screens for altered immune phenotypes.

In addition to regulation on the transcriptional level, the WRKY network is controlled by posttranslational modifications. Different MAPKs (Popescu et al. 2009) or the RLCK BIK1 (Lal et al. 2018) phosphorylate WRKYs probably to modulate their transcriptional activity. For example, phosphorylation of WRKY33 promotes its transactivation activity (Mao et al. 2011). In case of WRKY46 phosphorylation by MPK3/6 seems to negatively affect WRKY46 stability, while phosphorylation is required for full transactivation activity (Sheikh et al. 2016). A screen of WRKYs for *in vitro* phosphorylation by MPK3/6 in the same study suggests that most of the 48 tested WRKYs are putative MPK3/6 substrates but *in vivo* evidence is lacking for a majority of them.

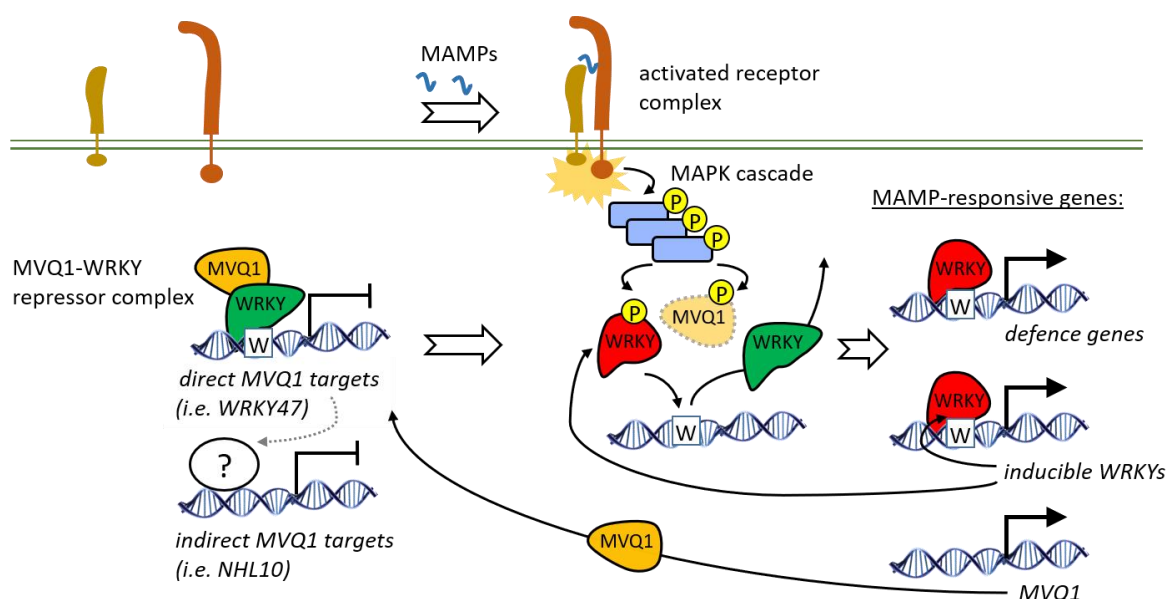


Fig. 32 Model of MVQ1 function within the WRKY network during MTI: MVQ1 engages with constitutively expressed WRKYs (green) in MVQ1-WRKY repressor complexes to suppress transcription of direct and indirect target genes in absence of MAMP stimuli. Upon MAMP-recognition and MAPK activation, MVQ1 is phosphorylated and removed from the complex. This possibly promotes substitution of repressor WRKYs with other inducible WRKYs (red), which bind promoters of MAMP-responsive genes to induce transcription. Inducible WRKYs activate transcription of their own genes providing a positive feedback loop. MAPKs further modulate transcription by phosphorylation of WRKYs. MAMP-induced activation of *MVQ1* transcription can serve as a negative feedback regulation to shut down MAMP-responsive transcription. Other VQs, which are not targeted by MAPKs might interact with WRKYs to influence transcription in a positive or negative manner. W indicate W-boxes and P indicate phosphorylation.

For future research on MVQ1 it will be important to pin down which WRKYs are interacting with MVQ1 in a given physiological situation and if they act as repressors or activators. Genes coding for proteins functioning in the same pathway are often co-expressed. Hence, in order to reduce the candidate list of possible WRKY interactors, the ATTED-II tool (Obayashi et al. 2018) was employed to search for WRKY genes that are co-expressed with *MVQ1*. *MVQ1* directly connects with *MKS1*, a galactose oxidase/kelch repeat superfamily protein (AT5G43190) and *WRKY15* in a network based on co-

expression data. However, WRKY15 belongs to group IId WRKYs and hence cannot be a direct MVQ1-interactor. Co-immunoprecipitation (Co-IP) followed by mass spectrometry analysis can help to identify WRKY interactors of MVQ1 and potential connections to other transcriptional regulators such as the mediator complex.

5. Summary

Plants respond to pathogen attacks with defence responses that involve transcriptional reprogramming. Accumulating experimental evidence implicates VQ-motif containing proteins (VQs) in the regulation of gene expression via interaction with transcription factors (e.g. WRKYs). Members of a subgroup of *Arabidopsis thaliana* VQs, termed MVQs, are substrates of the pathogen-responsive MAPKs MPK3/6. In agreement to their putative role as transcriptional co-regulators, all ten MVQs can localise to the nucleus, with additional cytoplasmic localisation of MVQ1-6. Defence gene promoter activation assays revealed that most MVQs suppressed or enhanced MAMP-induced activation of *pNHL10*, thus providing a first hint for a role of MVQs in transcriptional regulation of defence responses.

The identification of genes and pathways regulated by MVQ1 and the elucidation of the molecular mechanisms underlying MVQ1 function were the major aims of this work. A microarray analysis uncovered about 400 genes, whose MAMP-mediated induction is suppressed in MVQ1 OE lines, establishing MVQ1 as a novel negative transcriptional regulator of MTI. Consistent with this notion, MVQ1 OE lines displayed enhanced disease symptoms after infection with the necrotrophic fungus *Botrytis cinerea*, indicating a potential role of MVQ1 in plant immunity that warrants further exploration.

MVQ1 interacted with several WRKY TFs *in planta* and results from DNA-protein interaction assays suggested the existence of MVQ1-WRKY-DNA complexes. Successful isolation of DNA from immunoprecipitated MVQ1 (ChIP) confirmed this hypothesis and led to the identification of 232 direct MVQ1 target genes. These results represent the first experimental evidence of a VQ protein's association with DNA *in planta*. Overrepresentation of WRKY-binding motifs (W-boxes) at MVQ1 binding peaks and considerable overlap with direct WRKY targets underpin the notion of an indirect MVQ1-DNA interaction via WRKYs. Treatment with flg22 decreased the number and intensity of MVQ1 binding peaks indicating that phosphorylation by MAPKs liberates MVQ1 from the WRKY-DNA complex.

Interaction of MVQ1 with WRKYs increased DNA-binding activity of WRKYs *in vitro*. This led to the proposition of a model, in which MVQ1 engages with WRKYs in a repressor complex, promoting its DNA-binding activity to inhibit defence gene expression. Alternatively, MVQ1 might interfere with the recruitment of the transcription machinery by WRKYs with transactivation activity.

6. Zusammenfassung

Auf Angriffe durch Pathogene reagieren Pflanzen mit Abwehrreaktionen, die transkriptionelles Umprogrammieren erfordern. Proteine mit VQ-motiv (VQs) interagieren mit Transkriptionsfaktoren (TF), um die Genexpression zu modulieren und eine Untergruppe von *Arabidopsis thaliana* VQs, die MVQs genannt werden, stellen Substrate der Pathogen-responsiven MAPKs MPK3/6 dar. Entsprechend ihrer vermuteten Funktion als transkriptionelle Co-Regulatoren sind alle zehn MVQs im Zellkern zu finden, wobei MVQ1-6 zusätzlich im Cytoplasma zu finden sind. Promotoraktivierungsstudien zeigten, dass die meisten MVQs die MAMP-induzierte Aktivierung des *NHL10* Promotors unterdrücken oder verstärken können. Dies stellt einen ersten Hinweis auf eine Rolle von MVQs in der transkriptionellen Regulation der pflanzlichen Abwehrantwort dar.

Die Identifizierung von Genen und Prozessen, die von MVQ1 reguliert werden, sowie die Aufklärung der zu Grunde liegenden molekularen Mechanismen waren das hauptsächliche Ziel dieser Arbeit. Mittels Mikroarrayanalyse wurden etwa 400 Gene identifiziert, deren MAMP-vermittelte Aktivierung in MVQ1 Überexpressionslinien unterdrückt ist. Diese Ergebnisse etablieren MVQ1 als negativen transkriptionellen Regulator der MAMP-vermittelten Abwehrantwort

In Übereinstimmung mit diesen Ergebnissen wiesen MVQ1 Überexpressionslinien im Vergleich zum Wildtyp verstärkte Symptome nach Infektion mit dem nekrotrophen Pilz *Botrytis cinerea* auf. Dies legt eine mögliche Rolle von MVQ1 in der pflanzlichen Immunität, die jedoch tiefergehend untersucht werden sollte, nahe.

MVQ1 interagiert mit einigen WRKY TFs *in planta* und Ergebnisse von DNA-Protein Interaktionsstudien weisen auf die Existenz eines MVQ1-WRKY-DNA Komplexes hin. Die erfolgreiche Isolation von DNA aus immunoprecipitiertem MVQ1 mittels ChIP bestätigte diese Hypothese und führte zur Identifizierung von 232 Genen, die von MVQ1 gebunden werden. Diese Ergebnisse stellen den ersten experimentellen *in planta* Beweis für die enge Assoziierung eines VQ Proteins mit DNA dar. Die Überrepräsentation von WRKY-Bindemotiven (W-boxen) an MVQ1-Bindestellen und die Tatsache, dass diese Bindestellen erheblich mit bereits bekannten WRKY-Bindestellen überlappen, unterstreichen die Annahme, dass die Interaktion zwischen DNA und MVQ1 indirekt über WRKYs erfolgt. Nach Behandlung mit flg22 nahm die Anzahl und Intensität der Signale für MVQ1-Bindestellen ab. Dies weist darauf hin, dass die Phosphorylierung durch MAPKs zur Loslösung von MVQ1 aus dem WRKY-DNA-Komplex führt.

Die Interaktion zwischen MVQ1 und WRKYs erhöhte die DNA-Bindeaktivität der WRKYs *in vitro*. Daraufhin wurde ein Modell entwickelt, in dem MVQ1 mit WRKYs einen Repressorkomplex bildet und dessen DNA-Bindung verstärkt um die Expression von Genen zu verhindern. Alternativ könnte MVQ1 die Rekrutierung der Transkriptionsmaschinerie durch WRKYs mit Transaktivierungsaktivität stören.

7. References

- Adachi, H., T. Nakano, N. Miyagawa, N. Ishihama, M. Yoshioka, Y. Katou, T. Yaeno, K. Shirasu, and H. Yoshioka. 2015. 'WRKY Transcription Factors Phosphorylated by MAPK Regulate a Plant Immune NADPH Oxidase in *Nicotiana benthamiana*', *Plant Cell*, 27: 2645-63.
- Albert, I., H. Bohm, M. Albert, C. E. Feiler, J. Imkampe, N. Wallmeroth, C. Brancato, T. M. Raaymakers, S. Oome, H. Zhang, E. Krol, C. Grefen, A. A. Gust, J. Chai, R. Hedrich, G. Van den Ackerveken, and T. Nurnberger. 2015. 'An RLP23-SOBIR1-BAK1 complex mediates NLP-triggered immunity', *Nat Plants*, 1: 15140.
- Alonso, J. M., A. N. Stepanova, T. J. Leisse, C. J. Kim, H. Chen, P. Shinn, D. K. Stevenson, J. Zimmerman, P. Barajas, R. Cheuk, C. Gadrinab, C. Heller, A. Jeske, E. Koesema, C. C. Meyers, H. Parker, L. Prednis, Y. Ansari, N. Choy, H. Deen, M. Geralt, N. Hazari, E. Hom, M. Karnes, C. Mulholland, R. Ndubaku, I. Schmidt, P. Guzman, L. Aguilar-Henonin, M. Schmid, D. Weigel, D. E. Carter, T. Marchand, E. Risseeuw, D. Brogden, A. Zeko, W. L. Crosby, C. C. Berry, and J. R. Ecker. 2003. 'Genome-wide insertional mutagenesis of *Arabidopsis thaliana*', *Science*, 301: 653-7.
- Anderson, J. C., S. Bartels, M. A. Gonzalez Besteiro, B. Shahollari, R. Ulm, and S. C. Peck. 2011. 'Arabidopsis MAP Kinase Phosphatase 1 (AtMKP1) negatively regulates MPK6-mediated PAMP responses and resistance against bacteria', *Plant J*, 67: 258-68.
- Andreasson, E., T. Jenkins, P. Brodersen, S. Thorgrimsen, N. H. Petersen, S. Zhu, J. L. Qiu, P. Micheelsen, A. Rocher, M. Petersen, M. A. Newman, H. Bjorn Nielsen, H. Hirt, I. Somssich, O. Mattsson, and J. Mundy. 2005. 'The MAP kinase substrate MKS1 is a regulator of plant defense responses', *EMBO J*, 24: 2579-89.
- Asai, T., G. Tena, J. Plotnikova, M. R. Willmann, W. L. Chiu, L. Gomez-Gomez, T. Boller, F. M. Ausubel, and J. Sheen. 2002. 'MAP kinase signalling cascade in *Arabidopsis* innate immunity', *Nature*, 415: 977-83.
- Bailey, T. L., and P. Machanick. 2012. 'Inferring direct DNA binding from ChIP-seq', *Nucleic Acids Res*, 40: e128.
- Balcke, G. U., S. Bennewitz, N. Bergau, B. Athmer, A. Henning, P. Majovsky, J. M. Jimenez-Gomez, W. Hoehenwarter, and A. Tissier. 2017. 'Multi-Omics of Tomato Glandular Trichomes Reveals Distinct Features of Central Carbon Metabolism Supporting High Productivity of Specialized Metabolites', *Plant Cell*, 29: 960-83.
- Belhaj, K., A. Chaparro-Garcia, S. Kamoun, N. J. Patron, and V. Nekrasov. 2015. 'Editing plant genomes with CRISPR/Cas9', *Curr Opin Biotechnol*, 32: 76-84.
- Benjamini, Y., and Y. Hochberg. 1995. 'Controlling the False Discovery Rate - a Practical and Powerful Approach to Multiple Testing', *Journal of the Royal Statistical Society Series B-Methodological*, 57: 289-300.
- Bergmann, D. C., W. Lukowitz, and C. R. Somerville. 2004. 'Stomatal development and pattern controlled by a MAPKK kinase', *Science*, 304: 1494-7.
- Bethke, G., P. Pecher, L. Eschen-Lippold, K. Tsuda, F. Katagiri, J. Glazebrook, D. Scheel, and J. Lee. 2012. 'Activation of the *Arabidopsis thaliana* mitogen-activated protein kinase MPK11 by the flagellin-derived elicitor peptide, flg22', *Mol Plant Microbe Interact*, 25: 471-80.
- Bethke, G., T. Unthan, J. F. Uhrig, Y. Poschl, A. A. Gust, D. Scheel, and J. Lee. 2009. 'Flg22 regulates the release of an ethylene response factor substrate from MAP kinase 6 in *Arabidopsis thaliana* via ethylene signaling', *Proc Natl Acad Sci U S A*, 106: 8067-72.
- Bi, G., Z. Zhou, W. Wang, L. Li, S. Rao, Y. Wu, X. Zhang, F. L. H. Menke, S. Chen, and J. M. Zhou. 2018. 'Receptor-Like Cytoplasmic Kinases Directly Link Diverse Pattern Recognition Receptors to the Activation of Mitogen-Activated Protein Kinase Cascades in *Arabidopsis*', *Plant Cell*, 30: 1543-61.

- Birkenbihl, R. P., C. Diezel, and I. E. Somssich. 2012. 'Arabidopsis WRKY33 is a key transcriptional regulator of hormonal and metabolic responses toward Botrytis cinerea infection', *Plant Physiol*, 159: 266-85.
- Birkenbihl, R. P., B. Kracher, A. Ross, K. Kramer, I. Finkemeier, and I. E. Somssich. 2018. 'Principles and characteristics of the Arabidopsis WRKY regulatory network during early MAMP-triggered immunity', *Plant J*.
- Birkenbihl, R. P., B. Kracher, and I. E. Somssich. 2017. 'Induced Genome-Wide Binding of Three Arabidopsis WRKY Transcription Factors during Early MAMP-Triggered Immunity', *Plant Cell*, 29: 20-38.
- Boudsocq, M., M. R. Willmann, M. McCormack, H. Lee, L. Shan, P. He, J. Bush, S. H. Cheng, and J. Sheen. 2010. 'Differential innate immune signalling via Ca(2+) sensor protein kinases', *Nature*, 464: 418-22.
- Bozkurt, T. O., S. Schornack, M. J. Banfield, and S. Kamoun. 2012. 'Oomycetes, effectors, and all that jazz', *Curr Opin Plant Biol*, 15: 483-92.
- Brand, L. H., N. M. Fischer, K. Harter, O. Kohlbacher, and D. Wanke. 2013. 'Elucidating the evolutionary conserved DNA-binding specificities of WRKY transcription factors by molecular dynamics and in vitro binding assays', *Nucleic Acids Res*, 41: 9764-78.
- Brand, L. H., T. Kirchler, S. Hummel, C. Chaban, and D. Wanke. 2010. 'DPI-ELISA: a fast and versatile method to specify the binding of plant transcription factors to DNA in vitro', *Plant Methods*, 6: 25.
- Brutus, A., F. Sicilia, A. Macone, F. Cervone, and G. De Lorenzo. 2010. 'A domain swap approach reveals a role of the plant wall-associated kinase 1 (WAK1) as a receptor of oligogalacturonides', *Proc Natl Acad Sci U S A*, 107: 9452-7.
- Cao, F. Y., T. A. DeFalco, W. Moeder, B. Li, Y. Gong, X. M. Liu, M. Taniguchi, S. Lumba, S. Toh, L. Shan, B. Ellis, D. Desveaux, and K. Yoshioka. 2018. 'Arabidopsis ETHYLENE RESPONSE FACTOR 8 (ERF8) has dual functions in ABA signaling and immunity', *BMC Plant Biol*, 18: 211.
- Cao, Y., Y. Liang, K. Tanaka, C. T. Nguyen, R. P. Jedrzejczak, A. Joachimiak, and G. Stacey. 2014. 'The kinase LYK5 is a major chitin receptor in Arabidopsis and forms a chitin-induced complex with related kinase CERK1', *Elife*, 3.
- Chen, L., S. Xiang, Y. Chen, D. Li, and D. Yu. 2017. 'Arabidopsis WRKY45 Interacts with the DELLA Protein RGL1 to Positively Regulate Age-Triggered Leaf Senescence', *Mol Plant*, 10: 1174-89.
- Cheng, Y., Y. Zhou, Y. Yang, Y. J. Chi, J. Zhou, J. Y. Chen, F. Wang, B. Fan, K. Shi, Y. H. Zhou, J. Q. Yu, and Z. Chen. 2012. 'Structural and functional analysis of VQ motif-containing proteins in Arabidopsis as interacting proteins of WRKY transcription factors', *Plant Physiol*, 159: 810-25.
- Chi, Y., Y. Yang, Y. Zhou, J. Zhou, B. Fan, J. Q. Yu, and Z. Chen. 2013. 'Protein-protein interactions in the regulation of WRKY transcription factors', *Mol Plant*, 6: 287-300.
- Chinchilla, D., Z. Bauer, M. Regenass, T. Boller, and G. Felix. 2006. 'The Arabidopsis receptor kinase FLS2 binds flg22 and determines the specificity of flagellin perception', *Plant Cell*, 18: 465-76.
- Choi, J., K. Tanaka, Y. Liang, Y. Cao, S. Y. Lee, and G. Stacey. 2014. 'Extracellular ATP, a danger signal, is recognized by DORN1 in Arabidopsis', *Biochem J*, 463: 429-37.
- Ciolkowski, I., D. Wanke, R. P. Birkenbihl, and I. E. Somssich. 2008. 'Studies on DNA-binding selectivity of WRKY transcription factors lend structural clues into WRKY-domain function', *Plant Mol Biol*, 68: 81-92.
- Couto, D., and C. Zipfel. 2016. 'Regulation of pattern recognition receptor signalling in plants', *Nat Rev Immunol*, 16: 537-52.
- Crooks, G. E., G. Hon, J. M. Chandonia, and S. E. Brenner. 2004. 'WebLogo: a sequence logo generator', *Genome Res*, 14: 1188-90.
- Danquah, A., A. de Zelicourt, M. Boudsocq, J. Neubauer, N. Frei Dit Frey, N. Leonhardt, S. Pateyron, F. Gwinner, J. P. Tamby, D. Ortiz-Masia, M. J. Marcote, H. Hirt, and J. Colcombet. 2015. 'Identification and characterization of an ABA-activated MAP kinase cascade in Arabidopsis thaliana', *Plant J*, 82: 232-44.

- Day, B., D. Dahlbeck, J. Huang, S. T. Chisholm, D. Li, and B. J. Staskawicz. 2005. 'Molecular basis for the RIN4 negative regulation of RPS2 disease resistance', *Plant Cell*, 17: 1292-305.
- Denoux, C., R. Galletti, N. Mammarella, S. Gopalan, D. Werck, G. De Lorenzo, S. Ferrari, F. M. Ausubel, and J. Dewdney. 2008. 'Activation of defense response pathways by OGs and Flg22 elicitors in Arabidopsis seedlings', *Mol Plant*, 1: 423-45.
- Deslandes, L., and S. Rivas. 2012. 'Catch me if you can: bacterial effectors and plant targets', *Trends Plant Sci*, 17: 644-55.
- Djamei, A., A. Pitzschke, H. Nakagami, I. Rajh, and H. Hirt. 2007. 'Trojan horse strategy in Agrobacterium transformation: abusing MAPK defense signaling', *Science*, 318: 453-6.
- Dong, J., C. Chen, and Z. Chen. 2003. 'Expression profiles of the Arabidopsis WRKY gene superfamily during plant defense response', *Plant Mol Biol*, 51: 21-37.
- Dong, Q., S. Zhao, D. Duan, Y. Tian, Y. Wang, K. Mao, Z. Zhou, and F. Ma. 2018. 'Structural and functional analyses of genes encoding VQ proteins in apple', *Plant Sci*, 272: 208-19.
- Drerup, M. M., K. Schlucking, K. Hashimoto, P. Manishankar, L. Steinhorst, K. Kuchitsu, and J. Kudla. 2013. 'The Calcineurin B-like calcium sensors CBL1 and CBL9 together with their interacting protein kinase CIPK26 regulate the Arabidopsis NADPH oxidase RBOHF', *Mol Plant*, 6: 559-69.
- Duan, M. R., J. Nan, Y. H. Liang, P. Mao, L. Lu, L. Li, C. Wei, L. Lai, Y. Li, and X. D. Su. 2007. 'DNA binding mechanism revealed by high resolution crystal structure of Arabidopsis thaliana WRKY1 protein', *Nucleic Acids Res*, 35: 1145-54.
- Dubiella, U., H. Seybold, G. Durian, E. Komander, R. Lassig, C. P. Witte, W. X. Schulze, and T. Romeis. 2013. 'Calcium-dependent protein kinase/NADPH oxidase activation circuit is required for rapid defense signal propagation', *Proc Natl Acad Sci U S A*, 110: 8744-9.
- Dyson, M. R., S. P. Shadbolt, K. J. Vincent, R. L. Perera, and J. McCafferty. 2004. 'Production of soluble mammalian proteins in Escherichia coli: identification of protein features that correlate with successful expression', *BMC Biotechnol*, 4: 32.
- Earley, K. W., J. R. Haag, O. Pontes, K. Opper, T. Juehne, K. Song, and C. S. Pikaard. 2006. 'Gateway-compatible vectors for plant functional genomics and proteomics', *Plant J*, 45: 616-29.
- Eschen-Lippold, L., X. Jiang, J. M. Elmore, D. Mackey, L. Shan, G. Coaker, D. Scheel, and J. Lee. 2016. 'Bacterial AvrRpt2-Like Cysteine Proteases Block Activation of the Arabidopsis Mitogen-Activated Protein Kinases, MPK4 and MPK11', *Plant Physiol*, 171: 2223-38.
- Eulgem, T., P. J. Rushton, S. Robatzek, and I. E. Somssich. 2000. 'The WRKY superfamily of plant transcription factors', *Trends Plant Sci*, 5: 199-206.
- Eulgem, T., and I. E. Somssich. 2007. 'Networks of WRKY transcription factors in defense signaling', *Curr Opin Plant Biol*, 10: 366-71.
- Evrard, A., M. Kumar, D. Lecourieux, J. Lucks, P. von Koskull-Doring, and H. Hirt. 2013. 'Regulation of the heat stress response in Arabidopsis by MPK6-targeted phosphorylation of the heat stress factor HsfA2', *PeerJ*, 1: e59.
- Feng, F., F. Yang, W. Rong, X. Wu, J. Zhang, S. Chen, C. He, and J. M. Zhou. 2012. 'A Xanthomonas uridine 5'-monophosphate transferase inhibits plant immune kinases', *Nature*, 485: 114-8.
- Ferrari, S., D. V. Savatin, F. Sicilia, G. Gramegna, F. Cervone, and G. D. Lorenzo. 2013. 'Oligogalacturonides: plant damage-associated molecular patterns and regulators of growth and development', *Front Plant Sci*, 4: 49.
- Feys, B. J., M. Wiermer, R. A. Bhat, L. J. Moisan, N. Medina-Escobar, C. Neu, A. Cabral, and J. E. Parker. 2005. 'Arabidopsis SENESCENCE-ASSOCIATED GENE101 stabilizes and signals within an ENHANCED DISEASE SUSCEPTIBILITY1 complex in plant innate immunity', *Plant Cell*, 17: 2601-13.
- Gao, X., X. Chen, W. Lin, S. Chen, D. Lu, Y. Niu, L. Li, C. Cheng, M. McCormack, J. Sheen, L. Shan, and P. He. 2013. 'Bifurcation of Arabidopsis NLR immune signaling via Ca(2)(+)-dependent protein kinases', *PLoS Pathog*, 9: e1003127.
- Geilen, K., and M. Bohmer. 2015. 'Dynamic subnuclear relocalisation of WRKY40 in response to Abscisic acid in Arabidopsis thaliana', *Sci Rep*, 5: 13369.

- Geilen, K., M. Heilmann, S. Hillmer, and M. Bohmer. 2017. 'WRKY43 regulates polyunsaturated fatty acid content and seed germination under unfavourable growth conditions', *Sci Rep*, 7: 14235.
- Gendrel, A. V., Z. Lippman, R. Martienssen, and V. Colot. 2005. 'Profiling histone modification patterns in plants using genomic tiling microarrays', *Nat Methods*, 2: 213-8.
- Glazebrook, J. 2005. 'Contrasting mechanisms of defense against biotrophic and necrotrophic pathogens', *Annu Rev Phytopathol*, 43: 205-27.
- Grant, C. E., T. L. Bailey, and W. S. Noble. 2011. 'FIMO: scanning for occurrences of a given motif', *Bioinformatics*, 27: 1017-8.
- Grefen, C., N. Donald, K. Hashimoto, J. Kudla, K. Schumacher, and M. R. Blatt. 2010. 'A ubiquitin-10 promoter-based vector set for fluorescent protein tagging facilitates temporal stability and native protein distribution in transient and stable expression studies', *Plant J*, 64: 355-65.
- Group, Mapk. 2002. 'Mitogen-activated protein kinase cascades in plants: a new nomenclature', *Trends Plant Sci*, 7: 301-8.
- Guan, Y., X. Meng, R. Khanna, E. LaMontagne, Y. Liu, and S. Zhang. 2014. 'Phosphorylation of a WRKY transcription factor by MAPKs is required for pollen development and function in Arabidopsis', *PLoS Genet*, 10: e1004384.
- Gust, A. A., R. Biswas, H. D. Lenz, T. Rauhut, S. Ranf, B. Kemmerling, F. Gotz, E. Glawischnig, J. Lee, G. Felix, and T. Nurnberger. 2007. 'Bacteria-derived peptidoglycans constitute pathogen-associated molecular patterns triggering innate immunity in Arabidopsis', *J Biol Chem*, 282: 32338-48.
- Gust, A. A., R. Pruitt, and T. Nurnberger. 2017. 'Sensing Danger: Key to Activating Plant Immunity', *Trends Plant Sci*, 22: 779-91.
- Halter, T., J. Imkampe, S. Mazzotta, M. Wierzba, S. Postel, C. Bucherl, C. Kiefer, M. Stahl, D. Chinchilla, X. Wang, T. Nurnberger, C. Zipfel, S. Clouse, J. W. Borst, S. Boeren, S. C. de Vries, F. Tax, and B. Kemmerling. 2014. 'The leucine-rich repeat receptor kinase BIR2 is a negative regulator of BAK1 in plant immunity', *Curr Biol*, 24: 134-43.
- Han, L., G. J. Li, K. Y. Yang, G. Mao, R. Wang, Y. Liu, and S. Zhang. 2010. 'Mitogen-activated protein kinase 3 and 6 regulate Botrytis cinerea-induced ethylene production in Arabidopsis', *Plant J*, 64: 114-27.
- He, P., L. Shan, N. C. Lin, G. B. Martin, B. Kemmerling, T. Nurnberger, and J. Sheen. 2006. 'Specific bacterial suppressors of MAMP signaling upstream of MAPKKK in Arabidopsis innate immunity', *Cell*, 125: 563-75.
- Hillmer, R. A., K. Tsuda, G. Rallapalli, S. Asai, W. Truman, M. D. Papke, H. Sakakibara, J. D. G. Jones, C. L. Myers, and F. Katagiri. 2017. 'The highly buffered Arabidopsis immune signaling network conceals the functions of its components', *PLoS Genet*, 13: e1006639.
- Hoehenwarter, W., M. Thomas, E. Nukarinen, V. Egelhofer, H. Rohrig, W. Weckwerth, U. Conrath, and G. J. Beckers. 2013. 'Identification of novel in vivo MAP kinase substrates in Arabidopsis thaliana through use of tandem metal oxide affinity chromatography', *Mol Cell Proteomics*, 12: 369-80.
- Hoesel, B., and J. A. Schmid. 2013. 'The complexity of NF-kappaB signaling in inflammation and cancer', *Mol Cancer*, 12: 86.
- Hou, S., X. Wang, D. Chen, X. Yang, M. Wang, D. Turra, A. Di Pietro, and W. Zhang. 2014. 'The secreted peptide PIP1 amplifies immunity through receptor-like kinase 7', *PLoS Pathog*, 10: e1004331.
- Hsu, F. C., M. Y. Chou, S. J. Chou, Y. R. Li, H. P. Peng, and M. C. Shih. 2013. 'Submergence confers immunity mediated by the WRKY22 transcription factor in Arabidopsis', *Plant Cell*, 25: 2699-713.
- Hu, P., W. Zhou, Z. Cheng, M. Fan, L. Wang, and D. Xie. 2013. 'JAV1 controls jasmonate-regulated plant defense', *Mol Cell*, 50: 504-15.
- Hu, Y., L. Chen, H. Wang, L. Zhang, F. Wang, and D. Yu. 2013. 'Arabidopsis transcription factor WRKY8 functions antagonistically with its interacting partner VQ9 to modulate salinity stress tolerance', *Plant J*, 74: 730-45.

- Huffaker, A., G. Pearce, and C. A. Ryan. 2006. 'An endogenous peptide signal in Arabidopsis activates components of the innate immune response', *Proc Natl Acad Sci U S A*, 103: 10098-103.
- Huot, B., J. Yao, B. L. Montgomery, and S. Y. He. 2014. 'Growth-defense tradeoffs in plants: a balancing act to optimize fitness', *Mol Plant*, 7: 1267-87.
- Hussain, R. M. F., A. H. Sheikh, I. Haider, M. Quareshy, and H. J. M. Linthorst. 2018. 'Arabidopsis WRKY50 and TGA Transcription Factors Synergistically Activate Expression of PR1', *Front Plant Sci*, 9: 930.
- Jiang, S. Y., M. Sevugan, and S. Ramachandran. 2018. 'Valine-glutamine (VQ) motif coding genes are ancient and non-plant-specific with comprehensive expression regulation by various biotic and abiotic stresses', *BMC Genomics*, 19: 342.
- Jiang, Y., and D. Yu. 2016. 'The WRKY57 Transcription Factor Affects the Expression of Jasmonate ZIM-Domain Genes Transcriptionally to Compromise Botrytis cinerea Resistance', *Plant Physiol*, 171: 2771-82.
- Jing, Y., and R. Lin. 2015. 'The VQ Motif-Containing Protein Family of Plant-Specific Transcriptional Regulators', *Plant Physiol*, 169: 371-8.
- Jones, J. D. G., and J. L. Dangl. 2006. 'The plant immune system', *Nature*, 444: 323-29.
- Kadota, Y., J. Sklenar, P. Derbyshire, L. Stransfeld, S. Asai, V. Ntoukakis, J. D. Jones, K. Shirasu, F. Menke, A. Jones, and C. Zipfel. 2014. 'Direct regulation of the NADPH oxidase RBOHD by the PRR-associated kinase BIK1 during plant immunity', *Mol Cell*, 54: 43-55.
- Kaiserli, E., K. Paldi, L. O'Donnell, O. Batalov, U. V. Pedmale, D. A. Nusinow, S. A. Kay, and J. Chory. 2015. 'Integration of Light and Photoperiodic Signaling in Transcriptional Nuclear Foci', *Dev Cell*, 35: 311-21.
- Karin, M. 1999. 'How NF-kappaB is activated: the role of the IkappaB kinase (IKK) complex', *Oncogene*, 18: 6867-74.
- Khan, A., O. Fornes, A. Stigliani, M. Gheorghe, J. A. Castro-Mondragon, R. van der Lee, A. Bessy, J. Cheneby, S. R. Kulkarni, G. Tan, D. Baranasic, D. J. Arenillas, A. Sandelin, K. Vandepoele, B. Lenhard, B. Ballester, W. W. Wasserman, F. Parcy, and A. Mathelier. 2018. 'JASPAR 2018: update of the open-access database of transcription factor binding profiles and its web framework', *Nucleic Acids Res*, 46: D1284.
- King, S. R., H. McLellan, P. C. Boevink, M. R. Armstrong, T. Bukharova, O. Sukarta, J. Win, S. Kamoun, P. R. Birch, and M. J. Banfield. 2014. 'Phytophthora infestans RXLR Effector PexRD2 Interacts with Host MAPKKK{varepsilon} to Suppress Plant Immune Signaling', *Plant Cell*, 26: 1345-59.
- Kunze, G., C. Zipfel, S. Robatzek, K. Niehaus, T. Boller, and G. Felix. 2004. 'The N terminus of bacterial elongation factor Tu elicits innate immunity in Arabidopsis plants', *Plant Cell*, 16: 3496-507.
- Lai, Z., Y. Li, F. Wang, Y. Cheng, B. Fan, J. Q. Yu, and Z. Chen. 2011. 'Arabidopsis sigma factor binding proteins are activators of the WRKY33 transcription factor in plant defense', *Plant Cell*, 23: 3824-41.
- Lal, N. K., U. Nagalakshmi, N. K. Hurlburt, R. Flores, A. Bak, P. Sone, X. Ma, G. Song, J. Walley, L. Shan, P. He, C. Casteel, A. J. Fisher, and S. P. Dinesh-Kumar. 2018. 'The Receptor-like Cytoplasmic Kinase BIK1 Localizes to the Nucleus and Regulates Defense Hormone Expression during Plant Innate Immunity', *Cell Host Microbe*, 23: 485-97 e5.
- Lassowskat, I., C. Bottcher, L. Eschen-Lippold, D. Scheel, and J. Lee. 2014. 'Sustained mitogen-activated protein kinase activation reprograms defense metabolism and phosphoprotein profile in Arabidopsis thaliana', *Front Plant Sci*, 5: 554.
- Latrasse, D., T. Jegu, H. Li, A. de Zelicourt, C. Raynaud, S. Legras, A. Gust, O. Samajova, A. Veluchamy, N. Rayapuram, J. S. Ramirez-Prado, O. Kulikova, J. Colcombet, J. Bigeard, B. Genot, T. Bisseling, M. Benhamed, and H. Hirt. 2017. 'MAPK-triggered chromatin reprogramming by histone deacetylase in plant innate immunity', *Genome Biol*, 18: 131.
- Le Roux, C., G. Huet, A. Jauneau, L. Camborde, D. Tremousaygue, A. Kraut, B. Zhou, M. Levaillant, H. Adachi, H. Yoshioka, S. Raffaele, R. Berthome, Y. Coute, J. E. Parker, and L. Deslandes. 2015. 'A receptor pair with an integrated decoy converts pathogen disabling of transcription factors to immunity', *Cell*, 161: 1074-88.

- Lee, D., G. Bourdais, G. Yu, S. Robatzek, and G. Coaker. 2015. 'Phosphorylation of the Plant Immune Regulator RPM1-INTERACTING PROTEIN4 Enhances Plant Plasma Membrane H(+)-ATPase Activity and Inhibits Flagellin-Triggered Immune Responses in Arabidopsis', *Plant Cell*, 27: 2042-56.
- Lei, R., X. Li, Z. Ma, Y. Lv, Y. Hu, and D. Yu. 2017. 'Arabidopsis WRKY2 and WRKY34 transcription factors interact with VQ20 protein to modulate pollen development and function', *Plant J*, 91: 962-76.
- Lei, R., Z. Ma, and D. Yu. 2018. 'WRKY2/34-VQ20 Modules in Arabidopsis thaliana Negatively Regulate Expression of a Trio of Related MYB Transcription Factors During Pollen Development', *Front Plant Sci*, 9: 331.
- Lewis, L. A., K. Polanski, M. de Torres-Zabala, S. Jayaraman, L. Bowden, J. Moore, C. A. Penfold, D. J. Jenkins, C. Hill, L. Baxter, S. Kulasekaran, W. Truman, G. Littlejohn, J. Prusinska, A. Mead, J. Steinbrenner, R. Hickman, D. Rand, D. L. Wild, S. Ott, V. Buchanan-Wollaston, N. Smirnov, J. Beynon, K. Denby, and M. Grant. 2015. 'Transcriptional Dynamics Driving MAMP-Triggered Immunity and Pathogen Effector-Mediated Immunosuppression in Arabidopsis Leaves Following Infection with Pseudomonas syringae pv tomato DC3000', *Plant Cell*, 27: 3038-64.
- Li, B., S. Jiang, X. Yu, C. Cheng, S. Chen, Y. Cheng, J. S. Yuan, D. Jiang, P. He, and L. Shan. 2015. 'Phosphorylation of trihelix transcriptional repressor ASR3 by MAP KINASE4 negatively regulates Arabidopsis immunity', *Plant Cell*, 27: 839-56.
- Li, B., X. Meng, L. Shan, and P. He. 2016. 'Transcriptional Regulation of Pattern-Triggered Immunity in Plants', *Cell Host Microbe*, 19: 641-50.
- Li, F., C. Cheng, F. Cui, M. V. de Oliveira, X. Yu, X. Meng, A. C. Intorne, K. Babilonia, M. Li, B. Li, S. Chen, X. Ma, S. Xiao, Y. Zheng, Z. Fei, R. P. Metz, C. D. Johnson, H. Koiwa, W. Sun, Z. Li, G. A. de Souza Filho, L. Shan, and P. He. 2014. 'Modulation of RNA polymerase II phosphorylation downstream of pathogen perception orchestrates plant immunity', *Cell Host Microbe*, 16: 748-58.
- Li, H., Y. Ding, Y. Shi, X. Zhang, S. Zhang, Z. Gong, and S. Yang. 2017. 'MPK3- and MPK6-Mediated ICE1 Phosphorylation Negatively Regulates ICE1 Stability and Freezing Tolerance in Arabidopsis', *Dev Cell*, 43: 630-42 e4.
- Li, J., J. Wen, K. A. Lease, J. T. Doke, F. E. Tax, and J. C. Walker. 2002. 'BAK1, an Arabidopsis LRR receptor-like protein kinase, interacts with BRI1 and modulates brassinosteroid signaling', *Cell*, 110: 213-22.
- Li, L., M. Li, L. Yu, Z. Zhou, X. Liang, Z. Liu, G. Cai, L. Gao, X. Zhang, Y. Wang, S. Chen, and J. M. Zhou. 2014. 'The FLS2-associated kinase BIK1 directly phosphorylates the NADPH oxidase RbohD to control plant immunity', *Cell Host Microbe*, 15: 329-38.
- Li, Y., Y. Jing, J. Li, G. Xu, and R. Lin. 2014. 'Arabidopsis VQ MOTIF-CONTAINING PROTEIN29 Represses Seedling Deetiolation by Interacting with PHYTOCHROME-INTERACTING FACTOR1', *Plant Physiol*, 164: 2068-80.
- Liebrand, T. W., G. C. van den Berg, Z. Zhang, P. Smit, J. H. Cordewener, A. H. America, J. Sklenar, A. M. Jones, W. I. Tameling, S. Robatzek, B. P. Thomma, and M. H. Joosten. 2013. 'Receptor-like kinase SOBIR1/EVR interacts with receptor-like proteins in plant immunity against fungal infection', *Proc Natl Acad Sci U S A*, 110: 10010-5.
- Lippok, B., R. P. Birkenbihl, G. Rivory, J. Brummer, E. Schmelzer, E. Logemann, and I. E. Somssich. 2007. 'Expression of AtWRKY33 encoding a pathogen- or PAMP-responsive WRKY transcription factor is regulated by a composite DNA motif containing W box elements', *Mol Plant Microbe Interact*, 20: 420-9.
- Liu, J., J. M. Elmore, Z. J. Lin, and G. Coaker. 2011. 'A receptor-like cytoplasmic kinase phosphorylates the host target RIN4, leading to the activation of a plant innate immune receptor', *Cell Host Microbe*, 9: 137-46.
- Liu, S., B. Kracher, J. Ziegler, R. P. Birkenbihl, and I. E. Somssich. 2015. 'Negative regulation of ABA signaling by WRKY33 is critical for Arabidopsis immunity towards Botrytis cinerea 2100', *Elife*, 4: e07295.

- Liu, S., J. Ziegler, J. Zeier, R. P. Birkenbihl, and I. E. Somssich. 2017. 'Botrytis cinerea B05.10 promotes disease development in Arabidopsis by suppressing WRKY33-mediated host immunity', *Plant Cell Environ*, 40: 2189-206.
- Llorca, C. M., M. Potschin, and U. Zentgraf. 2014. 'bZIPs and WRKYs: two large transcription factor families executing two different functional strategies', *Front Plant Sci*, 5: 169.
- Lo Presti, L., and R. Kahmann. 2017. 'How filamentous plant pathogen effectors are translocated to host cells', *Curr Opin Plant Biol*, 38: 19-24.
- Lockstone, H. E. 2011. 'Exon array data analysis using Affymetrix power tools and R statistical software', *Brief Bioinform*, 12: 634-44.
- Logemann, E., R. P. Birkenbihl, B. Ulker, and I. E. Somssich. 2006. 'An improved method for preparing Agrobacterium cells that simplifies the Arabidopsis transformation protocol', *Plant Methods*, 2: 16.
- Lu, D., W. Lin, X. Gao, S. Wu, C. Cheng, J. Avila, A. Heese, T. P. Devarenne, P. He, and L. Shan. 2011. 'Direct ubiquitination of pattern recognition receptor FLS2 attenuates plant innate immunity', *Science*, 332: 1439-42.
- Lu, D. P., S. J. Wu, X. Q. Gao, Y. L. Zhang, L. B. Shan, and P. He. 2010. 'A receptor-like cytoplasmic kinase, BIK1, associates with a flagellin receptor complex to initiate plant innate immunity', *Proceedings of the National Academy of Sciences of the United States of America*, 107: 496-501.
- Macho, A. P., and C. Zipfel. 2014. 'Plant PRRs and the activation of innate immune signaling', *Mol Cell*, 54: 263-72.
- Maeo, K., S. Hayashi, H. Kojima-Suzuki, A. Morikami, and K. Nakamura. 2001. 'Role of conserved residues of the WRKY domain in the DNA-binding of tobacco WRKY family proteins', *Biosci Biotechnol Biochem*, 65: 2428-36.
- Maintz, J., M. Cavdar, J. Tamborski, M. Kwaaitaal, R. Huisman, C. Meesters, E. Kombrink, and R. Panstruga. 2014. 'Comparative analysis of MAMP-induced calcium influx in Arabidopsis seedlings and protoplasts', *Plant Cell Physiol*, 55: 1813-25.
- Maldonado-Bonilla, L. D., L. Eschen-Lippold, S. Gago-Zachert, N. Tabassum, N. Bauer, D. Scheel, and J. Lee. 2014. 'The Arabidopsis tandem zinc finger 9 protein binds RNA and mediates pathogen-associated molecular pattern-triggered immune responses', *Plant Cell Physiol*, 55: 412-25.
- Mao, G., X. Meng, Y. Liu, Z. Zheng, Z. Chen, and S. Zhang. 2011. 'Phosphorylation of a WRKY transcription factor by two pathogen-responsive MAPKs drives phytoalexin biosynthesis in Arabidopsis', *Plant Cell*, 23: 1639-53.
- Mathur, S., S. Vyas, S. Kapoor, and A. K. Tyagi. 2011. 'The Mediator complex in plants: structure, phylogeny, and expression profiling of representative genes in a dicot (Arabidopsis) and a monocot (rice) during reproduction and abiotic stress', *Plant Physiol*, 157: 1609-27.
- Mi, H., X. Huang, A. Muruganujan, H. Tang, C. Mills, D. Kang, and P. D. Thomas. 2017. 'PANTHER version 11: expanded annotation data from Gene Ontology and Reactome pathways, and data analysis tool enhancements', *Nucleic Acids Res*, 45: D183-D89.
- Miao, Y., T. Laun, P. Zimmermann, and U. Zentgraf. 2004. 'Targets of the WRKY53 transcription factor and its role during leaf senescence in Arabidopsis', *Plant Mol Biol*, 55: 853-67.
- Miya, A., P. Albert, T. Shinya, Y. Desaki, K. Ichimura, K. Shirasu, Y. Narusaka, N. Kawakami, H. Kaku, and N. Shibuya. 2007. 'CERK1, a LysM receptor kinase, is essential for chitin elicitor signaling in Arabidopsis', *Proc Natl Acad Sci U S A*, 104: 19613-8.
- Monaghan, J., S. Matschi, O. Shorinola, H. Rovenich, A. Matei, C. Segonzac, F. G. Malinovsky, J. P. Rathjen, D. MacLean, T. Romeis, and C. Zipfel. 2014. 'The calcium-dependent protein kinase CPK28 buffers plant immunity and regulates BIK1 turnover', *Cell Host Microbe*, 16: 605-15.
- Nakagawa, T., T. Kurose, T. Hino, K. Tanaka, M. Kawamukai, Y. Niwa, K. Toyooka, K. Matsuoka, T. Jinbo, and T. Kimura. 2007. 'Development of series of gateway binary vectors, pGWBs, for realizing efficient construction of fusion genes for plant transformation', *J Biosci Bioeng*, 104: 34-41.

- Navarro, L., C. Zipfel, O. Rowland, I. Keller, S. Robatzek, T. Boller, and J. D. Jones. 2004. 'The transcriptional innate immune response to flg22. Interplay and overlap with Avr gene-dependent defense responses and bacterial pathogenesis', *Plant Physiol*, 135: 1113-28.
- Nurnberger, T., F. Brunner, B. Kemmerling, and L. Piater. 2004. 'Innate immunity in plants and animals: striking similarities and obvious differences', *Immunol Rev*, 198: 249-66.
- Obayashi, T., Y. Aoki, S. Tadaka, Y. Kagaya, and K. Kinoshita. 2018. 'ATTED-II in 2018: A Plant Coexpression Database Based on Investigation of the Statistical Property of the Mutual Rank Index', *Plant Cell Physiol*, 59: 440.
- Oerke, E. C. 2006. 'Crop losses to pests', *Journal of Agricultural Science*, 144: 31-43.
- Ordon, J., J. Gantner, J. Kemna, L. Schwalgun, M. Reschke, J. Streubel, J. Boch, and J. Stuttmann. 2017. 'Generation of chromosomal deletions in dicotyledonous plants employing a user-friendly genome editing toolkit', *Plant J*, 89: 155-68.
- Palm-Forster, M. A., L. Eschen-Lippold, and J. Lee. 2012. 'A mutagenesis-based screen to rapidly identify phosphorylation sites in mitogen-activated protein kinase substrates', *Anal Biochem*, 427: 127-9.
- Pan, J., H. Wang, Y. Hu, and D. Yu. 2018. 'Arabidopsis VQ18 and VQ26 proteins interact with ABI5 transcription factor to negatively modulate ABA response during seed germination', *Plant J*, 95: 529-44.
- Pandey, S. P., and I. E. Somssich. 2009. 'The role of WRKY transcription factors in plant immunity', *Plant Physiol*, 150: 1648-55.
- Pecher, P., L. Eschen-Lippold, S. Herklotz, K. Kuhle, K. Naumann, G. Bethke, J. Uhrig, M. Weyhe, D. Scheel, and J. Lee. 2014. 'The Arabidopsis thaliana mitogen-activated protein kinases MPK3 and MPK6 target a subclass of 'VQ-motif'-containing proteins to regulate immune responses', *New Phytol*.
- Pesch, M., B. Dartan, R. Birkenbihl, I. E. Somssich, and M. Hulskamp. 2014. 'Arabidopsis TTG2 regulates TRY expression through enhancement of activator complex-triggered activation', *Plant Cell*, 26: 4067-83.
- Petersen, K., J. L. Qiu, J. Lutje, B. K. Fiil, S. Hansen, J. Mundy, and M. Petersen. 2010. 'Arabidopsis MKS1 is involved in basal immunity and requires an intact N-terminal domain for proper function', *PLoS One*, 5: e14364.
- Popescu, S. C., G. V. Popescu, S. Bachan, Z. Zhang, M. Gerstein, M. Snyder, and S. P. Dinesh-Kumar. 2009. 'MAPK target networks in Arabidopsis thaliana revealed using functional protein microarrays', *Genes Dev*, 23: 80-92.
- Qi, D., U. Dubiella, S. H. Kim, D. I. Sloss, R. H. Downen, J. E. Dixon, and R. W. Innes. 2014. 'Recognition of the protein kinase AVRPPHB SUSCEPTIBLE1 by the disease resistance protein RESISTANCE TO PSEUDOMONAS SYRINGAE5 is dependent on s-acylation and an exposed loop in AVRPPHB SUSCEPTIBLE1', *Plant Physiol*, 164: 340-51.
- Qi, J., J. Wang, Z. Gong, and J. M. Zhou. 2017. 'Apoplastic ROS signaling in plant immunity', *Curr Opin Plant Biol*, 38: 92-100.
- Qi, Z., R. Verma, C. Gehring, Y. Yamaguchi, Y. Zhao, C. A. Ryan, and G. A. Berkowitz. 2010. 'Ca²⁺ signaling by plant Arabidopsis thaliana Pep peptides depends on AtPepR1, a receptor with guanylyl cyclase activity, and cGMP-activated Ca²⁺ channels', *Proc Natl Acad Sci U S A*, 107: 21193-8.
- Qiu, J. L., B. K. Fiil, K. Petersen, H. B. Nielsen, C. J. Botanga, S. Thorgrimsen, K. Palma, M. C. Suarez-Rodriguez, S. Sandbech-Clausen, J. Lichota, P. Brodersen, K. D. Grasser, O. Mattsson, J. Glazebrook, J. Mundy, and M. Petersen. 2008. 'Arabidopsis MAP kinase 4 regulates gene expression through transcription factor release in the nucleus', *EMBO J*, 27: 2214-21.
- Qiu, J. L., L. Zhou, B. W. Yun, H. B. Nielsen, B. K. Fiil, K. Petersen, J. Mackinlay, G. J. Loake, J. Mundy, and P. C. Morris. 2008. 'Arabidopsis mitogen-activated protein kinase kinases MKK1 and MKK2 have overlapping functions in defense signaling mediated by MEKK1, MPK4, and MKS1', *Plant Physiol*, 148: 212-22.

- Ranf, S., L. Eschen-Lippold, K. Frohlich, L. Westphal, D. Scheel, and J. Lee. 2014. 'Microbe-associated molecular pattern-induced calcium signaling requires the receptor-like cytoplasmic kinases, PBL1 and BIK1', *BMC Plant Biol*, 14: 374.
- Ranf, S., N. Gisch, M. Schaffer, T. Illig, L. Westphal, Y. A. Knirel, P. M. Sanchez-Carballo, U. Zahringer, R. Huckelhoven, J. Lee, and D. Scheel. 2015. 'A lectin S-domain receptor kinase mediates lipopolysaccharide sensing in *Arabidopsis thaliana*', *Nat Immunol*, 16: 426-33.
- Rao, S., Z. Zhou, P. Miao, G. Bi, M. Hu, Y. Wu, F. Feng, X. Zhang, and J. M. Zhou. 2018. 'Roles of Receptor-Like Cytoplasmic Kinase VII Members in Pattern-Triggered Immune Signaling', *Plant Physiol*, 177: 1679-90.
- Rinerson, C. I., R. C. Rabara, P. Tripathi, Q. J. Shen, and P. J. Rushton. 2015. 'The evolution of WRKY transcription factors', *BMC Plant Biol*, 15: 66.
- Ritchie, M. E., B. Phipson, D. Wu, Y. Hu, C. W. Law, W. Shi, and G. K. Smyth. 2015. 'limma powers differential expression analyses for RNA-sequencing and microarray studies', *Nucleic Acids Res*, 43: e47.
- Roux, M. E., M. W. Rasmussen, K. Palma, S. Lolle, A. M. Regue, G. Bethke, J. Glazebrook, W. Zhang, L. Sieburth, M. R. Larsen, J. Mundy, and M. Petersen. 2015. 'The mRNA decay factor PAT1 functions in a pathway including MAP kinase 4 and immune receptor SUMM2', *EMBO J*, 34: 593-608.
- Rushton, P. J. 2002. 'Synthetic Plant Promoters Containing Defined Regulatory Elements Provide Novel Insights into Pathogen- and Wound-Induced Signaling', *The Plant Cell Online*, 14: 749-62.
- Rushton, P. J., I. E. Somssich, P. Ringler, and Q. J. Shen. 2010. 'WRKY transcription factors', *Trends Plant Sci*, 15: 247-58.
- Sarris, P. F., V. Cevik, G. Dagdas, J. D. Jones, and K. V. Krasileva. 2016. 'Comparative analysis of plant immune receptor architectures uncovers host proteins likely targeted by pathogens', *BMC Biol*, 14: 8.
- Sarris, P. F., Z. Duxbury, S. U. Huh, Y. Ma, C. Segonzac, J. Sklenar, P. Derbyshire, V. Cevik, G. Rallapalli, S. B. Saucet, L. Wirthmueller, F. L. H. Menke, K. H. Sohn, and J. D. G. Jones. 2015. 'A Plant Immune Receptor Detects Pathogen Effectors that Target WRKY Transcription Factors', *Cell*, 161: 1089-100.
- Schluttenhofer, C., and L. Yuan. 2015. 'Regulation of specialized metabolism by WRKY transcription factors', *Plant Physiol*, 167: 295-306.
- Schroeder, A., O. Mueller, S. Stocker, R. Salowsky, M. Leiber, M. Gassmann, S. Lightfoot, W. Menzel, M. Granzow, and T. Ragg. 2006. 'The RIN: an RNA integrity number for assigning integrity values to RNA measurements', *BMC Mol Biol*, 7: 3.
- Segonzac, C., A. P. Macho, M. Sanmartin, V. Ntoukakis, J. J. Sanchez-Serrano, and C. Zipfel. 2014. 'Negative control of BAK1 by protein phosphatase 2A during plant innate immunity', *EMBO J*, 33: 2069-79.
- Seybold, Heike, Fabian Trempel, Stefanie Ranf, Dierk Scheel, Tina Romeis, and Justin Lee. 2014. 'Ca²⁺ signalling in plant immune response: from pattern recognition receptors to Ca²⁺ decoding mechanisms', *New Phytologist*, 204: 782-90.
- Shankaranarayanan, P., M. A. Mendoza-Parra, M. Walia, L. Wang, N. Li, L. M. Trindade, and H. Gronemeyer. 2011. 'Single-tube linear DNA amplification (LinDA) for robust ChIP-seq', *Nat Methods*, 8: 565-7.
- Sheikh, A. H., L. Eschen-Lippold, P. Pecher, W. Hoehenwarter, A. K. Sinha, D. Scheel, and J. Lee. 2016. 'Regulation of WRKY46 Transcription Factor Function by Mitogen-Activated Protein Kinases in *Arabidopsis thaliana*', *Front Plant Sci*, 7: 61.
- Shinya, T., K. Yamaguchi, Y. Desaki, K. Yamada, T. Narisawa, Y. Kobayashi, K. Maeda, M. Suzuki, T. Tanimoto, J. Takeda, M. Nakashima, R. Funama, M. Narusaka, Y. Narusaka, H. Kaku, T. Kawasaki, and N. Shibuya. 2014. 'Selective regulation of the chitin-induced defense response by the *Arabidopsis* receptor-like cytoplasmic kinase PBL27', *Plant J*, 79: 56-66.
- Smakowska-Luzan, E., G. A. Mott, K. Parys, M. Stegmann, T. C. Howton, M. Layeghifard, J. Neuhold, A. Lehner, J. Kong, K. Grunwald, N. Weinberger, S. B. Satbhai, D. Mayer, W. Busch, M. Madalinski,

- P. Stolt-Bergner, N. J. Provart, M. S. Mukhtar, C. Zipfel, D. Desveaux, D. S. Guttman, and Y. Belkhadir. 2018. 'An extracellular network of Arabidopsis leucine-rich repeat receptor kinases', *Nature*, 553: 342-46.
- Sopena-Torres, S., L. Jorda, C. Sanchez-Rodriguez, E. Miedes, V. Escudero, S. Swami, G. Lopez, M. Pislewska-Bednarek, I. Lassowskat, J. Lee, Y. Gu, S. Haigis, D. Alexander, S. Pattathil, A. Munoz-Barrios, P. Bednarek, S. Somerville, P. Schulze-Lefert, M. G. Hahn, D. Scheel, and A. Molina. 2018. 'YODA MAP3K kinase regulates plant immune responses conferring broad-spectrum disease resistance', *New Phytol*, 218: 661-80.
- Southern, E. 2006. 'Southern blotting', *Nat Protoc*, 1: 518-25.
- Stegmann, M., J. Monaghan, E. Smakowska-Luzan, H. Rovenich, A. Lehner, N. Holton, Y. Belkhadir, and C. Zipfel. 2017. 'The receptor kinase FER is a RALF-regulated scaffold controlling plant immune signaling', *Science*, 355: 287-89.
- Su, J., B. J. Spears, S. H. Kim, and W. Gassmann. 2018. 'Constant vigilance: plant functions guarded by resistance proteins', *Plant J*, 93: 637-50.
- Su, J., L. Yang, Q. Zhu, H. Wu, Y. He, Y. Liu, J. Xu, D. Jiang, and S. Zhang. 2018. 'Active photosynthetic inhibition mediated by MPK3/MPK6 is critical to effector-triggered immunity', *PLoS Biol*, 16: e2004122.
- Sun, C. W., and J. Callis. 1997. 'Independent modulation of Arabidopsis thaliana polyubiquitin mRNAs in different organs and in response to environmental changes', *Plant J*, 11: 1017-27.
- Sun, T., Y. Nitta, Q. Zhang, D. Wu, H. Tian, J. S. Lee, and Y. Zhang. 2018. 'Antagonistic interactions between two MAP kinase cascades in plant development and immune signaling', *EMBO Rep*, 19.
- Sun, Y., L. Li, A. P. Macho, Z. Han, Z. Hu, C. Zipfel, J. M. Zhou, and J. Chai. 2013. 'Structural basis for flg22-induced activation of the Arabidopsis FLS2-BAK1 immune complex', *Science*, 342: 624-8.
- Szklarczyk, D., J. H. Morris, H. Cook, M. Kuhn, S. Wyder, M. Simonovic, A. Santos, N. T. Doncheva, A. Roth, P. Bork, L. J. Jensen, and C. von Mering. 2017. 'The STRING database in 2017: quality-controlled protein-protein association networks, made broadly accessible', *Nucleic Acids Res*, 45: D362-D68.
- Tang, J., Z. Han, Y. Sun, H. Zhang, X. Gong, and J. Chai. 2015. 'Structural basis for recognition of an endogenous peptide by the plant receptor kinase PEPR1', *Cell Res*, 25: 110-20.
- Thomma, B. P., T. Nurnberger, and M. H. Joosten. 2011. 'Of PAMPs and effectors: the blurred PTI-ETI dichotomy', *Plant Cell*, 23: 4-15.
- Thorvaldsdottir, H., J. T. Robinson, and J. P. Mesirov. 2013. 'Integrative Genomics Viewer (IGV): high-performance genomics data visualization and exploration', *Brief Bioinform*, 14: 178-92.
- Turck, F., A. Zhou, and I. E. Somssich. 2004. 'Stimulus-dependent, promoter-specific binding of transcription factor WRKY1 to its native promoter and the defense-related gene PcPR1-1 in Parsley', *Plant Cell*, 16: 2573-85.
- Valouev, A., D. S. Johnson, A. Sundquist, C. Medina, E. Anton, S. Batzoglou, R. M. Myers, and A. Sidow. 2008. 'Genome-wide analysis of transcription factor binding sites based on ChIP-Seq data', *Nat Methods*, 5: 829-34.
- Walter, M., C. Chaban, K. Schutze, O. Batistic, K. Weckermann, C. Nake, D. Blazevic, C. Grefen, K. Schumacher, C. Oecking, K. Harter, and J. Kudla. 2004. 'Visualization of protein interactions in living plant cells using bimolecular fluorescence complementation', *Plant J*, 40: 428-38.
- Wan, J., X. C. Zhang, D. Neece, K. M. Ramonell, S. Clough, S. Y. Kim, M. G. Stacey, and G. Stacey. 2008. 'A LysM receptor-like kinase plays a critical role in chitin signaling and fungal resistance in Arabidopsis', *Plant Cell*, 20: 471-81.
- Wang, A., D. Garcia, H. Zhang, K. Feng, A. Chaudhury, F. Berger, W. J. Peacock, E. S. Dennis, and M. Luo. 2010. 'The VQ motif protein IKU1 regulates endosperm growth and seed size in Arabidopsis', *Plant J*, 63: 670-9.
- Wang, C., J. Yao, X. Du, Y. Zhang, Y. Sun, J. A. Rollins, and Z. Mou. 2015. 'The Arabidopsis Mediator Complex Subunit16 Is a Key Component of Basal Resistance against the Necrotrophic Fungal Pathogen Sclerotinia sclerotiorum', *Plant Physiol*, 169: 856-72.

- Wang, H., Y. Hu, J. Pan, and D. Yu. 2015. 'Arabidopsis VQ motif-containing proteins VQ12 and VQ29 negatively modulate basal defense against *Botrytis cinerea*', *Sci Rep*, 5: 14185.
- Wang, H., Q. Xu, Y. H. Kong, Y. Chen, J. Y. Duan, W. H. Wu, and Y. F. Chen. 2014. 'Arabidopsis WRKY45 Transcription Factor Activates PHOSPHATE TRANSPORTER1; 1 Expression in Response to Phosphate Starvation1[W][OPEN]', *Plant Physiol*, 164: 2020-29.
- Wang, L., K. Tsuda, M. Sato, J. D. Cohen, F. Katagiri, and J. Glazebrook. 2009. 'Arabidopsis CaM binding protein CBP60g contributes to MAMP-induced SA accumulation and is involved in disease resistance against *Pseudomonas syringae*', *PLoS Pathog*, 5: e1000301.
- Weyhe, M., L. Eschen-Lippold, P. Pecher, D. Scheel, and J. Lee. 2014. 'Menage a trois: the complex relationships between mitogen-activated protein kinases, WRKY transcription factors, and VQ-motif-containing proteins', *Plant Signal Behav*, 9: e29519.
- William, D. A., Y. Su, M. R. Smith, M. Lu, D. A. Baldwin, and D. Wagner. 2004. 'Genomic identification of direct target genes of LEAFY', *Proc Natl Acad Sci U S A*, 101: 1775-80.
- Willmann, R., H. M. Lajunen, G. Erbs, M. A. Newman, D. Kolb, K. Tsuda, F. Katagiri, J. Fliegmann, J. J. Bono, J. V. Cullimore, A. K. Jehle, F. Gotz, A. Kulik, A. Molinaro, V. Lipka, A. A. Gust, and T. Nurnberger. 2011. 'Arabidopsis lysin-motif proteins LYM1 LYM3 CERK1 mediate bacterial peptidoglycan sensing and immunity to bacterial infection', *Proc Natl Acad Sci U S A*, 108: 19824-9.
- Xiang, T., N. Zong, Y. Zou, Y. Wu, J. Zhang, W. Xing, Y. Li, X. Tang, L. Zhu, J. Chai, and J. M. Zhou. 2008. 'Pseudomonas syringae effector AvrPto blocks innate immunity by targeting receptor kinases', *Curr Biol*, 18: 74-80.
- Xu, J., J. Meng, X. Meng, Y. Zhao, J. Liu, T. Sun, Y. Liu, Q. Wang, and S. Zhang. 2016. 'Pathogen-Responsive MPK3 and MPK6 Reprogram the Biosynthesis of Indole Glucosinolates and Their Derivatives in Arabidopsis Immunity', *Plant Cell*, 28: 1144-62.
- Xu, J., and S. Zhang. 2015. 'Mitogen-activated protein kinase cascades in signaling plant growth and development', *Trends Plant Sci*, 20: 56-64.
- Xu, X., C. Chen, B. Fan, and Z. Chen. 2006. 'Physical and functional interactions between pathogen-induced Arabidopsis WRKY18, WRKY40, and WRKY60 transcription factors', *Plant Cell*, 18: 1310-26.
- Yamada, K., K. Yamaguchi, T. Shirakawa, H. Nakagami, A. Mine, K. Ishikawa, M. Fujiwara, M. Narusaka, Y. Narusaka, K. Ichimura, Y. Kobayashi, H. Matsui, Y. Nomura, M. Nomoto, Y. Tada, Y. Fukao, T. Fukamizo, K. Tsuda, K. Shirasu, N. Shibuya, and T. Kawasaki. 2016. 'The Arabidopsis CERK1-associated kinase PBL27 connects chitin perception to MAPK activation', *EMBO J*, 35: 2468-83.
- Yamada, K., M. Yamashita-Yamada, T. Hirase, T. Fujiwara, K. Tsuda, K. Hiruma, and Y. Saijo. 2016. 'Danger peptide receptor signaling in plants ensures basal immunity upon pathogen-induced depletion of BAK1', *EMBO J*, 35: 46-61.
- Yamaguchi, Y., G. Pearce, and C. A. Ryan. 2006. 'The cell surface leucine-rich repeat receptor for AtPep1, an endogenous peptide elicitor in Arabidopsis, is functional in transgenic tobacco cells', *Proc Natl Acad Sci U S A*, 103: 10104-9.
- Yamasaki, K., T. Kigawa, S. Watanabe, M. Inoue, T. Yamasaki, M. Seki, K. Shinozaki, and S. Yokoyama. 2012. 'Structural basis for sequence-specific DNA recognition by an Arabidopsis WRKY transcription factor', *J Biol Chem*, 287: 7683-91.
- Yan, C., M. Fan, M. Yang, J. Zhao, W. Zhang, Y. Su, L. Xiao, H. Deng, and D. Xie. 2018. 'Injury Activates Ca(2+)/Calmodulin-Dependent Phosphorylation of JAV1-JAZ8-WRKY51 Complex for Jasmonate Biosynthesis', *Mol Cell*, 70: 136-49 e7.
- Yang, Y., L. Li, and L. J. Qu. 2016. 'Plant Mediator complex and its critical functions in transcription regulation', *J Integr Plant Biol*, 58: 106-18.
- Ye, Y. J., Y. Y. Xiao, Y. C. Han, W. Shan, Z. Q. Fan, Q. G. Xu, J. F. Kuang, W. J. Lu, P. Lakshmanan, and J. Y. Chen. 2016. 'Banana fruit VQ motif-containing protein5 represses cold-responsive transcription factor MaWRKY26 involved in the regulation of JA biosynthetic genes', *Sci Rep*, 6: 23632.

- Yoo, S. D., Y. H. Cho, and J. Sheen. 2007. 'Arabidopsis mesophyll protoplasts: a versatile cell system for transient gene expression analysis', *Nat Protoc*, 2: 1565-72.
- Yu, X., B. Feng, P. He, and L. Shan. 2017. 'From Chaos to Harmony: Responses and Signaling upon Microbial Pattern Recognition', *Annu Rev Phytopathol*, 55: 109-37.
- Yuan, P., E. Jauregui, L. Du, K. Tanaka, and B. W. Poovaiah. 2017. 'Calcium signatures and signaling events orchestrate plant-microbe interactions', *Curr Opin Plant Biol*, 38: 173-83.
- Zambelli, F., G. Pesole, and G. Pavesi. 2009. 'Pscan: finding over-represented transcription factor binding site motifs in sequences from co-regulated or co-expressed genes', *Nucleic Acids Res*, 37: W247-52.
- Zhang, J., W. Li, T. Xiang, Z. Liu, K. Laluk, X. Ding, Y. Zou, M. Gao, X. Zhang, S. Chen, T. Mengiste, Y. Zhang, and J. M. Zhou. 2010. 'Receptor-like cytoplasmic kinases integrate signaling from multiple plant immune receptors and are targeted by a *Pseudomonas syringae* effector', *Cell Host Microbe*, 7: 290-301.
- Zhang, J., F. Shao, Y. Li, H. Cui, L. Chen, H. Li, Y. Zou, C. Long, L. Lan, J. Chai, S. Chen, X. Tang, and J. M. Zhou. 2007. 'A *Pseudomonas syringae* effector inactivates MAPKs to suppress PAMP-induced immunity in plants', *Cell Host Microbe*, 1: 175-85.
- Zhang, L., L. Du, C. Shen, Y. Yang, and B. W. Poovaiah. 2014. 'Regulation of plant immunity through ubiquitin-mediated modulation of Ca(2+) -calmodulin-AtSR1/CAMTA3 signaling', *Plant J*, 78: 269-81.
- Zhang, Z. B., Y. N. Liu, H. Huang, M. H. Gao, D. Wu, Q. Kong, and Y. L. Zhang. 2017. 'The NLR protein SUMM2 senses the disruption of an immune signaling MAP kinase cascade via CRCK3', *Embo Reports*, 18: 292-302.
- Zheng, Z., S. A. Qamar, Z. Chen, and T. Mengiste. 2006. 'Arabidopsis WRKY33 transcription factor is required for resistance to necrotrophic fungal pathogens', *Plant J*, 48: 592-605.
- Zhou, J., S. Wu, X. Chen, C. Liu, J. Sheen, L. Shan, and P. He. 2014. 'The *Pseudomonas syringae* effector HopF2 suppresses Arabidopsis immunity by targeting BAK1', *Plant J*, 77: 235-45.
- Zipfel, C., G. Kunze, D. Chinchilla, A. Caniard, J. D. Jones, T. Boller, and G. Felix. 2006. 'Perception of the bacterial PAMP EF-Tu by the receptor EFR restricts *Agrobacterium*-mediated transformation', *Cell*, 125: 749-60.
- Zipfel, C., S. Robatzek, L. Navarro, E. J. Oakeley, J. D. Jones, G. Felix, and T. Boller. 2004. 'Bacterial disease resistance in Arabidopsis through flagellin perception', *Nature*, 428: 764-7.

8. Appendix

8.1 List of figures

Fig. 1	Scheme of <i>flg22</i> -triggered responses	8
Fig. 2	Consensus VQ-motif	12
Fig. 3	Yeast two-hybrid (Y2H) analysis of MVQ-WRKY interactions	14
Fig. 4	Subcellular localisation of MVQ1-10 and respective VQ-mutants in <i>A. thaliana</i> protoplasts	30
Fig. 5	Expression of GFP-tagged MVQs in <i>A. thaliana</i> protoplasts.....	30
Fig. 6	Co-localisation of MVQs with nuclear marker <i>ERF104</i>	31
Fig. 7	Subcellular localisation of MVQ1-6 and respective phosphosite-mutants (<i>Pmut</i>) in <i>A. thaliana</i> protoplasts.....	32
Fig. 8	Expression of GFP-tagged MVQ1-6 and respective phosphosite-mutants (<i>Pmut</i>) in <i>A. thaliana</i> protoplasts.....	33
Fig. 9	Effect of MVQ1 on the promoter activity of defence marker gene <i>NHL10</i>	34
Fig. 10	Effect of MVQs on promoter activity of defence marker gene <i>NHL10</i>	36
Fig. 11	Expression of HA-tagged MVQs in <i>A. thaliana</i> protoplasts.....	37
Fig. 12	Effect of MVQ1 on <i>flg22</i> -triggered activation of defence gene promoters.....	38
Fig. 13	Expression of MVQ1 and CFP in <i>A. thaliana</i> protoplasts.....	39
Fig. 14	Effect of WRKY33 and MVQ1 ^{<i>Pmut</i>} on activity of a -198 bp fragment of <i>pNHL10</i>	40
Fig. 15	Bimolecular fluorescence complementation of <i>cYFP-MVQ1</i> and <i>cYFP-MVQ1^{DL}</i> with <i>nYFP-WRKYs</i>	42
Fig. 16	Expression of <i>nYFP-WRKY</i> and <i>cYFP-MVQ1/MVQ1^{DL}</i> in <i>A. thaliana</i> protoplasts.....	43
Fig. 17	Characterisation of MVQ1 overexpressing line (MVQ1 OE K11) and T-DNA insertion line <i>mvq1</i>	45
Fig. 18	STRING network analysis of upregulated genes in MVQ1 OE vs. WT under control conditions	47
Fig. 19	STRING network analysis of differentially expressed genes in <i>mvq1</i> vs. WT under control conditions	47
Fig. 20	STRING network analysis of genes downregulated in MVQ1 OE vs. WT under control conditions.....	48
Fig. 21	Comparison of differentially expressed genes in <i>flg22</i> - vs. water treated plants from different genotypes	50
Fig. 22	Hierarchical clustering analysis of genes regulated by MVQ1 and/or <i>flg22</i>	51
Fig. 23	Expression analysis of selected genes in two MVQ1 OE lines after <i>flg22</i> treatment by qRT-PCR.....	54
Fig. 24	MVQ1 binds to a WRKY33-DNA complex.....	56
Fig. 25	Effect of MVQ1 on DNA binding of WRKY DBDs	58
Fig. 26	Effect of different MVQs on DNA binding of WRKY33 cDBD	60
Fig. 27	ChIP-seq reveals target genes bound by MVQ1 in MVQ1 OE line.....	62
Fig. 28	Motifs present in MVQ1 binding regions	62
Fig. 29	MVQ1 binding to different loci.....	64
Fig. 30	Infection of MVQ1 OE lines and WT with the fungal pathogen <i>Botrytis cinerea</i>	66
Fig. 31	Two alternative models describing the molecular mode of action of MVQ1	72
Fig. 32	Model of MVQ1 function within the WRKY network during MTI	77

8.2 List of tables

Tab. 1	Gateway compatible destination vectors used in this study	18
Tab. 2	List of antibodies used in this work	25
Tab. 3	Summary of MVQ effects on flg22-induced promoter activity of NHL10	37
Tab. 4	Differentially expressed genes in MVQ1 misexpression lines	46
Tab. 5	Selected flg22-activated genes that are suppressed in MVQ1 OE	52
Tab. 6	Selected target genes of MVQ1.....	63

8.3 List of supplementary figures

Fig. S1	Subnuclear localisation of MVQ7-10 and respective VQ-mutants in <i>A. thaliana</i> protoplasts.....	96
Fig. S2	Potential MAPK target sites in MVQ1-6	96
Fig. S3	MVQ1 ^{Pmut} interacts with WRKYs from group I and IIc	97
Fig. S4	Southern blot analysis of MVQ1 OE lines	97
Fig. S5	Transcript levels of MVQ1 in MVQ1 OE lines.....	98
Fig. S6	MVQ1 transcripts are induced by flg22 treatment	98
Fig. S7	Interaction of MVQ1 with WRKY DBDs.....	99
Fig. S8	Effect of MVQ1 on DNA binding of WRKY33 cDBD to different W-box probes	100
Fig. S9	Infection of MVQ1 OE K11 and WT with <i>Botrytis cinerea</i>	100
Fig. S10	Binding regions of MVQ1 and WRKYs at three different loci	101
Fig. S11	MVQ transcript levels in respective MVQ T-DNA insertion lines.....	102

8.4 List of supplementary tables

Tab. S1	List of primers used for generation of entry clones (pENTR/SD/D-TOPO).....	103
Tab. S2	List of primers and enzyme used for site-directed mutagenesis	103
Tab. S3	List of primers used for genotyping of T-DNA insertion lines	103
Tab. S4	List of primers used for qRT-PCR	104
Tab. S5	Primers for generation of the probe used in Southern blot analysis	105
Tab. S6	List of oligonucleotides used for generation of DNA-probes.....	105
Tab. S7	List of oligonucleotides used for generation of sgRNA shuttle vectors	106
Tab. S8	GO-enrichment analysis of 117 genes that are up-regulated ($FC \geq 2$) in <i>mvq1</i> vs. WT under control conditions.....	107
Tab. S9	GO-enrichment analysis of 21 genes that are down-regulated ($FC \leq 0.5$) in <i>mvq1</i> vs. WT under control conditions	107
Tab. S10	GO-enrichment analysis of 639 genes that are up-regulated ($FC \geq 2$) in MVQ1 OE (K11) vs. WT under control conditions	108
Tab. S11	GO-enrichment analysis of 431 genes that are down-regulated ($FC \leq 0.5$) in MVQ1 OE (K11) vs. WT under control conditions.....	109
Tab. S12	GO-enrichment analysis of 980 genes that are up-regulated ($FC \geq 2$) in WT 1 h after flg22 treatment compared to water control.....	111
Tab. S13	GO-enrichment analysis of 454 genes that are down-regulated ($FC \leq 0.5$) in WT 1 h after flg22 treatment compared to water control.....	114
Tab. S14	GO-enrichment analysis of 385 genes that are up-regulated ($FC \geq 2$) in <i>mvq1</i> but not in WT 1 h after flg22 treatment compared to respective water control.....	115
Tab. S15	GO-enrichment analysis of 160 genes that are up-regulated ($FC \geq 2$) in MVQ1 OE (K11) but not in WT 1 h after flg22 treatment compared to respective water control.....	116

<i>Tab. S16</i>	<i>Enrichment of TF-binding motifs in promoters of genes whose flg22-mediated induction is suppressed in MVQ1 OE (404 genes identified in clustering analysis)</i>	<i>118</i>
<i>Tab. S17</i>	<i>GO-enrichment analysis of 232 genes that were identified as targets of MVQ1 by ChIP-seq.....</i>	<i>119</i>

8.5 List of supplementary data files (see compact disc)

<i>File 1</i>	<i>Microarray data (Expression data for all identified genes)</i>
<i>File 2</i>	<i>HOPACH-Clustering of scaled expression data from differentially expressed genes in MVQ1OE, mvq1 and WT</i>
<i>File 3</i>	<i>HOPACH-Clustering of scaled expression data from differentially expressed genes in MVQ1OE and WT without mvq1</i>
<i>File 4</i>	<i>List of 404 genes that were identified in 4 different clusters as genes, whose activation by flg22 is strongly reduced in MVQ1OE</i>
<i>File 5</i>	<i>List of MVQ1 targets identified in ChIP-seq in control treatment samples</i>
<i>File 6</i>	<i>List of MVQ1 targets identified in ChIP-seq in flg22-treated samples (1 μM flg22, 1 h)</i>

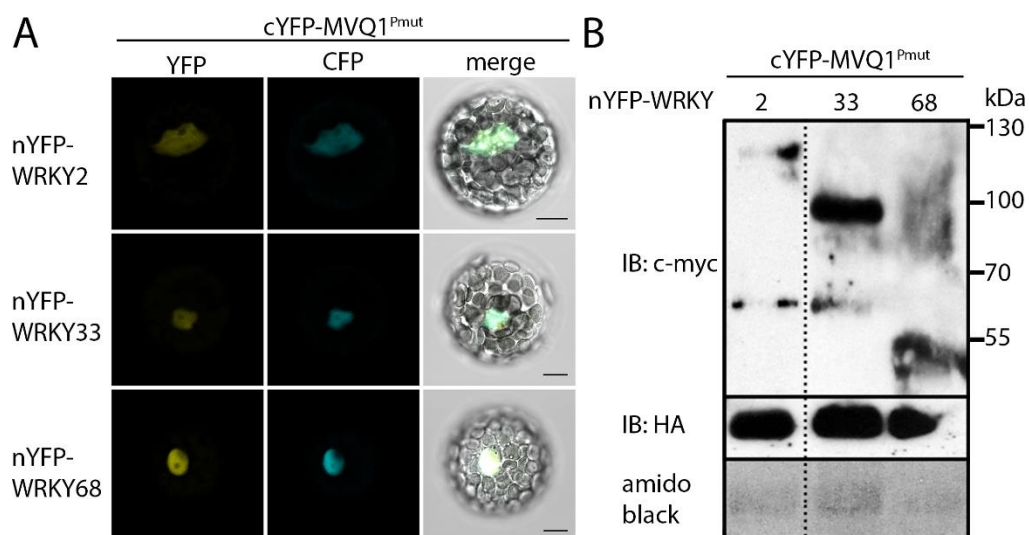


Fig. S3 **MVQ1^{Pmut} interacts with WRKYs from group I and IIc:** *A.* *thaliana* protoplasts were co-transfected with plasmids encoding cYFP-MVQ1^{Pmut} and n-YFP tagged WRKYs from subgroup I and IIc. A plasmid encoding ERF104-CFP was additionally transfected serving as a nuclear marker. **(A)** YFP reconstitution was analysed 16 h after transfection by confocal laser scanning microscopy. YFP-fluorescence (1st panel), CFP-fluorescence (2nd panel) and brightfield image were recorded in different channels and merged (3rd panel). Scale bars represent 10 μ m. **(B)** Immunoblot analysis confirmed expression of the nYFP-WRKY and cYFP-MVQ1^{Pmut} fusions.

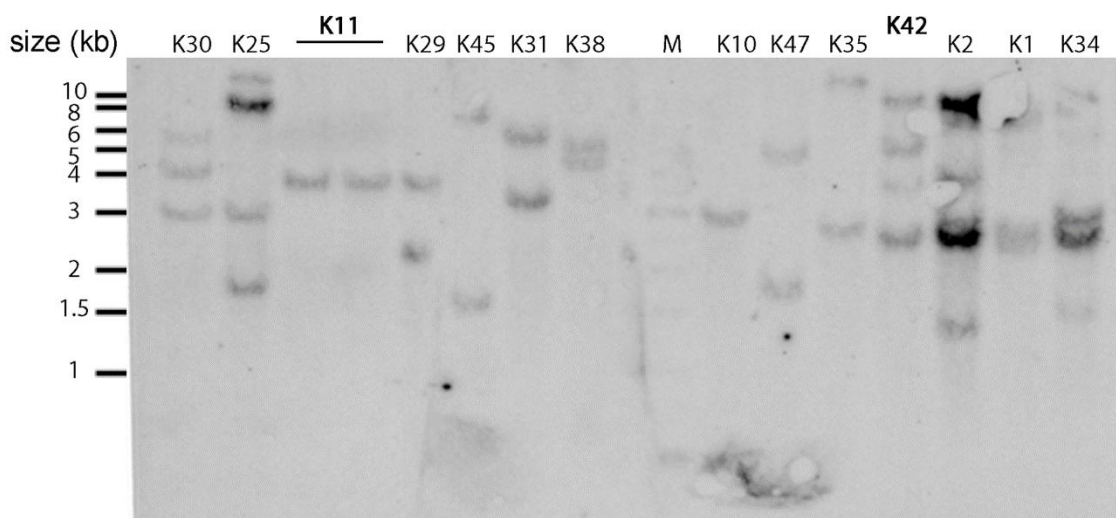


Fig. S4 **Southern blot analysis of MVQ1 OE lines:** Genomic DNA from different independent MVQ1 OE lines that carrying a pEarley203-MVQ1 construct was isolated and digested with EcoR1. Samples were subjected to agarose gel electrophoresis and southern blot analysis. The samples were hybridised with a radio-labelled probe that binds to the BASTA resistance gene of the pEarley203 construct. K11 was selected as a potential single copy line. Line 42 with multiple insertions was used as a second independent line in further experiments.

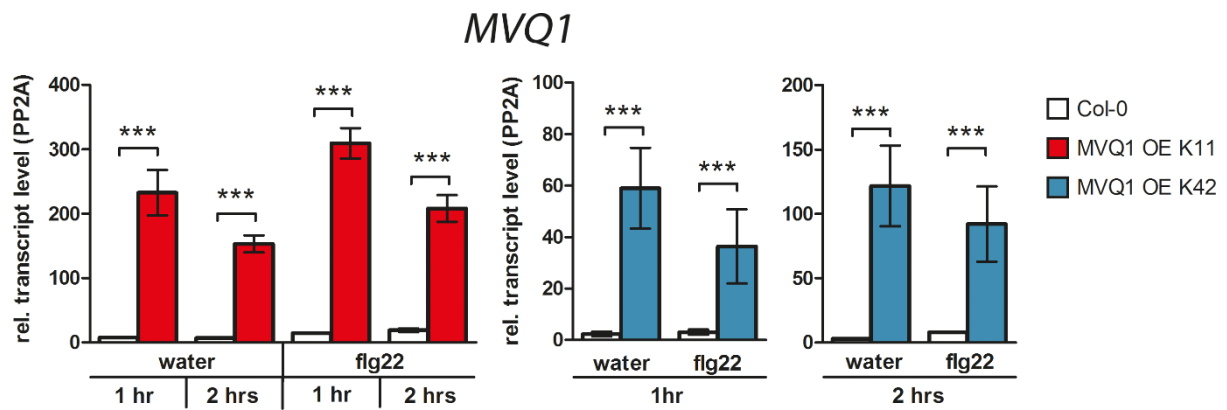


Fig. S5 Transcript levels of *MVQ1* in *MVQ1* OE lines : WT (Col-0) and plants from two independent *MVQ1* OE lines (K11 and K42) were infiltrated with 1 μ M flg22 or water as a control and samples were harvested after 1 h and 2 h. RNA was extracted for subsequent cDNA synthesis and analysis by qRT-PCR. *PP2A* served as a reference gene. For Col-0/K11 comparison, samples were derived from one experiment. For Col-0/K42 comparison, samples were derived from two independent experiments (one experiment for each time point) and therefore measured independently (see individual y-axis). Data is shown as mean and SEM, $n \geq 5$. Asterisks indicate statistically significant differences between Col-0 and respective *MVQ1* OE plants (unpaired two-tailed t-test after log₂ transformation, *** $p \leq 0.001$).

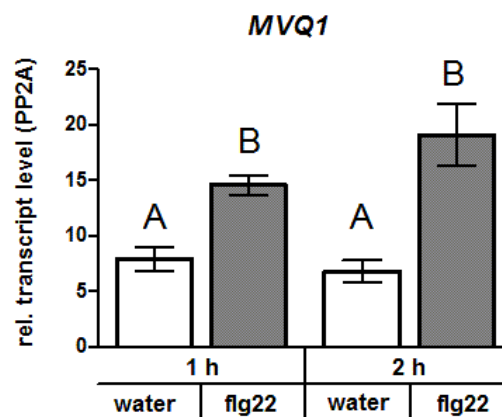


Fig. S6 *MVQ1* transcripts are induced by flg22 treatment: WT (Col-0) plants were infiltrated with 1 μ M flg22 or water as a control and samples were harvested after 1 h and 2 h. RNA was extracted for subsequent cDNA synthesis and analysis by qRT-PCR. *PP2A* served as a reference gene. Data is shown as mean and SEM, $n \geq 5$. Statistically different groups are denoted by letters (One-way ANOVA, Bonferroni multiple comparison post-test $p \leq 0.05$).

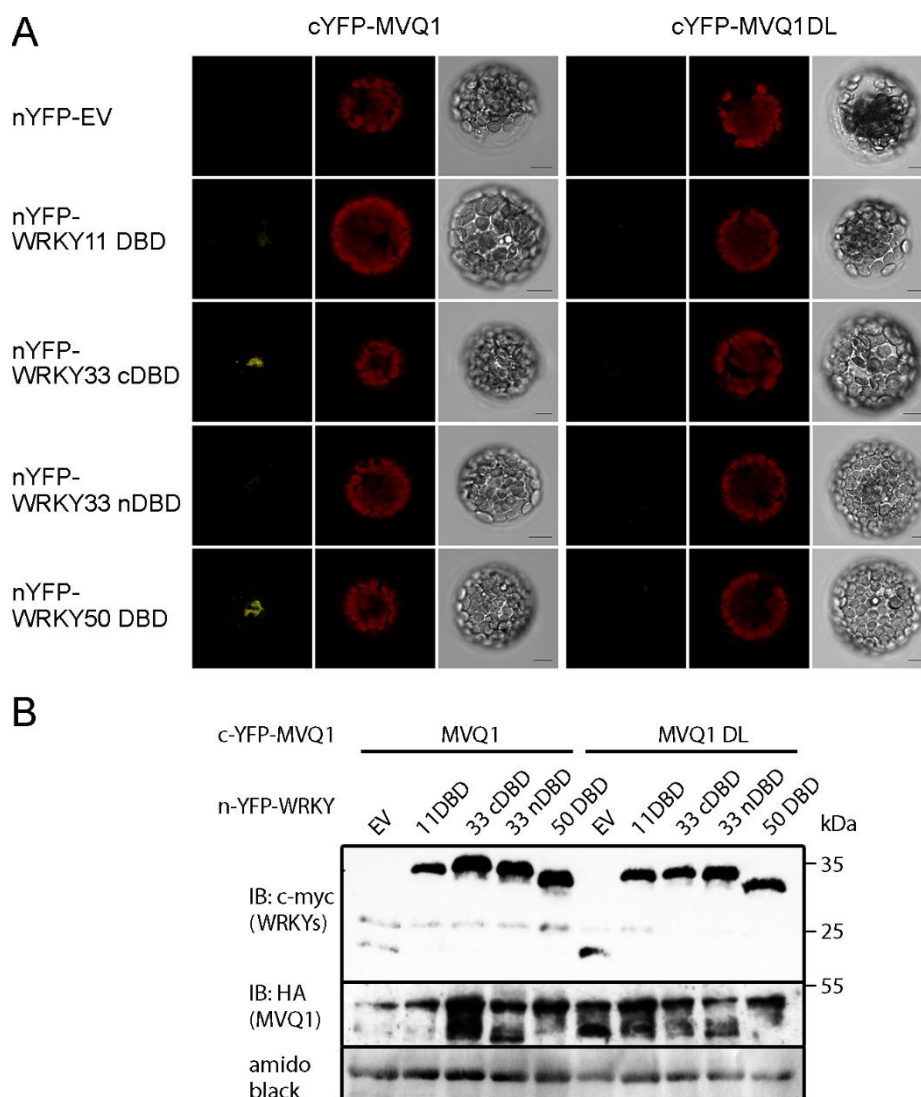


Fig. S7 Interaction of MVQ1 with WRKY DBDs: *A. thaliana* protoplasts were co-transfected with plasmids encoding cYFP-MVQ1 or cYFP-MVQ1^{DL} and n-YFP tagged WRKY DBDs or an empty vector control. YFP reconstitution was analysed 16 h after transfection by confocal laser scanning microscopy. **(A)** YFP-fluorescence (1st panel), chlorophyll fluorescence (2nd panel) and brightfield image (3rd panel) were recorded in different channels. Scale bars represent 10 μ m. Images are representative of three independent experiments with similar results. **(B)** Immunoblot analysis showed expression of the nYFP-WRKY DBDs and cYFP-MVQ1 fusions.

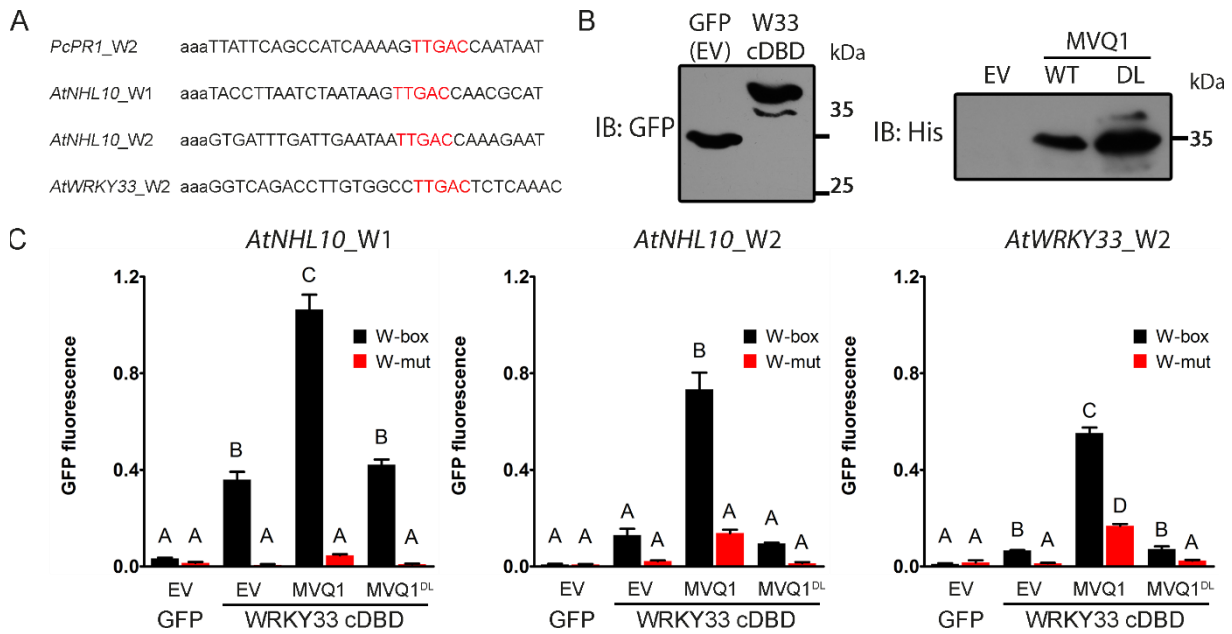


Fig. S8 Effect of MVQ1 on DNA binding of WRKY33 cDBD to different W-box probes: (A) Sequences of the W-box containing probes derived from promoters of defence-related genes in parsley and arabidopsis. **(B)** Bacterial protein extracts were subjected to SDS-PAGE and immunoblot analysis using antibodies against GFP (WRKY DBDs) or His (MVQ1) to confirm protein expression. **(C)** Crude *E. coli* extracts containing GFP (EV control) or GFP-tagged WRKY33 cDBD were pre-incubated with bacterial extracts containing MVQ1, MVQ1^{DL} or EV control and incubated with different immobilised W-box containing probes or W-mut versions harbouring a mutation in the W-box. After washing, GFP signal was quantified to assess the amount of WRKY DBD bound to the probe. Three independent extracts were used in independent experiments. Bars represent mean values with error bars indicating SEM. Statistically different groups are denoted by letters (One-way ANOVA, Bonferroni multiple comparison post-test $p \leq 0.05$).

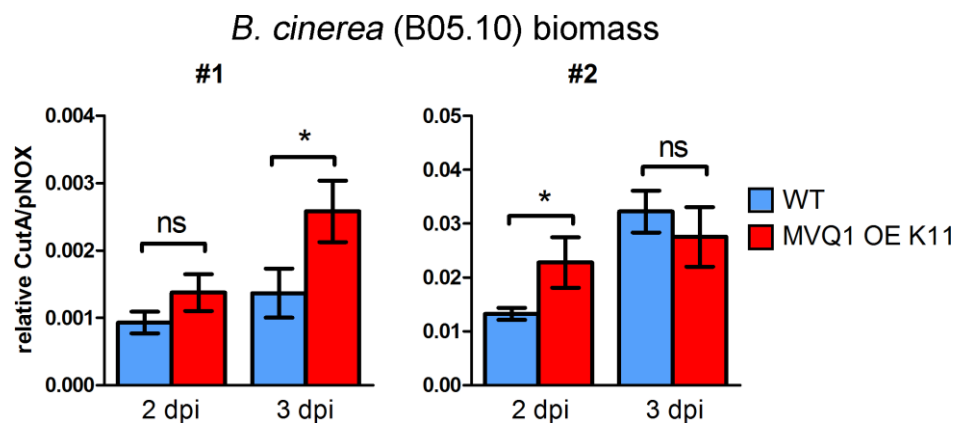


Fig. S9 Infection of MVQ1 OE K11 and WT with *Botrytis cinerea*: MVQ1 OE line (K11) and WT (Col-0) were grown for 5 weeks and infected with *B. cinerea* (strain B05.10) by drop inoculation ($10 \mu\text{l}$ of 2×10^5 spores/ml). Leaf discs ($d = 8 \text{ mm}$) from four infected leaves were harvested and pooled for each of the six plants per genotype and time point, $n = 6$ for quantification of fungal DNA by qPCR. DNA was extracted and spiked with plasmid DNA during extraction. Amount of fungal *CUTINASE A* was quantified and spiked plasmid DNA was used as reference. Data is presented as mean values with error bars indicating SEM. Asterisks indicate statistically significant differences between WT and MVQ1 OE K11 (unpaired two-tailed t-test after \log_2 -transformation, $* p \leq 0.05$, ns – not significant). Two independent experiments are shown.

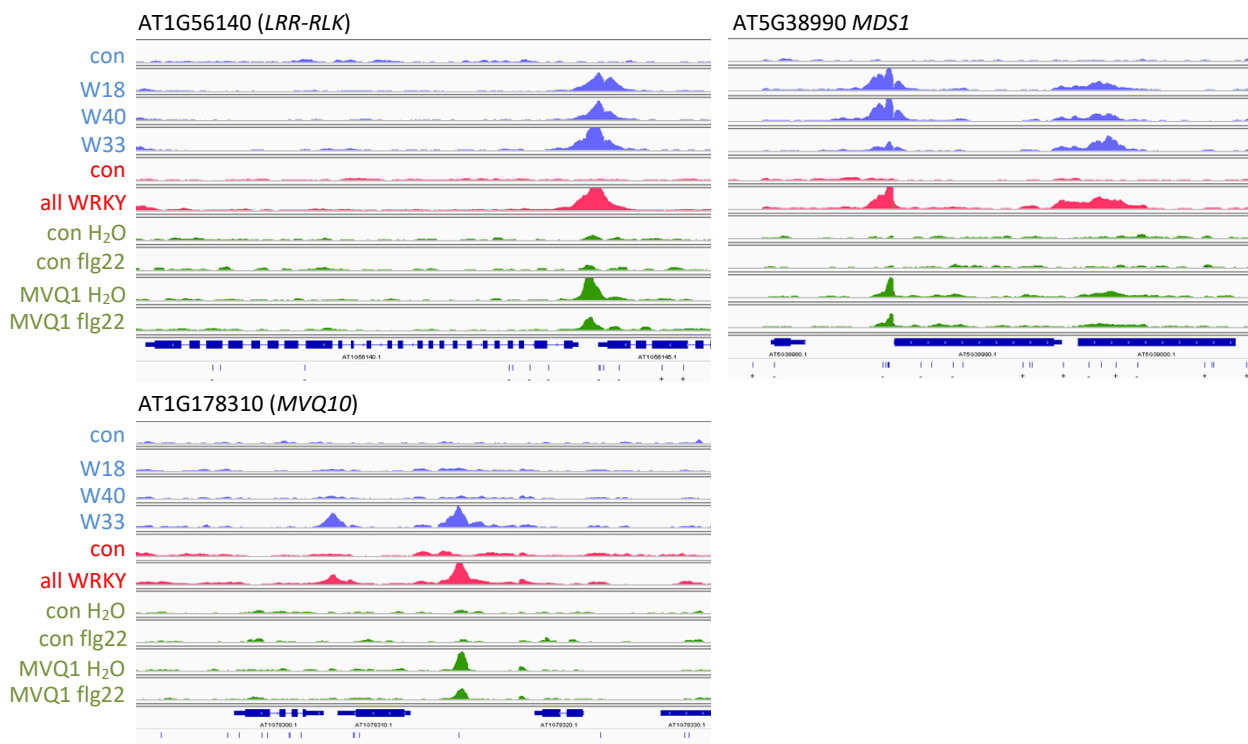


Fig. S10 Binding regions of MVQ1 and WRKYs at three different loci: Integrative Genomic Viewer (IGV) images of ChIP-seq results from different experiments. Analysis was performed by Dr. R. Birkenbihl using data from (Birkenbihl, Kracher, and Somssich 2017). Shown are three loci illustrating MVQ1 targets that are also targeted by WRKYs. WRKY18, WRKY40 WRKY33 and possibly additional WRKYs target **AT1G56140**. **AT5G38990** is targeted by WRKY18 and WRKY40 but not WRKY33. **AT1G178310** is only targeted by WRKY33 and potentially by additional WRKYs (other than WRKY18 or WRKY40). Read coverage histograms indicate binding of HA-tagged WRKY18, WRKY40 or WRKY33 (blue) 2 h after flg22 treatment in lines expressing respective HA-tagged WRKYs under native promoters compared to control samples (WT); binding of WRKYs 2 h after flg22 treatment detected by anti-all WRKY antibody in WT (red) compared to input control; binding of c-Myc-tagged MVQ1 in MVQ1 OE plants (K11) 1 h after control treatment or treatment with flg22 compared to control samples (WT). Last row displays gene structures and location of W-boxes is marked by blue lines.

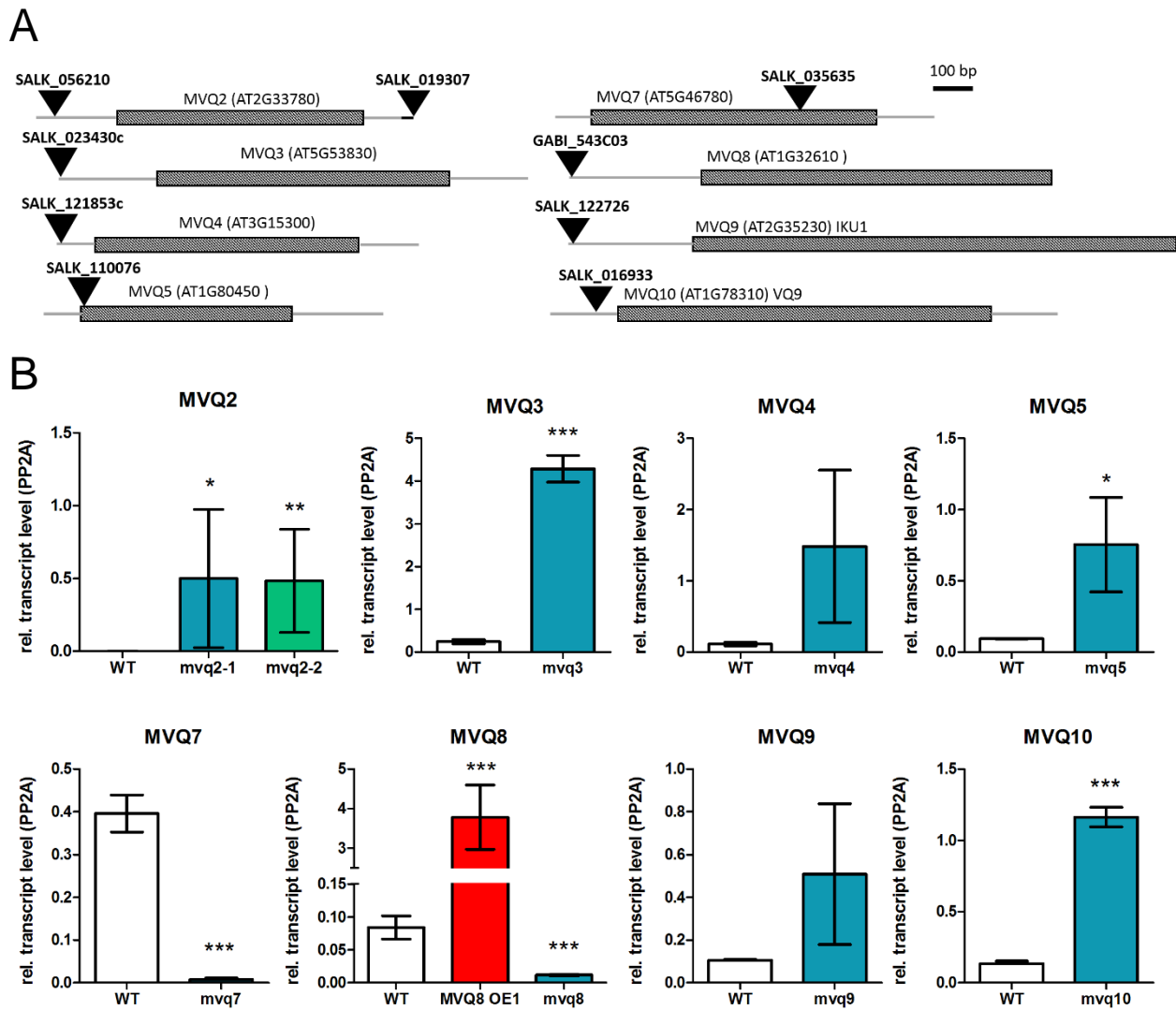


Fig. S11 MVQ transcript levels in respective MVQ T-DNA insertion lines: (A) Scheme drawn to scale of MVQ loci with coding region (box) and 5'/3' UTRs (grey lines). Location of T-DNA insertion is depicted by black triangle. **(B)** RNA was extracted from leaves of indicated plant lines and used for cDNA synthesis and subsequent analysis by qRT-PCR. PP2A served as reference gene. Relative transcript levels are represented by $2^{-\Delta ct}$ and error bars indicate SEM. Blue and green bars represent T-DNA insertion lines and red bars represent OE lines (pEarley203). mvq2-1 = SALK_056210, mvq2-2 = SALK_019307, in all other cases only one SALK or GABI line was used. For MVQ6 a SALK line (SALK_120763) was isolated but sequencing revealed that T-DNA insertion is in a different locus (AT1G27900). Asterisks indicate statistical different transcript levels compared to WT (Two-tailed t-test after log₂ transformation; *** $p \leq 0.001$, ** $p \leq 0.005$, * $p \leq 0.05$ $n=3$). Note break in y-axis for better visualisation of MVQ8 OE column.

8.6 Supplementary tables

Tab. S1 List of primers used for generation of entry clones (pENTR/SD/D-TOPO)

Name	Sequence
MVQ1_TOPO fwd	CACCATGGAGAATTCACCGAG
MVQ1_TOPO rev -stop	AGAAGTAGAAGCTGATGAAGAACC
MVQ2_TOPO fwd	CACCATGGAGAAATCACCAAGATAC
MVQ2_TOPO rev -stop	ATGATCATGAGGTGAAGGCGCCGG
MVQ3_TOPO fwd	CACCATGGAAGTTTCAACATC
MVQ3_TOPO rev-stop	AGAGTTCCTCGCCGGAG
MVQ4_TOPO fwd	CACCATGGAGATTTCAACAAA
MVQ4_TOPO rev -stop	CATCTCCGGCGATAATCTC
MVQ5_TOPO fwd	CACCATGAGTCACCAGCAGCC
MVQ5_TOPO rev -stop	AGAGTCTCGATGATTATCTTCATGAATCC
MVQ6_TOPO fwd	CACCATGAATAGCAAAGGGAG
MVQ6_TOPO rev -stop	TGGTTTGCCACTCGAATTG
MVQ8_TOPO fwd	CACCATGGATAGGACTTGTTG
MVQ8_TOPO rev-stop	GTAACCTCTCCATCTTTGACTAGATATTG

Tab. S2 List of primers and enzyme used for site-directed mutagenesis of pENTR/SD/D-TOPO-MVQ3 to generate MVQ3^{DL}

Name	Sequence	Enzyme
DL MVQ3 fw	AAAGGTCTCGATCTGATGCTTACCGGCTC	Bsal
DL MVQ3 rev	AAAGGTCTCCAGATCGACTTGTGGAAAGTAGAAG	

Tab. S3 List of primers used for genotyping of T-DNA insertion lines

Name	Sequence
LBb1.3	ATTTTGCCGATTTCCGGAAC
GKo8409	ATATTGACCATCATACTCATTGC
GKo8760	GGGCTACACTGAATTGGTAGCTC
GKo2588	CGCCAGGGTTTTCCAGTCACGACG
MVQ1-LP Salk_107266	ACTCTAGGAGAAGTCACCGGG
MVQ1-RP Salk_107266	AGAGCACATTTTTCTCCAC
MVQ2-LP Salk_019307	AAAAATGATTTCAAGAGTGTATGAGTG
MVQ2-RP Salk_019307	CCGAGATTTCTCTTTTTCAC
MVQ2-LP Salk_056210	AATTTGGTGTGCAGAGATTGC
MVQ2-RP Salk_056210	TGAAGGAAGCAAGTTCTTTGC
MVQ3-LP Salk_023430	AAAGGAACAAAAGAGCATGCC
MVQ3-RP Salk_023430	TGCTTGAACAAATGTTGTTGG
MVQ4-RP Salk_121853.54.50	GGGGAAATCAAGACAGCTAGG
MVQ4-RP Salk_121853.18.25	CTCTTCTCCGATAATGGC
MVQ5-LP Salk_110076	ATCAATCATTACGCAGTTGCC

MVQ5-RP Salk_110076	GAGAACGAAGAGGAAACAGGG
VQP6-RP Salk_120763	AATCATCAAGCATTGGATTGG
VQP6-LP Salk_120763	TCCAAGGATTTTTGGGTCTG
MVQ7-LP Salk_035635	GGTACAGTAAACGCGGATTTG
MVQ7-RP Salk_035635	CCAAGATTTGGATTTGCTCTG
MVQ8-LP GABI_543C03	TTTTGCAACTAGAGGAGGACC
MVQ8-RP GABI_543C03	TGAGGTAAACTCTCACGCGAC
MVQ9-LP Salk_152726	CGAGAGTTAAGCGGATATTCATC
MVQ9-RP Salk_152726	ACCCAACACCAAATATGACCC
MVQ10-LP Salk_016933	GGACTGCGTAAAGCCAATTAC
MVQ10-RP Salk_016933	TCACGTTATCAATCGTCCTCC

Tab. S4 List of primers used for qRT-PCR

Purpose	Name	Sequence
qRT-PCR	NHL10_F	ACGCCGGACAGTCTAGGA
	NHL10_R	CCCTAAGCCTGAACTTGATCTC
	PP2A_F	GACCGGAGCCAACTAGGAC
	PP2A_R	AAAAC TTGGTAACTTTCCAGCA
	RLP23_F	GATTAGAGGGCTTGTTCCTTCC
	RLP23_R	ACTGAATGAGGAAGGAACTTGG
	ProPep3 F	GCGAGGAAGATGAGAGTATCG
	ProPep3 R	TCAATGGTCATGCCATCTTCT
	AtFRK1_F	GAGACTATTTGGCAGGTAAAAGGT
	AtFRK1_R	AGGAGGCTTACAACCATTGTG
	MVQ1_qRT_F	TTGCGGTATGAGCAGTAGCA
	MVQ1_qRT_R	TTGGACGAATGTTGTCGGGT
	MVQ2_qRT_F	AAGCAGCTGCACCACTACAC
	MVQ2_qRT_R	CGGATGAAAGTGGTTTCATACATG
	MVQ3_qRT_F	TCTTCATCCATCTCCAGTCTCA
	MVQ3_qRT_R	CCGGAAAAAGAGGAAGAAGC
	MVQ4_qRT_F	CAACTCCGAGAGATTCTGAGC
	MVQ4_qRT_R	GCGATAATCTCGGAGAAGTCA
	MVQ5_qRT_F	TAACGACGCTTTCAGCCATT
	MVQ5_qRT_R	CCCAGAATGGGTCTAGGTGA
	MVQ7_qRT_F	AGTGTATTAATAATCCTGATGGTGGAT
	MVQ7_qRT_R	TGAAATGAGCAATTTTCTTTCTAGC
	MVQ8_qRT_F	CATCAATGGATCAACCTGGA
	MVQ8_qRT_R	AACCCCAAACGGAGATGC
	MVQ9_qRT_F	AGGGCCCTCTCAACCTAAC
	MVQ9_qRT_R	GGCACTGGGCTAGGAACTAA
MVQ10_qRT_F	CACCATCGCAGCATAACAGT	
MVQ10_qRT_R	AAACAGCAGAGGAAGGAGGA	

qRT-PCR Botrytis assay	BcCut_#7_5	ATAAGCGCCGAGCATGTG
	BcCut_#7_3	GGGATGACGGAAAAATAGACG
	StNOX_5	CTTCAGTTCATGAACAAGAATGTAGG
	StNOX_3	CATTCCATTAACAGCAAGTTGATCGA

Tab. S5 Primers for generation of the probe used in Southern blot analysis

Name	Sequence
BASTA-F	AACTTCGTACCGAGCCGCA
BASTA-R	GCTGAAGTCCAGCTGCCAGAAAC

Tab. S6 List of oligonucleotides used for generation of DNA-probes: W-boxes and mutated versions are marked in red

	Description	Name	Sequence
Cy5- labelled probes for EMSA	<i>PcPR1_W2</i>	W2-s	CY5-aaaTTATTCAGCCATCAAAAG TTGACCA AATAAT
		W2-as	ATTATT GGTCAA CTTTTGATGGCTGAATAATTT
	<i>PcPR1_W2mut</i>	W2m-s	CY5-aaaTTATTCAGCCATCAAAAG TTACCCA AATAAT
		W2m-as	ATTATT GGGTAA CTTTTGATGGCTGAATAATTT
Biotin- labelled probes for DPI-ELISA	<i>PcPR1_W2</i>	W2-S	BIO-aaaTTATTCAGCCATCAAAAG TTGACCA AATAAT
		W2-AS	ATTATT GGTCAA CTTTTGATGGCTGAATAATTT
	<i>PcPR1_W2mut</i>	W2mut-S	BIO-aaaTTATTCAGCCATCAAAAG TTACCCA AATAAT
		W2mut-AS	ATTATT GGGTAA CTTTTGATGGCTGAATAATTT
	<i>AtNHL10_W1</i>	pNHL10_W1-S	BIO-aaaTACCTTAATCTAATAAG TTGACCA ACGCAT
		pNHL10_W1-AS	ATGCGTT GGTCAA CTTATTAGATTAAGGTATTT
	<i>AtNHL10_W1mut</i>	pNHL10_W1mut-S	BIO-aaaTACCTTAATCTAATAAG TTACCCA ACGCAT
		pNHL10_W1mut-AS	ATGCGTT GGGTAA CTTATTAGATTAAGGTATTT
	<i>AtNHL10_W2</i>	pNHL10_W2-S	BIO-aaaGTGATTTGATTGAATAA TTGACCA AGAAT
		pNHL10_W2-AS	ATTCTTT GGTCAA ATTATTCAATCAAATCACTTT
	<i>AtNHL10_W2mut</i>	pNHL10_W2mut-S	BIO-aaaGTGATTTGATTGAATAA TTACCCA AGAAT
		pNHL10_W2mut-AS	ATTCTTT GGGTAA ATTATTCAATCAAATCACTTT
	<i>AtWRKY33_W2</i>	pWRKY33_W2-S	BIO-aaaGGTCAGACCTTGTTGGCC TTGACT CTCAAAC
		pWRKY33_W2-AS	GTTTGAG AGTCA AGGCCACAAGGTCTGACCTTT
	<i>AtWRKY33_W2mut</i>	pWRKY33_W2mut-S	BIO-aaaGGGTAGACCTTGTTGGCC TTACCT CTCAAAC
		pWRKY33_W2mut-AS	GTTTGAG AGGTAA AGGCCACAAGGTCTACCTTT

Tab. S7 List of oligonucleotides used for generation of sgRNA shuttle vectors: For each MVQ, 2 targets were generated

Gene	Name	Sequence	sgRNA target sequence
MVQ2 At2g33780	CAS_MVQ2t1o1	attgAGGATCGGTTCGGATGAAAG	AGGATCGGTTCGGATGAAAGTGG
	CAS_MVQ2t1o2	aaacCTTTCATCCGAACCGATCCT	
	CAS_MVQ2t7o1	attgCGTCACCGTCGACAACCTCCG	CGTCACCGTCGACAACCTCCGAGG
	CAS_MVQ2t7o2	aaacCGGAGTTGTGACGGTGACG	
MVQ3 At5g53830	CAS_MVQ3t1o1	attgGGAGATGAGATCATAGGAGG	GGAGATGAGATCATAGGAGGTGG
	CAS_MVQ3t1o2	aaacCCTCCTATGATCTCATCTCC	
	CAS_MVQ3t4o1	attgGGGTCATCGTTGCTTCTCAG	GGGTCATCGTTGCTTCTCAGTGG
	CAS_MVQ3t4o2	aaacCTGAGAAGCAACGATGACCC	
MVQ4 At3g15300	CAS_MVQ4t1o1	attgAGAGTCTGGAGATCTTGGGG	AGAGTCTGGAGATCTTGGGGAGG
	CAS_MVQ4t1o2	aaacCCCCAAGATCTCCAGACTCT	
	CAS_MVQ4t6o1	attgGACTGTAAAGTCAAGCTTG	GACTGTAAAGTCAAGCTTGGGG
	CAS_MVQ4t6o2	aaacCAAGCTTGCACTTAACAGTC	
MVQ5 At1g80450	CAS_MVQ5t2o1	attgGAACATGGTGTGGCTCGG	GAACATGGTGTGGCTCGGTGG
	CAS_MVQ5t2o2	aaacCCGAGCCAAACACCATGTTC	
	CAS_MVQ5t10o1	attgGGTGAGAGACGGGAGAGACG	GGTGAGAGACGGGAGAGACGAGG
	CAS_MVQ5t10o2	aaacCGTCTCTCCCGTCTCTACC	
MVQ6 At5g08480	CAS_MVQ6t1o1	attgAGTTGGCCTCTTTGTATGG	AGTTGGCCTCTTTGTATGGCGG
	CAS_MVQ6t1o2	aaacCCATACAAAAGAGGCCAACT	
	CAS_MVQ6t2o1	attgGTGGGCTTAAAGCTCAGAGG	GTGGGCTTAAAGCTCAGAGGAGG
	CAS_MVQ6t2o2	aaacCCTCTGAGCTTAAAGCCAC	
MVQ7 At5g46780	CAS_MVQ7t2o1	attgGGAGGTGGAGGTGGAGGTGG	GGAGGTGGAGGTGGAGGTGGAGG
	CAS_MVQ7t2o2	aaacCCACCTCCACCTCCACCTCC	
	CAS_MVQ7t9o1	attgGGAAATGGTGATCTTGGCTG	GGAAATGGTGATCTTGGCTGCGG
	CAS_MVQ7t9o2	aaacCAGCCAAGATCACCATTTC	
MVQ8 At1g32610	CAS_MVQ8t1o1	attgAGATTCCGAGGAAGAGGCTG	AGATTCCGAGGAAGAGGCTGAGG
	CAS_MVQ8t1o2	aaacCAGCCTCTCCTCGGAATCT	
	CAS_MVQ8t8o1	attgCGGTAAGCAGTTGGAGATTG	CGGTAAGCAGTTGGAGATTGTGG
	CAS_MVQ8t8o2	aaacCAATCTCCAACCTGCTTACCG	
MVQ9 At2g35230	CAS_MVQ9t1o1	attgGCAAAGTGGAGATGAGACTG	GCAAAGTGGAGATGAGACTGTGG
	CAS_MVQ9t1o2	aaacCAGTCTCATCTCAGTTTGC	
	CAS_MVQ9t9o1	attgGGGCCCTGCATGTTTCATTG	GGGCCCTGCATGTTTCATTGAGG
	CAS_MVQ9t9o2	aaacCGAATGAACATGCAGGGCCC	
MVQ10 At1g78310	CAS_MVQ10t1o1	attgTGCAGAGGCGGATACGGCGG	TGCAGAGGCGGATACGGCGGAGG
	CAS_MVQ10t1o2	aaacCCGCCGTATCCGCTCTGCA	
	CAS_MVQ10t10o1	attgGCCGTTACCACCGTTTACCG	GCCGTTACCACCGTTTACCGCGG
	CAS_MVQ10t10o2	aaacCGTGAACCGGTGGTAACGCG	

Tab. S8 GO-enrichment analysis of 117 genes that are up-regulated ($FC \geq 2$) in mvq1 vs. WT under control conditions

GO Biological process (related classes clustered together)	# of genes in genome (27502)	# of genes in upload list (117)	# of genes expected in upload list	GO Enrichment (fold)	P-value
maturation of LSU-rRNA from tricistronic rRNA transcript (SSU-rRNA, 5.8S rRNA, LSU-rRNA)	16	4	0.07	61.39	3.24E-03
maturation of LSU-rRNA	32	5	0.13	38.37	1.08E-03
ribosomal large subunit biogenesis	97	10	0.4	25.31	5.55E-08
ribonucleoprotein complex biogenesis	481	27	1.96	13.78	2.94E-19
cellular component biogenesis	1246	33	5.07	6.5	1.27E-14
cellular component organization or biogenesis	3089	39	12.58	3.1	1.36E-07
ribosome biogenesis	396	27	1.61	16.74	2.34E-21
rRNA processing	225	20	0.92	21.83	3.62E-17
rRNA metabolic process	237	20	0.97	20.72	9.42E-17
ncRNA metabolic process	414	21	1.69	12.46	1.82E-13
RNA metabolic process	1335	26	5.44	4.78	7.52E-08
nucleic acid metabolic process	1776	28	7.23	3.87	1.35E-06
nucleobase-containing compound metabolic process	2272	29	9.25	3.13	6.96E-05
organic cyclic compound metabolic process	2867	31	11.68	2.66	8.41E-04
cellular nitrogen compound metabolic process	3138	41	12.78	3.21	1.15E-08
nitrogen compound metabolic process	6477	47	26.38	1.78	4.67E-02
heterocycle metabolic process	2584	30	10.52	2.85	3.03E-04
cellular aromatic compound metabolic process	2748	30	11.19	2.68	1.13E-03
macromolecule metabolic process	5642	44	22.98	1.91	1.56E-02
ncRNA processing	336	21	1.37	15.35	3.29E-15
RNA processing	777	24	3.16	7.58	3.79E-11
gene expression	1605	37	6.54	5.66	6.04E-15
maturation of SSU-rRNA from tricistronic rRNA transcript (SSU-rRNA, 5.8S rRNA, LSU-rRNA)	39	6	0.16	37.78	7.64E-05
maturation of SSU-rRNA	50	6	0.2	29.47	2.94E-04
ribosomal small subunit biogenesis	83	8	0.34	23.67	1.00E-05
nucleocytoplasmic transport	122	6	0.5	12.08	3.87E-02
nuclear transport	122	6	0.5	12.08	3.87E-02
translation	588	12	2.39	5.01	1.67E-02
peptide biosynthetic process	593	12	2.41	4.97	1.81E-02
amide biosynthetic process	664	13	2.7	4.81	1.04E-02
Unclassified	4961	13	20.2	0.64	0.00E+00

Tab. S9 GO-enrichment analysis of 21 genes that are down-regulated ($FC \leq 0.5$) in mvq1 vs. WT under control conditions

GO Biological process (related classes clustered together)	# of genes in genome (27502)	# of genes in upload list (21)	# of genes expected in upload list	GO Enrichment (fold)	P-value
cellular response to hypoxia	27	3	0.02	> 100	3.61E-03
cellular response to decreased oxygen levels	29	3	0.02	> 100	4.40E-03
cellular response to oxygen levels	29	3	0.02	> 100	4.40E-03
response to abiotic stimulus	2097	10	1.52	6.56	1.68E-03

Appendix

response to hypoxia	66	3	0.05	62.5	4.57E-02
response to stress	3552	12	2.58	4.65	2.75E-03
cellular response to stress	943	8	0.69	11.67	4.71E-04
innate immune response	310	5	0.23	22.18	7.03E-03
immune response	316	5	0.23	21.76	7.71E-03
immune system process	373	5	0.27	18.43	1.71E-02
defense response	1513	9	1.1	8.18	1.25E-03
defense response to other organism	952	7	0.69	10.11	8.72E-03
response to other organism	1253	9	0.91	9.88	2.54E-04
response to external biotic stimulus	1253	9	0.91	9.88	2.54E-04
response to external stimulus	1659	10	1.21	8.29	1.89E-04
response to biotic stimulus	1266	9	0.92	9.78	2.77E-04
multi-organism process	1759	9	1.28	7.04	4.40E-03
Unclassified	4961	2	3.61	0.55	0.00E+00

Tab. S10 GO-enrichment analysis of 639 genes that are up-regulated ($FC \geq 2$) in MVQ1 OE (K11) vs. WT under control conditions

GO Biological process (related classes clustered together)	# of genes in genome (27502)	# of genes in upload list (639)	# of genes expected in upload list	GO Enrichment (fold)	P-value
respiratory burst	6	5	0.14	36.67	6.05E-03
toxin biosynthetic process	21	7	0.48	14.67	5.60E-03
toxin metabolic process	71	12	1.61	7.44	8.23E-04
secondary metabolic process	389	30	8.84	3.39	6.57E-05
secondary metabolite biosynthetic process	185	18	4.2	4.28	2.04E-03
defense response by callose deposition	18	6	0.41	14.67	3.08E-02
defense response	1513	80	34.38	2.33	2.43E-08
response to stress	3552	175	80.72	2.17	1.79E-19
response to stimulus	6214	266	141.22	1.88	2.13E-24
response to chitin	136	35	3.09	11.32	2.88E-20
response to drug	592	69	13.45	5.13	2.25E-23
response to chemical	2874	151	65.31	2.31	1.68E-18
response to oxygen-containing compound	1619	112	36.79	3.04	2.11E-21
response to organonitrogen compound	230	38	5.23	7.27	2.64E-16
response to nitrogen compound	294	41	6.68	6.14	2.25E-15
response to organic substance	2026	112	46.04	2.43	4.24E-14
jasmonic acid metabolic process	47	11	1.07	10.3	1.45E-04
small molecule metabolic process	1745	75	39.66	1.89	6.74E-04
hormone metabolic process	259	20	5.89	3.4	1.39E-02
regulation of hormone levels	409	25	9.29	2.69	4.58E-02
biological regulation	6055	192	137.6	1.4	1.71E-03
response to wounding	215	39	4.89	7.98	4.64E-18
indole-containing compound biosynthetic process	50	9	1.14	7.92	1.60E-02
indole-containing compound metabolic process	90	13	2.05	6.36	1.34E-03
response to jasmonic acid	213	28	4.84	5.78	2.96E-09
response to acid chemical	1198	82	27.23	3.01	1.68E-14

response to hormone	1728	86	39.27	2.19	8.05E-08
response to endogenous stimulus	1745	86	39.66	2.17	1.75E-07
regulation of response to biotic stimulus	90	11	2.05	5.38	4.27E-02
regulation of biological process	5383	168	122.33	1.37	3.22E-02
regulation of defense response	252	22	5.73	3.84	7.01E-04
regulation of response to stress	361	26	8.2	3.17	1.91E-03
response to antibiotic	306	23	6.95	3.31	4.25E-03
response to water deprivation	346	26	7.86	3.31	8.99E-04
response to water	353	26	8.02	3.24	1.28E-03
response to abiotic stimulus	2097	96	47.66	2.01	5.21E-07
response to inorganic substance	935	53	21.25	2.49	1.10E-05
response to ethylene	302	21	6.86	3.06	3.64E-02
response to oxidative stress	460	31	10.45	2.97	6.49E-04
immune system process	373	25	8.48	2.95	1.04E-02
response to osmotic stress	660	41	15	2.73	6.32E-05
response to abscisic acid	578	33	13.14	2.51	1.11E-02
response to alcohol	582	33	13.23	2.5	1.21E-02
response to other organism	1253	65	28.48	2.28	5.95E-06
response to external biotic stimulus	1253	65	28.48	2.28	5.95E-06
response to external stimulus	1659	85	37.7	2.25	3.00E-08
response to biotic stimulus	1266	66	28.77	2.29	3.78E-06
multi-organism process	1759	77	39.97	1.93	2.01E-04
small molecule biosynthetic process	737	37	16.75	2.21	4.59E-02
phosphorylation	1308	56	29.73	1.88	3.15E-02
phosphate-containing compound metabolic process	1900	80	43.18	1.85	5.57E-04
phosphorus metabolic process	1943	82	44.16	1.86	3.27E-04
oxidation-reduction process	1444	60	32.82	1.83	3.51E-02
cell communication	2009	82	45.66	1.8	1.66E-03
cellular response to stimulus	2697	101	61.29	1.65	2.65E-03
regulation of cellular process	4745	155	107.83	1.44	6.77E-03
Unclassified	4961	80	112.74	0.71	0.00E+00

Tab. S11 GO-enrichment analysis of 431 genes that are down-regulated ($FC \leq 0.5$) in MVQ1 OE (K11) vs. WT under control conditions

GO Biological process (related classes clustered together)	# of genes in genome (27502)	# of genes in upload list (431)	# of genes expected in upload list	GO Enrichment (fold)	P-value
photosynthesis, light harvesting in photosystem I	24	16	0.37	43.04	8.01E-16
photosynthesis, light harvesting	46	20	0.71	28.07	1.75E-17
generation of precursor metabolites and energy	367	32	5.68	5.63	7.00E-11
cellular metabolic process	7949	186	123.13	1.51	4.35E-07
cellular process	11448	243	177.33	1.37	6.73E-07
metabolic process	9472	218	146.72	1.49	7.37E-09
photosynthesis, light reaction	125	30	1.94	15.49	5.27E-21
photosynthesis	230	53	3.56	14.88	2.76E-38
photosynthesis, light harvesting in photosystem II	10	6	0.15	38.74	2.35E-04

Appendix

response to low light intensity stimulus	19	7	0.29	23.78	2.57E-04
response to light intensity	158	15	2.45	6.13	2.06E-04
response to light stimulus	741	45	11.48	3.92	8.75E-11
response to radiation	762	45	11.8	3.81	2.22E-10
response to abiotic stimulus	2097	82	32.48	2.52	5.19E-11
response to stimulus	6214	163	96.25	1.69	1.78E-09
chlorophyll biosynthetic process	41	15	0.64	23.62	1.11E-11
porphyrin-containing compound biosynthetic process	49	15	0.76	19.76	9.76E-11
porphyrin-containing compound metabolic process	73	15	1.13	13.27	1.39E-08
cofactor metabolic process	580	32	8.98	3.56	5.00E-06
tetrapyrrole metabolic process	74	15	1.15	13.09	1.65E-08
organic substance metabolic process	8341	175	129.2	1.35	9.82E-03
cofactor biosynthetic process	284	17	4.4	3.86	1.22E-02
biosynthetic process	3002	83	46.5	1.78	8.22E-04
tetrapyrrole biosynthetic process	52	15	0.81	18.62	2.03E-10
organic substance biosynthetic process	2874	80	44.52	1.8	1.13E-03
organic cyclic compound biosynthetic process	996	35	15.43	2.27	3.23E-02
chlorophyll metabolic process	60	15	0.93	16.14	1.20E-09
pigment biosynthetic process	122	18	1.89	9.53	1.49E-08
pigment metabolic process	144	19	2.23	8.52	2.23E-08
protein-chromophore linkage	44	15	0.68	22.01	2.62E-11
protoporphyrinogen IX biosynthetic process	15	5	0.23	21.52	2.84E-02
protoporphyrinogen IX metabolic process	15	5	0.23	21.52	2.84E-02
response to far red light	50	11	0.77	14.2	5.29E-06
response to red or far red light	221	16	3.42	4.67	2.33E-03
photosynthetic electron transport chain	43	7	0.67	10.51	2.85E-02
oxidation-reduction process	1444	47	22.37	2.1	8.82E-03
response to red light	68	11	1.05	10.44	8.94E-05
regulation of photosynthesis	44	7	0.68	10.27	3.26E-02
response to blue light	93	12	1.44	8.33	2.03E-04
response to high light intensity	81	9	1.25	7.17	2.67E-02
response to cold	422	22	6.54	3.37	4.38E-03
response to stress	3552	88	55.02	1.6	3.19E-02
response to inorganic substance	935	34	14.48	2.35	3.05E-02
response to chemical	2874	86	44.52	1.93	1.13E-05
response to hormone	1728	53	26.77	1.98	8.65E-03
response to organic substance	2026	60	31.38	1.91	6.69E-03
response to endogenous stimulus	1745	53	27.03	1.96	1.48E-02
Unclassified	4961	43	76.84	0.56	0.00E+00

Tab. S12 GO-enrichment analysis of 980 genes that are up-regulated ($FC \geq 2$) in WT 1 h after fl22 treatment compared to water control

GO Biological process (related classes clustered together)	# of genes in genome (27502)	# of genes in upload list (980)	# of genes expected in upload list	GO Enrichment (fold)	+/-	P-value
PAMP dependent induction by symbiont of host innate immune response	9	7	0.32	22.1	+	1.23E-03
PAMP dependent induction by organism of innate immune response of other organism involved in symbiotic interaction	9	7	0.32	22.1	+	1.23E-03
PAMP dependent modulation by organism of innate immune response in other organism involved in symbiotic interaction	9	7	0.32	22.1	+	1.23E-03
modulation by organism of innate immune response in other organism involved in symbiotic interaction	9	7	0.32	22.1	+	1.23E-03
modulation by organism of immune response of other organism involved in symbiotic interaction	12	8	0.42	18.94	+	4.17E-04
response to immune response of other organism involved in symbiotic interaction	12	8	0.42	18.94	+	4.17E-04
response to defenses of other organism involved in symbiotic interaction	13	8	0.46	17.48	+	6.53E-04
response to other organism	1253	133	44.1	3.02	+	2.94E-24
response to external biotic stimulus	1253	133	44.1	3.02	+	2.94E-24
response to external stimulus	1659	151	58.39	2.59	+	1.81E-21
response to stimulus	6214	418	218.72	1.91	+	1.48E-40
response to biotic stimulus	1266	134	44.56	3.01	+	2.33E-24
multi-organism process	1759	156	61.91	2.52	+	2.52E-21
modulation by organism of defense response of other organism involved in symbiotic interaction	13	8	0.46	17.48	+	6.53E-04
modification of morphology or physiology of other organism involved in symbiotic interaction	31	9	1.09	8.25	+	1.70E-02
positive regulation by organism of innate immune response in other organism involved in symbiotic interaction	9	7	0.32	22.1	+	1.23E-03
positive regulation by organism of immune response of other organism involved in symbiotic interaction	12	8	0.42	18.94	+	4.17E-04
positive regulation of immune response	79	19	2.78	6.83	+	1.98E-06
positive regulation of immune system process	79	19	2.78	6.83	+	1.98E-06
regulation of biological process	5383	262	189.47	1.38	+	9.53E-05
biological regulation	6055	292	213.12	1.37	+	1.90E-05
regulation of immune system process	139	30	4.89	6.13	+	2.87E-10
positive regulation of response to stimulus	253	32	8.9	3.59	+	1.03E-05
regulation of response to stimulus	683	60	24.04	2.5	+	2.23E-06
regulation of immune response	126	28	4.43	6.31	+	1.03E-09
positive regulation by organism of defense response of other organism involved in symbiotic interaction	9	7	0.32	22.1	+	1.23E-03
positive regulation of defense response	106	23	3.73	6.16	+	1.95E-07
regulation of defense response	252	43	8.87	4.85	+	2.37E-12
regulation of response to stress	361	49	12.71	3.86	+	6.93E-11
positive regulation of innate immune response	76	18	2.68	6.73	+	6.83E-06
regulation of innate immune response	119	27	4.19	6.45	+	1.77E-09
PAMP dependent modulation by symbiont of host innate immune response	9	7	0.32	22.1	+	1.23E-03
modulation by symbiont of host innate immune response	9	7	0.32	22.1	+	1.23E-03
modulation by symbiont of host immune response	12	8	0.42	18.94	+	4.17E-04
modulation by symbiont of host defense response	13	8	0.46	17.48	+	6.53E-04
response to host defenses	13	8	0.46	17.48	+	6.53E-04
response to host	13	8	0.46	17.48	+	6.53E-04
response to host immune response	12	8	0.42	18.94	+	4.17E-04

Appendix

positive regulation by symbiont of host innate immune response	9	7	0.32	22.1	+	1.23E-03
positive regulation by symbiont of host immune response	12	8	0.42	18.94	+	4.17E-04
positive regulation by symbiont of host defense response	9	7	0.32	22.1	+	1.23E-03
cellular response to hypoxia	27	12	0.95	12.63	+	1.03E-05
cellular response to decreased oxygen levels	29	12	1.02	11.76	+	1.95E-05
cellular response to oxygen levels	29	12	1.02	11.76	+	1.95E-05
response to oxygen levels	73	17	2.57	6.62	+	2.35E-05
response to abiotic stimulus	2097	143	73.81	1.94	+	6.29E-10
cellular response to chemical stimulus	1166	94	41.04	2.29	+	2.39E-09
cellular response to stimulus	2697	195	94.93	2.05	+	1.16E-17
cellular process	11422	515	402.03	1.28	+	2.31E-09
response to chemical	2874	242	101.16	2.39	+	9.88E-33
response to decreased oxygen levels	72	17	2.53	6.71	+	1.97E-05
response to hypoxia	66	17	2.32	7.32	+	6.40E-06
response to stress	3552	280	125.02	2.24	+	3.58E-34
cellular response to stress	943	78	33.19	2.35	+	7.61E-08
response to molecule of bacterial origin	34	15	1.2	12.53	+	1.24E-07
response to bacterium	493	81	17.35	4.67	+	2.60E-24
response to organic substance	2026	179	71.31	2.51	+	7.26E-25
endoplasmic reticulum unfolded protein response	17	7	0.6	11.7	+	2.94E-02
signal transduction	1750	131	61.6	2.13	+	1.12E-11
signaling	1779	131	62.62	2.09	+	3.24E-11
regulation of cellular process	4744	234	166.98	1.4	+	2.34E-04
cell communication	2009	150	70.71	2.12	+	8.71E-14
cellular response to unfolded protein	34	10	1.2	8.36	+	4.69E-03
response to unfolded protein	34	10	1.2	8.36	+	4.69E-03
response to topologically incorrect protein	54	11	1.9	5.79	+	3.04E-02
cellular response to topologically incorrect protein	50	11	1.76	6.25	+	1.61E-02
cellular response to organic substance	991	73	34.88	2.09	+	5.39E-05
negative regulation of programmed cell death	23	8	0.81	9.88	+	1.87E-02
regulation of cell death	79	14	2.78	5.03	+	8.42E-03
negative regulation of cell death	30	9	1.06	8.52	+	1.36E-02
response to chitin	136	47	4.79	9.82	+	1.39E-24
response to drug	592	95	20.84	4.56	+	2.74E-28
response to oxygen-containing compound	1619	173	56.98	3.04	+	3.46E-33
response to organonitrogen compound	230	54	8.1	6.67	+	1.17E-21
response to nitrogen compound	294	60	10.35	5.8	+	1.46E-21
aromatic amino acid family biosynthetic process	60	16	2.11	7.58	+	1.24E-05
organic substance metabolic process	8341	358	293.58	1.22	+	3.96E-02
metabolic process	9472	413	333.39	1.24	+	5.55E-04
organonitrogen compound metabolic process	4857	275	170.95	1.61	+	2.04E-12
nitrogen compound metabolic process	6477	299	227.97	1.31	+	8.40E-04
cellular metabolic process	7949	351	279.78	1.25	+	3.72E-03
aromatic amino acid family metabolic process	83	19	2.92	6.5	+	4.03E-06
recognition of pollen	42	11	1.48	7.44	+	3.75E-03
pollen-pistil interaction	50	11	1.76	6.25	+	1.61E-02
cell recognition	44	12	1.55	7.75	+	8.60E-04

defense response to fungus, incompatible interaction	45	10	1.58	6.31	+	3.94E-02
response to fungus	579	47	20.38	2.31	+	1.37E-03
defense response to other organism	952	94	33.51	2.81	+	2.39E-14
defense response	1513	158	53.25	2.97	+	7.66E-29
defense response, incompatible interaction	168	27	5.91	4.57	+	1.76E-06
innate immune response	310	52	10.91	4.77	+	4.20E-15
immune response	316	52	11.12	4.68	+	8.69E-15
immune system process	373	65	13.13	4.95	+	3.10E-20
indole-containing compound biosynthetic process	50	11	1.76	6.25	+	1.61E-02
indole-containing compound metabolic process	90	16	3.17	5.05	+	1.63E-03
plant-type hypersensitive response	73	16	2.57	6.23	+	1.33E-04
host programmed cell death induced by symbiont	74	16	2.6	6.14	+	1.57E-04
programmed cell death	102	18	3.59	5.01	+	3.59E-04
cell death	122	19	4.29	4.42	+	9.14E-04
defense response to oomycetes	69	14	2.43	5.76	+	2.06E-03
response to oomycetes	88	18	3.1	5.81	+	4.99E-05
negative regulation of defense response	55	11	1.94	5.68	+	3.53E-02
cellular response to drug	90	17	3.17	5.37	+	3.39E-04
response to hydrogen peroxide	78	14	2.75	5.1	+	7.38E-03
response to inorganic substance	935	80	32.91	2.43	+	8.63E-09
response to reactive oxygen species	175	26	6.16	4.22	+	1.58E-05
response to oxidative stress	460	53	16.19	3.27	+	2.23E-09
response to antibiotic	306	42	10.77	3.9	+	3.59E-09
regulation of response to biotic stimulus	90	16	3.17	5.05	+	1.63E-03
regulation of response to external stimulus	95	16	3.34	4.79	+	3.07E-03
defense response to bacterium	394	62	13.87	4.47	+	3.45E-17
protein autophosphorylation	202	29	7.11	4.08	+	4.29E-06
protein phosphorylation	963	115	33.9	3.39	+	1.88E-24
phosphorylation	1308	140	46.04	3.04	+	4.55E-26
phosphate-containing compound metabolic process	1900	165	66.88	2.47	+	1.05E-21
phosphorus metabolic process	1943	169	68.39	2.47	+	2.05E-22
cellular protein modification process	2328	178	81.94	2.17	+	3.62E-18
protein modification process	2328	178	81.94	2.17	+	3.62E-18
protein metabolic process	3640	204	128.12	1.59	+	1.14E-07
macromolecule modification	2741	179	96.48	1.86	+	1.06E-11
cellular protein metabolic process	3270	189	115.1	1.64	+	7.57E-08
cellular macromolecule metabolic process	4335	211	152.58	1.38	+	3.63E-03
response to wounding	215	29	7.57	3.83	+	1.52E-05
response to salicylic acid	203	27	7.15	3.78	+	6.62E-05
response to acid chemical	1198	108	42.17	2.56	+	3.09E-14
response to organic cyclic compound	344	37	12.11	3.06	+	3.44E-05
response to hormone	1728	121	60.82	1.99	+	1.08E-08
response to endogenous stimulus	1745	124	61.42	2.02	+	1.98E-09
secondary metabolite biosynthetic process	185	22	6.51	3.38	+	6.94E-03
secondary metabolic process	389	33	13.69	2.41	+	2.68E-02
response to heat	221	24	7.78	3.09	+	1.04E-02

Appendix

response to abscisic acid	578	51	20.34	2.51	+	4.97E-05
response to alcohol	582	51	20.48	2.49	+	5.47E-05
response to lipid	787	65	27.7	2.35	+	5.09E-06
cellular response to oxygen-containing compound	633	53	22.28	2.38	+	1.15E-04
cellular response to acid chemical	449	37	15.8	2.34	+	1.61E-02
response to salt stress	585	44	20.59	2.14	+	2.65E-02
response to osmotic stress	660	52	23.23	2.24	+	7.81E-04
cellular response to hormone stimulus	881	58	31.01	1.87	+	3.72E-02
cellular response to endogenous stimulus	898	61	31.61	1.93	+	8.12E-03
Unclassified	4961	132	174.61	0.76	-	0.00E+00
macromolecule biosynthetic process	1361	20	47.9	0.42	-	2.34E-02
RNA processing	777	6	27.35	0.22	-	5.13E-03
RNA metabolic process	1335	9	46.99	0.19	-	6.68E-08
nucleic acid metabolic process	1776	16	62.51	0.26	-	8.39E-09
nucleobase-containing compound metabolic process	2272	42	79.97	0.53	-	7.47E-03
gene expression	1605	10	56.49	0.18	-	1.02E-10
peptide biosynthetic process	593	2	20.87	0.1	-	1.29E-03

Tab. S13 GO-enrichment analysis of 454 genes that are down-regulated ($FC \leq 0.5$) in WT 1 h after flg22 treatment compared to water control

GO Biological process (related classes clustered together)	# of genes in genome (27502)	# of genes in upload list (454)	# of genes expected in upload list	GO Enrichment (fold)	P-value
response to nitrate	31	7	0.51	13.62	6.56E-03
response to inorganic substance	935	39	15.5	2.52	1.02E-03
response to chemical	2874	89	47.65	1.87	3.73E-05
response to stimulus	6214	162	103.03	1.57	1.66E-06
response to oxygen-containing compound	1619	68	26.84	2.53	1.44E-08
response to acid chemical	1198	56	19.86	2.82	2.67E-08
sterol biosynthetic process	37	7	0.61	11.41	1.83E-02
cellulose biosynthetic process	47	8	0.78	10.27	8.04E-03
beta-glucan biosynthetic process	59	8	0.98	8.18	3.63E-02
glucan biosynthetic process	112	11	1.86	5.92	1.58E-02
polysaccharide metabolic process	443	28	7.35	3.81	1.43E-05
carbohydrate metabolic process	1025	50	17.00	2.94	9.21E-08
cellular carbohydrate metabolic process	403	21	6.68	3.14	2.13E-02
polysaccharide biosynthetic process	201	18	3.33	5.40	6.65E-05
carbohydrate biosynthetic process	340	29	5.64	5.14	1.03E-08
cellular glucan metabolic process	211	16	3.50	4.57	3.16E-03
glucan metabolic process	219	16	3.63	4.41	4.98E-03
cellulose metabolic process	75	9	1.24	7.24	2.58E-02
rhythmic process	123	11	2.04	5.39	3.59E-02
response to red or far red light	221	16	3.66	4.37	5.56E-03
response to light stimulus	741	36	12.29	2.93	6.68E-05
response to radiation	762	36	12.63	2.85	1.30E-04
response to abiotic stimulus	2097	81	34.77	2.33	7.56E-09

response to water deprivation	346	24	5.74	4.18	3.44E-05
response to water	353	24	5.85	4.10	4.93E-05
cell wall biogenesis	225	15	3.73	4.02	2.93E-02
cell wall organization or biogenesis	657	37	10.89	3.40	9.85E-07
cell wall organization	504	30	8.36	3.59	1.48E-05
external encapsulating structure organization	541	30	8.97	3.34	6.68E-05
cell growth	359	21	5.95	3.53	3.88E-03
growth	413	23	6.85	3.36	2.74E-03
cellular response to oxygen-containing compound	633	28	10.50	2.67	1.39E-02
cellular response to chemical stimulus	1166	42	19.33	2.17	1.15E-02
cellular response to stimulus	2697	81	44.72	1.81	6.06E-04
response to lipid	787	34	13.05	2.61	2.22E-03
response to organic substance	2026	68	33.59	2.02	1.29E-04
hormone-mediated signaling pathway	770	31	12.77	2.43	3.09E-02
response to endogenous stimulus	1745	63	28.93	2.18	3.47E-05
response to hormone	1728	63	28.65	2.2	2.79E-05
signal transduction	1750	56	29.02	1.93	1.26E-02
signaling	1779	56	29.50	1.90	1.62E-02
regulation of biological process	5383	129	89.25	1.45	2.78E-02
biological regulation	6055	141	100.40	1.40	3.91E-02
cell communication	2009	66	33.31	1.98	5.02E-04
Unclassified	4961	49	82.26	0.60	0.00E+00

Tab. S14 GO-enrichment analysis of 385 genes that are up-regulated ($FC \geq 2$) in *mvq1* but not in WT 1 h after flg22 treatment compared to respective water control

GO Biological process (related classes clustered together)	# of genes in genome (27502)	# of genes in upload list (385)	# of genes expected in upload list	GO Enrichment (fold)	P-value
defense response to bacterium, incompatible interaction	42	8	0.58	13.68	1.05E-03
defense response, incompatible interaction	168	13	2.34	5.56	4.01E-03
innate immune response	310	23	4.32	5.33	8.04E-07
immune response	316	23	4.4	5.23	1.14E-06
response to stimulus	6214	166	86.54	1.92	1.48E-15
immune system process	373	26	5.19	5.01	1.95E-07
defense response	1513	72	21.07	3.42	5.40E-16
response to stress	3552	120	49.47	2.43	4.63E-17
defense response to other organism	952	47	13.26	3.55	5.75E-10
response to other organism	1253	60	17.45	3.44	6.61E-13
response to external biotic stimulus	1253	60	17.45	3.44	6.61E-13
response to external stimulus	1659	67	23.1	2.9	2.89E-11
response to biotic stimulus	1266	60	17.63	3.4	1.04E-12
multi-organism process	1759	67	24.5	2.74	4.11E-10
defense response to bacterium	394	32	5.49	5.83	2.33E-11
response to bacterium	493	37	6.87	5.39	1.76E-12
plant-type hypersensitive response	73	11	1.02	10.82	5.91E-05
cellular response to stress	943	34	13.13	2.59	2.20E-03

Appendix

cellular response to stimulus	2697	79	37.56	2.1	1.22E-06
host programmed cell death induced by symbiont	74	11	1.03	10.67	6.71E-05
programmed cell death	102	12	1.42	8.45	1.63E-04
cell death	122	12	1.7	7.06	9.75E-04
response to chitin	136	14	1.89	7.39	6.09E-05
response to drug	592	35	8.24	4.25	7.60E-09
response to chemical	2874	79	40.02	1.97	1.95E-05
response to oxygen-containing compound	1619	59	22.55	2.62	8.19E-08
response to organonitrogen compound	230	16	3.2	5	9.59E-04
response to nitrogen compound	294	18	4.09	4.4	1.06E-03
response to organic substance	2026	61	28.21	2.16	5.87E-05
response to oomycetes	88	9	1.23	7.34	2.14E-02
regulation of immune system process	139	11	1.94	5.68	2.11E-02
regulation of defense response	252	18	3.51	5.13	1.22E-04
regulation of response to stress	361	21	5.03	4.18	2.55E-04
regulation of response to stimulus	683	34	9.51	3.57	1.23E-06
response to wounding	215	14	2.99	4.68	1.07E-02
response to salicylic acid	203	13	2.83	4.6	2.79E-02
response to antibiotic	306	17	4.26	3.99	7.77E-03
response to acid chemical	1198	47	16.68	2.82	1.09E-06
response to hormone	1728	48	24.06	1.99	1.97E-02
response to endogenous stimulus	1745	48	24.3	1.98	3.35E-02
negative regulation of response to stimulus	205	13	2.85	4.55	3.08E-02
protein phosphorylation	963	37	13.41	2.76	1.53E-04
phosphorylation	1308	43	18.22	2.36	1.10E-03
phosphate-containing compound metabolic process	1900	60	26.46	2.27	1.95E-05
phosphorus metabolic process	1943	61	27.06	2.25	1.49E-05
cellular protein modification process	2328	68	32.42	2.1	2.90E-05
protein modification process	2328	68	32.42	2.1	2.90E-05
organonitrogen compound metabolic process	4857	103	67.64	1.52	2.21E-02
macromolecule modification	2741	69	38.17	1.81	5.35E-03
response to abiotic stimulus	2097	63	29.2	2.16	3.29E-05
signal transduction	1750	49	24.37	2.01	1.30E-02
signaling	1779	49	24.77	1.98	2.45E-02
cell communication	2009	57	27.98	2.04	1.53E-03
Unclassified	4961	48	69.09	0.69	0.00E+00

Tab. S15 GO-enrichment analysis of 160 genes that are up-regulated ($FC \geq 2$) in MVQ1 OE (K11) but not in WT 1 h after flg22 treatment compared to respective water control

GO Biological process (related classes clustered together)	# of genes in genome (27502)	# of genes in upload list (160)	# of genes expected in upload list	GO Enrichment (fold)	P-value
protoporphyrinogen IX biosynthetic process	15	4	0.09	45.55	1.10E-02
porphyrin-containing compound biosynthetic process	49	8	0.29	27.89	3.93E-06

porphyrin-containing compound metabolic process	73	9	0.43	21.06	3.42E-06
cofactor metabolic process	580	18	3.4	5.3	3.97E-05
cellular metabolic process	7949	86	46.53	1.85	3.45E-07
cellular process	11422	104	66.87	1.56	1.27E-05
metabolic process	9472	97	55.45	1.75	8.96E-08
tetrapyrrole metabolic process	74	9	0.43	20.78	3.82E-06
organonitrogen compound metabolic process	4857	56	28.43	1.97	6.06E-04
organic substance metabolic process	8341	80	48.83	1.64	1.17E-03
nitrogen compound metabolic process	6477	64	37.92	1.69	1.64E-02
cofactor biosynthetic process	284	12	1.66	7.22	4.99E-04
cellular biosynthetic process	2758	39	16.15	2.42	5.80E-04
biosynthetic process	3001	43	17.57	2.45	8.14E-05
tetrapyrrole biosynthetic process	52	8	0.3	26.28	6.00E-06
cellular nitrogen compound biosynthetic process	1366	28	8	3.5	2.50E-05
organonitrogen compound biosynthetic process	1500	30	8.78	3.42	1.17E-05
organic substance biosynthetic process	2873	42	16.82	2.5	5.52E-05
protoporphyrinogen IX metabolic process	15	4	0.09	45.55	1.10E-02
pigment metabolic process	144	8	0.84	9.49	8.74E-03
pigment biosynthetic process	122	8	0.71	11.2	2.70E-03
photosynthesis, light harvesting in photosystem I	24	6	0.14	42.7	5.14E-05
photosynthesis, light harvesting	46	8	0.27	29.71	2.51E-06
generation of precursor metabolites and energy	367	15	2.15	6.98	2.10E-05
photosynthesis, light reaction	125	9	0.73	12.3	2.63E-04
photosynthesis	230	21	1.35	15.6	5.48E-15
chlorophyll biosynthetic process	41	8	0.24	33.33	1.12E-06
chlorophyll metabolic process	60	9	0.35	25.62	7.05E-07
carbon fixation	23	4	0.13	29.71	4.79E-02
regulation of stomatal movement	87	6	0.51	11.78	4.87E-02
defense response to bacterium	394	13	2.31	5.64	2.29E-03
response to bacterium	493	14	2.89	4.85	4.78E-03
response to stimulus	6214	67	36.38	1.84	2.14E-04
defense response to other organism	952	18	5.57	3.23	4.16E-02
response to stress	3552	45	20.79	2.16	1.11E-03
translation	588	14	3.44	4.07	3.39E-02
peptide biosynthetic process	593	14	3.47	4.03	3.72E-02
peptide metabolic process	671	15	3.93	3.82	3.40E-02
cellular amide metabolic process	808	17	4.73	3.59	1.90E-02
amide biosynthetic process	664	15	3.89	3.86	3.01E-02
carboxylic acid metabolic process	971	19	5.68	3.34	1.47E-02
oxoacid metabolic process	1126	21	6.59	3.19	9.44E-03
organic acid metabolic process	1129	21	6.61	3.18	9.83E-03
small molecule metabolic process	1745	26	10.22	2.55	3.27E-02
response to abiotic stimulus	2097	36	12.28	2.93	1.36E-05
Unclassified	4961	16	29.04	0.55	0.00E+00

Tab. S16 **Enrichment of TF-binding motifs in promoters of genes whose flg22-mediated induction is suppressed in MVQ1 OE (404 genes identified in clustering analysis)**

Matrix ID	Matrix Name	p-value	family	core Seq
MA1310.1	WRKY42	8.50E-26	WRKY	TTGAC(T/C)
MA1297.1	WRKY26	3.90E-25	WRKY	TTGAC(T/C)
MA1307.1	WRKY31	4.75E-24	WRKY	TTGAC(T/C)
MA1302.1	WRKY65	1.12E-23	WRKY	TTGAC(T/C)
MA1305.1	WRKY55	1.45E-23	WRKY	TTGAC(T/C)
MA1089.1	WRKY57	1.57E-23	WRKY	TTGAC(T/C)
MA1079.1	WRKY21	1.71E-23	WRKY	TTGAC(T/C)
MA1314.1	WRKY14	2.41E-23	WRKY	TTGAC(T/C)
MA1295.1	WRKY20	3.09E-23	WRKY	TTGAC(T/C)
MA1087.1	WRKY45	4.70E-23	WRKY	TTGAC(T/C)
MA1300.1	WRKY6	5.02E-23	WRKY	TTGAC(T/C)
MA1083.1	WRKY30	1.69E-22	WRKY	TTGAC(T/C)
MA1308.1	WRKY70	7.37E-22	WRKY	TTGAC(T/C)
MA1301.1	WRKY33	1.48E-21	WRKY	TTGAC(T/C)
MA1306.1	WRKY11	1.80E-21	WRKY	TTGAC(T/C)
MA1309.1	WRKY3	1.95E-21	WRKY	TTGAC(T/C)
MA1094.1	WRKY8	2.06E-21	WRKY	TTGAC(T/C)
MA1315.1	WRKY24	2.44E-21	WRKY	TTGAC(T/C)
MA1080.1	WRKY23	3.23E-21	WRKY	TTGAC(T/C)
MA1084.1	WRKY38	3.60E-21	WRKY	TTGAC(T/C)
MA1311.1	WRKY28	5.044E-21	WRKY	TTGAC(T/C)
MA1303.1	WRKY22	5.91E-21	WRKY	TTGAC(T/C)
MA1076.1	WRKY15	9.23E-21	WRKY	TTGAC(T/C)
MA1298.1	WRKY29	2.59E-20	WRKY	TTGAC(T/C)
MA1318.1	WRKY27	3.57E-20	WRKY	TTGAC(T/C)
MA1299.1	WRKY17	3.12E-19	WRKY	TTGAC(T/C)
MA1304.1	WRKY59	5.13E-19	WRKY	TTGAC(T/C)
MA1086.1	WRKY43	5.77E-19	WRKY	TTGAC(T/C)
MA1316.1	WRKY71	7.85E-19	WRKY	TTGAC(T/C)
MA1313.1	WRKY7	2.78E-18	WRKY	TTGAC(T/C)
MA1075.1	WRKY12	2.85E-18	WRKY	TTGAC(T/C)
MA1088.1	WRKY48	3.56E-18	WRKY	TTGAC(T/C)
MA1312.1	WRKY47	8.44E-17	WRKY	TTGAC(T/C)
MA1091.1	WRKY62	1.20E-16	WRKY	TTGAC(T/C)
MA1093.1	WRKY75	7.73E-16	WRKY	TTGAC(T/C)
MA1317.1	WRKY50	1.65E-14	WRKY	TTGAC(T/C)
MA1077.1	WRKY18	2.24E-14	WRKY	TTGAC(T/C)
MA1090.1	WRKY60	2.64E-14	WRKY	TTGAC(T/C)
MA1296.1	WRKY46	1.29E-13	WRKY	TTGAC(T/C)
MA1092.1	WRKY63	1.32E-13	WRKY	TTGAC(T/C)
MA1085.2	WRKY40	2.38E-13	WRKY	TTGAC(T/C)
MA1081.1	WRKY25	6.17E-13	WRKY	TTGAC(T/C)
MA1078.1	WRKY2	1.96E-12	WRKY	TTGAC(T/C)

MA1069.1	TGA6	1.22E-5	bZIP	TGACGT
MA0589.1	ZAP1	1.54E-5	WRKY	TTGAC(T/C)
MA1047.1	TGA5	3.19E-5	bZIP	TGACGT
MA1161.1	TSO1	6.94E-5	CPP	AAATTTAAA
MA0983.1	DOF5.6	7.44E-5	C2H2	AAAG
MA0982.1	DOF2.4	8.00E-5	C2H2	AAAG
MA0973.1	CDF2	0.00014	C2H2	AAAG
MA1028.1	KAN4	0.00019	GARP	GAATATTC
MA1344.1	bZIP28	0.00020	bZIP	ACGTG(G/T)
MA1043.1	NAC083	0.00023	NAC/NAM	ACG(C/T)AA
MA0933.1	AHL20	0.00023	AT-hook	AATTAAT
MA0931.1	ABI5	0.00026	bZIP	CACGTG
MA0558.1	FLC	0.00028	MADS box	CC(A/T)6GG
MA0096.1	bZIP910	0.00031	bZIP	TGACGT
MA0989.1	PHYPADRAFT_153324	0.00032	C2H2	AAAG
MA1280.1	OBP4	0.00037	C2H2	AAAG
MA1279.1	COG1	0.00038	C2H2	AAAG
MA0552.1	PIF1	0.00038	bZIP	CACGTG
MA1338.1	AREB3	0.00039	bZIP	ACGTG(G/T)
MA1347.1	bZIP68	0.00048	bZIP	CCACGT

Tab. S17 GO-enrichment analysis of 232 genes that were identified as targets of MVQ1 by ChIP-seq

GO Biological process (related classes clustered together)	# of genes in genome (27502)	# of genes in upload list (232)	# of genes expected in upload list	GO Enrichment (fold)	P-value
response to chitin	136	13	1.1	11.84	6.88E-07
response to drug	592	17	4.78	3.56	2.56E-02
response to chemical	2874	59	23.2	2.54	4.30E-08
response to stimulus	6214	95	50.16	1.89	8.03E-08
response to oxygen-containing compound	1619	40	13.07	3.06	1.00E-06
response to organonitrogen compound	230	15	1.86	8.08	4.08E-06
response to nitrogen compound	294	17	2.37	7.16	1.83E-06
response to organic substance	2026	47	16.35	2.87	1.69E-07
hormone-mediated signaling pathway	770	22	6.22	3.54	1.29E-03
cellular response to hormone stimulus	881	24	7.11	3.37	8.71E-04
cellular response to endogenous stimulus	898	24	7.25	3.31	1.22E-03
response to endogenous stimulus	1745	37	14.09	2.63	2.52E-04
cellular response to organic substance	991	27	8	3.38	1.50E-04
cellular response to chemical stimulus	1166	35	9.41	3.72	9.98E-08
cellular response to stimulus	2697	58	21.77	2.66	1.07E-08
response to hormone	1728	37	13.95	2.65	1.98E-04
signal transduction	1750	40	14.13	2.83	8.94E-06
signaling	1779	40	14.36	2.79	1.41E-05
regulation of cellular process	4745	69	38.3	1.8	1.86E-03
regulation of biological process	5383	73	43.45	1.68	9.94E-03
biological regulation	6055	80	48.88	1.64	5.59E-03

Appendix

cell communication	2009	46	16.22	2.84	4.32E-07
protein phosphorylation	963	24	7.77	3.09	4.03E-03
phosphorylation	1308	29	10.56	2.75	3.08E-03
phosphate-containing compound metabolic process	1900	36	15.34	2.35	5.54E-03
phosphorus metabolic process	1943	37	15.68	2.36	3.48E-03
response to inorganic substance	935	22	7.55	2.91	2.74E-02
response to acid chemical	1198	26	9.67	2.69	1.68E-02
regulation of transcription, DNA-templated	2125	38	17.15	2.22	1.08E-02
regulation of nucleic acid-templated transcription	2126	38	17.16	2.21	1.09E-02
regulation of RNA biosynthetic process	2126	38	17.16	2.21	1.09E-02
regulation of RNA metabolic process	2203	38	17.78	2.14	2.69E-02
regulation of nucleobase-containing compound metabolic process	2290	39	18.49	2.11	3.73E-02
response to stress	3552	55	28.67	1.92	4.80E-03
Unclassified	4961	33	40.05	0.82	0.00E+00

Danksagung

An dieser Stelle möchte ich mich bei allen bedanken, die die Entstehung dieser Arbeit durch experimentelle Unterstützung, wissenschaftliche Diskussionen, ihr gezeigtes Interesse am Gelingen des Projekts und wertvolle Ratschläge ermöglicht haben:

Mein besonderer Dank geht an Dr. Justin Lee und Prof. Dierk Scheel für die Betreuung meiner Promotionsarbeit und die vielen Freiheiten und Möglichkeiten, die mir bei der Bearbeitung dieses Themas eingeräumt wurden. Meiner SFB 648-Mentorin Dr. Katharina Bürstenbinder danke ich für die vielen Ideen und Kommentare.

Dem SFB 648 und allen Beteiligten danke ich für die Finanzierung des MVQ-Projektes und den inspirierenden Austausch mit anderen Wissenschaftlern, der in diesem Rahmen ermöglicht wurde.

Den Gutachtern der vorliegenden Arbeit und der Prüfungskommission danke ich für Ihre aufgebrachte Zeit zur Begutachtung der Arbeit.

Mein Dank gilt Dr. Luise Brand, Stefan Fischer Prof. Dirk Wanke und Prof. Klaus Harter für ihre Hilfe bei der Etablierung des DPI-ELISA, das Teilen unveröffentlichter Expressionsvektoren und die freundliche Zusammenarbeit in Tübingen. Dr. Benedikt Athmer danke ich für die enorme Unterstützung bei der Prozessierung und Auswertung der Microarray Daten.

Dr. Rainer Birkenbihl und Prof. Imre Somssich danke ich für die Zusammenarbeit bei der ChIP-seq Analyse, anregende Diskussionen und das Teilen ihrer WRKY und ChIP Expertise. Dr. Michal Sikorski danke ich für das WRKY33 Expressionskonstrukt.

Dank gilt auch meinen Ex-Masterstudenten Samuel Grimm und Florian Rist für ihre Arbeiten an MVQ-Projekten.

Dr. Lennart Eschen-Lippold danke ich besonders für seine wertvollen Erfahrungen und die enthusiastische Hilfsbereitschaft im Labor. Großer Dank gebührt meiner "Labornachbarin" Dr. Naheed Tabassum für aufmunternde Worte, meine bescheidenen Hindi-Kenntnisse und all den großartigen Spaß. Herzlich möchte ich mich bei Nicole Bauer für die außerordentlich hilfreiche technische Unterstützung bedanken.

Der gesamten Arbeitsgruppe "Zelluläre Signaltransduktion" (Naheed Tabassum, Manaswita Baruah, Xiyuan Jiang, Fabian Trepel, Annekatriin Missal, Nicole Bauer, Dr. Lennart Eschen-Lippold, Dr. Lore Westphal) danke ich für die wunderbare Arbeitsatmosphäre und die schönen Unternehmungen. Der Kaffeerunde mit der "Induzierten Pathogenabwehr" danke ich für den Spaß am Nachmittag, der stets Quell von Motivation und Energie war. Allen Mitgliedern der Abteilung Stress- und Entwicklungsbiologie am Leibniz Institut für Pflanzenbiochemie möchte ich für alle Freundlichkeiten und Unterstützung danken.

Den Gärtnern, Handwerkern, IT-Fachleuten und Mitarbeitern der Verwaltung möchte ich ausdrücklich für die Bereitstellung der exzellenten Infrastruktur am IPB danken.

Meiner Familie und Freunden danke ich für die liebevolle Unterstützung in allen Lebenslagen und das Glück einen solchen Mittelpunkt im Leben zu haben.

DANKE!

Curriculum vitae

Persönliche Informationen

Name: Martin Weyhe
Nationalität: deutsch
Geboren: am 14.03.1987 in Merseburg
Anschrift: Karl-Liebknecht-Straße 4, 06114 Halle (Saale)

Ausbildung & wissenschaftlicher Werdegang

- 04/2013 – 03/2018 **Doktorand** in der AG “Zelluläre Signaltransduktion”
Prof. Dierk Scheel, Dr. Justin Lee
Leibniz Institut für Pflanzenbiochemie (IPB), Halle
Titel der Dissertation: “Transcriptional regulation of defence gene expression by a VQ-motif containing protein”
- 10/2012 – 04/2013 **Wissenschaftlicher Mitarbeiter**
AG “Glanduläre Trichome & Isoprenoidbiosynthese”
Prof Alain Tissier, Prof. Bettina Hause
Leibniz Institut für Pflanzenbiochemie (IPB), Halle
- 03/2012 – 08/2012 **Forschungspraktikum** EU-Stipendiat „Leonardo da Vinci”
Division of plant science, Prof. Paul Birch
James Hutton Institute, Dundee, United Kingdom
Thema: „Identification of host targets of Phytophthora RXLR-effectors“
- 03/2011 – 02/2012 **Diplomarbeit** in der AG “Jasmonatfunktion & Mykorrhiza”
Prof. Bettina Hause
Leibniz Institut für Pflanzenbiochemie (IPB), Halle
Thema: “Untersuchungen zur Funktion von Jasmonaten in der Blütenentwicklung von Tomate”
- 10/2006 – 02/2012 **Studium Biologie** Diplom (Abschlussnote: 1,2)
Martin Luther Universität (MLU), Halle-Wittenberg
- 09/2001 – 07/2006 **Allgemeine Hochschulreife** (Abschlussnote: 1,7)
Gymnasium Landesschule Pforta, Naturwissenschaftlicher Zweig
-

Publikationen

Dobritzsch, S., Weyhe, M., Schubert, R., Dindas, J., Hause, G., Kopka, J., and Hause, B. (2015): Dissection of jasmonate functions in tomato stamen development by transcriptome and metabolome analyses. *BMC biology* 13:28.

Weyhe, M., Eschen-Lippold, L., Pecher, P., Scheel, D., and Lee, J. (2014): Menage a trois: The complex relationships between mitogen-activated protein kinases, WRKY transcription factors and VQ-motif-containing proteins. *Plant signaling & behavior* 9.

Pecher, P., Eschen-Lippold, L., Herklotz, S., Kuhle, K., Naumann, K., Bethke, G., Uhrig, J., Weyhe, M., Scheel, D., and Lee, J. (2014): The *Arabidopsis thaliana* mitogen-activated protein kinases MPK3 and MPK6 target a subclass of 'VQ-motif'-containing proteins to regulate immune responses. *The New phytologist* 203:592-606.

Halle (Saale), 20.12.2018

Martin Weyhe

Eidesstattliche Erklärung

Hiermit erkläre ich an Eides statt, dass die vorliegende Arbeit selbstständig und ohne fremde Hilfe von mir verfasst wurde. Ich habe keine anderen als die von mir angegebenen Hilfsmittel verwendet. Wörtlich oder inhaltlich aus anderen Arbeiten entnommene Stellen habe ich als solche kenntlich gemacht.

Mit dieser Dissertationsschrift bewerbe ich mich erstmalig um die Erlangung eines Doktorgrades.

Martin Weyhe

Halle (Saale), _____